NASA-CR-176455
19860007385

A Reproduced Copy

OF

N86-16855

Reproduced for NASA

by the

NASA Scientific and Technical Information Facility

JPL PUBLICATION 85-63

Satellite-Derived Sea Surface Temperature: Workshop-III

February 22-24, 1984
Pasadena, California

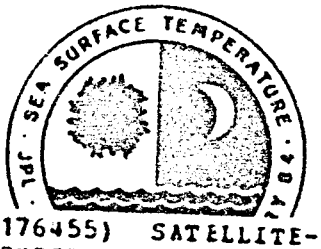

October 15, 1985

NASA
National Aeronautics and Space Administration

Jet Propulsion Laboratory
California Institute of Technology
Pasadena, California

JPL PUBLICATION 85-63

Satellite-Derived Sea Surface Temperature: Workshop-III

February 22-24, 1984
Pasadena, California

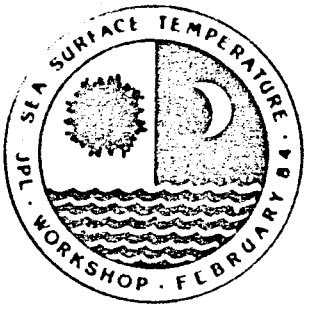

October 15, 1985

National Aeronautics and
Space Administration

Jet Propulsion Laboratory
California Institute of Technology
Pasadena, California

This publication was prepared by the Jet Propulsion Laboratory, California Institute of Technology, under a contract with the National Aeronautics and Space Administration.

ABSTRACT

This is the third report in a series of three workshops, sponsored by the National Aeronautics and Space Administration, to investigate the state of the art in global sea surface temperature measurements from space. Three workshops were necessary to process and analyze sufficient data from which to draw conclusions on the accuracy and reliability of the satellite measurements. In this workshop (Workshop III), the final two (out of a total of four) months of satellite and in situ data chosen for study were processed and evaluated. Results from the AVHRR, HIRS, SMMR, and VAS sensors, in comparison with in situ data from ships, XBTs, and buoys, confirmed satellite rms accuracies in the 0.5 to 1.0°C range, but with variable biases. These accuracies may degrade under adverse conditions for specific sensors. A variety of color maps, plots, and statistical tables are provided for detailed study of the individual sensor SST measurements.

FOREWORD

This report documents the proceedings of a Satellite-Derived Sea Surface Temperature Workshop, held at the Jet Propulsion Laboratory, Pasadena, California, on February 22 to 24, 1984. The workshop was the third and final of a series designed to compare directly SST measurements from existing satellite sensors, thereby evaluating their global accuracies and enabling informed decisions to be made concerning future sensor development. Motivation for the comparisons arose from reports of approximately 1°C accuracy in SST measurement by four different satellite sensors, and from the need for oceanographers and climate scientists to understand conditions under which better or worse performance could be expected from each sensor type. The workshops were convened under the sponsorship of the Oceanic Processes Branch, Office of Space Science and Applications of the National Aeronautics and Space Administration.

A first planning meeting for the workshop series was held at the NASA/Goddard Space Flight Center on April 16, 1982, at which the principal workshop participants met to discuss approaches to the proposed satellite and in situ data comparisons. Subsequent workshop organization took place at JPL to facilitate archiving and processing of the satellite and in situ data sets on the JPL Pilot Ocean Data System.

A substantial effort was required to assimilate, process, and analyze several months of satellite and in situ data of divergent sampling densities, spatial resolutions, and formats. The first workshop, held January 27 to 28, 1983, was thus limited to a single satellite sensor (SMMR) and one month of data (November 1979), and to evaluation of approaches developed to compare the satellite data sets with each other and with climatology, ship, XBT, and buoy observations. The second workshop, held June 22 to 24, 1983 included data from the SMMR, HIRS, and AVHRR, for November 1979 and December 1981. Finally, the third workshop was held February 22 to 24, 1984, and included data from the SMMR, HIRS, AVHRR, and VAS, for the additional months of March and July 1982. An improved set of display products for analysis was developed for this workshop.

Since the completion of these workshops, increasing attention has been paid by the scientific research community to the question of utilizing satellite SST data in large-scale ocean and atmosphere observing programs. A Tropical Oceans and Global Atmosphere (TOGA) Workshop on Sea Surface Temperature and Net Surface Radiation was held in La Jolla, California, March 28 to 30, 1984, and a Committee for Space Research (COSPAR) International Workshop on Satellite-Derived Sea Surface Temperatures for Global Climate Applications was held in Washington, D.C., May 29 to 31, 1985. Ensuring the long-term availability and accuracy of satellite SST measurements is now a high priority for ocean and climate research applications.

Participation in the three NASA/JPL Workshops was varied. Those who participated in Workshop III and contributed to this report are listed in Appendix D. The efforts of all those who contributed to the organization of the workshops are gratefully acknowledged. Special thanks are due to Jeff Hilland and the staff of the JPL Pilot Ocean Data System, through whose tireless efforts the wide array of processed SST comparison products was generated and made available for the workshops.

Eni G. Njoku
Workshop Chairman

This Page Intentionally Left Blank

TABLE OF CONTENTS

TABLE OF CONTENTS (Continued)

FIGURES (Continued)

TABLES

TABLE OF CONTENTS (Continued)

TABLES (Continued)

TABLE OF CONTENTS (Continued)

TABLES (Continued)

SECTION I

SUMMARY

E. Njoku
Jet Propulsion Laboratory, California Institute of Technology

In the series of three Satellite-Derived Sea Surface Temperature (SST) Workshops, held at the Jet Propulsion Laboratory (JPL) between January 1983 and February 1984, satellite measurements of SST were reviewed and evaluated in detail. The emphasis was on global-scale evaluations, to complement the many investigations previously carried out using high-resolution or regional data, and to address the SST measurement objectives of large-scale ocean and climate programs.

Four satellite sensors and their associated retrieval techniques were reviewed: the Advanced Very High Resolution Radiometer (AVHRR), the High-Resolution Infrared Sounder/Microwave Sounding Unit (HIRS/MSU), the Visible-Infrared Spin-Scan Radiometer Atmospheric Sounder (VAS), and the Scanning Multichannel Microwave Radiometer (SMMR). Data from these sensors were compared with each other and with in situ data from ships, expendable bathythermographs (XBTs), and drifting buoys. Four months of data were studied: November 1979, December 1981, March 1982, and July 1982.

Principal investigators for each sensor provided JPL with "raw" SST data to be processed on the JPL Pilot Ocean Data System (PODS). A variety of display products was generated from these data so that results from all sensors could be compared in a common format. The display products included color maps, histograms, scatterplots, and tables of comparison statistics. Data were compared either by point-to-point match-ups (raw data comparisons) or as monthly averaged fields on a $2^{\circ} \times 2^{\circ}$ latitude-longitude grid (binned data comparisons). Workshop investigators then examined the display products and sought to draw conclusions as to the accuracy and error characteristics of the sensor SST measurements.

Conclusions and recommendations arising from Workshops I and II have been documented in the reports of those workshops (JPL 1983 and 1984) and in the report of a subsequent TOGA Workshop on Sea Surface Temperature and Net Surface Radiation (WCP 1984). Conclusions and recommendations from Workshop III have been summarized by Njoku (1985) and detailed results from the workshop series will be published as a special collection of papers in the November 1985 issue of the Journal of Geophysical Research (JGR Oceans). This report, therefore, serves mainly to provide details of the new data and analysis methods used in Workshop III and to supplement discussions appearing in the JGR issue.

As a very broad and general conclusion, which will be expanded upon in the following sections, the workshops have shown that present satellite sensors can measure global SST with rms accuracies in the range of 0.5 to $1.0^{\circ}C$. Future emphasis must, however, be placed on improved validation and monitoring techniques to understand the nature of residual spatial and temporal bias variations. The present accuracies and geographical distributions of in situ sensors are inadequate for this purpose. Fortunately, large-scale ocean/

atmosphere experiments (TOGA and WOCE) of the World Climate Research Program now provide a focus for continuing efforts to improve satellite SST accuracies beyond the 0.5°C level (COSPAR 1985).

N86
16856

UNCLAS

SECTION II

DATA SETS AND PRODUCTS

J. Hilland and E. Njoku
Jet Propulsion Laboratory, California Institute of Technology

A. BACKGROUND

Since 1981, the Advanced Very High Resolution Radiometer (AVHRR) on the NOAA satellites has made SST measurements in the infrared portion of the spectrum using a multi-channel technique developed by McClain et al. (1983). In order to determine SST more accurately under partially cloudy conditions, infrared soundings from the High-Resolution Infrared Sounder (HIRS) and microwave soundings from the Microwave Sounding Unit (MSU), also on NOAA satellites, have been combined in a scheme described by Susskind et al. (1984). Another instrument, the Visible-Infrared Spin Scan Atmospheric Sounder (VAS), has provided SST retrievals from geostationary orbit (Smith and Woolf 1982). The ocean surface has also been viewed in the microwave portion of the spectrum by the Scanning Multichannel Microwave Radiometer aboard Nimbus-7. Wilheit et al. (1983) have described the SMMR SST retrieval techniques in detail.

In contrast to satellite methods, in situ data collected from ships, expendable bathythermographs (XBTs), and moored or drifting buoys have provided direct bulk measurements of SST. These platforms have long served as oceanographers' primary tools. Hence, a large body of knowledge has been compiled on in situ accuracies, with estimates in the range 0.2 to 1.0°C (Saur 1963; Tabata 1982).

Against this background of spacecraft and in situ measurements, participants at the JPL workshops sought to review the sensor performances (including calibration problems), understand the different SST retrieval algorithms, evaluate the sensor SST accuracies, and discuss directions for future sensor development. The issue of utilization of satellite SSTs in climate, air-sea interaction, and mesoscale oceanography studies was not the main focus of the workshops, but did have a bearing on the recommendations that arose from the discussions. Workshop planning and initial results from SMMR were discussed in JPL (1983). Workshop II results were more comprehensive as a result of refinements in the analysis procedures. In addition, more data were available for analysis with the acquisition of AVHRR (MCSST), HIRS/MSU, and VAS data sets as described in JPL (1984). In Workshop III, the subject of this report, the acquisition and analysis of data were completed, recommendations for future research and sensor development were discussed, and plans were made for eventual publication of results from the workshop series in the open literature.

B. DATA SET CHARACTERISTICS

Each sensor collected data in a unique manner, due to resolution and scanning methods, as well as a result of sensor processing and duty cycles (the percentage of time the sensor provided data satisfactorily relative to the total time). Therefore, the data distribution varied greatly. Table 2-1 summarizes pertinent sampling parameters for each sensor. The comparison shows

Table 2-1. Sensors Evaluated During the SST Workshops and Resolution of Derived SSTs

Platform	Sensor	Duty Cycle (%)	Spatial Resolution of Derived SST (km)	Coverage
TIROS-N, NOAA-7	AVHRR	100	25	Global
TIROS-N, NOAA-7	HIRS/MSU	100	125	Global
Nimbus-7	SMMR	30	150	Global
GOES	VAS	75	50	N.W. Atlantic S.E. Pacific
Ships	Thermometer			Global (mostly northern hemisphere)
XBT	Thermistor			N. Pacific
FGGE	Thermistor			Southern hemisphere

that the high resolution, nearly continuous duty cycle of the visible-infrared sensors yields an enormous number of discrete radiances. Spacecraft-measured radiances were averaged as part of the conversion process to geophysically meaningful temperatures before delivery to JPL, thus somewhat reducing the data volume. Details of the sensor modes of operation were reported in JPL (1983 and 1984), but will be summarized below for reference.

1. AVHRR

Global, day/night coverage across a 2,500 km wide swath at 4 km resolution characterizes the fundamental global sampling of AVHRR instruments aboard the NOAA satellites. Prior to mid-November 1981 the Global Operational Sea Surface Temperature Computation (GOSSTCOMP) provided 50 km resolution SST retrievals using a single window (centered at 11 μm) algorithm. After this date the improved five-channel instrument was used to derive SST from the 3.7, 11, and 12 μm windows, utilizing the triple-window technique known as the multi-channel sea surface temperature (MCSST) algorithm. A spatial resolution of 25 km was retained. The standard NOAA GOSSTCOMP and MCSST products provided geolocated SSTs and supporting parameters such as platform source, data quality, and day/night status.

2. HIRS/MSU

The HIRS and MSU instruments flown on TIROS-N and NOAA-7 served as sources for derived SSTs. The large number of infrared and microwave channels are combined in a physical algorithm to produce surface temperatures under clear or cloudy conditions. Arrays of HIRS soundings (instantaneous field of view 17.4 km at nadir) are averaged across the 2,300 km wide swath to form

SSTs at a spatial resolution of 125 km. Because the retrievals are spatially averaged, points within 60 km of land tend to be contaminated by warmer land temperatures. For workshop purposes, space/time location and quality parameters were provided so that information could be segregated for various study months, regions, and sampling conditions such as day/night and clear/cloudy.

3. SMMR

Dual polarized microwave radiance measurements at 6.6, 10.7, 18, and 21 GHz were the fundamental input to SMMR SST algorithms. The SMMR samples along a nadir-centered 780 km wide swath with a spatial resolution of 150 km at 6.6 GHz. Various quality control criteria were applied to the data by the Nimbus-7 algorithm development team, but the most obvious and influential, with regard to workshop processing, was a land proximity mask. All data within 600 km of land, including large islands, were eliminated due to possible antenna sidelobe contamination. Furthermore, in order to distinguish the highest quality values, data sent to JPL were flagged for day/twilight/night status and cell (1-5) location in the swath. The instrument was turned on and off every other day due to spacecraft/power limitations. Furthermore, the end cells in the swath were deemed unreliabile due to polarization correction errors. Thus, the overall duty cycle was reduced to 30%.

4. VAS

The Geostationary Operational Earth Satellite (GOES), carrying VAS, provided a stable platform for scanning the full disc. Daytime-only IR and VIS data were collected as part of the normal operations. These data were screened for cloud-free areas as part of the SST derivation scheme. Three of the twelve thermal bands sensed by VAS were used to derive SSTs at a spatial resolution of ~50 km. Finally, retrievals from the eastern tropical Pacific and northwestern Atlantic were provided for evaluation.

5. In Situ

The primary surface data set consisted of ship intake temperature measurements collected from radio reports by the Fleet Numerical Oceanography Center (FNOC). Typically, intake temperatures are accurate to the nearest 1°C. Additionally, biases on the order of tenths of a degree Celsius have been reported (JPL 1983). However, these data are the sole source of global in-situ measurements and at best provide spotty spatial coverage in the southern hemisphere. The temporal resolution of most reports is six hours. Marine reports were closely scrutinized for pathological errors related to erroneous ship locations and extreme temperatures.

Complementary data sets consisting of XBT drops across the northern and tropical Pacific and measurements from drifting buoys in the southern Pacific provided additional validation information. XBT drops between North America, Japan, Hawaii, Tahiti, and the Panama Canal are made about every 200 km, yielding 400 to 1,000 observations during any month. Reported accuracies are 0.1°C with biases of about +0.2°C relative to salinity-temperature-depth (STD) instruments.

Drifting buoys launched during the First GARP Global Experiment (FGGE) supplemented ship observations in the southern hemisphere from 20 S to 65 S. More than 100 buoys reported SSTs at roughly 6-hr intervals throughout each study month. In an examination of the buoy program (Garrett 1981), comparisons made with ship measurements within 1 hour and 100 km of the buoy observation yielded a worst-case standard deviation of 1.48°C and an average bias of +0.28°C relative to the ships. Allowing for buoy temperature sensor stabilization reduced the standard deviation and bias to 1.15°C and +0.75°C when compared to intake temperatures and 0.56°C and +0.18°C, respectively, when compared to bucket measurements. It should be noted that these statistics were determined for buoy SSTs taken 24 hours after the ship recording.

C. ANALYSIS TECHNIQUES

Very different spatial and temporal sampling characteristics, as well as a low signal-to-noise ratio, characterized the data. Hence, analysis procedures were designed to reduce the noise by forming monthly, 2° latitude by 2° longitude average SST anomaly fields. Noise levels were determined from point-to-point or "spot" comparisons of SST anomalies. An anomaly is defined as the departure of absolute SST from climatology. Anomalies were computed by linearly interpolating, in space and time, a 1° by 1° climatology generated by Reynolds (1982) to the irregularly spaced satellite or surface point and subtracting the climatology from the measured temperature, T. The resultant value, hereafter referred to as a "raw" anomaly, ΔT, was used as the fundamental signal rather than the absolute SST. Thus, a picture of ocean variability was depicted by each sensor.

A variety of statistical and display routines, summarized in Table 2-2, was used to portray raw-anomaly quantitative results and spatial features. First and second moments were computed in the usual Gaussian sense:

$$\Delta\bar{T} = 1/n \sum_{i=1}^{n} \Delta\bar{T}_i \qquad (2\text{-}1)$$

and

$$\Delta T_{rmsd} = [1/n \sum_{i=1}^{n} (\Delta T_i - \Delta\bar{T})^2]^{1/2} \qquad (2\text{-}2)$$

where n is the total number of points, ΔT_i is the raw anomaly located at latitude y and longitude x at time t, and ΔT_{rmsd} is the root-mean-square deviation about the mean.

Monthly average fields were formed from raw anomalies by averaging all points that fell within a 2^{o} by 2^{o} cell centered on odd latitudes and longitudes. The average temperature or "binned" anomaly for latitude, j, and longitude, i, is simply expressed as

$$\overline{T}_{ji} = 1/m \sum_{k=1}^{m} T_{yx} \qquad (2\text{-}3)$$

where m is the total number of points in cell j, i, and T_{yx} is the k^{th} raw anomaly located at latitude y and longitude x within the cell centered at j, i.

Statistics of the binning process were retained for the purpose of comparing sampling charateristics, temperature extremes, and data dispersion within each cell. Raw anomalies exceeding $\pm 5.75^{o}C$ were eliminated before binned anomaly fields were formed, because the natural variability of the ocean is typically much less than this magnitude. It follows that any signal of this intensity is the result of poor sensor performance or algorithm deficiencies, except perhaps in the case of a strong El Niño. No further quantitative editing was performed on SST anomalies. However, the data were stratified into latitude/longitude bands and segregated based on a qualitative interpretation of the status flag associated with each observation. Table 2-2 summarizes the screening procedures applied to each data set. Field-data statistics were calculated as in Eqs. (2-1) and (2-2) by substituting the mean anomalies for the raw values.

Sensor and algorithm performance were measured relative to climatology and to each sensor. Statistics of the relationships quantified the bias, standard deviation, and correlation. The correlation between any two sensors (climatology was treated as a sensor) is given by:

$$R_{12} = \frac{\sum_{n=1}^{N} \overline{T}_{1n}\,\overline{T}_{2n} - \frac{1}{N}\sum_{n=1}^{N} \overline{T}_{1n} \sum_{m=1}^{N} \overline{T}_{2m}}{\left[\sum_{n=1}^{N}\left(\overline{T}_{1n} - \frac{1}{N}\sum_{m=1}^{N}\overline{T}_{1m}\right)2\right]1/2\left[\sum_{n=1}^{N}\left(\overline{T}_{2n} - \frac{1}{N}\sum_{m=1}^{N}\overline{T}_{2m}\right)2\right]1/2} \qquad (2\text{-}4)$$

where subscripts 1 and 2 refer to sensor pairs and subscripts n and m denote the cells common to both sensors.

Table 2-2. Analysis and Graphical Display Techniques Applied to Satellite-Derived SSTs

Techniques	Data Type Analyzed: Raw Absolute	Raw Anomaly	Binned Anomaly
Compute raw anomalies by interpolating climatology to satellite point and subtracting	X		
Form 2° latitude x 2° longitude monthly averages (binning)		X	
Calculate absolute SST by adding binned anomalies to 2° binned climatological SST	X		X
Prepare a histogram of SST and summary statistics; mean, standard deviation, and number of observations		X	
Prepare a contour map of binned absolute SST	X		X
Prepare a thematic map of binned anomalies			X
Prepare a thematic map of anomaly differences			X
Draw a thematic map of number density within a 2° cell			X
Make a scatter diagram of binned anomaly SST versus Reynolds climatological SST: summary statistics, bias, standard deviation about bias, correlation and number of observations	X		X
Prepare cross correlation tables: statistics, correlation, bias, standard deviation about bias, and number of 2° cells			X
Calculate error partitioning tables: statistics and overall rms error contributed by each sensor and rms error for each sensor combined with two other sensors			X
Make a scatter diagram of sensor versus sensor: statistics, correlation, bias, standard deviation about bias, and number of 2° cells		X	X
Make a scatter diagram of binned anomaly differences for a sensor pair versus number of observations in 2° cells for either sensor			X

Another information extraction technique, error partitioning, was used to ascribe a measurement error to each sensor. This method employs sensor triplets in a set of three simultaneous equations which can be solved for each sensor's contribution to the total error in an rms sense. The mean-square difference between binned anomalies from two sensors is expressed as:

$$D_{12} = \langle(\overline{T}_1 - \overline{T}_2)^2\rangle = 1/N \sum_{n=1}^{N} (\overline{T}_{1n} - \overline{T}_{2n})^2 \qquad (2\text{-}5)$$

where $\langle\ \rangle$ indicates the sample mean computed over all binned points, n, that are common to the sensor triplet, and $\overline{T}_1$ and $\overline{T}_2$ are the binned SST anomalies. The error in the measured anomaly is

$$\varepsilon_k = T_k - T_t \qquad (2\text{-}6)$$

where T_k is the measurement from sensor k and T_t is the true anomaly. Then, it is possible to express Eq. (2-5) as:

$$D_{12} = \langle(\varepsilon_1 - \varepsilon_2)^2\rangle = \langle\varepsilon_1^2\rangle + \langle\varepsilon_2^2\rangle \qquad (2\text{-}7)$$

It has been assumed that sensor errors are uncorrelated; hence, the mean cross-product of the errors is zero. Similar expressions may be derived for D_{13} and D_{23}, thus forming a set of three equations that can be solved for the sensor errors, $\langle\varepsilon_k^2\rangle$, k = 1,2,3 [JPL (1983), Appendix G].

In this manner, error estimates for sensors forming the triplet can be determined. For M sensors there will be $(M^2 - 3M + 2)/2$ possible triplet combinations containing a given sensor. An overall error estimate can be obtained for each sensor by averaging the partitioned error for that sensor in each triplet combination.

These analytical techniques were applied to the binned anomaly fields and raw anomalies. Results were displayed from field data on monthly global and regional scales and from raw data in the form of "spot" comparisons on spatial and temporal scales commensurate with sensor sampling and geophysical variability. The space-time scales used for preparing analysis products are presented in Table 2-3.

Table 2-3. Data Analysis Products Spatial and Temporal Length Scales[1]

Analysis Product	Global[2,6]	North Pacific[3]	South Pacific[4]	North Atlantic[5]	Monthly Average
Anomaly histogram	X	X	X	X	X
Absolute SST contour map	X	X	X	X	X
Thematic map of binned anomalies	X	X	X	X	X
Thematic map of anomaly differences	X				X
Thematic map of number density	X				X
Scatter diagram of anomaly SST versus climatological SST	X	X	X	X	X
Cross correlation table	X	X	X	X	X
Error partitioning table	X	X	X	X	X
Scatter diagram sensor versus sensor		X	X	X	Spot merge $\pm\overline{6}$, $\pm\overline{12}$ hr; $\overline{20}$, $\overline{100}$ km
Scatter diagram anomaly difference versus numerical observ. in 2^{o} cell		X	X	X	

1. For some products the Pacific study area was separated into 3 regions of latitude to separate the tropics and extratropics. These regions were latitudes: (1) below 20^{o}S, (2) between 20^{o}S and 20^{o}N, and (3) above 20^{o}N.

2. Global study area; 60^{o} S to 60^{o} N, 0^{o} to 360^{o} E.

3. North Pacific study area: 0^{o} to 60^{o} N, 100^{o} to 290^{o} E.

4. South Pacific study area: 60^{o} S to 0^{o}, 100^{o} to 290^{o} E.

5. North Atlantic study area: 0^{o} to 60^{o} N, 290^{o} to 360^{o} E.

6. Global and regional thematic maps and scatter diagrams within 20^{o} latitude bands extended to 60^{o} latitude. All other products terminated at 55^{o} latitude to eliminate possibly spurious points due to sea ice.

Spot comparisons of the raw data were made using a number of different space-time "windows" in which sensor data points were matched within a given time tolerance (± hr) and radial distance (km). Table 2-4 provides the window specifications for matching any given sensor to the sensors listed in the Table.

D. WORKSHOP III RESULTS

Detailed analysis results from Workshop III have been compiled into a special collection of papers to be published in the November 1985 issue of the Journal of Geophysical Research (JGR Oceans). In this report, some additional sets of data products are provided. Tables of correlations and other statistics can be found in Appendix A. Error partitioning results are provided in Appendix B, and selected color images of SST anomaly fields are shown in Appendix C. A lengthy set of histograms and scatterplots were also generated for the Workshop and can be individually copied and supplied by request to the authors. Individual summaries of findings from the Workshop data are provided in Sections III to VIII.

1. Data Sets

Table 2-5 shows the satellite and in situ data sets processed during the three JPL workshops. In Workshop III, data from all sensors for the months of March and July 1982, and also HIRS data for December 1981, were evaluated. Details of the procedures used to derive the SST data can be found in Sections III to VI, or in previous workshop reports (JPL 1983 and 1984). Prior to Workshop III some changes were made in the HIRS SST algorithm to improve its performance. These changes included a higher-resolution climatology to define land points, tightened criteria for internal consistency checking, and retention of more data samples in each cloud analysis area (see Section IV). This new version of HIRS data was named "Version 2." In addition, both HIRS versions were provided with data quality weights which could be applied in the binning process. Those SST data with weights applied were referred to as HIRS "weighted."

Another data set unique to Workshop III was provided by T. Wilheit. This "SMMR/ship" data set consisted of a blended monthly averaged SST field on a $2^{\circ} \times 2^{\circ}$ grid, for the Pacific Ocean region, comprising original raw SST data from the SMMR and from FNOC ships. The mechanism for blending the SMMR and ship data is outlined in Section VI and, in essence, uses the ship data, where available, in an objective analysis scheme to remove spatial biases in the SMMR SST field.

2. Analysis Products

A great improvement in Workshop III was the availability of color images, or "thematic maps," to display global SST anomaly fields and data distributions. Table 2-6 lists the complete set of global color maps that were produced, including retrospective processing of maps for November 1979 and December 1981. Those maps, which have been referenced by discussions in Sections III through VI, are shown in Appendix C. The maps are self-explanatory.

Table 2-4. Time-Space Windows Used for Merging Sensor Data to Data from Other Sensors Listed in the Table

Sensor	Time (±hr)	Radial Distance (km)
AVHRR	12	100
Ships	6	100
XBT	12	20, 100
FGGE Buoys	12	20

Table 2-5. Data Sets Available for Workshop Processing

	November 1979	December 1981	March 1982	July 1982
SMMR	1	2	3	3
AVHRR	2	2	3	3
HIRS/MSU	2	3	3	3
VAS	-	-	3	3
FNOC Ship	1	2	3	3
FGGE Buoy	2	-	-	-
TRANSPAC XBT	2	2	3	3

Key: 1 = available for Workshop I
2 = available for Workshop II
3 = available for Workshop III

Table 2-6. SST Workshop Color Maps (Global)

	Nov 79	Dec 81	Mar 82	Jul 82
Data Distribution:				
AVHRR	✓	✓	✓	✓
HIRS	✓	✓	✓	✓
SMMR	✓	✓	✓	✓
VAS	0	0	✓	✓
Ship	✓	✓	✓	✓
XBT	✓	✓	✓	✓
FGGE Buoy	✓	0	0	0
SST Anomalies:				
AVHRR	✓	✓	✓	✓
HIRS	✓	✓	✓	✓
SMMR	✓	✓	✓	✓
SMMR/Ship	0	0	✓	✓
VAS	0	0	✓	✓
Ship	✓	✓	✓	✓
XBT	✓	✓	✓	✓
FGGE Buoy	✓	0	0	0
SST Anomaly Differences:				
AVHRR (day-night)	0	✓	✓	✓
HIRS-AVHRR	✓	✓	✓	✓
SMMR-AVHRR	✓	✓	✓	✓
SMMR/Ship-AVHRR	0	0	✓	✓
VAS-AVHRR	0	0	✓	✓
HIRS-SMMR	✓	✓	✓	✓
AVHRR-Ship	✓	✓	✓	✓
HIRS-Ship	✓	✓	✓	✓
SMMR-Ship	✓	✓	✓	✓
SMMR/Ship-Ship	0	0	✓	✓
VAS-Ship	0	0	✓	✓
XBT-Ship	✓	✓	✓	✓
XBT-AVHRR	✓	✓	✓	✓

Key: ✓ Available
0 Not available

The tables in Appendix A provide statistics (as discussed in Section II.C) for pair-wise sensor comparisons of binned data for all months. All data have been masked up to 600 km from land to conform to the SMMR areal coverage. Another benefit of the masking is that high-gradient coastal current regions, which could cause sampling errors in the 2^{o}-binned analyses, are largely eliminated. For each month, there is one global set of statistics and another set for each of four ocean regions. This allows the contrasting of statistics for tropics and extratropics, or for North Atlantic and North Pacific. A second table (A-2) was generated using the same data as for Table A-1, but with a 3 x 3 cell two-dimensional spatial filter applied. The weights for the filter were as follows (normalized by a factor of 16):

1	2	1
2	4	2
1	2	1

The motivation for applying the filter was to investigate any reduction in the standard deviation or increase in the correlation therefrom. (Climate-scale models can accommodate data on 2^{o} x 5^{o} or even 5^{o} x 5^{o} spatial scales.) However, care must be taken in interpreting the statistics of Table A-2 since the 2^{o}-binned sensor data are no longer strictly independent after the spatial filter has been applied. Finally, Table A-3 has been included to show the effects of using the HIRS algorithm quality weights on the March 1982 data (see Section IV).

The error-partitioning tables in Appendix B follow from the discussion in Section IIC. Only the four data sets with truly global coverage have been included. Results could be significantly skewed by the addition of ship data, unless all data were restricted to the North Atlantic or North Pacific. Separate tables for these regions were not produced, however, at the Workshop. As in Appendix A, separate tables were generated for unsmoothed and smoothed data sets. The HIRS data used was Version 2. For each sensor, the partitioned error from each of three possible triplets (or triads) was averaged to give an overall average rms error. These average errors have been collected together for convenience in Table B-3.

E. DISCUSSION

The data products (maps, plots, statistics) generated for the Workshops led to very detailed discussions concerning sensor calibration, algorithm performance, error characteristics, error sources, validation problems, and future research. Participants were encouraged to submit summaries of their evaluations for the Workshop report. These investigator summaries are provided in Sections III through VIII. (Some investigators chose to postpone publication of their analyses until the JGR Oceans special issue.)

SECTION III

ADVANCED VERY HIGH RESOLUTION RADIOMETER (AVHRR) SENSOR COMPARISON CHARACTERISTICS

E. Paul McClain

National Oceanic and Atmospheric Administration

A. INTRODUCTION

Multi-channel sea surface temperature (MCSST) techniques make use of the AVHRR on the NOAA satellites (Schwalb 1978), which delivers 1.1-km and 4-km resolution measurements in four (or five) channels: 0.58-0.68, 0.725-1.10, 3.55-3.93, and 10.3-11.3 μm (also 11.5-12.5 μm for five-channel AVHRRs). Various combinations of the four or five AVHRR data channels are used in the important initial cloud-filtering stages. Thresholds of the bi-directional reflectance in the visual and reflected-IR channels, and of brightness temperature in the thermal-IR channels, have been established for cloud-free conditions. Homogeneity tests take advantage of the low radiometer noise levels and the high degree of spatial uniformity in the ocean surface reflectance and temperature fields in the absence of clouds. Details of the cloud tests are given in McClain et al. 1983, and in Part II, pp. 1-8, in the SST Workshop II Report (JPL 1984).

The brightness temperatures measured in a given window channel of the AVHRR are corrected for atmospheric attenuation by use of the brightness temperatures from two or all three of the atmospheric windows, each of these spectral bands being characterized by a different atmospheric transmittance. The relationships between the atmospheric correction and various combinations of brightness temperature differences is linear with exceptionally small scatter, as was determined from simulation data bases (McClain 1981). Satellite and buoy measurements matched to within 25 km and 24 hours have been used to derive a small but significant temperature-dependent bias correction term for the simulation equations. Further details of deriving multichannel sea surface temperatures from AVHRR measurements are given in McClain et al. 1983.

B. ADVANTAGES OF THE AVHRR (MCSST) TECHNIQUE

The principal advantages of the AVHRR-derived sea surface temperatures are high resolution, broad geographic coverage, general consistency, and good accuracy. The MCSSTs have been produced on an operational basis since November, 1981, and they are available globally from NOAA/NESDIS as a monthly mean (65N-65S, 2.5° grid) or as a weekly composite (70N-70S, 100-km grid), and as selected regional (50-km grid) or local charts (14-km grid). The basic retrievals are obtained from 2 x 2 arrays of AVHRR data over an area nominally 8 km on a side, then one or more of the retrievals per 25-km box are resolved onto the various grid intervals listed above. MCSSTs can be obtained within 10-20 km of a land, ice, or cloud edge; and except in regions of extremely persistent and continuous cloud cover, most areas of the world are sampled at least once on a 100-km grid every 5-10 days.

In comparison with in situ sensors, particularly those on ships of opportunity, the AVHRR with its nearly continuous onboard calibration generates an internally uniform set of brightness temperature measurements orbit after orbit, day after day. Except for quite unusual circumstances, such as the El Chichon eruptions and the electrical interference problems that have plagued the 3.7 μm data during certain periods (discussed in next section), the operationally derived MCSSTs generally comprise a spatially and temporally consistent data base. The few changes that have been made in the operational algorithms have affected the root mean square (rms) differences with respect to drifting buoy temperatures only at the <0.25C level. Recent drifting buoy spot comparisions over a wide range of temperatures, geographic area, and seasons consistently indicate biases of <0.1C and rms differences (or scatters) of 0.5-0.6C (Strong and McClain 1984). Comparisons with screened ship observations, after removal of a common ship-based climatology to derive anomalies, are summarized for the various periods and regions in Table 3-1 along with the statistics for the other sensors studied during the several JPL SST Workshops. It is evident that the AVHRR, compared with the other sensors, was almost always and everywhere oer the globe characterized by the largest number of matchups, the lowest bias and scatter, and the highest correlation relative to the Pazan set of screened ship observations (the prncipal exception to this occurred in July 1982 in connection with the El Chichon eruption effects).

Table 3-1 gives the various statistics for each sensor with respect to ship matchups more than 600 km from any land or ice surface. The use of a 600 km mask is necessary in order to equalize the coverage for the AVHRR, HIRS/MSU, and VAS, which can obtain observations near coastlines and ice edges, with that available for the SMMR, which is constrained to operate at least 600 km away. Furthermore, it should be noted that there are no measurements from the SMMR over the North Atlantic in November 1979, and the VAS coverage is limited to two areas in March and July of 1982, one about 25° latitude by 30° longitude on a side in the southwestern North Atlantic and the other about 40° latitude by 40° longitude in the extreme eastern equatorial and northeastern South Pacific.

Table 3-1 also enables comparison of sensor statistics for ship matchups >600 km from land or ice and those for the same matchups after a special 3 x 3 weighted smoother[1] is applied. This procedure was used on all available 2° latitude-longitude bins >600 km from land or ice. A sharp drop in sample size resulted from loss of outer rows and columns of bins and from no computation being made for arrays where inadequate in situ or satellite data resulted in no bin average being computed for one or more bins of the 3 x 3 array. This was a particularly acute problem in the case of the FGGE buoy set; e.g., the unsmoothed global data set of N=400 for the AVHRR matchups was reduced to N=1 for the smoothed set.

---

[1] A smoothing set of weights is applied to the monthly mean SST anomalies (T_1, T_2, ..., T_9) in overlapping 3 x 3 arrays of the two-degree bins.

$$\begin{matrix} T_1 & T_2 & T_3 \\ T_4 & T_5 & T_6 \\ T_7 & T_8 & T_9 \end{matrix}$$

$$T'_5 = 4*T_5 + 2*(T_2 + T_4 + T_6 + T_8) + T_1 + T_3 + T_7 + T_9) /16$$

Table 3-1. Sensor Sea Surface Temperatures Compared With Pazan Screened Ship Temperatures (>5 per bin). Values in Parentheses Are After a 3x3 Center-Weighted Smoother Was Applied (A = AVHRR; S = SMMR; V = VAS, H = HIRS/MSU).

	Nov 1979			Dec 1981			March 1982				July 1982			
Number of Bin Matchups	A	S	H	A	S	H	A	S	H	V	A	S	H	V
Global	723 (324)	395 (152)	735 (324)	729 (235)	677 (226)	729 (235)	795 (368)	690 (368)	795 (368)	109 (51)	644 (274)	522 (230)	662 (327)	992 (38)
North Pacific (20-56S)	397 (176)	353 (148)	397 (176)	376 (1727)	361 (126)	376 (127)	434 (210)	392 (200)	434 (210)	— —	320 (117)	278 (127)	337 (170)	— —
Mid-Pacific (20S-20N)	34 (4)	41 (4)	43 (4)	41 (6)	40 (4)	41 (6)	38 (5)	37 (5)	38 (5)	1 (0)	37 (0)	22 (0)	27 (0)	4 (0)
South Pacific (20-56S	1 (0)	1 (0)	1 (0)	12 (0)	10 (0)	12 (0)	11 (0)	9 (0)	11 (0)	2 (0)	11 (0)	7 (0)	11 (C)	— —
North Atlantic (0-56N)	270 (144)	— —	270 (144)	255 (102)	227 (96)	255 (102)	267 (153)	213 (95)	267 (153)	106 (51)	258 (57)	193 (103)	259 (157)	88 (38)
Bias (ship minus satellite)														
Global	-0.19 (-0.24)	-0.52 (-0.72)	+0.04 (+0.20)	+0.30 (+0.33)	-0.72 (-0.71)	-0.13 (-0.21)	+0.36 (+0.44)	+0.21 (+0.17)	-0.30 (-0.29)	-0.90 (-0.91)	+0.48 (+0.35)	+0.43 (+0.69)	+0.07 (-0.09)	-0.48 (-0.53)
North Pacific	-0.21 (-0.27)	-0.66 (-0.76)	-0.06 (+0.06)	+0.44 (+0.43)	-1.08 (-0.95)	-0.31 (-0.21)	+0.50 (+0.54)	-0.05 (-0.13)	-0.47 (-0.42)	— —	+0.37 (+0.17)	+0.22 (+0.39)	+0.01 (-0.14)	— (—)
Mid-Pacific	-0.17 (-0.05)	+0.65 (+0.79)	+0.29 (+0.65)	+0.27 (+0.41)	+0.46 (+0.71)	+0.27 (+0.16)	+0.21 (+0.43)	+0.62 (+0.86)	-0.05 (+0.03)	— —	+1.03 —	+0.36 —	+0.69 —	-0.06 —
South Pacific	— —	— —	— —	-0.02 —	+0.04 —	+0.74 —	-0.40 —	-0.46 —	+0.05 —	— —	+0.11 —	-0.40 —	-0.11 —	— —
North Atlantic	-0.17 (-0.20)	— —	+0.13 (+0.35)	+0.15 (+0.19)	-0.42 (-0.47)	-0.10 (-0.24)	+0.29 (+0.30)	+0.76 (+0.77)	-0.16 (-0.12)	-0.89 (-0.91)	+0.57 (+0.48)	+0.88 (+1.07)	+0.08 (-0.04)	-0.90 (-0.53)
Standard Deviation (Scatter)														
Global	0.58 (0.33)	1.27 (0.81)	1.01 (0.52)	0.50 (0.28)	1.17 (0.79)	0.88 (0.42)	0.51 (0.29)	1.11 (0.79)	0.92 (0.41)	0.56 (0.26)	0.79 (0.52)	0.97 (0.60)	0.69 (0.38)	0.46 (0.22)
North Pacific	0.61 (0.33)	1.26 (0.78)	1.08 (0.65)	0.50 (0.29)	1.10 (0.72)	0.89 (0.45)	0.48 (0.29)	0.99 (0.67)	0.95 (0.41)	— —	0.93 (0.62)	0.87 (0.48)	0.72 (0.39)	— —
Mid-Pacific	0.47 (0.04)	0.77 (0.21)	0.70 (0.08)	0.54 (0.21)	0.68 (0.16)	0.72 (0.12)	0.39 (0.10)	0.75 (0.120)	0.46 (0.07)	— —	0.49 —	0.61 —	0.48 —	0.43 —
South Pacific	— —	— —	— —	0.60 —	0.77 —	0.96 —	0.78 —	1.07 —	1.00 —	— —	0.19 —	0.912 —	0.49 —	— —
North Atlantic	0.57 (0.38)	— —	0.95 (0.52)	0.41 (0.18)	1.14 (0.76)	0.77 (0.39)	0.42 (0.21)	1.19 (0.69)	0.84 (0.35)	0.52 (0.26)	0.60 (0.37)	0.93 (0.51)	0.62 (0.36)	0.43 (0.22)
Cross Correlation														
Global	0.69 (0.78)	0.34 (0.54)	0.31 (0.41)	0.76 (0.91)	0.21 (0.40)	0.21 (0.45)	0.67 (0.77)	0.24 (0.15)	0.10 (0.40)	0.40 (0.79)	0.62 (0.70)	0.46 (0.55)	0.49 (0.79)	0.49 (0.42)
North Pacific	0.74 (0.85)	0.39 (0.58)	0.32 (0.40)	0.77 (0.92)	0.22 (0.34)	0.29 (0.56)	0.52 (0.58)	0.37 (0.54)	0.13 (0.39)	— —	0.59 (0.53)	0.54 (0.62)	0.43 (0.52)	— —
South Pacific	— — (0.41)	— —	— — (0.49)	0.74 (0.93)	0.33 (0.59)	0.13 (0.04)	0.67 (0.80)	-0.05 (-0.09)	-0.01 (0.43)	0.50 (0.79)	0.66 (0.84)	0.32 (0.66)	0.51 (0.85)	0.46 (0.42)

The effect of the smoother on the bias is mixed at best, but there is definite (often dramatic) improvement in the scatter (i.e. standard deviation) and cross correlation statistics in nearly every case for every sensor. This is noteworthy in particular, for it demonstrates just how important a factor is the uneven quality of the in situ temperature observations when one is using them in an attempt to validate satellite-derived temperatures.

Table 3-2 displays the statistics for AVHRR/ship matchups >600 km from land or ice with various types of in-situ data (viz., Pazan ships, >5 and >20 per cell; FGGE buoys; and Transpac XBTs); and Table 3-3 shows AVHRR/ship matchup statistics separated into day and night. Table 3-4 enables comparison of two types of in situ observations, viz., Pazan ships the Transpac XBTs.

C. LIMITATIONS OF AVHRR (MCSST) TECHNIQUE

Perhaps chief among the limitations of the MCSST, or any other infrared method, is lack of retrievals in areas of persistent and essentially continuous cloud cover. The relatively high resolution of the AVHRR does enable more retrievals to be made in areas of patchy cloud cover than can be done wth the other sensors. The cloud detection tests appear to work well in that retrievals are seldom made using cloud-contaminated data, including contamination by thin cirrus or sub-resolution cumulus fields.

Severe volcanic eruptions or dust storms can produce extraordinary aerosol loadings in the atmosphere and thereby greatly increase attenuation of the infrared signal reaching the satellite, as well as interfere with those cloud detection tests that depend on visible-band measurements. El Chichon, because of the large mass of H_2SO_4 droplets found at very high altitudes in the atmosphere, was particulary severe in its impact on the MCSSTs, especially in the Northern Hemisphere tropics and subtropics. Daytime retrievals were virtually eliminated between 5N-30N for up to six months, and nighttime retrievals were biased too low by up to 2-4C from April to October 1982 (Strong et al. 1983). Recent research indicates the very real possibility of using a different formulation of the triple-window MCSST equation, one that appears to be nearly insensitive to the concentration of El Chichon type aerosols (Walton 1985). Furthermore, daytime visible band data from the AVHRR can probably be used to obtain a point-to-point measure of the aerosol loading, thus leading to other possibilities for correction of the retrieval temperatures (Stowe 1984).

Use of any triple-window equation obviously needs noise-free measurements in all three IR-window channels. The noise level has been exceptionally low <0.1 K, in the 11 and 12μm channels. The 3.7 μm window data, however, tend to have an acceptable noise figure (<0.2 K) during the first 12 months or so after each satellite launch, but then become increasingly contaminated by electrical interference thereafter. Fortunately, so-called "outgassing" procedures that were implemented recently[2] successfully reduced the complex but coherent noise in the 3.7 μm data to levels comparable to those measured immediately after launch. More recent experience indicates that outgassing must probably be repeated every 6-12 months to control this problem. Although the noise level in this channel was moderately high in July 1982, this was reflected primarily in a loss of nighttime MCSSTs from failure of the MCSST Intercomparison Test (see McClain in Part II, pp. 1-8, JPL 1984) rather than a decrease in accuracy.

[2]On 6/15/83 for NOAA-6, on 9/27/83 for NOAA-7, and on 9/8/83 for NOAA-8.

Table 3-2. AVHRR Multichannel Sea Surface Temperatures Compared With In Situ Temperatures. Values in Parentheses Are After a 3x3 Center-Weighted Smoother Was Applied (P5 = Pazan Screened Ships, >5/Bin; P20 = Pazan Screened Ships, >20/Bin; F = FGGE Buoys; T = Transpac XBT's).

	Nov 1979				Dec 1981			March 1982			July 1982		
Number of Bin Matchups	P5	P20	F	T	P5	P20	T	P5	P20	T	P5	P20	T
Global	723 (324)	113 (6)	400 (1)	457 (30)	729 (235)	129 (2)	284 (13)	795 (348)	265 (23)	447 (18)	644 (274)	218 (7)	288 (3)
North Pacific (20-56N)	397 (176)	— —	— —	258 (29)	376 (1237)	— —	188 (13)	434 (210)	— —	251 (18)	320 (117)	— —	169 (3)
Mid-Pacific (20N-20S)	36 (4)	— —	65 (0)	199 (1)	41 (6)	000 —	98 (0)	38 (5)	— —	196 (0)	27 (0)	— —	119 (0)
South Pacific (20-56S)	1 (0)	— —	172 (0)	0 —	12 (0)	— —	0 —	11 (0)	— —	— —	11 (0)	— —	— —
North Atlantic (0-56N)	270 (144)	— —	— —	— —	255 (107)	— —	— —	267 (153)	— —	— —	258 (157)	— —	— —
Bias (in situ minus satellite)													
Global	-0.19 (-0.24)	-0.28 (-0.32)	-0.24 —	-0.19 (-0.20)	+0.30 (+0.33)	+0.27 —	+0.30 (+0.53)	+0.36 (+0.44)	+0.39 (+0.60)	+0.16 (+0.14)	+0.48 (+0.35)	+0.44 (+0.45)	+0.49 (+0.10)
North Pacific	-0.21 (-0.27)	— —	— —	-0.21 (-0.21)	+0.44 (+0.43)	— —	+0.46 (+0.63)	+0.50 (+0.54)	— —	+0.30 (+0.14)	+0.37 (+0.17)	— —	(+0.33) (+0.10)
Mid-Pacific	-09.17 (=0.05)	— —	+0.10 —	-0.17 —	+0.27 (+0.41)	— —	-0.02 —	+0.21 (+0.43)	— —	-0.02 —	+1.03 —	— —	+0.73 —
South Pacific	— —	— —	-0.04 —	— —	-0.02 —	— —	— —	-0.40 (-)	— —	— —	+0.11 —	— —	— —
North Atlantic	-0.17 (-0.20)	— —	— —	— —	+0.15 (+0.19)	— 000	— 000	+0.29 (+0.30)	— —	— —	+0.57 (+0.48)	— —	— —
Standard Deviation (Scatter)													
Global	0.58 (0.35)	0.50 (0.12)	0.96 —	0.70 (0.32)	0.50 (0.28)	0.46 —	0.69 (0.33)	0.51 (0.29)	0.53 (0.28)	0.70 (0.35)	0.79 (0.52)	.78 (0.43)	1.08 (0.77)
North Pacific	0.61 (0.33)	— —	— —	0.78 (0.32)	0.50 (0.29)	— —	0.71 (0.33)	0.48 (0.29)	— —	0.82 (0.35)	0.93 (0.62)	— —	1.26 (0.77)
Mid-Pacific	0.47 (0.04)	— —	0.90 —	0.58 —	0.54 (0.21)	— —	0.53 —	0.39 (0.10)	— —	0.46 —	0.49 —	— —	0.67 —
South Pacific	— —	— —	0.87 —	— —	0.60 —	— —	— —	0.78 —	— —	— —	0.19 —	— —	— —
North Atlantic	0.57 (0.38)	— —	— —	— —	0.41 (0.18)	— —	— —	0.42 (0.21)	— —	— —	0.60 (0.37)	— —	— —
Cross Correlation													
Global	0.69 (0.78)	0.60 (0.87)	0.57 —	0.72 (0.78)	0.76 (0.91)	0.72 —	0.73 (0.73)	0.67 (0.77)	0.64 (0.92)	0.59 (0.70)	0.62 (0.70)	0.71 (0.90)	0.57 (-0.98)
North Pacific	0.74 (0.85)	— —	— —	065 (0.76)	0.77 (0.92)	— —	0.75 (0.73)	0.52 (0.58)	— —	0.52 (0.70)	0.59 (0.63)	— —	0.42 (-0.98)
Mid-Pacific	0.54 (0.99)	— —	0.54 —	0.56 —	0.42 (0.71)	— —	0.49 (-)	0.38 (0.84)	— —	0.53 —	0.53 —	— —	0.61 —
South Pacific	— —	— —	0.71 —	— —	0.07 —	— —	— —	0.00 —	— —	— —	0.86 —	— —	— —
North Atlantic	0.43 (0.41)	— —	— —	— —	0.74 (0.93)	— —	— —	0.67 (0.80)	— —	— —	0.66 (0.84)	— —	— —

Table 3-3. AVHRR Multichannel Sea Surface Temperatures Compared With Pazen Screened Ship Temperatures (>5/Bin) by Day and by Night. Values in Parentheses Are After a 3x3 Center-Weighted Smoother Was Applied.

	Dec 1981		Mar 1982		Jul 1982	
Number of Bin Matchups	DAY	NIGHT	DAY	NIGHT	DAY	NIGHT
Global	690 (232)	729 (213)	691 (239)	795 (368)	375 (74)	640 (296)
North Pacific (20-56N)	364 (127)	376 (108)	344 (95)	434 (210)	172 (27)	317 (112)
Mid-Pacific (20N-20S)	41 (6)	41 (3)	36 (5)	38 (5)	7 (0)	26 (0)
South Pacific (20-56S)	12 (0)	12 (0)	11 (0)	11 (0)	11 (0)	11 (0)	
North Atlantic (0-56N)	233 (99)	255 (102)	255 (139)	267 (153)	164 (47)	258 (157)
Bias (ship minus satellite)						
Global	+0.32 (+0.36)	+0.31 (+0.83)	+0.09 (+0.10+	+0.49 (+0.57)	-0.43 (-0.79)	+0.72 (+0.67)
North Pacific	+0.48 (+0.45)	+0.44 (+0.87)	+0.22 (+0.21)	+0.59 (+0.65)	-0.67 (-1.07)	+0.73 (+0.68)
Mid-Pacific	+0.32 (+0.58)	+0.11 (+1.12)	+0.07 (+0.18)	+0.26 (+0.47)	+0.50 ---	+1.08 ---
South Pacific	-0.59 ---	+0.99 ---	-0.62 ---	-0.07 ---	+0.10 ---	+0.17 ---
North Atlantic	+0.22 (+0.22)	+0.11 (+0.79)	+0.04 (+0.03)	+0.44 (+0.46)	-0.35 (-0.62)	+0.73 (+0.65)
Standard Deviation (Scatter)						
Global	0.57 (0.29)	0.52 (0.73)	0.67 (0.33)	0.46 (0.23)	1.00 (0.52)	0.65 (0.35)
North Pacific	0.54 (0.33)	0.50 (0.51)	0.66 (0.28)	0.46 (0.24)	1.10 (0.59)	0.73 (0.41)
Mid-Pacific	0.69 (0.25)	0.51 (0.10)	0.58 (0.21)	0.36 (0.14)	0.37 ---	0.48 ---
South Pacific	0.63 ---	0.56 ---	0.84 ---	0.77 ---	0.20 ---	0.19 ---
North Atlantic	0.44 (0.17)	0.42 (0.92)	0.60 (0.35)	0.41 (0.17)	0.85 (0.39)	0.52 (0.31)
Cross Correlation						
Global	0.72 (0.89)	0.75 (-0.11)	0.56 (0.74)	0.69 (0.82)	0.52 (0.83)	0.70 (0.83)
North Pacific	0.75 (0.67)	0.77 (0.79)	0.34 (0.43)	0.56 (0.72)	0.49 ---	0.64 ---
Mid-Pacific	0.45 (0.67)	0.34 (0.79)	0.26 (0.43)	0.43 (0.72)	0.61 ---	0.46 ---
South Pacific	0.17 ---	0.49 ---	-0.08 ---	0.04 ---	0.85 ---	0.86 ---
North Atlantic	0.69 (0.90)	0.75 (-0.80)	0.57 (0.64)	0.66 (0.83)	0.63 (0.94)	0.73 (0.89)

Table 3-4. Pazan Screened Ship Temperatures (>5/Bin) Compared With Transpac XBTs and AVHRR Multichannel Sea Surface Temperatures. Values in Parentheses Are After a 3x3 Center-Weighted Smoother Was Applied (A = AVHRR; T = Transpac XBTs).

	Nov 1979		Dec 1981		March 1982		July 1982	
Number of Bin Matchups	A	T	A	T	A	T	A	T
Global	723 (324)	232 (29)	729 (235)	158 (8)	795 (368)	242 (18)	644 (274)	154 (2)
North Pacific (20-56N)	397 (176)	223 (29)	376 (127)	155 (8)	343 (210)	227 (28)	320 (117)	146 (7)
Mid-Pacific (20N-20S)	34 (4)	9 (0)	41 (6)	3 (0)	38 (5)	15 (0)	27 (0)	8 (0)
South Pacific (20-56S)	1 (0)	0 —	12 (0)	0 —	11 (0)	11 (0)	0 —	0 —
North Atlantic (0-56N)	270 (144)	0 —	255 (102)	0 —	267 (153)	0 —	258 (157)	0 —
Bias (ship minus other)								
Global	-0.19 (-0.24)	-0.11 (-0.15)	+0.30 (+0.33)	+0.03 (-0.24)	+0.36 (-0.44)	+0.27 (+0.47)	+0.48 (+0.35)	+0.22 (-0.06)
North Pacific	-0.21 (-0.27)	-0.12 (-0.15)	+0.44 (+0.43)	+0.04 (-0.24)	+0.50 (+0.54)	+0.29 (+0.47)	+0.37 (+0.17)	+0.23 (-0.06)
Mid-Pacific	-0.17 (-0.05)	-0.09 —	+0.27 (+0.41)	-0.36 —	+0.21 (+0.43)	+0.05 —	+1.03 —	+0.03 —
South Pacific	— —	— —	-0.59 —	— —	-0.40 —	-0.11 —	— —	— —
North Atlantic	-0.17 (-0.20)	— —	+0.15 (+0.19)	— —	+0.29 (+0.30)	— —	+0.57 (+0.48)	— —
Standard Deviation (Scatter)								
Global	0.58 (0.35)	0.79 (0.34)	0.50 (0.28)	0.84 (0.27)	0.51 (0.29)	0.89 (0.35)	0.79 (0.52)	0.94 (0.28)
North Pacific	0.61 (0.33)	0.80 (0.34)	0.50 (0.29)	0.84 (0.27)	0.48 (0.29)	0.91 (0.35)	0.93 (0.62)	0.96 (0.28)
Mid-Pacific	0.47 (0.04)	0.38 —	0.54 (0.21)	0.73 —	0.39 (0.10)	0.30 —	0.49 —	0.52 —
South Pacific	— —	— —	0.63 —	— —	0.78 —	— —	0.19 —	— —
North Atlantic	0.57 (0.38)	— —	0.41 (0.18)	— —	0.42 (0.21)	— —	0.60 (0.37)	— —
Cross Correlation								
Global	0.69 (0.78)	0.53 (0.68)	0.76 (0.91)	0.63 (0.50)	0.67 (0.77)	0.39 (0.70)	0.62 (0.70)	0.58 (-0.99)
North Pacific	0.74 (0.85)	0.62 (0.68)	0.77 (0.92)	0.63 (0.50)	0.52 (0.58)	0.38 (0.70)	0.59 (0.63)	0.55 (-0.99)
Mid-Pacific	0.54 (0.99)	0.79 —	0.42 (0.71)	-0.24 —	0.38 (0.84)	0.42 —	0.53 — —	0.11 —
South Pacific	— —	— —	0.17 —	— —	0.00 —	— —	0.86 —	— —
North Atlantic	0.43 (0.41)	— —	0.74 (0.93)	— —	0.67 (0.80)	— —	0.66 (0.84)	— —

Although the brightness temperature at 3.7 μm can be significantly elevated above the emission value by even small amounts of specularly reflected solar radiation (>1.7% normalized bi-directional reflectance) and present operational MCSST procedures use only split-window, i.e., 11 and 12 μm brightness temperatures in the daytime for this reason, recent tests indicate that no detectable solar contamination exists at satellite zenith angles greater than 5-10° on the anti-solar side of the satellite subpoint track. Thus dual-window (3.7 and 11 μm) or triple-window MCSST equations can be used in the daytime over large areas of the globe.

Concern has been raised over use of the standard MCSST equations, particularly the split-window one, when steep temperature inversions are present in the atmosphere just over a water surface (see Condal et al. in Part II, pp. 29-31, JPL 1984). Such conditions are prevalent at times over the Great Lakes in late spring and early summer, and can occur in any mid-latitude coastal waters during this season if offshore winds are blowing. Recent investigations of this with buoy data from the Great Lakes in 1982 and 1983 found that the operational split-window MCSST equation actually performed rather well except under the most extreme inversion conditions. No reliable methods for satellite detection of the presence of these extreme conditions, and correcting for their effects on the temperature retrieval, have been found to date.

The old problem remains of skin-versus-bulk temperature, as satellite IR techniques yield skin temperatures at depths of less than a millimeter and in situ methods of observation give bulk temperatures at depths ranging from a few centimeters (towed thermistors), to a meter or two (buoys), to three to ten meters (ship intakes). The use in the MCSST method of a temperature-dependent bias correction derived from satellite/buoy matchup data presumably incorporates some sort of average skin-vs-1 m depth temperature adjustment, but this effect is almost always negative (i.e., the skin is cool) and generally amounts to 0.1-0.5C in magnitude (Robinson et al. 1984). It is not uncommon for the top few tens of cm of the water surface to become heated under low amounts of cloudiness and when very light winds result in little mechanical stirring; this has been termed the "diurnal thermocline" (Robinson et al. 1984).

D. ABILITY TO SATISFY USER NEEDS

Obviously the higher the temporal and spatial resolution, and accuracy, and the more complete the coverage under all meteorological conditions, the more user needs will be satisfied by the satellite-derived SST measurements. Lesser resolution data in time and space presumably can always be derived from the original observations. With its capability to produce relatively high resolution daily to weekly observations very close to coastlines or ice edges, the AVHRR can satisfy many users, both oceanographic (including fisheries) and meteorological, although extensive cloud cover may be constraining in some areas and times. Good global MCSST coverage for the relatively low-resolution monthly mean charts is virtually always available for climatological users.

E. ERROR CHARACTERISTICS OF MCSST`S FROM STATISTICAL TABLES

In addition to the various statistics summarized in Table 3-1, which all refer to the Pazan set of screened ship data, and where all anomalies were derived using the Reynolds` climatology (Reynolds 1982), numerous ship and satellite anomaly fields, and associated difference fields, were also produced in connection with the workshops. The ship anomaly fields suffer from the traditional lack of observational coverage in the Southern Hemisphere and some other areas. The Transpac XBT fields are severely constrained by limited geographical coverage. With this in mind, a discussion of each data period follows.

1. November 1979 Data Period

This first data period is different from the other three in that no MCSSTs were yet available, the NOAA operational product at that time being an improved AVHRR/HIRS version of the earlier GOSSTCOMP (Global Operational SST Computation), which was based on data from the SR/VTPR instruments on the pre-TIROS-N generation of NOAA operational polar satellites (Walton 1980). Compared with the SR/VTPR data, the AVHRR/HIRS measurements are of better quality and higher spatial resolution. Consequently, although still based on a single AVHRR window channel, the satellite retrievals based on the GOSSTCOMP procedures from 1979 through mid November of 1981 were generally of higher quality than those in 1978 and earlier.

Table 3-1 indicates that AVHRR biases are comparable or a bit larger than those for HIRS/MSU, but significantly smaller than those for SMMR. AVHRR scatter and correlation values are much better than for HIRS/MSU and very much better than for SMMR.

Table 3-1 also demonstrates the very substantial improvement in scatter and cross correlation figures for all three sensors and in nearly every area that results from the 3 x 3 weighted smoothing procedure (the mid-Pacific values are of dubious reliability because of the small sample): the AVHRR statistics are especially impressive (scatter of 0.33-0.38C and cross correlation of 0.41-0.85), whether on an absolute basis or compared with the other sensors. Biases generally worsen somewhat for all sensors when the 3 x 3 smoother is used.

In Table 3-2 (AVHRR only) comparisons by in situ data type are limited by sampling constraints, especially after the 3 x 3 smoother is applied, so not all regions are represented. There is very little difference in bias from one type of in-situ data to another, but scatter values are clearly worse relative to FGGE buoys[3] and a bit worse relative to Transpac XBTs. Cross correlation comparison are mixed. Scatter and correlation figures generally improve substantially when the 3 x 3 smoother is used.

---

[3]This was unexpected as previous studies have found lower bias and scatter relative to buoys than to ships (Strong and McClain 1984). An independent study of the FGGE buoy data set for Nov. 1979 for another purpose by a NOAA/NESDIS contractor found that some of the FGGE buoy observations were seriously in error. This is significant because neither the buoys nor the XBTs were given the same kind of extensive screening as were the Pazan ships.

2. December 1981 Data Period

This was the first full month of operational MCSST processing; and as in the Nov. 79 period, Table 3-1 indicates that AVHRR biases were comparable to HIRS/MSU ones and significantly better than those associated with SMMR, and the AVHRR biases tend to be better with the 600 km mask in place. Likewise, scatter magnitudes are much better for AVHRR than for HIRS/MSU, the latter being significantly better in turn than for SMMR. Cross correlations are generally comparable for HIRS/MSU and SMMR (0.13-0.33), being much lower than for AVHRR (0.74-0.77). Scatter and cross correlation figures almost always improve substantially when the 3 x 3 smoother is used, but the relative rankings given above still hold. The 3 x 3 weighted smoother statistics for the AVHRR are quite respectable indeed, being 0.18-0.29C for scatter and 0.91-0.93 for cross correlation.

Table 3-2 again has adequate AVHRR bin matchup sampling in only some of the regions especially after the smoother is applied, and there are no FGGE buoys. Bias and cross correlation values are comparable for all the in situ data sets, but scatter is somewhat worse for the Transpac XBT than the Pazan ships, although even this reverses when the 3 x 3 smoother is used. As before, the 3 x 3 smoother greatly improves the AVHRR/ship comparisons of scatter and cross correlation (see remarks on Table 3-1 just above), but generally worsened the biases somewhat.

3. March 1982 Data Period

This is the last full month of operational MCSSTs prior to the eruption of El Chichon and about the beginning of the period when the 3.7 μm noise level began to climb significantly. The statistics in Table 3-1 indicate generally lower biases for the AVHRR than for the HIRS/MSU, SMMR, or VAS. The AVHRR scatter values are superior to those of the other sensors, and they are particularly noteworthy when the 3 x 3 smoother is used, viz., 0.21-0.29C (see Table 3-1). The AVHRR cross correlation values are comparable with those of VAS and substantially better than those for HIRS/MSU and SMMR, and as with previous periods, those correlations associated with the 3 x 3 smoothing are higher (reaching 0.58-0.84 for the AVHRR).

Table 3-2, which has the same coverage restrictions as in the previous period, shows somewhat lower bias values for Transpac XBTs than for Pazan ships, and again has about comparable cross correlations and higher scatter values relative to the Transpac XBTs.

4. July 1982 Data Period

By this month the El Chichon volcanic aerosol cloud had girdled the Earth several times, but generally had remained just north of the equator, and this severely reduced the numbers of daytime AVHRR retrievals in the region of the aerosol cloud. Nighttime MCSST observations in that same zone exhibit large positive biases (AVHRR lower than in situ data because of aerosol attenuation in the high stratosphere). Chief effects of the increased 3.7 μm noise level are reduced observational densities and somewhat higher scatter, the latter from occasional erroneous passing of the uniform low stratus test, both at night. Table 3-1 reflects these factors in the large positive AVHRR bias

values. Unfortunately, the 3 x 3 smoothing procedures results in a zero sample in the Mid-Pacific zone. AVHRR scatter is adversely affected also, making it higher than the VAS, comparable to the HIRS/MSU, but still rather better than the SMMR. AVHRR cross correlations are poorer than in the previous periods, but still comparable to or even better than for the other sensors.

Table 3-3 shows AVHRR statistics are comparable relative to all the in situ data, and that all are generally worse than for the previous months studied. As with the other periods, scatter and cross correlation statistics are significantly improved by the 3 x 3 smoothing scheme, whereas the effects of the smoother on the biasing is mixed.

5. Diurnal Variations

Table 3-3 summarizes the AVHRR/ship comparisons for the three data periods when both day and night statistics are available. Excluding for the moment the month of July 1982, in which El Chichon had a strong influence that differed by day and night, there appears a systematic diurnal difference in the bias in the March period of 1982, larger positive (ship SST higher than MCSST) at night than in the daytime, that is not evident in December 1981. Standard deviations are somewhat lower, and cross correlations somewhat higher, at night for all data periods. Both these statistics generally improve substantially when the 3 x 3 weighted smoother is used. The rather drastic change from a moderate to a large negative bias in the daytime to an even larger positive bias at night during June 1982 reflects the impact of El Chichon. Monitoring of drifting buoy/MCSST matchups during the first half of 1982 also detected a nighttime positive bias of about 0.4C in the NOAA operational product. This bias was effectively removed after mid-September 1982 by re-derivation of the temperature-dependent bias correction (see discussion in Sec. F.5).

6. Summary

With the partial exception of the El Chichon impacted July 1982 period, the error characteristics of the operational AVHRR-based SSTs as exhibited by the statistical measures given in Tables 3-1 and 3-2 are predominantly as follows: biases are generally a few tenths of a degree and positive in sign (AVHRR lower than in situ temperatures) except for the earliest data period when the GOSSTCOMP instead of the MCSST method was in use. Scatter (i.e. standard deviation) magnitude tended to be in the range 0.5-0.6C, and when the latter are subjected to a 3 x 3 weighted smoothing scheme, the scatter further decreases to a remarkable 0.2-0.4! Cross correlations, except in the tropics where the extremely small range in surface temperature generally mediates against high values for this type of statistic, generally fall in the range 0.3-0.7; use of the 3 x 3 smoothing results in a further increase to 0.5-0.9.

It helps to put the foregoing discussion of the AVHRR/MCSST matchup comparisons with the Pazan ship and Transpac XBT data sets into better perspective if one looks at the statistics for the matchups between the Pazan screened ship observations and the Transpac XBT measurements (see Table 3-4). The biases associated with the Transpac XBTs tend to be one to three tenths of a degree smaller than those found with the AVHRR, but the standard deviations and cross correlations of the AVHRR are consistently and significantly better than those relative to the XBTs. As has been noted in the previous remarks, the 3 x 3

weighted smoother has variable results on the bias values for both data sets, generally worsening them somewhat, while substantially improving both scatter and cross correlation figures. The XBT standard deviations tend to have larger reductions than the AVHRR when the smoother is applied, thus rendering them quite comparable in magnitude. This was particularly the case in the July 1982 data period when the scatter for the XBTs became smaller than for the AVHRR, presumably because of the adverse effects of El Chichon on the MCSSTs.

The foregoing once again emphasizes the uncertainties in assessing the "true" accuracy of the satellite-derived SSTs when the correlative in situ measurements evidently contain significant but unknown errors of their own. It would be desirable to cross compare the Pazan ship, Transpac XBT, and FGGE buoy data sets in this connection, but the number of ship/buoy, and XBT/buoy bin matchups is N=1 and N=14, respectively. The statistics for the latter are not particularly impressive: B = -0.49, S = 1.11, and C = -0.03, but confidence in them is low with such a small sample.

Unlike the favorable effects on the other statistical measures for all data periods and regions, use of the 3 x 3 smoothing had mixed results on the bias values, generally tending to worsen them slightly. The notable exception is the July 1982 data period when the El Chichon eruption cloud belt adversely affected all the AVHRR statistics generally. Even in this case the large positive biases were decreased somewhat by the smoother. Use of only those two-degree bins having more than 20 ship observations appeared to have only a slight, and mixed, effect on all the statistical parameters.

F. REGIONAL AVHRR ERROR CHARCTERISTICS FROM GLOBAL ANOMALY CHARTS

When using the global charts of SST anomalies or anomaly differences between AVHRR and in situ data sources, it is necessary to be reminded that valid comparisons can be made only in areas where there is an adequate distribution of both types of observations. Whereas the density of AVHRR-based SSTs was generally good to excellent on a world-wide basis (the exception being the Nov 1979 GOSSTCOMP distribution, which is poor south of 45S and in parts of the tropical belt, particularly the zone from 90E to 180E), the ship SST distribution for any of the data periods is of adequate density only in parts of the North Atlantic and North Pacific and a few narrow tracks elsewhere (Figure C-1 is an example, see Appendix C). The Transpac XBT data coverage is even poorer than that of the ships, being concentrated along a few heavily travelled shipping lanes, and only a few of the two-degree bins have >4-6 observations for a given month (Figure C-1 is an example). The data distribution for the FGGE buoys (Nov. 1979 only) is all in the Southern Hemispere, but it provides some spotty coverage in regions rarely visited by ships (see Figure C-1).

1. November 1979 Data Period

There is general agreement between AVHRR- and ship-derived anomaly patterns, but some differences in amplitude are evident (Figure C-2). General agreement with the anomalies derived from Transpac XBTs and from the FGGE buoys (Figure C-2) is apparent also, though again not on a bin-by-bin basis. Some of the >3.5C positive anomalies seem suspect, particularly those on the edge of the AVHRR data void in the Southern Hemisphere. Parts of the South Atlantic area also appears too warm in the AVHRR.

2. December 1981 Data Period

The coverage and density of AVHRR/MCSST in this data period is better than it was with the AVHRR/GOSSTCOMP in November 1979, particularly in the central and western North Pacific, central and eastern South Pacific, and the high latitudes of the Southern Hemisphere generally. There is still a paucity of observations in the deep tropics of the western Pacific (Indonesia/Micronesia areas). As in the November 1979 period, if one looks at the larger, more coherent anomaly features, there is good general agreement between the satellite-derived pattern and the ship-derived pattern (Figure C-3), although the overall amplitude of the MCSST anomaly field tends to be greater. The strength of the large positive MCSST anomaly northeast of New Guinea, as well as a weaker one northeast of Madagascar, and a strong ship-based anomaly southeast of the tip of Africa, all appear suspect.

3. March 1982 Data Period

Although MCSST data densities during this period are poorer in the northern and eastern North Pacific than in December 1981, they are higher in the Indian, South Atlantic, and Southern Oceans. As previously, the Indonesia/Micronesia area is relatively poorly observed. Once again, the larger scale patterns generally match, but the amplitudes of the MCSST maxima are generally somewhat greater than the ship ones (Figure C-4). The positive MCSST anomaly in the Indonesia/Micronesia area and westward appears to have no counterpart in the ship-based pattern.

4. July 1982 Data Period

The drastic impact of the El Chichon aerosol cloud and the increased 3.7 μm noise on MCSST observational densities is seen in Figure C-5. Excellent coverage remains, however, in the central North Atlantic and in the Southern Hemisphere down to at least 45S. If one disregards the "El Chichon negative anomaly" stretching around the globe between roughly 5N-30N, there is yet again reasonably good conformance between the MCSST-based and ship-based (Figure C-5) anomaly fields, although the amplitude of the MCSST negative anomaly in the mid North Pacific is somewhat too large.

5. Diurnal Effects

Global AVHRR day-minus-night charts (Figure C-9) were produced for the Dec. 1981, March 1982, and July 1982 data periods. Although some systematic difference patterns are evident, their interpretation or explanation is hampered because no separate day and night anomaly charts were produced. Unfortunately, little recourse can be made to the separate day and night tabulations in the statistical tables (e.g., see Table 3-4), as they are broken out only by rather large regions.

A pronounced positive day-minus-night difference of several degrees extends around the Earth between about 25-40S in the December 1981 data period. This positive difference appears in a far weaker, more irregular or interrupted form and generally at somewhat lower latitudes of the Southern Hemisphere in the March 1982 period. It is absent there altogether in July 1982, but appears

in similar latitudes of the Northern Hemisphere that month. This seasonal behavior, probably associated with northward shift of the most intense solar heating from the Southern Hemisphere at the time of the summer solstice there to the Northern Hemisphere at the time of its summer solstice, is consistent with a widespread "diurnal thermocline" developing in the weak wind regimes of the central subtropical anticyclone belts.

The other major day-to-night difference that appears during all three periods is a positive one extending westward from the Indonesia area into the central Indian Ocean near the equator. In December 1981, this is clearly related to too large an atmosphere correction from a quadratic term in the operational daytime split-window equation (see discussion in Sec. G.2). In March and July of 1982, however, a linear form of the split-window equation was in daytime use, so an alternate explanation must be sought for what appears to be a persistent overcorrection for very high moisture. When the coefficients of the operational daytime and nighttime equations were adjusted slightly in October 1982 on the basis of a larger and more representative sample of buoy/MCSST matchups (see McClain in Appendix C, pp. C-1 to C-16, JPL, 1983), one of the results was to diminish this tendency toward a negative daytime and positive nighttime bias in those regions of the tropics that are extremely moist, and thus to lessen diurnal differences of the type noted here.

6. Summary

The larger-scale MCSST anomaly patterns are in fair to good agreement with the corresponding ship-derived fields almost everywhere and during every data period where there was adequate common coverage. Looking only at the small-scale, bin-to-bin values, it is difficult to see the relatively large degree of pattern similarity that really exists overall. In isolated areas there are suspect anomalies during the several data periods, and the amplitude of the AVHRR anomaly field seems somewhat larger overall than the ship field, but generally there is surprisingly good correspondence in view of the probable errors inherent in both fields. These errors combine (adding or subtracting) in a variable and unknown way in their difference field. The diurnal variations apparent in the global day-minus-night charts are sometimes difficult to account for in the absence of separate day and night anomaly fields, but the prevalence of positive day/night differences can often be attributed to the "diurnal thermocline" effect in areas where lack of wind has inhibited mixing of the uppermost layer.

G. POSSIBLE CAUSES FOR ERRORS IN THE AVHRR-BASED ANOMALY FIELDS

The general subject of sources of error in SSTs obtained from the AVHRR using the GOSSTCOMP or MCSST methods is addressed in Section C, but a few additional remarks directed specifically to possible errors noted in the above discussion of anomaly fields are in order.

1. November 1979

The tendency for a positive anomaly rimming the edge of the data at 45-50S (Figure C-2) is probably something peculiar to the GOSSTCOMP method, as it does not appear in any of the three MCSST data periods. On the other hand, the rather scattered two-degree bins with ship-based anomalies do tend to support the presence of warmer than normal water in that part of the southern

Indian Ocean (Figure C-2). The relatively cooler water extending from near the southwest tip of Africa northwestward into the central South Atlantic is supported in the AVHRR/GOSSTCOMP anomaly field (Figure C-2) only by a tongue of relatively less warm water. This could be a "diurnal thermocline" effect, as this area of the subtropical Atlantic was characterized by anticyclonic conditions with light winds at the surface and low amounts of cloudiness[5] in November 1979. There is no obvious explanation for the lack in the AVHRR of any real indication of the strong negative anomaly evident in the ship data some distance to the east of the southern part of South America.

2. December 1981

The large positive anomaly northeast of New Guinea, and to a lesser extent the weaker ones just northeast of Madagascar and along the northeast coast of Australia (Figure C-3) do not appear to be supported by the ship-based anomaly field (Figure C-3), although ship data were very scarce in the first area mentioned. The Australian case would seem to be a manifestation of the "diurnal thermocline" in the IR-based SSTs. This area was under weak mean monthly pressure gradients near sea level (light winds), and there was a mean monthly albedo of <20%, indicating very little cloudiness. The New Guinea and Madagascar cases may also have an element of this effect, but the situation there was aggravated by the use of a quadratic term in the daytime split-window MCSST equation (see Sec. F.5). This term was found to produce erroneously high MCSSTs, but only in areas where atmospheric water vapor was exceedingly large (i.e. precipitble water >5 cm), a characteristic of the region extending westward from Micronesia/Indianesia into the central Indian Ocean. Further confirmation of a moisture maximum there is afforded by a SMMR-derived precipitable water chart for December 1981 provided by NASA/GSFC. The positive anomaly southeast of South Africa seems rather too large in magnitude in the ship-derived field, but there is a large amplitude and equally dubious negative anomaly in the MCSST field just to the south of it in a large region devoid of ship data. There is no obvious explanation of either of these.

3. March 1982

Aside from the previously noted tendency for greater amplitude in the MCSST-derived anomalies than in the ship-based ones (see particularly the negative anomaly features in the North Pacific and North Atlantic (Figure C-4), the only unsupported feature is the positive anomaly in the far western Pacific and Indian Oceans centered roughly on the equator. This corresponds climatologically to the moistest portion of the tropics, and this is corroborated by the SMMR-based precipitable water charts supplied by NASA/GSFC. A similar, but rather stronger, positive anomaly in December 1981 was largely accounted for by use of a quadratic daytime MCSST equation, discontinued in February 1982. The fact that an apparently erroneous positive anomaly persists in March and July 1982 indicates that the limited set of buoy matchups used in deriving the original temperature dependent bias corrections to the MCSST simulation equations evidently still did not adequately account

---

[5]This information obtained or inferred from charts of monthly mean pressure at sea level from NCAR, monthly mean SMMR wind speeds (NASA/GSFC), and of monthly mean albedo and outgoing long wave radiation from NOAA/NESDIS.

for the atmosphere/ocean conditions in this region. This positive anomaly vanished when re-derived bias corrections, based on a much larger and more representative buoy matchup data base, were incorporated in the operational equations in October 1982.

4. July 1982

The large belt of negative anomaly stretching around the Earth from roughly 5-30N is, as discussed previously, almost entirely a consequence of the volcanic aerosol from eruptions of El Chichon in Mexico in early April 1982. The cold aerosol cloud almost eliminated daytime MCSSTs in this belt and severely attenuated the emitted radiation from the Earth's surface. The difference between monthly mean SSTs derived solely from satellite MCSSTs and solely from ship and other in situ measurements has been used by Strong et al. (1983) to track the month-to-month coverage of the volcano cloud during 1982. His charts indicate a southward transport of the aerosol near central West Africa, and a northward transport in the west central North Pacific, which is consistent with distortion in the negative anomaly belt in those regions (Figure C-5). The ship-based anomaly field (Figure C-5) also shows negative anomaly features in those two areas, but the greater extent and amplitude in the AVHRR chart is attributed to the added influence of the volcano cloud. The source of the large negative MCSST anomaly along a large part of the extreme southern edge of the chart, especially southwest of Australia, is suspected to be deficiencies in the climatology there (the ship-derived anomaly chart has a data void all through that region). The NOAA/NESDIS anomaly charts, which are based on the Robinson/Baur climatology, show only two small (in area) negative anomalies (maximum of -1.5C) anywhere in this zonal belt, one southwest of Australia at about 50-53S and another southeast of New Zealand near 55-58S.

The general tendency, in all data periods, for the amplitude of the AVHRR-based anomalies to be somewhat greater than the ship-derived anomalies, is possibly a consequence of to factors: (1) the sparser and more irregular sampling of ship data going into the bin averages; and (2) the skin temperature.

H. POSITIVE FINDINGS

Despite the difficulty of comparing satellite sensors with differing spatial resolution and geographical coverge, and matching each of these in turn with common in situ data sets that are themselves highly irregular in density of coverage in many regions and are of variable quality (furthermore, they are "spot" measurements at depths of one to several meters, whereas the AVHRR senses a kind of "skin" temperature over an area about ten kilometers on a side), there is surprisingly good correspondence in the sign and location of the major anomaly features; the correspondence in the amplitude of the anomaly maxima is only fair.

As expressed by the bias, scatter, and cross-correlation statistics for the globe and for the North Pacific, Mid-Pacific, South Pacific, and North Atlantic regions, the operational NOAA/NESDIS AVHRR product, the MCSST, generally compares better with the Pazan screened ship data set than do any of the other satellite sensors. This is especially true in the case of the standard deviation (scatter) and the cross correlation, with the AVHRR having been lower scatter and higher correlation with respect to the Pazan ships than do the

Transpac XBTs. This, and the fact that the AVHRR similarly has better statistics relative to the Pazan screened ships than it has relative to either the Transpac XBTs or the FGGE buoys, suggests that the latter two data sets should have had an equally comprehensive screening to delete incorrect observations.

When a modest amount of additional spatial smoothing (using the 3 x 3 center-weighted smoother) is done, the AVHRR/MCSST figures for scatter and cross correlation become impressive even on an absolute basis, attaining values of 0.2-0.4C for the former statistic and 0.7-0.9 for the latter. This high a correlation is noteworthy when one is reminded that it refers to anomaly values, which have a much smaller range than the temperature values from which they were derived.

1. RECOMMENDATIONS FOR IMPROVED COMPARISONS OF SENSOR AND IN SITU DATA

In view of the substantial improvement in statistics that resulted from application of the 3 x 3 center-weighted smoother, with its implications about the noise level remaining in the bin averages of ship and some of the sensor data, three recommendations are made: (1) Find a way to include 3 x 3 arrays having up to a total of say four side and/or corner bins missing from the 3 x 3 array; this would cut down the erroneous reduction in sample size that results from the present way of doing the 3 x 3 smoothing (i.e., no bin can be missing). (2) Try using 4 x 4 deg. lat./long. bins instead of 2 x 2 in the basic monthly mean anomaly chart. (3) If the effect on the statistics is salutory after doing either of the above, produce new global anomaly charts, either color-coded or contoured.

If global day-minus-night charts are to be properly interpreted, then it is necessary to produce separate daytime and nighttime global anomaly charts. Otherwise, one cannot tell if a feature in the difference field comes about because the daytime values are high, or the nighttime values are low, or both, or vice versa.

SECTION IV

RETRIEVAL OF SEA-SURFACE TEMPERATURES FROM HIRS2/MSU

J. Susskind and D. Reuter
Goddard Laboratory for Atmospheric Sciences

The methods used at the Goddard Laboratory for Atmospheres (GLA) to retrieve sea surface temperatures from HIRS2/MSU data for the four months of the NASA sea surface temperature intercomparison workshop are described. Results are shown comparing anomaly fields produced using data from ships, AVHRR, HIRS2/MSU, SMMR and VAS for the last three of these months. Fields from AVHRR and HIRS2 show the highest accuracy compared to ship fields. Errors in the HIRS2 fields appear more random while AVHRR data shows large area, spatially coherent errors. The random errors in the HIRS2 fields can be further reduced by performing the retrievals at a higher spatial resolution.

A. OVERVIEW OF THE GLA RETRIEVAL SCHEME

HIRS2 and MSU are the 20 channel infrared and 4 channel microwave passive sounders on the operational, low earth orbiting satellites. They monitor emissions, arising primarily from the earth's surface and the atmosphere up to the mid stratosphere. These, together with the SSU, a three channel pressure modulated infrared radiometer which monitors emission from the mid-upper stratosphere, comprise the TOVS (TIROS Operational Vertical Sounder) system.

The TOVS data are analyzed operationally by NOAA NESDIS to produce vertical temperature-humidity profiles using a method based primarily on statistical regression relationships between observed radiances and atmospheric parameters (Smith 1980). The approach used at GLA is fundamentally different from the current operational approach. Rather than rely on empirical relationships between observations and meteorological conditions, we attempt to find surface and atmospheric conditions which, when substituted in the radiative transfer equations describing the dependence of the observations on the meteorological conditions, match the observations to a specified amount. A physically based retrieval scheme has a number of advantages over a statistically based scheme. The single most important advantage is the ability to correct for the effects of auxiliary factors such as surface temperature, surface emissivity, surface elevation, reflected solar radiation, satellite zenith angle, and most significant of all, clouds on the observations. All of these parameters are either solved for, or directly accounted for, together with the atmospheric temperature profile, in an iterative scheme. As a result of this, the data analyzed produce not only global fields of atmospheric temperature profiles, which are necessary for the initialization of atmospheric models for numerical weather prediction, but also other auxiliary fields. These include the following monthly mean fields: sea/land surface temperature and their day-night difference which, over land, is related to soil moisture; fractional cloud cover, cloud-top temperature, and cloud-top pressure and their day-night differences; and ice and snow cover which is derived from combined use of the surface emissivity at 50.3 GHz and the ground temperature. Another important advantage of the physical retrieval is the ability to identify those areas where a satisfactory solution to the radiative transfer equations cannot be found, in which case the retrieved parameters are flagged as questionable.

The details of an earlier version of the GLA retrieval algorithm, as well as results of analysis of data from January 1979, are given in Susskind et al. (1984). The GLA processing system consists of the following main steps: 1) the forward calculation of radiances as a function of atmospheric and surface conditions; 2) accounting for cloud and surface radiative effects on the observations; 3) determining atmospheric temperature profiles by the inverse solution of the radiative transfer equation; and 4) determination of auxiliary meteorological parameters. Steps 1-3 are performed iteratively until convergence is reached. The effects of clouds on the infrared observations must be accounted for before either ground or atmospheric temperatures can be determined. The cloud-filtering algorithm utilizes MSU channel 2, which has a transmittance of about 0.1 at the surface and is sensitive to the surface emissivity. Therefore, after the calculation of radiances, microwave surface emissivity is calculated next in the iterative scheme, using MSU channel 1, followed by the cloud correction, the retrieval of ground temperature, and finally, the update of atmospheric temperature profile. If sufficient agreement between observed and calculated radiances is found, the procedure is terminated and step 4 is performed. Otherwise, the iterative procedure is continued with recalculation of radiances, surface emissivity, etc.

Table 4-1 shows the channels, centers, and peaks of the weighting functions $d\tau/d\ln P$, and radiance contribution function $Bd\tau/d\ln P$, and other relevant information, for the channels on MSU and HIRS2. The current analysis does not employ the SSU observations. Those channels utilized by GLA in analysis of the data and their primary function are indicated.

The months of data for the sea-surface temperature workshop were November 1979, December 1981, and March and July of 1982. HIRS2/MSU data for the first month were taken from TIROS-N. The remaining data were from NOAA-7, on which the channels of HIRS are slightly but significantly different from those on TIROS-N. Consequently, one change had to be made to the processing system described in Susskind et al. (1984) for the NOAA-7 data. Other changes and improvements in the processing were also made during the course of the workshop.

The data from November 1979, the first month of the workshop, would have been analyzed exactly as described in Susskind et al. (1984), but essentially one half of the month of data were missing including a big gap from November 10 to November 17 and a number of smaller gaps. Therefore, in order to have more data points and cut down the random noise component of the monthly mean fields, retrievals were run in both the warmest (least cloudy) and second warmest (second least cloudy) 125 x 125 km quadrants of the 250 x 250 km grid (see Figure 4-1), rather than in only the warmest quadrant as had been done earlier.

Significant changes were made to the processing system used to analyze the data for December 1981 and March 1982. One change, affecting the clear column radiance algorithm, was made primarily because of the change in characteristics of channel 13 and channel 14 of HIRS2 on NOAA-7 from those of the same channels of HIRS2 on TIROS-N. The improved algorithm, shown in the next section, has been found to be superior even with TIROS-N data, and has now been incorporated, together with other changes, for use in the re-analysis of TIROS-N data. The second change involved use of the 11 μm window data, in addition to the 3.7 and 4.0 μm window data, in the retrieval of ground temperatures. In addition, individual soundings were assigned weights to be used in the generation of monthly mean fields. After studying the December 1981 and March 1982

Table 4-1. HIRS2 and MSU Channels

Channel	λ(μm)	ν(cm^{-1})	Peak of dτ/dlnp (mb)	Peak of Bdτ/dlnp (mb)
H1	14.96	668.40	30	20
H2[a]	14.72	679.20	60	50
H3	14.47	691.10	100	100
H4[a,c]	14.21	703.60	280	360
H5[c]	13.95	716.10	475	575
H6[c]	13.65	732.40	725	875
H7[c]	13.36	748.30	Surface	Surface
H8[b,c]	11.14	897.70	Window, sensitive to water vapor	
H9	9,73	1027.90	Window, sensitive to O_3	
H10	8.22	1217.10	Lower tropospheric water vapor	
H11	7.33	1363.70	Middle tropospheric water vapor	
H12	6.74	1484.40	Upper tropospheric water vapor	
H13[a,d]	4.57	2190.40	Surface	Surface
H14[a,d]	4.52	2212.60	650	Surface
H15[a]	4.46	2240.10	340	675
H16	4.39	2276.30	170	425
H17	4.33	2310.70	15	2
H18[b]	3.98	2512.00	Window, sensitive to solar radiation	
H19[b]	3.74	2671.80	Window, sensitive to solar radiation	
M1[e]	0.596*	50.30**	Window, sensitive to surface emissivity	
M2[d]	0.558*	53.74**	500	
M3[a]	0.546*	54.96**	300	
M4[a]	0.518*	57.95**	70	

[a]used by GLA to compute temperature profiles
[b]used by GLA to compute surface temperature
[c]used by GLA to compute cloud fields
[d]used by GLA in cloud correction
[e]used by GLA to compute surface emissivity
*λ in cm
**ν in GHz

sea surface temperature fields in Workshop III, a number of other changes were made to further reduce noise in the field. The newest system, called HIRS version 2 in the workshop, was used to reprocess March 1982 data and to process July 1982 data. For this reason, results for July 1982 and the reprocessed data for March 1982 are better indicators of the capabilities of HIRS2/MSU for retrieval of surface temperature than those of the earlier months. Modifications to Susskind et al. (1984) used in the analysis of workshop data for December 1981 and March 1982, and in the analysis of July 1982 and re-analysis of March 1982, are described in the next two sections.

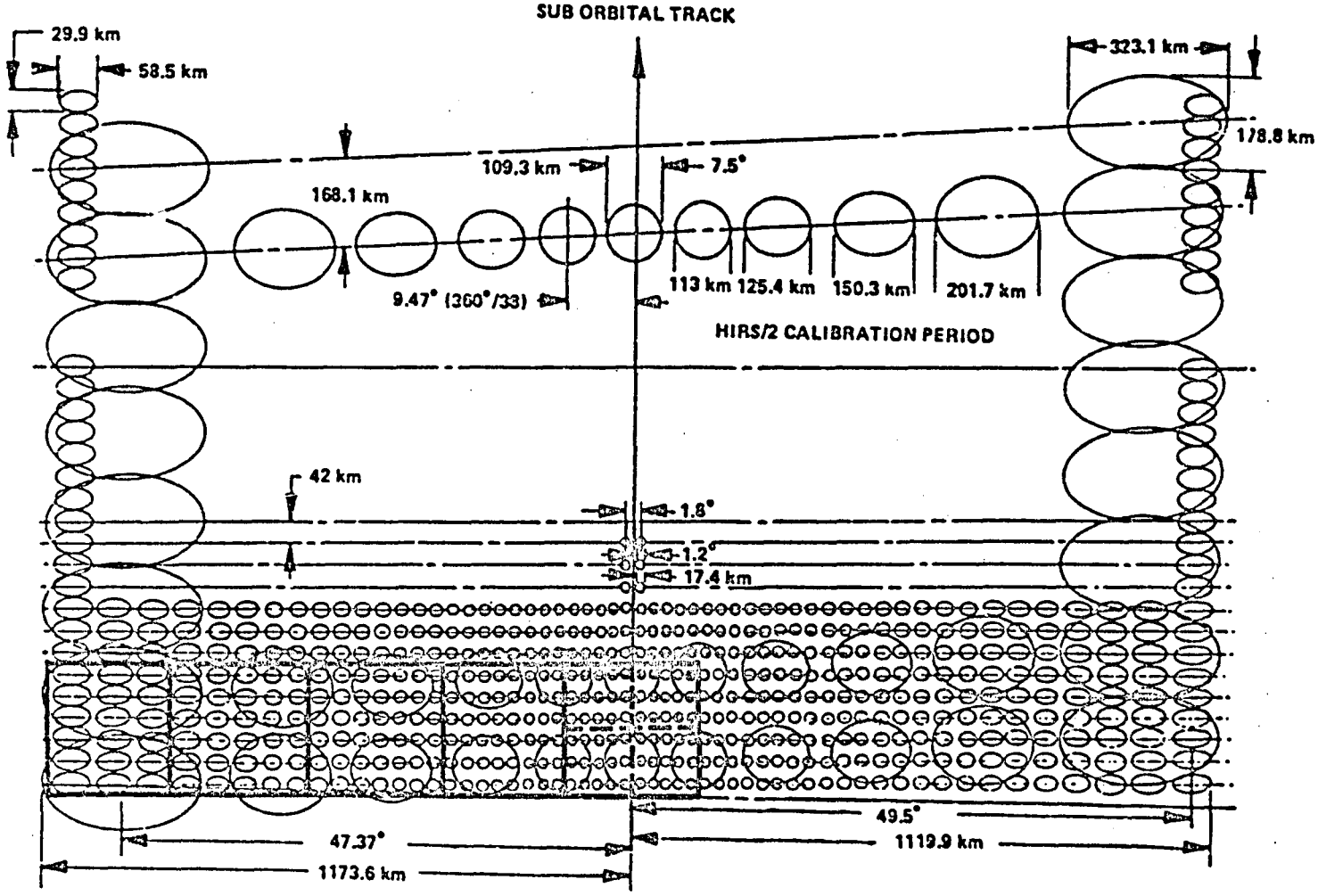

Figure 4-1. Retrievals were run in the warmest and second warmest 125 x 125 km quadrants of the 250 x 250 km grid.

B. IMPROVEMENTS TO THE SYSTEM USED IN ANALYSIS OF DECEMBER 1981 AND MARCH 1982 DATA

HIRS2/MSU data for December 1981 and March 1982 were analyzed exactly as in Susskind et al. (1984), except for modifications which were made to improve the clear column radiance algorithm and the sea/land surface temperature algorithm. These are described below.

1. Improved Estimation of Clear Column Infrared Radiances

Infrared observations are highly sensitive to the presence of clouds in the field of view and, hence, accounting for their effects on the observations becomes perhaps the most important step in the retrieval process. If one looks at an otherwise homogeneous but partially cloudy scene with cloud fraction α, then to a reasonable approximation, one can write the radiance observed in channel i to be

$$R_i = (1-\alpha)\, R_{i,CLR} + \alpha\, R_{i,CLD} \qquad (4\text{-}1)$$

where $R_{i,CLR}$ is the radiance one would observe in a cloud-free area and $R_{i,CLD}$ is the radiance one would observe in a completely cloud-covered area. $R_{i,CLD}$ depends not only on the atmospheric variables but also on the detailed properties of the clouds. Rather than assume or attempt to determine the cloud properties simultaneously with the determination of atmospheric and surface properties, the method attempts to estimate, or "reconstruct" from the observed radiances, the clear column radiances which would have been observed if no clouds were present. These reconstructed clear column radiances, $\tilde{R}_i$, are used in determiation of the atmospheric temperature profile as well as in the determination of sea surface or ground temperature. The cloud field parameters are determined only after a complete atmospheric and surface solution is obtained. This method of treating clouds is fundamentally different from the approach used in analysis of AVHRR data, in which high spatial resolution is used to attempt to identify clear spots. Sea-surface temperatures are not determined in AVHRR spots thought to have any cloud contamination.

A two field-of-view approach, similar to one originally introduced by Smith (1968), is used to extrapolate observed radiances to obtain reconstructed clear column radiances, $\tilde{R}_i$. We express $\tilde{R}_i$ as

$$\tilde{R}_i = R_{i,1} + \eta[R_{i,1} - R_{i,2}] \qquad (4\text{-}2)$$

where $R_{i,1}$ is the observed radiance for channel i in the field of view having the larger 11 μm radiance, and $R_{i,2}$ is the observation of channel i in the second field of view.

If $R_{i,CLR}$ is known for a given channel, then η can be solved for according to

$$\eta = \frac{R_{1,CLR} - R_{1,1}}{R_{1,1} - R_{1,2}} \tag{4-3}$$

Since $\eta = \alpha_1/(\alpha_1 - \alpha_2)$, it should not be dependent on the channel used. In Susskind et al. (1984), η was determined by combined use of HIRS2 channel 13 and MSU channel 2. $R^N_{13,CLR}$ is computed in each iteration (N) using the N^{th} iterative temperature profile and ground temperature. If the N^{th} guess is too warm (or cold), $R^{(N)}_{I,CLR}$ would be too large (or small). The effect on the computed brightness temperature of channel 13 of a bias in the temperature profile in the troposphere is accounted for, to first order, by modifying the brightness temperature according to

$$\Theta'_{13} = \Theta^N_{13,CLR} + \Theta_{M2} - \Theta^N_{M2} \tag{4-4}$$

where $\Theta^N_{13,CLR}$ is the equivalent brightness temperature to $R^N_{13,CLR}$, Θ_{M2} is the observed brightness temperature in MSU channel 2, which is sensitive to the average tropospheric temperature, and Θ^N_{M2} is the computed brightness temperature in MSU channel 2. This procedure works reasonably well even though channel 13 is sensitive primarily to radiation much closer to the surface than that of MSU channel 2. Then, η_{13} is computed according to

$$\eta_{13} = \frac{B_{13}[\Theta'_{13}] - R_{13,1}}{R_{13,1} - R_{13,2}} \tag{4-5}$$

where $B(\Theta')$, the black body function of the corrected equivalent brightness temperature, is the corrected estimate of the clear column radiance. While results using equations (4-2) through (4-5) are quite good, it has been found that in cases where the initial guess has a lapse rate error, improved results are obtained by defining η_{14} in an analogous manner to η_{13} in equations (4-4) and (4-5) and setting η equal to the average of η_{13} and η_{14} weighted by the square of the difference in radiances for each channel in each field of view:

$$\eta = \frac{\eta_{13}(R_{13,1}-R_{13,2})^2 + \eta_{14}(R_{14,1}-R_{14,2})^2}{(R_{13,1}-R_{13,2})^2 + (R_{14,1}-R_{14,2})^2} \tag{4-6}$$

Including channel 14 radiances in the determination of η has the effect of utilizing a single infrared channel with a broader weighting function, more in line with that of the microwave channel, to correct for cloud effects. Combined use of channels 13 and 14 was especially necessary for NOAA-7 data be-

cause the weighting functions for both channels 13 and 14 were shifted lower in the atmosphere relative to TIROS-N and channel 13 provided even a poorer match with MSU channel 2. The procedure gives improved results with TIROS-N data as well.

2. Improved Determination of Sea-Surface Temperatures and Ground Temperatures

Once η is obtained in any iteration, reconstructed clear column radiances, $\tilde{R}_i^N$, are obtained for each channel using equation (4-2). These radiances are used to get the updated estimates of ground temperature and atmospheric temperature profile. One can solve for ground temperature at night from any window channel observation (8, 18, or 19) in a straightforward manner given the clear column radiance, the estimated temperature-humidity profile, and an estimate of the surface emissivity. During the day, solar radiation reflected off the ground contributes significantly to the observed radiances in the short-wave window channels 18 and 19. A sea surface or ground temperature can be obtained during the day by simultaneous use of the two shortwave channel observations, with the additional assumption that the surface bidirectional reflectance of radiation from the sun, in the direction of the satellite, is the same at both 4.0 and 3.7 μm (Susskind et al. 1984).

In Susskind et al. (1984) only the two short wave channels were used to obtain both day and night global surface temperatures. The 11 μm channel was not used because attenuation due to water vapor becomes very significant in humid atmospheres. The differences between the retrieved January 1979 monthly mean day and night sea surface temperature were almost all less than 1°C as expected. This gives evidence that the procedures used to correct the short wave observations for solar contamination are valid.

While the results using this method were quite good, several new improvements have been made to the system. The first change involves including radiances in the 11 μm window channel 8 in the estimate of sea/land surface temperature. As alluded to earlier, under very humid conditions, significant attenuation of radiation leaving the surface by water vapor absorption at channel 8 frequencies produces a large potential source of error in the determination of ground temperatures both because of uncertainties in water vapor distribution, and even more significantly, low response of the radiances to changes in surface temperatures. Nevertheless, inclusion of 11 μm radiances introduces additional surface temperature information, which becomes quite accurate at low and moderate water vapor conditions. In addition, during the day, under some conditions, the long wave observations are superior to short wave observations which have a potential error source due to the reflected solar radiation. In order to determine the proper mix of channels to be used to get ground temperatures in a given situation, ground temperatures were retrieved for all channels, that is, three independent estimates, T_{s8}, T_{s18}, and T_{s19}, were made at night, and two independent estimates, T_{s8} and $T_{s18,19}$ were made during the day. Each estimate was given a weight, Q_i, which decreased according to the magnitude of the cloud correction and atmospheric and solar radiation corrections that had to be made to obtain the ground temperature T_{si} from the observed brightness temperatures. The weight was defined as

$$Q_i^{-1} = \left|\tilde{\theta}_i - \theta_{i,1}\right| + \left|\tilde{\theta}_i - T_{si}\right| \qquad (4\text{-}7)$$

where $\tilde{\theta}_i - \theta_{i,1}$ is the difference between the reconstructed brightness temperature and that observed in field of view 1 for channel i, and $\tilde{\theta}_i - T_{si}$ is the difference between the reconstructed clear column brightness temperature used to obtain a surface temperature and the surface temperature obtained. The first term represents the cloud correction and the second factor represents the atmospheric and solar radiation correction.

In the case of daytime retrievals, the brightness temperature of channel 18, which is less affected by solar radiation than that of channel 19, is used in equation (4-7) together with $T_{18,19}$, to get $Q_{18,19}$. For a given sounding, an estimate of surface temperature is given a zero weight if its weight as obtained from equation (4-7) is not at least half the average of the rest of the weights. In addition, any weight less than 1/30 was set equal to zero. No surface temperature is retrieved if all weights are zero. Otherwise, the surface temperature T_s is taken as the weighted sum of $T_{s,i}$

$$T_s = \left(\sum_i Q_i T_{s,i}\right)/\sum_i Q_i \qquad (4\text{-}8)$$

The entire sounding is also given a weight, W, which reflects the number of independent estimates of sea surface temperature as well as the weight of each estimate

$$W = \left[\sum_i Q_i^2\right]^{1/2} \qquad (4\text{-}9)$$

T_s is weighted by W in generating monthly mean fields. Given a set of sea-surface temperatures T_j and weights W_j for a grid box k, the (weighted) monthly mean sea surface temperature anomaly field $\bar{A}_k^W$ should be produced according to

$$\bar{A}_k^W = \sum W_j(T_j - T_{CLIM,j})/\sum W_j \qquad (4\text{-}10)$$

where $T_{CLIM,j}$ is the Reynolds (1982) sea surface climatology interpolated in time and space to the location of the sounding j. As a consequence of equations (4-7) through (4-10), more optimal use is made of the three window channels for a given sounding, and relatively clear and/or dry soundings are weighted more than cloudy or humid ones in generating monthly mean fields. In addition, night-time soundings are given more weight than day-time soundings (not necessarily a good result) because night soundings have 3 independent estimates instead of 2, which tends to increase W, and also because the night-time values of Q tend to be higher in shortwave channels than the day values.

W, the weight for each sounding, equation (4-9), was sent to the workshop along with the corresponding T_s, equation (4-8), so that weighted anomaly fields, equation (4-10), could be produced. Unfortunately, the workshop did not initially utilize the weights provided to them in generating the monthly mean anomaly fields and treated all soundings as having equal weight.

Figure C-3 (see Appendix C) shows the anomaly fields derived by the workshop from data from ships, AVHRR, HIRS and SMMR for December 1981. The small scale noisy nature of the HIRS field is evident. In addition, large spurious warm anomalies are observed in the HIRS field in the vicinity of land and especially in the Gulf of Mexico, the Sea of Japan, and the Yellow Sea. Similar characteristics are found in the March 1982 anomaly field generated using this method. The errors close to land were found to be the result of the inadvertent use of a $4^o \times 5^o$ topography which was used to define land and water in the retrieval program. This land-water flag is used to specify the surface emissivity, which is taken as higher over ocean than over land. Using an emiscivity with too low a value in analysis of data off the coasts of continents resulted in spuriously warm retrieved surface temperatures. It was also observed i.. Workshop III that the small scale noise in the HIRS fields is greatly reduced by applying a 9 point smoothing to the anomaly fields

$$\bar{A}_k^s = \sum S_{kl} \bar{A}_l^w / \sum S_{kl} \qquad (4\text{-}11)$$

where grid points l are adjacent to k and S_{kl} is a smoothing matrix. As a result of this, the workshop generated some statistics for smoothed anomaly fields derived from all sensors and ships. This produced some interesting findings which will be shown later.

C. MODIFICATIONS MADE TO REPROCESS MARCH 1982 AND PROCESS JULY 1982 - HIRS VERSION 2

As a result of the findings on the HIRS fields originally produced for December 1981 and March 1982, a number of further modifications were made to the program. The first change involved simply replacing the $4^o \times 5^o$ topography by a $1^o \times 1^o$ topography. This eliminated the large errors near the coasts. The second change involved the processing of more data to reduce the effects of random noise. It was found that retrievals performed in each of the three quadrants having the largest brightness temperatures (see Figure 4-1) produced geophysical parameters of comparable accuracy to those obtained only from analysis of data from the warmest quadrant as seen by the 11 μm window. This tripling of the data density did little to change the sea-surface temperature anomaly patterns, but greatly reduced the random noise component. In addition, improved fields of ground temperature and ice and snow cover resulted from the increased data density.

A consistency check was also added to the sea surface temperatures $T_{s,i}$ obtained for a given sounding with channel i. Ir the case of three estimates of sea surface temperature for a given sounding, Q_i was set equal to zero if T_{si} was different from T_s, computed in equation (4-8) using Q_i, by more than 1.5^oC. In this case, T_s was recomputed using equation (4-8) with

$Q_i = 0$. In the case of two estimates of $T_{s,i}$ for a given sounding, the less reliable sounding was eliminated if the difference between the two soundings was greater than 3°C. The less reliable sounding was defined as the one differing the most from climatology. This does not eliminate large differences from climatology as long as the result is supported by more than one channel for a given sounding. This system, called HIRS version 2, was used to reprocess March 1982 and process July 1982 data. As in the system described in Section A, equations (4-1) through (4-9) were used and temperatures and weights were sent to the workshop. Comparison of results for December 1981, March 1982, and July 1982 with those produced from ship data are shown in the next section for HIRS fields and other fields in the workshop.

D. COMPARISON OF RETRIEVED ANOMALY FIELDS WITH THOSE OBTAINED FROM SHIP DATA

One way of judging the accuracy of sea surface temperatures retrieved by various sensors is to compare characteristics of the monthly mean anomaly fields derived from the sensors and from ship measurement. Climatology is also treated as a sensor in this comparison. Tables 4-2 to 4-4, taken from values generated by the JPL workshop, show: C, the correlation coefficient; B, the bias (sensor-ship); S, standard deviation; and N, the number of grid point samples ($2^\circ \times 2^\circ$ grid) comparing anomaly fields from a number of sensors with ship fields. Statistics are given for global colocations and also for those in the North Pacific and North Atlantic Oceans. Results are given for the unsmoothed field, and also for 9-point smoothed fields, in which case, both the ship field and retrieved field were smoothed and then compared to each other. All 8 points surrounding a grid point were needed to perform the smoothing. Therefore, only points for which unsmoothed anomalies were available for all surrounding points were included in the smoothed statistics. As a result of this, many ship and XBT observations were dropped from the smoothed fields because these fields have more data gaps, especially in the tropics and southern oceans.

To interpret the significance of standard deviation from ships, an anomaly field produced by a sensor can be considered skillful if its standard deviation from ships is at least as low as that of climatology, which is representative of the ocean signal. Statistical results for December 1981 are shown in Table 4-2. It is interesting to see that climatology differs from ships with a standard deviation of about 0.6°C when no smoothing is applied and about 0.4°C when smoothing is applied. This drop in "signal" is most likely due to noise in the unsmoothed ship field. It is also possible that further deviations from climatology exist in those grid points which are excluded from the statistics because ships did not report in all the surrounding grid points, but it is unlikely that this would explain all the reduction in standard deviation.

Table 4-2. Comparison of Monthly Mean Anomaly Fields with Ships > 5/Cell, December 1981

		Unsmoothed			Smoothed		
		Global	N. Pac.	N. Atl.	Global	N. Pac.	N. Atl.
AVHRR	C	0.76	0.77	0.74	0.91	0.93	0.93
	B	-0.30	-0.44	-0.15	-0.33	-0.43	-0.19
	S	0.50	0.50	0.41	0.28	0.29	0.18
	N	729	376	255	235	127	102
HIRS	C	0.21	0.29	0.13	0.45	0.56	0.04
	B	0.13	0.31	0.10	0.21	0.21	0.24
	S	0.88	0.89	0.77	0.42	0.45	0.39
	N	729	376	255	235	127	102
SMMR	C	0.21	0.22	0.33	0.40	0.34	0.59
	B	0.72	1.08	0.42	0.71	0.95	0.47
	S	1.17	1.10	1.15	0.79	0.72	0.76
	N	677	361	227	226	126	96
XBT	C	0.63	0.63		C 50	0.50	
	B	-0.03	-0.04		0.24	0.24	
	S	0.84	0.84		0.27	0.27	
	N	158	155		8	8	
CLIM	C	0.00	0.00	0.00	0.00	0.00	0.00
	B	0.03	0.18	-0.14	0.08	0.12	0.01
	S	0.61	0.61	0.55	0.38	0.41	0.35
	N	729	376	255	235	127	102

Table 4-3. Comparison of Monthly Mean Anomaly Fields with Ships > 5/Cell, March 1982

		Unsmoothed			Smoothed		
		Global	N. Pac.	N. Atl.	Global	N. Pac.	N. Atl.
AVHRR	C	0.67	0.52	0.67	0.77	0.58	0.80
	B	-0.36	-0.50	-0.29	-0.44	-0.54	-0.30
	S	0.51	0.48	0.42	0.29	0.29	0.21
	N	795	434	267	368	210	153
HIRS	C	0.10	0.13	-0.01	0.40	0.39	0.43
	B	0.30	0.47	0.16	0.29	0.42	0.12
	S	0.92	0.95	0.84	0.42	0.41	0.35
	N	795	434	267	368	210	153
HIRS Version 2	C				0.55	0.30	0.66
	B				0.29	0.36	0.21
	S				0.31	0.34	0.22
	N				368	210	153
SMMR Night	C	0.24	0.37	-0.05	0.15	0.54	-0.09
	B	-0.21	0.05	-0.76	-0.17	0.13	-0.77
	S	1.11	0.99	1.19	0.79	0.67	0.69
	N	690	392	213	300	200	95
SMMR/Ship Composite	C	0.58	0.57		0.75	0.75	
	B	0.04	0.03		0.07	0.07	
	S	0.47	0.46		0.25	0.25	
	N	438	394		207	203	
VAS	C	0.40		0.50	0.79		0.79
	B	0.90		0.89	0.91		0.91
	S	0.56		0.52	0.26		0.26
	N	109		106	51		51
XBT	C	0.39	0.38		0.70	0.70	
	B	-0.27	-0.29		-0.47	-0.47	
	S	0.89	0.91		0.35	0.35	
	N	242	227		18	18	
CLIM	C	0.00	0.00	0.00	0.00	0.00	0.00
	B	0.09	0.27	-0.05	0.13	0.29	-0.10
	S	0.52	0.48	0.42	0.35	0.32	0.27
	N	795	434	267	368	210	153

Table 4-4. Comparison of Monthly Mean Anomaly Fields with Ships > 5/Cell, July 1982

		Unsmoothed			Smoothed		
		Global	N. Pac.	N. Atl.	Global	N. Pac.	N. Atl.
AVHRR	C	0.62	0.59	0.66	0.70	0.63	0.84
	B	-0.48	-0.37	-0.57	-0.35	-0.17	-0.46
	S	0.79	0.93	0.60	0.52	0.62	0.37
	N	644	320	258	274	117	157
HIRS Version 2	C	0.49	0.43	0.51	0.78	0.52	0.85
	B	-0.07	0.01	-0.08	0.09	0.14	0.04
	S	0.69	0.72	0.62	0.38	0.39	0.36
	N	662	337	259	327	170	157
HIRS Version 2 Weighted	C	0.52	0.45	0.56	0.79	0.45	0.88
	B	-0.37	-0.31	-0.37	-0.25	-0.23	-0.27
	S	0.69	0.74	0.61	0.38	0.43	0.30
	N	662	337	259	327	170	157
SMMR Night	C	0.46	0.54	0.32	0.55	0.62	0.66
	B	-0.43	-0.22	-0.88	-0.69	-0.39	-1.07
	S	0.97	0.87	0.93	0.60	0.48	0.51
	N	522	278	193	230	127	103
SMMR/Ship	C	0.76	0.74		0.86	0.86	
	B	-0.04	-0.06		-0.10	-0.10	
	S	0.53	0.54		0.27	0.27	
	N	316	282		137	137	
VAS	C	0.49		0.46	0.42		0.42
	B	0.48		0.50	0.55		0.55
	S	0.46		0.45	0.22		0.22
	N	92		88	38		38
XBT	C	0.58	0.55				
	B	-0.22	-0.23				
	S	0.94	0.96				
	N	154	146				
CLIM	C		0.00	0.00	0.00	0.00	0.00
	B		0.67	0.26	0.70	0.96	0.40
	S		0.73	0.69	0.63	0.50	0.64
	N		338	259	336	179	157

One reason the global deviation from climatology is small is that extensive areas have deviations very close to zero. On the other hand, large spatially coherent areas of anomalies > 0.5°C also exist, as evident in Figure C-3a showing the ship anomaly field for December 1981. A much better indicator of skill is the correlation of the sensor anomaly field with that of ships. This correlation is high if the anomalies lie in the right place and are of the right sign. The correlations are reduced by random noise, especially if the noise is of comparable magnitude to the signal. In addition, large areas of small anomaly will also reduce the correlations because the magnitude of the signals in these areas is comparable to noise. Climatology, by definition, has zero anomaly correlation and zero skill.

As seen in Table 4-2, smoothing has reduced the noise and increased the correlation coefficients for all cases (except XBT which contains only 8 points in the smoothed field). Part of this is due to random noise reduction in the ship field and part due to noise reduction in the field being compared to ships. The AVHRR field shows skill both in the standard deviation sense and in the correlation sense in the unsmoothed fields, while both the HIRS and SMMR fields show poor skill in the unsmoothed fields. It is interesting to note the XBTs also appear noisy in the unsmoothed fields with regard to standard deviation, but not correlation coefficient. This may be in part due to noise, but it is also due to the fact that the portion of the North Pacific Ocean measured by XBTs had a larger anomaly than the North Pacific Ocean as a whole. In the smoothed fields, AVHRR shows remarkable skill in both categories. In addition, the statistics for HIRS have improved greatly so as to show moderate skill in correlations and noise level. It should be noted that these statistics are for the unweighted HIRS2 field. The weighted field (not shown) provides better visual agreement with the ship field, but statistics were not initially computed using the weighted field. The SMMR field statistics also improved to show some skill in anomaly correlation, but the noise levels are high compared to the signal.

While AVHRR appears extremely good statistically, some aspects of the anomaly field, shown in Figure C-3b, are disturbing. In particular, the region from about 75°E to 155°E, 5°N to 5°S, shows a coherent warm anomaly of between 0.5° and 2.5°C, which is not supported by the few ship measurements in the area. In fact this area did not enter into the statistics for two reasons: first, the scarcity of ships in the area, and secondly because of the "SMMR Mask" (see Figure C-3d) which was applied to statistics of all fields so similar areas could be compared statistically. This mask is applied to SMMR data because accurate SMMR retrievals cannot be obtained less than 600 km from land. A second problem is that the AVHRR data has regional biases. Table 4-2 shows a cold bias in both the Atlantic and Pacific Oceans, with the Pacific Ocean bias being about 0.2° larger. Figure C-3b shows the biases to be largest in the high latitudes, which represent the coldest, driest air. On the other hand, the western Pacific tropical area previously mentioned, which is the one with the highest water vapor content, was spuriously warm. It is possible that the algorithm used to correct the AVHRR soundings for water vapor undercorrects the effect for low water vapor content and overcorrects in the case of high water vapor content. This is consistent with theoretical studies showing that the effects of water vapor content on brightness temperature grow in less than a linear fashion.

Statistical results for March 1982 are shown in Table 4-3. This table includes results of the reprocessed March 1982 HIRS data, as described in Section B, called HIRS version 2 in the table. Only statistics for the smoothed version 2 data were generated. Also included in the table are statistics for the field derived using SMMR data and ship data simultaneously, and for the VAS retrievals, which were primarily in a small area in the North Atlantic Ocean. The SMMR/SHIP composite field was produced only in the Pacific Ocean because of calibration difficulties with the SMMR in the Atlantic Ocean.

Comparison of ships with climatology shows smaller anomalies in March 1982 than in December 1981. Indeed, the signal in the North Pacific and North Atlantic Oceans is on the order of 0.3°C. Statistics for AVHRR in March 1982 are similar to those of December 1981, but the correlations are reduced somewhat, most likely because the signal is reduced. Statistics for the HIRS2 are again similar to those of December 1981. It should be noted that HIRS version 2 is significantly better than HIRS, both with regard to standard deviation and anomaly correlation.

Smoothing has reduced the noise and increased the correlation coefficients for all cases. Part of this is due to random noise reduction in the ship field and part due to noise reduction in the field being compared to ships. The unsmoothed AVHRR field in March 1982, shown in Figure C-4b, shows marginal skill in the standard deviation sense and good skill in the correlation sense. Statistics for the unsmoothed March HIRS version 2 fields were not generated at the workshop. It is interesting to note the XBTs also appear noisy in the unsmoothed fields with regard to standard deviation and correlation coefficient.

In the smoothed fields, AVHRR shows increased skill in both categories. The statistics for the smoothed HIRS2 fields are almost as good as those of AVHHR with regard to standard deviation, but the correlations are considerably lower. It should be noted that these statistics are for the unweighted HIRS2 field shown in Figure C-6. The weighted field, shown in Figure C-6b, provides better visual agreement with the ship field, but statistics were not computed using the weighted field. The weighted SMMR field is much more noisy, but shows some correlation skill in the North Pacific Ocean. An additional field, produced using both SMMR data and ship data, shows good agreement in the vicinity of ships as expected. Surprisingly, the statistics are only marginally better than those of AVHRR or HIRS2, which did not have the benefit of including the ship data used to verify the fields. VAS shows good results for that portion of the North Atlantic Ocean where observations were made but has a disturbingly large bias of 0.9°C too warm.

Figure C-4a indicates that March 1982 had only small areas showing more than 0.5° deviation from climatology, especially in the North Atlantic Ocean. In the North Pacific Ocean, there are small cold anomalies centered at about 160°W, 35°N and 175°E, 28°N and a small warm anomaly about 115°W, 20°N. The weighted HIRS2/MSU field likewise shows small anomalies in the North Pacific Ocean, of the correct sign, centered at the appropriate locations. The anomaly centered at 35°N is weaker than in the ship field, and is less apparent in the HIRS2 field because it is between 0 and -0.5°, showing up as white in the picture, but on the cold side of the 0° contour. The small anomalies in the Atlantic Ocean are in almost perfect agreement with those in the ship field. The AVHRR field, on the other hand, indicates extensive areas of cold

anomaly in both the North Atlantic and Pacific Ocean, sometimes exceeding 1.5° in magnitude. This feature is consistent with the cold bias of 0.3°C to 0.5°C indicated in Table 4-3 for AVHRR. The weighted HIRS2 field, like the ship field, shows a warm anomaly in the Bay of Bengal, which is absent in the AVHRR field, and an area of negligible anomaly along the equator from 75°E to 155°E. In contrast, the AVHRR field has a very large spurious warm anomaly in this region. Agreement of all fields in the southern hemisphere is reasonable, but the AVHRR warm anomalies are larger than those indicated by HIRS2/MSU or the ships. The unweighted HIRS2 field is somewhat warmer than the weighted field and has essentially no anomalies in the North Pacific Ocean. It is not surprising that small correlation coefficients were found in the North Pacific Ocean for the unweighted HIRS2 version 2 field.

Statistics for July 1982 are shown in Table 4-4. For this month, statistics were generated for both the weighted and unweighted HIRS2 version 2 fields. As observed from looking at the statistics comparing climatology with ships, July 1982 was much more anomalous than other months in the workshop with a standard deviation of about 0.6°C about a cold bias (Table 4-4 shows climatology-ships) of 0.96°C in the North Pacific Ocean and 0.4°C in the North Atlantic Ocean. Therefore signals are large and one expects larger correlations between retrieved anomaly fields and ship anomaly fields. Correlations for AVHRR are similar to those in March 1982, but the standard deviations are considerably larger than in the other months. HIRS2 statistics show improved correlation over March 1982, as expected, with standard deviations slightly degraded over those of March 1982. Statistics for the weighted HIRS2 field, relative to the unweighted field, show the weighted soundings have become colder on the average by about 0.35°C. Results have improved slightly in the Atlantic Ocean and degraded somewhat in the Pacific Ocean. SMMR results have improved over previous months, both in the standard deviation sense and in the sense of error correlation. The SMMR/ship field, as expected, shows good agreement with the ships used to produce the field and shows more of an improvement, with regard to standard deviation over the HIRS2 field, which did not have the benefit of including ships, than in March. VAS continues to have good agreement with regard to standard deviation in the small region of the North Atlantic Ocean where colocations with smoothed ships exist. VAS retrievals also continue to have a large warm bias, which is about 0.4°C less than in March 1982.

Figures C-7a, b, and c and C-6c show the retrieved anomaly fields determined from ships, AVHRR, HIRS, and weighted HIRS data. HIRS again shows very good agreement with the ship anomaly fields, which this time are quite large and extensive in both the North Atlantic and North Pacific Oceans. The HIRS field does have a few areas of spurious cold anomaly in July, located mainly within a thin latitude band running from about 15°N to 25°N over most of the ocean, and off the west coast of South America from 15°S to about the equator. These spurious anomalies, which are mostly of the order 0.5° - 1°C, may be due to the effects of aerosols put into the atmosphere by the eruption of El Chichon which occurred in Mexico in April 1982. The errors are amplified in the weighted field, which is colder in general. The effects of this eruption on the determination of sea surface temperatures are much more evident in the AVHRR anomaly pattern which shows a large block of spurious cold anomaly from 10°N to 35°N running across the entire oceanic area, with magnitudes of the order of 2°C.

As shown in Figures C-6 and C-7, the weighted HIRS2 fields tend to be slightly cooler than the unweighted fields. The same result was found for December 1981. The weighted fields show better agreement with ship fields in December 1981 and March 1982. July 1982 is a special case where spurious cold anomalies already existed, possibly due to effects of the El Chichon eruption, and results were slightly worse in the weighted fields.

Weighted fields count clear cases more than cloudy ones and night somewhat more than day. A simple explanation for weighted fields being colder would be the heavier weight placed on nighttime soundings. To test this, weighted fields were produced using only nighttime data and using only daytime data and compared to the unweighted fields at the appropriate time of day. This comparison showed the weighted fields again to be cooler than the unweighted ones in both cases, with the effect being larger at night. It appears then that sea surface temperature soundings in an area are warmer under cloudy conditions than under clear conditions. This implies the effects of clouds are somewhat over-corrected in the system by the use of equations (4-2) through (4-6).

E. SUMMARY AND FUTURE PROSPECTS

Prospects for improved sea surface temperature fields obtained from sounders such as HIRS2/MSU appear bright. The current test shows HIRS2/MSU fields to be statistically comparable to those of AVHRR in March 1982 and superior in July 1982, where the El Chichon eruption had drastic consequences on the AVHRR data, but much smaller effects on HIRS2/MSU data. Errors in the AVHRR data tend to be systematic and spatially coherent, providing spurious warm anomalies in the most humid areas of the tropics and possibly spurious cold anomalies at high latitudes. HIRS2 errors tend to be more random in nature and resultant fields are improved considerably by averaging more data. Our plans in the near future involve reprocessing all data at a roughly 60 km spatial resolution, corresponding to 4 x 4 sets of HIRS2 spots broken up into 2 x 2 quadrants. We have currently completely vectorized the retrieval code for use on the CYBER 205 computer and one-day global retrievals at 60 km resolution takes only 10 minutes CPU time. We feel this is the finest resolution with which retrievals can be done using HIRS2 data because of the need for at least four spots in a quadrant to allow for distinct separation of radiances into fields of view for the purpose of cloud filtering. These higher resolution retrievals should produce much better anomaly fields both because of the reduction of random errors by a larger sample, and also because the individual retrievals will become more accurate due to increased homogeneity in the sounding area both with regard to clouds (assumption of a single cloud formation is implicit in the cloud filtering algorithm) and the sea surface temperature itself.

Hardware modifications in the near future will also improve results. The HIRS2 to be flown starting on NOAA-H (~1987) will have a modification in its channel 17, now centered at 2360 cm^{-1}. The current channel monitors emission from the upper stratosphere and is highly affected by non-local thermodynamic equilibrium. Consequently little use has been made of observations in this channel either operationally or experimentally. The new frequency will be at 2420 cm^{-1} and can be used together with channel 18, at 2500 cm^{-1}, to get

improved sea surface temperatures during the day. The new combination is superior to the current channel 18,19 combination for several reasons. The new channel 17 is less sensitive to solar radiation than 19; therefore, the effect of solar radiation is smaller. Also, channel 17 is insensitive to water vapor (atmospheric N_2 is the biggest absorber), while channel 19 has moderate sensitivity to water vapor, which sometimes causes problems in tropical areas during the day. The spurious cold anomaly in the central Pacific Ocean in March, derived from HIRS2 data, in fact appeared only in daytime soundings. This problem will not occur with the new channel. Another significant improvement in the new channel 17 is that its bandpass is about 50 cm^{-1} rather than 200 cm^{-1} in channel 19. This makes the concept of "effective channel central frequency," which is used in converting back and forth from brightness temperature to radiance, more meaningful. The broader bandpass of channel 19 introduces an extra source of noise in the data.

Perhaps the ultimate in measurement of sea surface temperatures will come from an advanced infrared sounder, AMTS, described in Chahine et al. (1984), which may fly on polar orbit in the 1990's. This instrument has a number of "super-window" channels with atmospheric transmittance ≈0.98, even in very humid atmospheres, and 10 km spatial resolution with contiguous coverage. Simulation studies show soundings with about a 40 km resolution can be performed in up to 90% cloudiness with instantaneous accuracy of about 0.4°C. It is expected that monthly mean fields with accuracies of the order of 0.2°C can be obtained at a spatial resolution of about 50 km. This will go a long way toward meeting the needs of monitoring sea surface temperatures, at least in the climatological sense, and will make possible detailed studies relating the effects of sea surface temperatures anomalies in the tropics on atmospheric circulation.

SECTION V

SEA SURFACE TEMPERATURES FROM VAS MSI DATA

J. Bates

University of Wisconsin
Madison, Wisconsin

A. SST INTERCOMPARISON WORKSHOP

1. Introduction

The results of the SST intercomparison workshop series (JPL 1983) are the first examination of monthly mean SSTs derived from MSI data provided by the VAS instrument on the GOES series satellites. While VAS instruments are currently only on the U.S. geostationary satellites, limiting coverage to the western hemisphere, it is hoped that the success of VAS will encourage the European Space Agency, Japan, and India to consider installing a VAS instrument on their future geostationary satellites. Because the procedure to derive SSTs from VAS data is still in the developmental stage, several changes in the procedure were made between the processing of data for March 1982 and processing the data for July 1982. The most significant change was the use of the three window channel algorithm (3.9, 11.0, and 12.6 μm) in the processing of the July data as opposed to the use of only the two window channel (11.0/12.6 μm) algorithm for the March data. Initially only the two channel algorithm was used in order to extend the analysis of SST into areas of sunglint in the tropics. However, the analysis of the March data showed that little additional data was gained by doing this. In addition, further satellite/buoy matches indicated that the triple window channel algorithm showed a smaller standard deviation than the two window channel algorithm and was less sensitive to the effects of volcanic aerosol contamination and low level inversion conditions. This is due to the smaller brightness temperature attenuation by aerosols and water vapor at 3.9 μm than at 11.0 and 12.6 μm. Thus, the decision was made to use the best product (i.e., the three window channel algorithm) for processing the July data.

2. March 1982 Results

Two large regions were chosen for analysis of VAS data from GOES-East, one in the western North Atlantic and one in the eastern Tropical Pacific. Since ship observations of surface layer temperature provide the only long-term climatology of SST, Reynolds (1982) climatology has been used as a standard from which satellite SST monthly mean anomaly fields were produced. Data from all sensors were binned on a two by two degree latitude/longitude grid for each month. SMMR data were required to be more than 600 km from land in order to avoid contamination from land. Thematic contour charts of sensor anomaly fields from climatology for March are shown in Figure C-8 (see Appendix C). VAS, AVHRR, and ship data all show a pattern of cold to warm to cold to warm proceeding southeast off the U.S. east coast; however the

VAS data have a warm bias of 0.5 to 1.0°C. In the South Pacific, the VAS data show only a slight warm bias and again are highly correlated with the AVHRR, ships, and XBTs. In particular, the VAS and AVHRR thematic contour anomaly charts show similar patterns with warm water along the coast from 20° to 30°S and extending to the west along 30°S, a pool of cold water along the coast from 0 to 10°S, another cold anomaly offshore, and near normal conditions elsewhere. The HIRS data show generally weaker anomaly patterns and a warm bias near the coastlines due to problems in accurately specifying the land/water boundaries (Susskind, personal communication). The HIRS data do show a warm anomaly along 30°S in the eastern South Pacific and a large warm anomaly in the western North Atlantic. Little correlation in patterns is found between the VAS and the SMMR product.

Table 5-1 summarizes the cross correlation statistics for each satellite verses ship-of-opportunity measurements for March 1982. VAS estimates of SST show a warm bias relative to ships for all regions ranging from +0.35 to 1.73°C. The largest biases (1.73°C and 1.05°C) are found with the lowest numbers of matches (21 and 53) and also occur at the largest satellite zenith angles (North Pacific region 20-56°N and South Pacific regions 20-56°S). This indicates that the magnitude of the warm bias for the two channel algorithm may increase with increasing satellite zenith angle but also suggests that noisy ship data may be partly responsible for some of the bias.

The uniform warm bias in all regions, however, indicates a diurnal sampling bias and a possible bias in the matches used to tune the empirical algorithm. Satellite/buoy matches are continuing to be collected in order to ensure that a seasonally and geographically diverse set of matches is used to update the coefficients for the empirical algorithms. It does appear though that the diurnal sampling of VAS data is largely responsible for the warm bias. VAS data were generally processed at 1530 and 1830 GMT (1030 and 1330 LST at the GOES-East subpoint) and only cloud-free observations were used. Thus, VAS SSTs might be expected to have a warm bias relative to estimates of SST that average day and night data. Diurnal heating of the ocean skin temperature as observed by satellite infrared data has also been reported by Strong (1984) and by Deschamps and Frouin (1984). Future intercomparisons must take into account possible diurnal sampling biases of each sensor.

Additional cross correlation statistics for March show VAS with a scatter relative to ships of 0.79-1.24°C. The statistics show VAS well correlated with ships, and shows regional correlations very similar to those of the AVHRR. The one exception is the far South Pacific region (20-56°S). This again is the region of fewest matches and thus should be given little weight.

3. July 1982 Results

In the thematic anomaly charts for July (Figure C-8), the effects of the El Chichon volcanic aerosol are very evident in the AVHRR data as a zonal band of cold anomalies from 10-30°N. VAS data, however, do not show an analagous anomaly in those latitudes. This result is due to differences in the spectral channels of the VAS and AVHRR, differences in the processing

Table 5-1. Cross Correlations of Satellite SST Estimates Versus Ship SST Estimates for March 1982

	Number of Matches				Bias				Standard Deviation				Cross Correlation			
	AVHRR	SMMR	HIRS	VAS	AVHRR	SMMR	HIRS	VAS	AVHRR	SMMR	HIRS	VAS	AVHRR	SMMR	HIRS	VAS
Global	4322	1972	—	425	-0.06	-0.01	—	+0.63	0.81	1.20	—	0.96	0.58	0.25	—	0.59
North Pacific (0-56°N)	1563	815	—	127	-0.26	-0.05	—	+0.52	0.67	0.99	—	0.92	0.64	0.29	—	0.61
North Pacific (20-56°N)	1033	529	1054	53	-0.39	-0.01	+0.54	+1.05	0.65	1.03	1.07	0.89	0.60	0.36	0.28	0.63
Tropical Pacific (20°N-20°S)	837	412	858	165	+0.10	-0.22	+0.23	+0.20	0.73	0.87	0.93	0.90	0.13	0.08	0.03	0.10
South Pacific (20-56°S)	535	202	541	21	+0.24	+0.55	+0.05	+1.73	0.78	1.19	1.11	1.24	0.42	0.08	0.28	-0.39
South Pacific (0-56°S)	984	328	—	112	+0.26	+0.17	—	+0.52	0.80	1.14	—	1.20	0.29	0.11	—	0.23
VAS Pacific Region (14°N-30°S)	178	81	—	181	+0.06	-0.16	—	+0.35	0.89	0.91	—	1.06	0.23	-0.08	—	0.03
Global AVHRR El Chichon Mask	2214	1088	2229	211	+0.03	+0.12	+0.20	+0.55	0.86	1.11	1.04	1.12	0.48	0.29	0.20	0.41
North Atlantic (0-56°N)	715	315	—	186	-0.33	-0.92	—	+0.76	0.61	1.18	—	0.79	0.58	-0.02	—	0.65

algorithms, and differences in the average viewing geometry. The VAS, SMMR, and ship data all show a warm anomaly in the eastern tropical Pacific.

In the North Atlantic VAS region, the VAS data appears to be slightly warmer than the ship data, but again shows similar patterns. The VAS and AVHRR data show some correlation near the coast of the U.S., but meaningful comparisons between the two are hampered by the volcanic aerosol contamination in the AVHRR data. The anomaly patterns are much the same in a comparison of the VAS/SMMR data, however, the SMMR data is contaminated by "cold" instrument warmup noise in much of the North Atlantic (Milman, personal communication). In the VAS region of the Pacific, the VAS, SMMR, and ship data all show warming. Here, the VAS and SMMR data show a high correlation with a pattern of warm anomalies along the coast and extending westward along the equator. In contrast, the HIRS data, while not showing any consistent bias in the El Chichon region, does show a large cold anomaly in this region.

Cross correlation statistics for July 1982 are summarized in Table 5-2. VAS SSTs again show a slight warm bias in all regions. The very large warm bias at large local zenith angles evident in the March 1982 data, however, has been eliminated by the use of the three window channel algorithm. Little bias is evident in the region of the El Chichon volcanic aerosol (approximately 10-30°N). In this region, the AVHRR data show a cold bias of 0.50-0.75°C relative to ships. The VAS standard deviations are also generally smaller in July than in March due to the use of the three window channel algorithm. The cross correlations of VAS data with ship data, however, are much weaker in July than March.

After SST Intercomparison Workshop III, additional cross correlation tables were generated to try to answer some of the questions raised during the workshop. Most important to the interpretation of VAS data was the stratification of AVHRR data into day and night so that the daytime only VAS data could be directly compared to daytime only AVHRR data. Although the new cross correlation tables are masked to include only data greater than 600 km from land (to normalize the comparison between SMMR and the other sensors, but greatly reducing the number of VAS/ship matches), some trends are clearly evident. In March 1982, AVHRR shows a global average day minus night difference relative to ships of +0.43°C. This reduces the VAS minus AVHRR day bias to +0.23°C. The VAS verses ship biases remain unchanged since ships measure SST at some depth beneath the surface and are relatively insensitive to diurnal heating of the ocean skin. In July, on a global basis, the AVHRR day product is 0.43°C warmer than ships while the AVHRR night product is 0.72°C colder than ships. There is no discernable bias between AVHRR day SSTs and VAS SSTs outside the El Chichon zone (i.e., in the South Pacific and North Atlantic), while within the El Chichon zone (the mid-Pacific) AVHRR day is 0.69°C colder than VAS and 0.50°C colder than ships. These data clearly show that the diurnal heating of the ocean skin is being detected by VAS and AVHRR, and demonstrates that most of the VAS warm bias relative to the other sensors is due to this diurnal variability.

Table 5-2. Cross Correlations of Satellite SST Estimates Versus Ship SST Estimates for July 1982

	Number of Matches				Bias				Standard Deviation				Cross Correlation			
	AVHRR	SMMR	HIRS	VAS	AVHRR	SMMR	HIRS	VAS	AVHRR	SMMR	HIRS	VAS	AVHRR	SMMR	HIRS	VAS
Global	3962	1826	—	437	-0.54	-0.18	--	+0.60	0.90	1.08	—	0.85	0.44	0.38	—	0.26
North Pacific (0-56°N)	1368	708	--	116	-0.69	+0.26	—	+0.91	0.95	0.89	—	0.80	0.41	0.46	—	0.17
North Pacific (20-56°N)	514	221	—	26	-0.18	+0.11	—	+0.40	0.64	1.13	—	1.25	0.50	0.24	—	-0.10
Tropical Pacific (20°N-20°S)	779	366	—	165	-0.69	+0.10	—	+0.77	0.83	0.83	—	1.00	0.30	0.27	—	0.07
South Pacific (20-56°S)	958	480	—	51	-0.54	-0.31	—	+0.61	0.98	0.92	—	0.50	0.46	0.44	—	0.11
South Pacific (0-56°S)	883	359	—	126	-0.23	+0.06	—	+0.50	0.67	1.03	—	1.05	0.41	0.26	—	0.00
VAS Pacific Region (14°N-30°S)	162	104	—	174	-0.38	+0.16	—	+0.68	0.81	1.10	—	1.08	0.25	0.05	—	0.01
Global AVHRR El Chichon Mask	2305	1112	—	216	-0.20	+0.02	—	+0.49	0.77	1.08	—	0.90	0.49	0.41	—	0.26
North Atlantic (0-56°N)	695	324	—	195	-0.81	-1.06	—	+0.49	0.87	1.06	—	0.67	0.38	0.21	—	0.40

B. EVALUATION OF OTHER PRODUCTS

1. AVHRR

The AVERR MCSST is the only operational satellite SST analysis currently and is the most accurate and consistent product evaluated at the workshop series. As with all SST data sources, care and understanding must be used when evaluating and applying this data. Studies such as that by Legeckis and Pichel (1984) are particularly useful in interpreting the weekly MCSST analyses. Users must also understand the nature and variability of ocean surface skin temperature measurements as opposed to ship bulk surface layer measurements. For example, the MCSST analysis for March 1982 has been criticized for showing a warm anomaly along the equator from the western Pacific into the western Indian Ocean; an area where ship climatology shows little monthly variability. The AVHRR day-night thematic contour analysis (Figure C-9), however, shows that this warm anomaly may be the result of diurnal warming of the ocean surface. In fact, the AVHRR day-night analyses show a distinct diurnal pattern of solar heating from December 1981 to March 1982 to July 1982. In December 1981, a consistent zonal band of warm daytime SST anomalies is found from about 30-50°S, in the southern (summer) hemisphere. In March 1982, the warm anomaly has become more diffuse and shows the largest anomalies on the equator. By July 1982, the warm anomaly evident as a zonal band in the northern (summer) hemisphere. Diurnal variability of the oceans skin is being measured by satellite sensors, as is evident from the analysis of AVHRR day-night measurements.

2. SMMR

The problems with the SMMR SST product are largely due to instrumental difficulties. The SMMR calibration biases are large and vary in time and space, and sidelobe interference requires observations to be greater than 600 km from land. In spite of these difficulties, SMMR analyses of the Pacific and Indian Oceans appear reasonable. Unfortunately, the calibration problem makes it difficult to evaluate the problem of microwave emissivity changes of the ocean surface with wind speed, while the land mask restricts analysis of the important boundary currents. The SMMR/ship product is an improvement on SMMR alone, but it does not take full advantage of all the different sensors for measuring SST.

3. HIRS/MSU

Evaluation of the HIRS/MSU product is difficult because of changes in the product from one time to the next and because the data were presented late. The HIRS/MSU anomaly patterns generally look noisy and weaker than the anomaly patterns of the other sensors. In March 1982, the HIRS/MSU shows no correlation with any of the other products and a standard deviation from climatology of about 1°C. The July 1982 statistics are better, but the anomaly patterns are inconsistent, showing an overall cool bias. Particularly troublesome is a cool anomaly in the eastern Equatorial Pacific where all the other sensors show a warm anomaly.

C. RECOMMENDATIONS

1. Improvements in Infrared Sensors

Recent theoretical and empirical studies of the infrared portion of the earth's spectrum have revealed that neither VAS nor AVHRR have the optimal channel selection for SST detection. Studies are now underway to determine which window regions using a filtered radiometer would yield the most accurate SSTs. In the long term, though, an infrared spectrometer interferometer instead of a filtered radiometer will be a much better instrument since it would permit use of all portions of the infrared window regions to be utilized.

2. A Combined Product

Efforts should begin on a combined satellite SST product that takes advantage of the benefits of each sensing system discussed in the workshop series. Such an approach should use the raw data from each instrument, not just the finished products such as the SMMR/Ship composite. The McIDAS system has the capability of processing raw data from all sensors used in the workshop series. It is time to begin a program to produce an operational SST analysis.

3. Research Panel on SST Sensing

A research panel to set research program goals, evaluate present systems, and recommend areas for further study should be set up under the direction of NSF or other appropriate agency. This panel should coordinate efforts between ongoing ocean research programs and the remote sensing community. This panel could also serve as the focus for the development of a combined SST product.

SECTION VI

BLENDED SST FIELDS USING COMBINED SMMR/SHIP DATA (SUMMARY OF TECHNIQUE)

T. Wilheit and D. Han

NASA/Goddard Space Flight Center
Greenbelt, MD

A. INTRODUCTION

All remote sensors have bias problems which vary in space and time, albeit rather slowly. The SMMR can in this regard be considered a pathological example of a more general truth. Even ship measurements have a token bias of the order of a few tenths of a degree caused by heating of the thermistor by the hot engine room environment. This ship bias can be neglected if one dealt in SST anomaly (departure from climatology) since ships with a similar bias are the principal source of the data used to generate the climatology. The ships, however, are very poorly distributed globally, and individually represent very noisy measurements. Each remote sensor has its own distribution of data as well. The infrared measurements are very sparse in cloudy areas; the SMMR has coverage limitations due to the interference of land areas and only half-time operation. If one simply averaged the data from these various sources, the combination of the biases and varying sampling would introduce artifacts into the analyzed product which would reflect the sampling and which could be quite misleading. What is needed is an analysis scheme which uses the strength of each type of measurement to compensate for the weakness of the other. In particular, the remote sensors provide reasonable estimates of gradients of SST over length scales greater than the sensor resolution but smaller than hemispheric. Ships can be considered unbiased but are poorly distributed on small scales except in the densest shipping lanes. An analysis scheme based on a suggestion by Holl (1981) has been developed which exploits just this approximately complementarity to provide an improved SST analysis. The resulting accuracy appears to be in the required ~0.5°C range for the particular case of using SMMR and ship data to produce two degree latitude by two degrees longitude monthly analyses. Proper use of other data sources could only improve this product. Moreover, it could easily be argued that the mathematics used in this analysis technique are not particularly sophisticated or even rigorous and a more precise treatment may be of benefit. However the technique is very precisely targeted to the problems actually observed in the measurements, and extreme care must be taken, in any attempt to improve the mathematical foundation of the technique, not to lose sight of the measurement realities with which the technique is designed to deal. It could also be argued that biases of the sort observed here are inherent to all currently available remote sensing approaches to the measurement of any geophysical variable, and that the SST case studied here is only one of the simpler examples of a more general problem.

B. DESCRIPTION OF THE TECHNIQUE

Consider an analysis algorithm as depicted in Figure 6-1. This analysis algorithm accepts measurement values with associated uncertainties at the grid points of the field. It also accepts values for the first and second derivatives of the field in finite difference form, again with associated uncertainties. If there are enough values of the field and its derivative specified, then the field is overdetermined and the analysis algorithm derives a minimum weighted square error solution as the resultant field. An associated uncertainty field is a by-product of this computation. An analysis technique of this form is the basic building block of the Bias Removal Analysis Technique (BRAT). The specific finite differences used are:

Differences of adjacent cells row-wise:

$$R(i,j) = F(i+1,j) - F(i,j)$$

Differences of adjacent cells column-wise:

$$C(i,j) = F(i,j+1) - F(i,j)$$

Differences of adjacent cells diagonally (both ways):

$$D1(i,j) = F(i+1,j+1) - F(i,j)$$

$$D2(i,j) = F(i+1,j-1) - F(i,j)$$

Two-space differences both column and row-wise:

$$R2(i,j) = F(i+2,j) - F(i,j)$$

$$C2(i,j) = F(i,j+2) - F(i,j)$$

Finally, the Lambertian (a second difference operator):

$$L(i,j) = 4F(i,j) - F(i+1,j) - F(i-1,j) - F(i,j+1) - F(i,j-1)$$

The weight applied to any observation is the inverse square of its presumed uncertainty. For present purposes one degree celcius is used

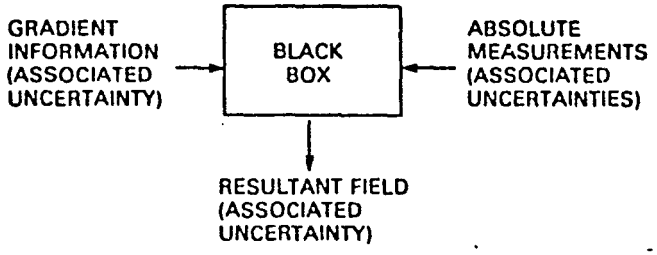

Figure 6-1. Generalized Analysis Algorithm Which is the Basic Building Block of the Bias Removal Analysis Technique.

as the uncertainty for individual SMMR and ship measurements. The weight of any of the differences is similarly the inverse square of the uncertainty which is derived directly from the uncertainties of the associated points in the field from which the finite differences are derived. The resulting problem is to solve for a set of values for F'(i,j) which minimizes the function:

$$E = \sum_{i,j} \left| \frac{[F(i,j) - F^1(i,j)]^2}{W_F(i,j)} + \frac{[A(i,j) - A^1(i,j)]^2}{W_A(i,j)} + \right.$$

$$\left. + \frac{[B(i,j) - B^1(i,j)]^2}{W_B(i,j)} + \ldots\ldots + \frac{[L(i,j) - L^1(i,j)]^2}{W_L(i,j)} \right|$$

where the unprimed quantities are given and the primed are solved for. The $\sum_{i,j}$ denotes summation over all grid points, and the W(i,j) represent data weights. Traditionally, this equation is reduced to a matrix form which results in a formal solution:

$$\bar{S} = \bar{A}\,\bar{F}$$

$$\bar{F} = \bar{A}^{-1}\,\bar{S}$$

If F is not particularly large the equation can actually be solved this way. However, in a practical case the field could be defined on a 50 x 50 array; this would result in the F vector in the above equations having a length of 2,500 and the matrix A would be 2,500 x 2,500. The direct inversion of such a matrix would hardly be a practical matter. One alternative is to solve for F by minimizing the error summation with respect to each element of F individually and to iterate through all the locations until satisfactory convergence is obtained. It can readily be shown that such a procedure is convergent (in a mathematical sense). It was however found that the convergence in the present application was unreasonably slow. Fortunately, a compromise between the two extremes of solving for all elements of F or a single element at a time is possible. It was found that solving for 5 elements at a time provided reasonable convergence and the inversion of a 5 x 5 matrix is a simple matter on any modern computer.

Figure 6-2 illustrates the use of this basic building block in a typical application of BRAT. In this case we have treated the SMMR day and night data as though they come from different sensors since the bias and drift problems are independent on the day and night portions of the orbit. In principle, other sensor types could be included at this level; each sensor should be self-consistent as far as bias and drift are concerned so this same day/night separation would seem appropriate for any current space-borne remote sensor. At this level, no derivative information is available so climatology is used with an extremely small weight (10^{-6}) simply to prevent numerical problems.

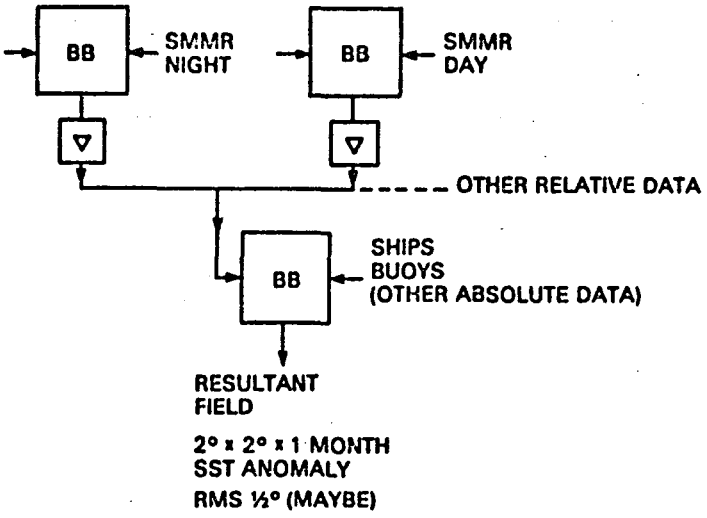

Figure 6-2. Application of the Basic Building Block in the Bias Removal Analysis Technique

Each application of the building block of this level results in a sea surface temperature anomaly field with an associated uncertainty. Each of these resultant SST fields is differentiated and the weights of the derivatives are determined from the weights of the elements of the SST field. The derivative fields are averaged with their associated weights. The weighted average of the resulting set of derivative fields is used as input to the final application of the building block along with the ship data. In this manner any constant bias in the SMMR or other remotely sensed data is automatically removed, and any slowly changing bias is overpowered in the weighted least square error solution as long as there are enough ship data. Conversely, random noise in the ship data is smoothed out by the derivative constraints provided by the SMMR data. However, any bias in the ship data is passed through the analysis unmodified.

In order to test this bias removal analysis technique (BRAT), we have chosen an area in the Pacific Ocean from 50°S to 50°N and from 13°E to 80°W. We have produced monthly analyses of SST anomaly (with respect to the Robinson-Bauer climatology (Reynolds 1983) with a spatial grid size of 2 x 2 degrees. We have used the day and night observations of the SMMR as different relative sensors and the file of ship observations available from NOAA as the absolute sensors. We have used all beam positions in the SMMR night data but

a restricted set of day data to reduce the impact of ionospheric Faraday rotation on the resulting analysis. This will provide an extremely demanding test of the ability of the analysis to reduce large scale biases since the various SST workshops showed that in this respect the SMMR was the most severely afflicted of the remote sensing techniques examined.

Figure C-10c (Appendix C) shows the results of application of BRAT to the data from July 1980. One can easily see patterns of anomalies which look reasonable. They rarely exceed 2°C in magnitude and are spatially coherent. An exception one might be inclined to question is the cold anomaly extending across the South Pacific which exceeds 2.5°C. Because of the interference of large land areas with the SMMR retrievals, there are large data gaps around the continents. The data gap in the Micronesia area suggests excessive conservatism in protecting SMMR retrievals against this interference.

Figures C-10a and C-10b show analyses for the same period based on ship-only and SMMR-only data respectively. Note that the ship data have large gaps particularly in the Southern Hemisphere. Note also that even where the ship data are dense the SSTs have a great deal of uncorrelated structure suggesting a noisy product. It is particularly worthy of note that the suspicious feature in the South Pacific discussed in the previous paragraph is, in fact, supported in the ship data although there is not nearly enough data to delineate its form.

On the other hand, the SMMR-only product is quite smooth and delineates the anomaly pattern of figure C-10a quite well. However there is a noticeable drift in the absolute value which is particularly noticeable in the North Pacific. This is precisely the sort of error that the bias removal analysis technique is designed to reduce. Quantitative estimates of the quality of these analysis products are difficult. However, estimates have been attempted and suggests an rms error of the order of 0.5°C.

SECTION VII

INTERCOMPARISON OF GLOBAL SST FIELDS DERIVED FROM SATELLITE SENSORS AND SHIP OBSERVATIONS

S. E. Pazan

Scripps Institution of Oceanography
La Jolla, California

A. INTRODUCTION

Near global comparisons have been made between binned forms of SST obtained from different satellite instruments, ship meteorological observations, and the output of a meteorological model. Binning hereinafter means gridding by simple summation of data values in a bin, which in this study was a 2° x 2° box or a 10° x 10° box surrounding a grid node. In the binned comparisons, the question is asked: are the binned data from two instruments drawn from the same population? The first two measures of statistical moments of the populations are used to test the hypothesis that they are.

Comparisons were also attempted between raw forms of the various SST retrievals, using a structure function analysis. The results of this analysis were relatively uninteresting and are therefore omitted for the sake of brevity.

B. DATA SOURCES

Five different types of SST field estimates were available for intercomparison. They were: 1. Multi-channel sea surface temperatures (MCSST) from the Advanced Very High Resolution Radiometer (AVHRR); 2. the Scanning Multichannel Microwave Radiometer (SMMR); 3. the High-Resolution Infrared Sounder (HIRS); 4. ship engine intake temperatures collected for marine weather analyses; 5. Fleet Numerical Oceanography Center (FNOC) sea surface temperature monthly mean analyses. The instruments, data collection procedures, and error budgets of the respective SST analyses have been discussed elsewhere in the NASA/JPL SST workshop reports (JPL 1983 and 1984), and will not be discussed further here.

C. ANALYSIS TECHNIQUES

The "pool-permutation procedure" (PPP) described by Preisendorfer and Barnett (1983) has been used to determine whether the first and second moments of SST anomaly fields produced by the different instruments are statistically identical. The PPP measure of the difference between first moments is called "SITES", and the measure of the difference between second moments is called "SPRED." The PPP method allows a rigorous, nonparametric test of the contention that the satellite-derived SST fields are similar to each other

and/or a SST field derived from conventional ship data. The power of the method (detection level) is estimable. Further, the technique is robust for relatively limited data sets (only 4 realizations in our case).

The PPP test statistics values ("SITES" and "SPRED") fall into eight categories; the hypothesis of statistical identity is considered to be shown to be false only if the statistic falls in the last category, the category with the largest SITES or SPRED statistic value. If the PPP test were applied to a completely random set of data fields, any randomly selected permutation would fall into the last category 1 out of every 8 times; in this sense, the test has a confidence level of 7 out of 8, or 88%.

For further discussion of this method, the reader is referred to Preisendorfer and Barnett (1983).

D. RESULTS

The PPP tests were applied to the data sets discussed in Section B. As discussed above, the PPP test statistic values fall into 8 unique values, called "categories."

1. Sensitivity Test

Before drawing any conclusions from the results of PPP intercomparisons it is useful to have some idea of the power of the test, in particular testing the validity of applying this statistical test to a time series only four months long. Tests of the PPP were done using modified versions of the ship data sets, i.e., four month 'test data' sets were constructed using a transformation. $T' = F(\mu,\sigma) + T$, where F represents a random population with a mean of μ and a standard deviation of σ. Several realizations of the PPP test were made for each pair of μ and σ values Table 7-1.

For μ not equal to zero and large σ, the SITES test poorly discriminates between the T and T' fields; that is, the ability of this test to discriminate between fields actually degrades with increasing σ. For instance, given a $\mu = 0.05$, the SITES test was able to discriminate between T and T' for a σ of 0.06, but it was not able to discriminate for a σ of 0.35. On the other hand, the SPRED test discriminates well between data sets differing by a random noise element of the mean bias is small. As the mean bias increases, this test is less capable of discriminating. Thus, when $\mu = 0$ statistical identity is rejected for $\sigma > 0.35$ both in the northern and southern regions. However, if μ is increased to 0.2, σ must be 0.46 before statistical identity is uniformly rejected. For a plausible bias, μ, and random noise, σ, the SPRED test also seems quite sensitive and complements the SITES test well.

a. Comparisons of Global Satellite Data Fields. Results of the global SST comparisons are shown in Tables 7-2, 7-3, and 7-4. Since other results have indicated that AVHRR may have problems with water vapor contami-

TABLE 7-1. Results of PPP Intercomparisons of Ship Injection Temperatures T With an Artifical Data Set T', Where Each Temperature T'(*) = F(μ,σ) + T(*). F is a Random Function With a Mean of μ and a Standard Deviation of σ. These Intercomparisons Were Run 20 Times for 20 Independent Random Realizations and the Number of Times a PPP Test Rejected the Statistical Identity of T' and T is Tabulated vs. the Number of Times a PPP Test Accepted the Statistical Identity of T' and T.

SITES Tests:

Northern Region (30°N - 50°N)
Number of Rejections/Number of Acceptances

μ	σ = .06	0.12	0.17	0.23	0.35	0.46
0.00	6/14	1/19	1/19	6/14	1/19	4/16
0.05	20/ 0	20/ 0	20/ 0	19/ 1	13/ 7	9/11
0.10	20/ 0	20/ 0	20/ 0	20/ 0	20/ 0	19/ 1

Southern Region (50°S - 30°S)
Number of Rejections/Number of Acceptances

μ	σ = .06	0.12	0.17	0.23	0.35	0.46
0.00	3/17	5/15	3/17	3/17	5/15	3/17
0.05	20/ 0	20/ 0	17/ 3	11/ 9	3/17	6/14
0.10	20/ 0	20/ 0	20/ 0	20/ 0	17/ 3	14/ 6

SPRED Tests:

Northern Region (30°N - 50°N)
Number of Rejections/Number of Acceptances

μ	σ = .06	0.12	0.17	0.23	0.35	0.46
0.00	12/ 8	19/ 1	20/ 0	20/ 0	20/ 0	20/ 0
0.05	0/20	2/18	15/ 5	19/ 1	20/ 0	20/ 0
0.10	0/20	0/20	0/20	13/ 7	20/ 0	20/ 0
0.20	0/20	0/20	0/20	0/20	17/ 3	20/ 0
0.40	0/20	0/20	0/20	0/20	1/19	18/ 2
0.60	0/20	0/20	0/20	0/20	0/20	7/13

Southern Region (50°S - 30°S)
Number of Rejections/Number of Acceptances

μ	σ = .06	0.12	0.17	0.23	0.35	0.46
0.00	3/17	7/13	15/ 5	18/ 2	20/ 0	20/ 0
0.05	0/20	2/18	12/ 8	17/ 3	20/ 0	20/ 0
0.10	0/20	0/20	2/18	13/ 7	20/ 0	20/ 0
0.20	0/20	0/20	0/20	1/19	14/ 6	20/ 0
0.40	0/20	0/20	0/20	0/20	5/15	19/ 1
0.60	0/20	0/20	0/20	0/20	0/20	12/ 8

TABLE 7-2. Number of Space Grid Points. Below and Left of the Data Matrix Diagonal, the Number of Space Points in the Data Swarms Used in the PPP Tests are Printed. Row and Column Numbers Indicate These Instruments: 1) AVHRR, 2) SMMR, 3) HIRS, 4) Ship, and 5) FNOC.

a) North Temperate (30°N-60°N, 0°-360°E)

		1	2	3	4
AVHRR	1				
SMMR	2	223			
HIRS	3	1140	234		
Ship	4	984	233	1040	
FNOC	5	517	235	535	525

b) Global Tropics (30°S-30°N, 0°-360°E)

		1	2	3	4
AVHRR	1				
SMMR	2	1250			
HIRS	3	3210	1430		
Ship	4	1110	289	1360	
FNOC	5	936	824	1150	470

c) South Temperate (60°S-30°S, 0°-360°E)

		1	2	3	4
AVHRR	1				
SMMR	2	470			
HIRS	3	2080	470		
Ship	4	192	5	192	
FNOC	5				

TABLE 7-3. Pool Permutation Procedure, SITES Statistics on 2° Binned Data. Test the Hypothesis That Two Datasets are Drawn From the Same Population. Below and Left of the First Data Matrix Diagonal, the Relative Category of the SITES Comparison Between the Observed Data Swarms is Printed; the PPP Test Statistics Fall Into Eight Unique Values, Called "Categories". Above the Right of the Data Matrix Diagonal, T(rue)/F(alse) is Printed, Indicating Whether or Not the Hypothesis is Supported or Rejected, Respectively. Below and Left of the Second Data Matrix Diagonal, the Percentage of the Artificially Constructed Data Swarm Test Values Which Fall Below the Observed Swarms' Test Value is Printed; Above and to the Right of the Second Data Matrix Diagonal, the SITES Test Value for the Observed Data Swarms is Printed.

SITES Statistics

a) North Temperate (30°N-60°N, 0°-360°E)

	Category/Hypothesis					Percent/Test Value				
	1	2	3	4	5	1	2	3	4	5
AVHRR	1	F	F	T	F	1	1.5	1.0	0.32	11
SMMR	2 8		F	F	F	2 88		0.82	1.2	6.3
HIRS	3 8	8		F	F	3 88	88		1.0	9.5
Ship	4 6	8	8		F	4 59	88	88		12
FNOC	5 8	8	8	8		5 88	88	88	88	

b) Global Tropics (30°S-30°N, 0°-360°E)

	Category/Hypothesis					Percent/Test Value				
	1	2	3	4	5	1	2	3	4	5
AVHRR	1	F	F	T	F	1	0.86	0.89	0.63	3.7
SMMR	2 8		F	F	F	2 82		1.3	0.98	3.3
HIRS	3 8	8		T	F	3 82	82		1.0	2.7
Ship	4 6	8	7		F	4 67	82	72		3.4
FNOC	5 8	8	8	8		5 82	82	82	82	

c) South Temperate (60°S-30°S, 0°-360°E)

	Category/Hypothesis				Percent/Test Value			
	1	2	3	4	1	2	3	4
AVHRR	1	F	F	F	1	1.1	1.7	0.60
SMMR	2 8		F	T	2 83		1.3	1.1
HIRS	3 8	8		F	3 83	83		1.2
Ship	4 8	5	8		4 83	46	83	

Table 7-4. SITES Statistics on 10° Binned Data. (See Table 7-3 for Explanation of the Organization of This Table.)

SITES Statistics

a) North Temperate (30°N-60°N, 0°-360°E)

	Category/Hypothesis Test					Percent/Test Value				
	1	2	3	4	5	1	2	3	4	5
AVHRR	1	F	F	T	F	1	2.4	1.0	0.17	13
SMMR	2 8		F	F	F	2 88		1.1	1.8	6.8
HIRS	3 8	8		T	F	3 88	88		1.2	15
Ship	4 2	8	7		F	4 10	88	73		17
FNOC	5 8	8	8	8	1	5 88	88	88	88	

b) Global Tropics (30°S-30°N, 0°-360°E)

	Category/Hypothesis Test					Percent/Test Value				
	1	2	3	4	5	1	2	3	4	5
AVHRR	1	F	F	T	F	1 82	1.1	1.2	0.57	4.0
SMMR	2 8		F	F	F	2 82		1.8	1.2	5.1
HIRS	3 8	8		T	F	3 82	82		1.1	4.0
Ship	4 7	7	7		F	4 67	82	72		4.6
FNOC	5 8	8	8	8	1	5 82	82	82	82	

c) South Temperate (60°S-30°S, 0°-360°E)

	Category/Hypothesis Test				Percent/Test Value			
	1	2	3	4	1	2	3	4
AVHRR	1	F	F	T	1	1.3	2.7	0.59
SMMR	2 8		F	T	2 83		2.7	1.2
HIRS	3 8	8		T	3 83	83		1.5
Ship	4 7	5	7		4 73	46	63	

nation in the Tropics, the tests were taken on data swarms for three areas: the first north of 30°N; the second between 30°S and 30°N; and the third south of 30°S. These tests are displayed in a compact matrix form, in which rows and columns each represent data swarms for particular instruments. The column and row order are always the same: AVHRR, SMMR (nighttime), HIRS, ship, and FNOC. For example, the entry for the first row and second column (and vice-versa) is an AVHRR-SMMR test result. Different results are shown above and below the matrix diagonal, in order to show results in a compact form.

Figure 7-1 shows the spatial pattern of grid points used in each PPP comparison. Since the time and space distribution for each data swarm differs, the spatial pattern of coincident grid points differs for each sensor combination. The maximum number of space points is found in the AVHRR vs. HIRS comparison. Because of the coastline mask on SMMR data, comparisons with SMMR have fewer space points. The number of observations in the tropics (Table 7-2(b)) tends to be somewhat larger than in the northern regions; SMMR comparisons no longer have the fewest spatial points, reflecting the fact that relatively less ocean lies adjacent to coastland in the tropics; therefore the SMMR land mask is not as important. The southern region (Table 7-2(c)) generally has fewer data points in the comparisons; its FNOC analysis is absent south of the equator, while ship data is much sparser. SMMR comparisons are sparse in the southern hemisphere also.

b. 2° SITES Tests. Results of the 2° binned SITES test for the northern region (Table 7-3(a)) indicate that the data swarms are not drawn from the same population for any comparisons except the AVHRR - ship comparison. The test category for the AVHRR - ship SITES comparison is 6, indicating an imperfect agreement. The SITES test values are all greater than 0.8 except for the AVHRR - ship comparison.

Results of the 2° binned SITES test for the tropics (Table 7-3(b)) indicate that ship and AVHRR SST and ship and HIRS are statistically identical. Interestingly enough, the hypothesis of statistical identity was rejected for the AVHRR vs. HIRS. Since the El Chichon volcanic eruption contaminated AVHRR dat for July, 1982, this result demands a closer examination. Figure 7-1(c) shows the data distribution of ships vs. AVHRR and indicates very few spatial points were present in the tropics. This is probably due to the paucity of ship data. On the other hand, a color plate (Figure C-7) of AVHRR SST - ship SST indicates that some of the areas of greatest difference in this month are not present in the joint distribution map, apparently because one of the other months was deficient in either ship or AVHRR data in those regions. Also, south of the equator, the thematic map indicates that the SST differences are very small. The consequence of this is that over the four months the PPP tests are unable to discriminate effectively between tropical ship SST and AVHRR SST, in spite of widespread El Chichon contamination.

c. 10° SITES Tests. SITES statistics for 10° binned data are shown in Table 7-4. In the northern and tropical regions the results are identical to 2° binned data SITES results. The southern region differs for 10° bins in that statistical identity is accepted between AVHRR and ships and HIRS and ships.

ORIGINAL PAGE IS
OF POOR QUALITY

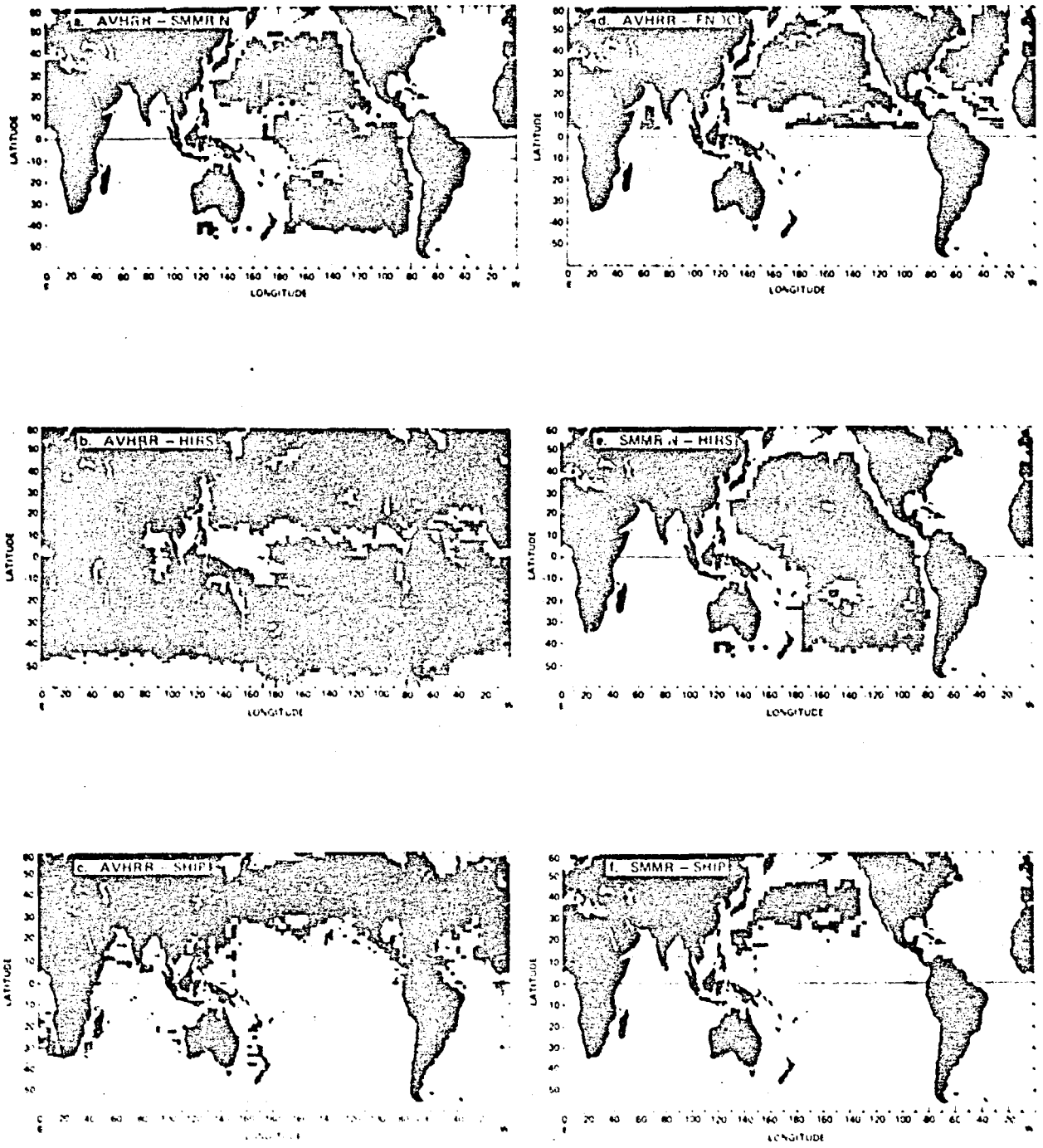

Figure 7-1. Spatial distributions of grid points used in PPP comparisons: a) AVHRR vs. SMMR; b) AVHRR vs. HIRS; c) AVHRR vs. ship; d) AVHRR vs. FNOC; e) SMMR vs. HIRS; f) SMMR vs. ship; g) SMMR vs. FNOC; h) HIRS vs. ship; i) HIRS vs. FNOC; j) ship vs. FNOC; k) ship vs. ship.

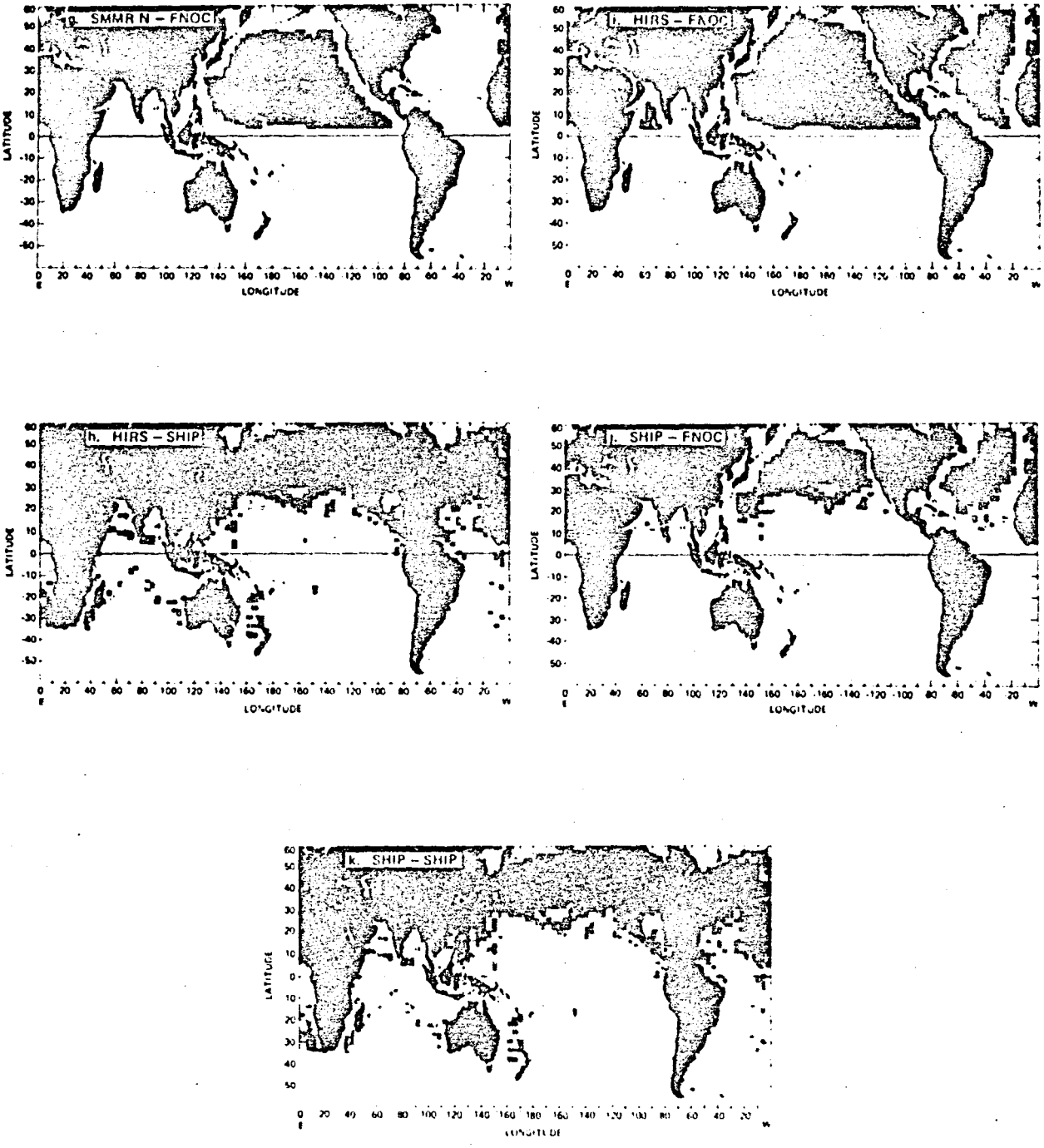

Figure 7-1. (Continued)

d. 2° SPRED Tests. Results of the SPRED test, i.e., the equality of the second moments, for the northern region (Table 7-5(a)), indicate that the data sets are not drawn from the same statistical population for all SMMR comparisons except SMMR vs. AVHRR, and reject the statistical identity of ships and AVHRR. On the other hand, this test indicates statistical identity between any pair drawn from the AVHRR, ship, or HIRS data swarms. In the tropics, the SPRED test (Table 7-5(b)) rejects statistical identity only for HIRS vs. ship. The test otherwise accepts statistical identity for every comparison test. In the southern regions, the test (Table 7-5(c)) rejects statistical identity in AVHRR vs. SMMR and HIRS vs. SMMR. Ship vs. SMMR indicates statistical identity, but with very few spatial points as mentioned before.

However, as has been concluded previously, where SITES comparisons indicate a possible bias, SPRED test results indicating identity should be suspect. This would invalidate many of the positive SPRED comparisons. Conversely, where SITES comparisons are good, very small SPRED values indicate no identity by the SPRED test. For this reason, ship vs. AVHRR comparisons, indicating statistical identity, are suspect.

e. 10° SPRED Tests. Table 7-6 shows SPRED results for 10° binned data; the results are essentially the same as the 2° bin SPRED test.

E. SUMMARY

The SITES test accepts statistical identity between AVHRR and ship data swarms. The SPRED test is consistent with these results, in the following sense. The presence or absence of a large SITES test value can bias the SPRED test towards acceptance of statistical identity, or rejection of statistical identity, respectively. Therefore, the rejection of statistical identity in the SPRED tests between AVHRR and ships and the North temperate regions is probably due to the enhanced sensitivity of the SPRED test when SITES values are small. Contrariwise, acceptance of statistical identity in the SPRED test between SMMR and FNOC in the tropics, for instance, is made suspect by the clear rejection of statistical identity in the SITES tests between that particular pair.

HIRS and ships show good agreement in both SPRED and SITES at times, but this is more inconsistent than the PPP test results of AVHRR and ship comparisons.

The general rejection of statistical identity in comparisons between satellite sensors themselves is noteworthy. Not even AVHRR and HIRS were statistically alike by the PPP tests. This seems to imply that the level of noise in AVHRR and HIRS was larger than that in the binned ship data. It implies that although at least two satellite sensors approach ship SST by the statistical measures used in this study, all of the binned satellite SSTs were noisier than the binned in situ ship SST. SMMR differs by particularly large PPP statistic values from other satellite sensors, and the FNOC SST fields show the least agreement with other sensors.

Table 7-5. Pool Permutation Procedure, SPRED Statistics on 2° Binned Data. Test the Hypothesis That Two Datasets are Drawn From the Same Population. Below and Left of the First Data Matrix Diagonal, the Relative Category of the SPRED Comparison Between the Observed Data Swarms is Printed; Above and Right of the Data Matrix diagonal, T(rue)/F(alse) is Printed, Indicating Whether or Not the Hypothesis is Supported or Rejected, Respectively. Below and Left of the Second Data Matrix Diagonal, the Percentage of the Artificially Constructed Data Swarm Test Values Which Fall Below the Observed Swarms' Test Value is Printed; Above and to the Right of the Second Data Matrix Diagonal, the SPRED Test Value for the Observed Data Swarms is Printed.

SPRED Statistics

(a) North Temperate (30°N-60°N, 0°-360°E)

	Category/ Hypothesis					Percent/Test Value				
		1	2	3	4	5		1	2	3	4	5
AVHRR	1		T	T	F	T	1		0.14	0.66×10^{-5}	0.066	0.22×10^{-3}
SMMR	2	6		F	F	F	2	63		0.13	0.45	0.47
HIRS	3	1	8		T	T	3	1.0	88		0.055	0.36×10^{-5}
Ship	4	8	8	7		T	4	88	88	73		0.037
FNOC	5	1	8	1	5		5	1.0	88	1.0	49	

(b) Global Tropics (30°S-30°N, 0°-360°E)

	Category/ Hypothesis					Percent/Test Value				
		1	2	3	4	5		1	2	3	4	5
AVHRR	1		T	T	T	T	1		0.0087	0.57×10^{-4}	0.078	0.12
SMMR	2	3		T	T	T	2	32		0.0018	0.017	0.047
HIRS	3	1	1		F	T	3	1.0	1.0		0.15	0.048
Ship	4	4	6	8		T	4	26	59	82		0.0057
FNOC	5	4	7	5	2		5	37	75	54	11	

(c) South Temperate (60°S-30°S, 0°-360°E)

	Category/ Hypothesis					Percent/Test Value			
		1	2	3	4		1	2	3	4
AVHRR	1		F	T	T	1		0.035	0.0057	0.00098
SMMR	2	8		F	T	2	83		0.11	0.0033
HIRS	3	4	8		T	3	41	83		0.018
Ship	4	3	2	7		4	21	21	63	

Table 7-6. SPRED Statistics on 10° Binned Data. (See Table 7-5 for Explanation of the Organization of This Table.)

SPRED Statistics

(a) North Temperate (30°N-60°N, 0°-360°E)

	Category/ Hypothesis Test					Percent/Test Value				
	1	2	3	4	5	1	2	3	4	5
AVHRR	1		T	T	F	T	1	0.12	0.055	0.11	0.033
SMMR	2	6		F	F	F	2 63		0.47	0.58	0.27
HIRS	3	7	8		T	F	3 71	88		0.053	0.19
Ship	4	8	8	7		F	4 88	88	73		0.29
FNOC	5	5	8	8	8	1	5 49	88	88	88	

(b) Global Tropics (30°S-30°N, 0°-360°E)

	Category/ Hypothesis Test					Percent/Test Value				
	1	2	3	4	5	1	2	3	4	5
AVHRR	1		T	T	T	T	1	0.051	0.012	0.19	0.25
SMMR	2	5		T	T	T	2 57		0.015	0.0063	0.030
HIRS	3	1	6		F	T	3 1.0	64		0.20	0.0050
Ship	4	7	1	8		T	4 67	1.0	82		0.0096
FNOC	5	5	3	1	5	1	5 53	22	1.0	44	

(c) South Temperate (60°S-30°S, 0°-360°E)

	Category/ Hypothesis Test				Percent/Test Value			
	1	2	3	4	1	2	3	4
AVHRR	1		T	T	F	1	0.012	0.17	0.076
SMMR	2	6		F	T	2 66		0.46	0.032
HIRS	3	4	8		T	3 41	83		0.016
Ship	4	8	1	5		4 83	1.0	50	

The similarity of 10° binned results and 2° binned results indicates that the sensitivity of the PPP test is not affected by changing bin size on these scales. This implies that the noise problems cannot be overcome easily by simply gathering more data.

N86
16862

UNCLAS

N86-16862

SECTION VIII

REQUIREMENTS FOR SEA SURFACE TEMPERATURE GROUND TRUTH IN THE INDONESIAN REGION

J. Penrose

Western Australia Institute of Technology

The comparatively low density of ship and XBT observations in large areas of the Southern Hemisphere and the tropics limits the extent to which satellite SST estimates can be validated on a global basis. The additional difficulties associated with previous SST estimates in the tropics have been recognized for some time (Barnett et al., 1979) and are still residually apparent in the region centered on the Indonesian archipelago (JPL 1983, p. 3-4) where both extensive cloud cover and high atmospheric water vapor content occur, notably in the October to April periods of each year. These factors affect AVHRR retrievals particularly and substantially degrade SST returns which, in drier areas appear to give useful agreement with ship derived values. SMMR returns and to a lesser extent HIRS returns are affected by the distributed nature of the land mass in the Indonesian region. AVHRR has the advantages in this region of high sampling density and small footprint. Present methods of SST retrieval applied in this region provide apparent high positive temperature anomalies where cloud cover allows retrievals to proceed. While this is presumably a consequence of over correction for atmospheric water vapor effects, adequate analysis is difficult to achieve because of limited ground truth availability in the region.

Two related problems thus arise in evaluating AVHRR SST retrievals in the Indonesian region. One concerns the regional nature of the processing apparently required for AVHRR data and the second concerns the requirements and availability of ground truth information. AVHRR regression coefficients derived in one set of regional environmental conditions can result in large SST errors when applied to data in other regions (JPL 1983, p. 5-3). Pending a fuller understanding of the global atmosphere it may be necessary to develop regional processing algorithms for multichannel water vapor corrections, a process particularly called for in the Indonesian region. This in turn calls for improved ground truth data sets both of SST and atmospheric water vapor.

The small AVHRR footprint is better suited to comparison with ship point measurements than the larger HIRS and SMMR footprints, SST retrievals from which are better compared with binned ship data. The nature of shipping in the Indonesian region suggests that point, rather than binned ship data are more likely to arise. This raises a difficulty already experienced in working with differently conditioned ground truth data sets. Reynolds (1982) has indicated that the widespread availability of ship near-surface temperature estimates, notwithstanding the substantial noise in such data, makes it more valuable than the more precise, but less dense XBT data. Further, single point observations of SST are usually assumed to be representative of an ensemble mean value over the spatial dimensions characterizing one or more pixels (JPL 1983, p. 5-7). This assumption may require examination in parts of the Indonesian region where comparatively large horizontal temperature gradients may be expected.

Recommendations:

(1) Attention should be given to developing regional multichannel processing techniques applicable to the tropical region centered on Indonesia. This will call for improved ground truth data sets in the area.

(2) Because the spatial density of ground truth data sets in the Indonesian region can be expected to remain low, attention should be given both to the development of high accuracy in ground truth wherever possible and to the statistical significance of comparisons made with the data sets that do become available.

(3) Wherever possible, SST ground truth data in the Indonesian region should include measurements illustrative of the spatial character of the temperature field, notably over length scales comparable with the AVHRR footprint.

(4) Cooperation in items (1)-(3) above should be sought from scientists and institutions active in the Indonesian region in order to maximize the amount of ground truth data made available.

SECTION IX

REFERENCES

Barnett, T. P., W. C. Patzert, S. C. Webb, and B. R. Bean, 1979: Climatological usefulness of satellite determined sea surface temperatures in the tropical Pacific. Bull. Am. Met. Soc., 60, 197-205.

Chaline, M. T., N. L. Evans, V. Gilbert, and R. D. Haskins, 1984: Requirements for a passive IR advanced moisture and temperature sounder. Appl. Opt., 23, 979-989.

COSPAR, (1985): International workshop on satellite derived sea surface temperature for global climate applications. Report of workshop held May 29-31, 1985, Washington, D.C. (in preparation).

Deschamps, P. Y. and R. Frouin, 1984: Large diurnal heating of the sea surface observed by the HCMR experiment. J. Phys. Oceanog., 14, 177-184.

Garret, J., 1981: The performance of the FGGE drifting buoy system. Adv. Space Res., 1, 87-94, Pergamon Press, Oxford.

Holl, M. M., 1981: Alternating parallel analysis. In: The Scientific/Technical Report for the Expanded Ocean Thermal Structure Analysis System (Contract #N0028-80-c-y751, U. S. Navy Fleet Numerical Oceanography Center), Meteorology International Inc., Monterey, CA.

JPL, 1983: Satellite-derived sea surface temperature: Workshop-I. JPL Publication 83-34, Jet Propulsion Laboratory, California Inst. of Technology, Pasadena, CA, 147 pp.

JPL, 1984: Satellite-derived sea surface temperature: Workshop-II. JPL Publication 84-5, Jet Propulsion Laboratory, California Inst. of Technology, Pasadena, CA, 145 pp.

Legeckis, R. and W. Pichel, 1984: Monitoring of long waves in the eastern equatorial Pacific 1981-83 using satellite multi-channel sea surface temperature charts. NOAA Tech. Report, NESDIS 8, NOAA/NESDIS, Washington, D.C.

McClain, E. P., 1981: Multiple atmospheric window techniques for satellite-derived sea surface temperatures. Oceanography from Space, Plenum Press, New York, pp. 73-85.

McClain, E. P., W. G. Pichel, C. C. Walton, A. Ahmad, and J. Sulton, 1983: Multi-channel improvements to satellite-derived global sea surface temperatures. Adv. Space Res., 2, 43-47, Pergamon Press, Oxford.

Njoku, E. G., 1985: Satellite derived sea surface temperature: Workshop comparisons. Bull. Am. Met. Soc., 66, 274-281.

Preisendorfer, R. and T. P. Barnett, 1983: Numerical model-reality intercomparison tests using small-sample statistics. J. Atm. Sci., 40, 1884-1896.

Reynolds, R., 1982: A monthly averaged climatology of sea surface temperature. NOAA Tech. Report NWS 31, NOAA/NWS, Silver Spring, MD, 35 pp.

Reynolds, R. W., 1983: A comparison of sea surface temperature climatologies. J. Clim. Appl. Meteoral., 22, 447-459.

Robinson, I. S., N. C. Wells, and H. Chamock, 1984: The sea surface thermal boundary layer and its relevance to the measurement of sea surface temperature by airborne and spaceborne radiometers. Int. J. Rem. Sens., 5, 19-45.

Saur, J. F. T., 1963: A study of the quality of sea water temperatures reported in logs of ships' weather observations. J. Appl. Meteorol., 2, 417-425.

Schwalb, A., 1978: The TIROS N/NOAA A-G satellite series. NOAA Tech. Memo. NESS 95, NOAA/NESDIS, Washington, D.C., 75 pp.

Smith, W. L., 1968: An improved method for calculating tropospheric temperature and moisture from satellite radiometer measurements. Mon. Wea. Rev., 96, 387-396.

Smith, W. L., 1980: Operational sounding algorithms. VAS Demonstration Sounding Workshop. NASA Conf. Publ. 2157, NASA/Goddard Space Flight Center, Greenbelt, MD, pp. 1-10.

Smith, W. L. and H. M. Woolf, 1982: Algorithms used to retrieve surface skin temperature and vertical moisture and temperature profiles from VISSR Atmospheric Sounder (VAS) radiance observations. Proc. AMS 4th Conf. Atmos. Rad., Toronto, Canada, American Meterological Soc., Boston, MA.

Stowe, L. L., 1984: Personal communication (address: Climate and Earth Sciences Laboratory, NOAA/NESDIS, E/RA11, Washington, D.C. 20233).

Strong, A. E., L. L. Stowe, and C. C. Walton, 1983: Using the NOAA-7 AVHRR data to monitor El Chichon aerosol evaluation and subsequent sea surface temperature anomalies. Proc. 17th Int. Symp. Rem. Sens. Env., Univ. of Michigan, Ann Arbor, MI, pp. 107-122.

Strong, A. E. and E. P. McClain, 1984: Improved ocean surface temperatures from space - comparisons with drifting buoys. Bull. Am. Met. Soc., 65, 138-142.

Strong, A. E., 1984: Use of drifting buoys to improve accuracy of satellite sea surface temperature measurements. Trop. Ocean-Atm. Newsl., 25, 16-18.

Susskind, J., J. Rosenfield, D. Reuter, and M. T. Chahine, 1984: Remote sensing of weather and climate parameters from HIRS2/MSU on TIROS-N. J. Geophys. Res., 89, 4677-4697.

Tabata, S., 1982: An evaluation of the quality of sea surface temperatures and salinities measured at Station P and Line P in the northeast Pacific Ocean. J. Geophys. Res., 17, pp. 374-385.

Walton, C. C., 1980: Deriving sea surface temperatures from TIROS-N data. Remote Sensing of Atmospheres and Oceans, Academic Press, New York, pp. 547-578.

Walton, C. C., 1985: Satellite measurements of sea surface temperatures in the presence of volcanic aerosol. J. Clim. Appl. Meteoral., 24, 501-507.

WCP, 1984: Report of the TOGA workshop on sea surface temperature and net surface radiation, La Jolla, CA, March 1984. World Climate Program Report WCP-92, WMO, C.P. 5, 1211 Geneva 20, Switzerland.

Wilheit, T. T., J. Gatlin, D. Han, B. M. Krupp, A. S. Milman, and E. Chang, 1983: Retrieval of ocean surface parameters from the scanning multichannel microwave radiometer (SMMR) on the Nimbus-7 satellite. IEEE Trans. Geosci. Rem. Sens., 15, 225-224.

APPENDIX A

CORRELATION TABLES

Table A-1. Statistical Comparisons Between 2° Latitude-Longitude Binned SST Anomaly Fields. All Data Masked up to 600 km from Land: (a) November 1979, Global.

Two Degree Average SST Anomaly Cross Correlations
Region: 56 0 deg N to 56 0 deg S, 0 0 deg E to 348 0 deg E

At least 1 observation(s) at common grid points
(C--Cross Correlation, B--Bias, S--Standard Deviation about Bias, N--Number of common valid observations)
Bias is average over column temperatures minus row temperatures

		NOAA AVHRR NOV		SUSSKIND HIRS		WILHEIT/ MILMAN SMMR NIGHT CELL 234		PAZAN SHIPS)5/CELL		PAZAN SHIPS)28/CELL		FGGE BUOYS		TRANSPAC XBT		CLIMATOL
NOAA AVHRR NOV	..	C	0 18	C	0 48	C	0 69	C	0 68	C	0 57	C	0 72	C	0 88
	..	B	-0 58	B	-0 67	B	-0 19	B	-0 28	B	-0 24	B	-0 19	B	-0 69
	..	S	1 89	S	1 11	S	0 58	S	0 58	S	0 96	S	0 78	S	0 83
	..	N	4894	N	2139	N	723	N	113	N	488	N	457	N	4184
SUSSKIND HIRS	..			C	0 18	C	0 31	C	0 88	C	0 25	C	0 37	C	0 88
	..			B	-0 22	B	0 64	B	0 27	B	0 45	B	0 12	B	-0 85
	..			S	1 25	S	1 01	S	1 12	S	1 28	S	1 86	S	0 92
	..			N	2385	N	735	N	115	N	427	N	473	N	4595
WILHEIT/ MILMAN SMMR NIGHT CELL 234	..					C	0 34	C	0 41	C	0 58	C	0 29	C	0 88
	..					B	-0 52	B	-1 09	B	1 88	B	0 81	B	0 87
	..					S	1 27	S	1 31	S	1 86	S	1 33	S	1 18
	..					N	395	N	65	N	212	N	451	N	2386
PAZAN SHIPS)5/CELL	..							C	1 88	C	0 88	C	0 63	C	0 88
	..							B	0 88	B	1 33	B	0 11	B	0 88
	..							S	0 88	S	0 88	S	0 79	S	0 89
	..							N	115	N	1	N	232	N	735
PAZAN SHIPS)28/CELL	..									C	0 56	C	0 88
	..									B	0 62	B	-0 22
	..									S	0 76	S	0 58
	..									N	54	N	115
FGGE BUOYS	..											C	-0 83	C	0 88
	..											B	-0 49	B	-0 66
	..											S	1 11	S	1 83
	..											N	14	N	428
TRANSPAC XBT	..													C	0 88
	..													B	-0 19
	..													S	0 99
	..													N	473
CLIMATOL	..														
	..														
	..														

(b) November 1979, North Pacific

Two Degree Average SST Anomaly Cross Correlations
Region: 54 0 deg N to 28 0 deg N, 188 0 deg E to 298 0 deg E

At least 1 observation(s) at common grid points
(C--Cross Correlation, B--Bias, S--Standard Deviation
about bias, N--Number of common valid observations)
Bias is average over column temperatures minus row temperatures

	NOAA AVHRR NOV	BUSSKIND HIRS	WILHEIT/ MILMAN SMMR NIGHT CELL 234	PAZAN SHIPS)S/CELL	TRANSPAC XBT	CLIMATOL
NOAA AVHRR NOV	..	C .. 0 28	C .. 0 53	C .. 0 74	C .. 0 65	C .. 0 88
	..	B -0 84	B .. 0 29	B -0 21	B -0 21	B .. 0 00
	..	S .. 0 99	S .. 1 07	S .. 0 61	S .. 0 78	S .. 0 74
	..	N .. 595	N .. 524	N .. 397	N .. 258	N .. 595
BUSSKIND HIRS	..	..	C .. 0 16	C .. 0 32	C .. 0 21	C .. 0 38
	..	..	B .. 1 41	B -0 84	B -0 81	B .. 0 74
	..	..	S .. 1 42	S .. 1 08	S .. 1 27	S .. 0 98
	..	..	N .. 524	N .. 397	N .. 258	N .. 595
WILHEIT/ MILMAN SMMR NIGHT CELL 234	..	..	..	C .. 0 39	C .. 0 39	C .. 0 00
	..	..	..	B -0 66	B -0 64	B -0 36
	..	..	..	S .. 1 25	S .. 1 31	S .. 1 26
	..	..	..	N 353	N 237	N .. 524
PAZAN SHIPS)S/CELL	..	..	..	..	C .. 0 62	C .. 0 00
	..	..	..	..	B .. 0 12	B .. 0 20
	..	..	..	..	S .. 0 00	S .. 0 00
	..	..	..	..	N .. 223	N .. 397
TRANSPAC XBT	..	..	..	..	..	C .. 0 00
	..	..	..	..	..	B .. 0 24
	..	..	..	..	..	S .. 1 01
	..	..	..	..	..	N 258
CLIMATOL	..	..	..	..	..	..
	..	..	..	..	..	..
	..	..	..	..	..	..
	..	..	..	..	..	..

(c) November 1979, Mid Pacific

Two Degree Average SST Anomaly Cross Correlations
Region: 28.0 deg N to 20.0 deg S; 180.0 deg E to 290.0 deg E

At least 1 observation(s) at common grid points
(C--Cross Correlation, B--Bias, S--Standard Deviation
about bias, N--Number of common valid observations)
Bias is average over column temperatures minus row temperatures

	NOAA AVHRR NOV	SUOMI HIRS	WILHEIT/ MILMAN SMMR NIGHT CELL 234	PAZAN SHIPS)S/CELL	FGGE BUOYS	TRANSPAC XBT	CLIMATOL
NOAA	C.. 0.47	C.. 0 25	C.. 0 54	C.. 0 54	C.. 0 54	C.. 0 56	C. 0 00
AVHRR	B. -0.42	B -0 81	B. -0 17	B. 0 10	B. -0 17	B. -0 36
NOV	S.. 0 72	S.. 0 94	S.. 0.47	S.. 0 90	S.. 0 50	S.. 0 72
	N.. 893	N.. 877	N.. 34	N.. 65	N.. 199	N.. 894
SUOMI HIRS	.. ..	C.. 0 87	C.. 0 87	C.. 0 32	C.. 0 35	C.. 0 00
	.. ..	B. -0 32	B. 0.29	B. 0 57	B. 0 27	B. -0 41
	.. ..	S.. 1 94	S.. 0.78	S.. 1 64	S.. 0 73	S.. 0.78
	.. ..	N.. 1842	N.. 43	N.. 73	N.. 215	N.. 1863
WILHEIT/ MILMAN SMMR NIGHT CELL 234	.. .. ..	C.. 0 33	C.. 0 85	C.. 0 21	C.. 0 00
	.. .. ..	B. 0 65	B. 0 86	B. 0 74	B. -0 18
	.. .. ..	S.. 0 77	S.. 1 31	S.. 0 92	S.. 0 82
	.. .. ..	N.. 41	N.. 72	N.. 214	N.. 1843
PAZAN SHIPS)S/CELL	.. ..	C.. 0 79	C.. 0 00
	.. ..	B. 0 69	B. -0 17
	.. ..	S.. 0.38	S.. 0 58
	.. ..	N.. 9	N.. 43
FGGE BUOYS	.. ..	C..-0 83	C.. 0 00
	.. ..	B. -2 49	B. -1 23
	.. ..	S.. 1 11	S.. 1 02
	.. ..	N.. 14	N.. 73
TRANSPAC XBT	.. ..	C.. 0 00
	.. ..	B. -0 78
	.. ..	S.. 0 67
	.. ..	N.. 215
CLIMATOL	.. ..
	.. ..
	.. ..
	.. ..

(d) November 1979, South Pacific

Two Degree Average SST Anomaly Cross Correlations
Region: 28.0 deg S to 56.0 deg S, 180.0 deg E to 298.0 deg E

At least 1 observation(s) at common grid points
(C--Cross Correlation, B--Bias, S--Standard Deviation about bias, N--Number of common valid observations)
Bias is average over column temperatures minus row temperatures

	NOAA AVHRR NOV	SUBSKIND HIRS	WILHEIT/ HILMAN SMMR NIGHT CELL 234	PAZAN SHIPS >5/CELL	FCCE BUOYS	CLIMATOL
NOAA AVHRR NOV	..	C.. 0.14	C.. 0.66	C.. 0.00	C.. 0.71	C.. 0.00
	..	B. -0.06	B. -1.19	B. -0.55	B. -0.64	B. -0.69
	..	S.. 1.21	S.. 0.66	S.. 0.00	S.. 0.87	S.. 0.96
	..	N.. 1023	N.. 738	N.. 1	N.. 172	N.. 1038
SUBSKIND HIRS	..	..	C.. 0.21	C.. 0.00	C.. 0.32	C.. 0.00
	..	..	B. -0.54	B. -0.09	B. 0.52	B. 0.23
	..	..	S.. 1.23	S.. 0.00	S.. 1.16	S.. 0.92
	..	..	N.. 739	N.. 1	N.. 174	N.. 1079
WILHEIT/ HILMAN SMMR NIGHT CELL 234	..	..	..	C.. 0.00	C.. 0.68	C.. 0.38
	..	..	..	B. 0.46	B. 1.07	B. 0.63
	..	..	..	S.. 0.00	S.. 0.09	S.. 1.09
	..	..	..	N.. 1	N.. 148	N.. 739
PAZAN SHIPS >5/CELL	..	..	..	..	..	C.. 0.00
	..	..	..	..	..	B. 0.25
	..	..	..	..	..	S.. 0.60
	..	..	..	..	..	N.. 1
FCCE BUOYS	..	..	..	..	..	C.. 0.00
	..	..	..	..	..	B. -0.58
	..	..	..	..	..	S.. 1.05
	..	..	..	..	..	N.. 174
CLIMATOL	..	..	..	..	..	..
	..	..	..	..	..	..
	..	..	..	..	..	..
	..	..	..	..	..	..

(e) November 1979, North Atlantic

Two Degree Average SST Anomaly Cross Correlations
Region: 56.0 deg N to 0.0 deg S, 278.0 deg E to 360.0 deg E

At least 1 observation(s) at common grid points
(C--Cross Correlation, B--Bias, S--Standard Deviation
about bias, N--Number of common valid observations)
Bias is average over column temperatures minus row temperatures

	NOAA AVHRR NOV	SUBSKIND HIRS	PAZAN SHIPS)5/CELL	CLIMATOL
NOAA AVHRR NOV	..	C.. 0.19	C.. 0.43	C.. 0.89
	..	B. -0.17	B. -0.17	B. -0.35
	..	S.. 0.88	S.. 0.57	S.. 0.47
	..	N.. 414	N.. 278	N.. 414
SUBSKIND HIRS	..	..	C.. 0.27	C.. 0.80
	..	..	B. 0.13	B. -0.10
	..	..	S.. 0.95	S.. 0.84
	..	..	N.. 278	N.. 428
PAZAN SHIPS)5/CELL	..	..	..	C.. 0.88
	..	..	..	B. -0.21
	..	..	..	S.. 0.59
	..	..	..	N.. 278
CLIMATOL	..	..	..	..
	..	..	..	..
	..	..	..	..
	..	..	..	..

(f) December 1981, Global

Two Degree Average SST Anomaly Cross Correlations
Region: 56.0 deg N to 56.0 deg S, 0.0 deg E to 363.0 deg E

At least 1 observation(s) at common grid points
(C--Cross Correlation, B--Bias, S--Standard Deviation about Bias, N--Number of common valid observations)
Bias is average over column temperatures minus row temperatures

		NOAA AVHRR DAY AND	NOAA AVHRR NIGHT	NOAA AVHRR	BUSSEIND HIRS	NILMAN SMMR NIGHT CELL 234	NILMEIT/ HAN SMMR/SHIP COMPOSITE	BATES VAS	PAZAN SHIPS)5/CELL	PAZAN SHIPS)20/CELL	TRANSPAC XBT	CLIMATOL
NOAA AVHRR DAY AND	C	0.88	0.96	0.48	0.49	0.51	0.24	0.56	0.45	0.51	0.00
	B	-0.37	-0.18	-0.43	-0.27	-6.11	0.23	0.09	0.08	-1.87	-0.36
	S	0.43	0.24	0.95	1.03	0.60	0.67	0.67	0.78	0.79	0.92
	N	4294	4327	4327	3547	2295	435	691	215	364	4327
NOAA AVHRR NIGHT	C			0.96	0.35	0.54	0.61	0.24	0.69	0.67	0.58	0.00
	B			0.18	-0.02	0.14	0.29	0.62	0.49	0.51	0.27	0.04
	S			0.23	0.92	0.95	0.52	0.82	0.44	0.49	0.71	0.79
	N			4579	4579	3810	2474	439	795	265	443	4579
NOAA AVHRR	C				0.35	0.54	0.58	0.28	0.67	0.64	0.59	0.00
	B				-0.28	-0.06	0.11	0.46	0.36	0.39	0.16	-0.14
	S				0.75	0.97	0.59	0.88	0.51	0.53	0.78	0.85
	N				4612	3848	2505	439	795	265	447	4612
BUSSEIND HIRS	C					0.13	0.13	0.31	0.18	0.13	0.11	0.00
	B					0.18	0.28	0.37	-0.38	-0.27	-0.29	0.06
	S					1.26	0.98	0.79	0.92	0.98	1.08	0.82
	N					3852	2517	439	795	265	450	4624
NILMAN SMMR NIGHT CELL 234	C						0.69	0.04	0.24	0.07	0.26	0.00
	B						0.23	0.06	0.21	0.15	-0.10	-0.14
	S						0.62	1.20	1.11	1.15	1.10	1.12
	N						2261	425	698	240	418	3852
NILMEIT/ HAN SMMR/SHIP COMPOSITE	C							-0.10	1.53	0.62	0.47	0.00
	B							0.27	-0.04	-0.11	-0.23	-0.14
	S							0.94	0.47	0.42	0.72	0.56
	N							316	438	118	427	2517
BATES VAS	C								0.48	0.42	-0.15	0.00
	B								-0.91	-0.88	-0.87	-0.57
	S								0.56	0.57	0.75	0.88
	N								189	55	16	439
PAZAN SHIPS)5/CELL	C									1.00	0.39	0.00
	B									0.00	-0.27	0.09
	S									0.00	0.59	0.52
	N									265	242	795
PAZAN SHIPS)20/CELL	C										0.34	0.00
	B										-0.34	-0.02
	S										0.80	0.50
	N										75	265
TRANSPAC XBT	C											0.00
	B											0.10
	S											0.85
	N											450
CLIMATOL												

(g) December 1981, North Pacific

Two Degree Average SST Anomaly Cross Correlations
Region: 56.0 deg N to 28.0 deg N, 180.0 deg E to 290.0 deg E

At least 1 observation(s) at common grid points
(C--Cross Correlation, B--Bias, S--Standard Deviation
about bias, N--Number of common valid observations)
Bias is average over column temperatures minus row temperatures

	NOAA AVHRR DAY DEC	NOAA AVHRR NIGHT	NOAA AVHRR	BUSSKIND HIRS	WILHEIT/ MILMAN SMMR NIGHT CELL 234	PAZAN SHIPS)5/CELL	TRANSPAC XBT	CLIMATOL
NOAA AVHRR DAY DEC	..	C.. 0.95 B.. 0.06 S.. 0.25 N.. 581	C.. 0.99 B.. 0.03 S.. 0.11 N.. 581	C.. 0.41 B.. 0.74 S.. 0.89 N.. 581	C.. 0.60 B.. 1.31 S.. 1.28 N.. 571	C.. 0.75 B.. 0.48 S.. 0.54 N.. 364	C.. 0.73 B.. 0.48 S.. 0.72 N.. 189	C.. 0.88 B.. 0.57 S.. 0.82 N.. 581
NOAA AVHRR NIGHT	..	..	C.. 0.98 B.. -0.03 S.. 0.16 N.. 595	C.. 0.43 B.. 0.68 S.. 0.86 N.. 595	C.. 0.68 B.. 1.25 S.. 1.27 N.. 572	C.. 0.77 B.. 0.44 S.. 0.58 N.. 376	C.. 0.75 B.. 0.47 S.. 0.78 N.. 188	C.. 0.88 B.. 0.58 S.. 0.80 N.. 595
NOAA AVHRR	..	..	..	C.. 0.43 B.. 0.71 S.. 0.86 N.. 595	C.. 0.69 B.. 1.28 S.. 1.26 N.. 572	C.. 0.77 B.. 0.44 S.. 0.58 N.. 376	C.. 0.75 B.. 0.46 S.. 0.71 N.. 188	C.. 0.88 B.. 0.53 S.. 0.80 N.. 595
BUSSKIND HIRS	..	..	..	..	C.. 0.86 B.. 0.57 S.. 1.28 N.. 572	C.. 0.29 B.. -0.31 S.. 0.89 N.. 376	C.. 0.27 B.. -0.39 S.. 1.28 N.. 188	C.. 0.88 B.. -0.18 S.. 0.80 N.. 595
WILHEIT/ MILMAN SMMR NIGHT CELL 234	..	..	..	..	..	C.. 0.22 B.. -1.68 S.. 1.18 N.. 361	C.. 0.25 B.. -1.39 S.. 1.29 N.. 189	C.. 0.88 B.. -0.74 S.. 1.04 N.. 572
PAZAN SHIPS)5/CELL	..	..	..	..	..	..	C.. 0.63 B.. -0.04 S.. 0.84 N.. 155	C.. 0.88 B.. 0.18 S.. 0.61 N.. 376
TRANSPAC XBT	..	..	..	..	..	..	..	C.. 0.88 B.. 0.43 S.. 1.06 N.. 188
CLIMATOL	..	..	..	..	..	..	..	..

(h) December 1981, Mid Pacific

Two Degree Average SST Anomaly Cross Correlations
Region: 28.0 deg N to 28.0 deg S; 180.0 deg E to 290.0 deg E

At least 1 observation(s) at common grid points
(C--Cross Correlation, B--Bias, S--Standard Deviation
about bias, N--Number of common valid observations)
Bias is average over column temperatures minus row temperatures

	NOAA AVHRR DAY DEC	NOAA AVHRR NIGHT	NOAA AVHRR	SUSSKIND HIRS	WILHEIT/ MILMAN SMMR NIGHT CELL 234	PAZAN SHIPS >5/CELL	TRANSPAC XBT	CLIMATOL
NOAA AVHRR DAY DEC	..	C.. 0.58 B. -0.13 S.. 0.62 N.. 996	C.. 0.92 B. -0.07 S.. 0.33 N.. 1889	C.. 0.19 B. -0.39 S.. 0.87 N.. 1809	C.. 0.33 B. -0.35 S.. 0.95 N.. 983	C.. 0.45 B. 0.32 S.. 0.69 N.. 41	C.. 0.28 B. -0.21 S.. 0.79 N.. 91	C.. 0.00 B. -0.12 S.. 0.79 N.. 1809
NOAA AVHRR NIGHT	..	..	C.. 0.77 B. 0.05 S.. 0.36 N.. 1843	C.. 0.29 B. -0.26 S.. 0.58 N.. 1843	C.. 0.39 B. -0.24 S.. 0.79 N.. 1015	C.. 0.34 B. 0.11 S.. 0.51 N.. 41	C.. 0.58 B. 0.11 S.. 0.43 N.. 98	C.. 0.00 B. 0.01 S.. 0.42 N.. 1843
NOAA AVHRR	..	..	..	C.. 0.25 B. -0.33 S.. 0.70 N.. 1856	C.. 0.36 B. -0.38 S.. 0.85 N.. 1026	C.. 0.42 B. 0.27 S.. 0.54 N.. 41	C.. 0.49 B. -0.02 S.. 0.53 N.. 98	C.. 0.00 B. -0.06 S.. 0.60 N.. 1856
SUSSKIND HIRS	..	..	..	..	C.. 0.01 B. 0.02 S.. 1.01 N.. 1033	C..-0.03 B. 0.27 S.. 0.72 N.. 41	C.. 0.43 B. 0.37 S.. 0.57 N.. 98	C.. 0.00 B. 0.27 S.. 0.55 N.. 1864
WILHEIT/ MILMAN SMMR NIGHT CELL 234	..	..	..	..	..	C.. 0.53 B. 0.46 S.. 0.68 N.. 48	C.. 0.58 B. 0.42 S.. 0.70 N.. 93	C.. 0.00 B. 0.25 S.. 0.66 N.. 1033
PAZAN SHIPS >5/CELL	..	..	..	..	..	..	C..-0.24 B. 0.36 S.. 0.73 N.. 3	C.. 0.00 B. -0.09 S.. 0.43 N.. 41
TRANSPAC XBT	..	..	..	..	..	..	..	C.. 0.00 B. -0.18 S.. 0.53 N.. 98
CLIMATOL	..	..	..	..	..	..	..	..

(i) December 1981, South Pacific

Two Degree Average SST Anomaly Cross Correlations
Region: 28.0 deg S to 56.0 deg S, 180.0 deg E to 298.0 deg E

At least 1 observation(s) at common grid points
(C--Cross Correlation, B--Bias, S--Standard Deviation
about bias, N--Number of common valid observations)
Bias is average over column temperatures minus row temperatures

	NOAA AVHRR DAY DEC	NOAA AVHRR NIGHT	NOAA AVHRR	SUSSKIND HIRS	WILHEIT/ MILMAN SMMR NIGHT CELL 234	PAZAN SHIPS)S/CELL	CLIMATOL
NOAA AVHRR DAY DEC	..	C.. 0.58 B. -0.96 S.. 0.75 N.. 1049	C.. 0.89 B. -0.38 S.. 0.36 N.. 1053	C.. 0.58 B. -0.86 S.. 0.83 N.. 1052	C.. 0.25 B. -0.78 S.. 1.00 N.. 714	C.. 0.17 B. -0.59 S.. 0.63 N.. 12	C.. 0.00 B. -0.17 S.. 0.81 N.. 1053
NOAA AVHRR NIGHT	..	..	C.. 0.71 B. 0.55 S.. 0.55 N.. 1095	C.. 0.37 B. 0.09 S.. 0.98 N.. 1094	C.. 0.11 B. 0.43 S.. 1.10 N.. 732	C.. 0.49 B. 0.99 S.. 0.56 N.. 12	C.. 0.00 B. 0.00 S.. 0.72 N.. 1095
NOAA AVHRR	..	..	..	C.. 0.49 B. -0.47 S.. 0.82 N.. 1098	C.. 0.14 B. -0.23 S.. 1.05 N.. 736	C.. 0.07 B. -0.02 S.. 0.60 N.. 12	C.. 0.00 B. 0.24 S.. 0.73 N.. 1099
SUSSKIND HIRS	..	..	..	..	C.. 0.16 B. 0.12 S.. 1.12 N.. 735	C..-0.01 B. 0.74 S.. 0.95 N.. 12	C.. 0.00 B. 0.71 S.. 0.67 N.. 1098
WILHEIT/ MILMAN SMMR NIGHT CELL 234	..	..	..	..	..	C.. 0.04 B. 0.04 S.. 0.77 N.. 10	C.. 0.00 B. 0.31 S.. 0.93 N.. 736
PAZAN SHIPS)S/CELL	..	..	..	..	..	..	C.. 0.00 B. -0.14 S.. 0.55 N.. 12
CLIMATOL	..	..	..	..	..	..	..

(j) December 1981, North Atlantic

Two Degree Average SST Anomaly Cross Correlations
Region: 56.0 deg N to 0.0 deg S, 298.0 deg E to 360.0 deg E

At least 1 observation(s) at common grid points
(C--Cross Correlation, B--Bias, S--Standard Deviation about bias, N--Number of common valid observations)
Bias is average over column temperatures minus row temperatures

	NOAA AVHRR DAY DEC	NOAA AVHRR NIGHT	NOAA AVHRR	SUSSKIND HIRS	WILHEIT/ MILMAN SMMR NIGHT CELL 234	PAZAN SHIPS)5/CELL	CLIMATOL
NOAA AVHRR DAY DEC	..	C.. 0.91 B.. 0.03 S.. 0.39 N.. 344	C.. 0.90 B.. 0.00 S.. 0.29 N.. 344	C.. 0.28 B.. 0.16 S.. 0.79 N.. 344	C.. 0.11 B.. 0.21 S.. 1.29 N.. 333	C.. 0.69 B.. 0.22 S.. 0.44 N.. 233	C.. 0.00 B.. -0.10 S.. 0.66 N.. 344
NOAA AVHRR NIGHT	..	..	C.. 0.97 B.. -0.02 S.. 0.13 N.. 420	C.. 0.18 B.. 0.14 S.. 0.74 N.. 420	C.. 0.32 B.. 0.08 S.. 1.18 N.. 373	C.. 0.75 B.. 0.11 S.. 0.42 N.. 255	C.. 0.00 B.. -0.13 S.. 0.57 N.. 420
NOAA AVHRR	..	..	..	C.. 0.19 B.. 0.16 S.. 0.73 N.. 420	C.. 0.26 B.. 0.10 S.. 1.21 N.. 373	C.. 0.74 B.. 0.15 S.. 0.41 N.. 255	C.. 0.00 B.. -0.10 S.. 0.56 N.. 420
SUSSKIND HIRS	..	..	..	..	C.. 0.00 B.. -0.02 S.. 1.35 N.. 373	C.. 0.13 B.. -0.10 S.. 0.77 N.. 255	C.. 0.00 B.. -0.27 S.. 0.58 N.. 420
WILHEIT/ MILMAN SMMR NIGHT CELL 234	..	..	..	..	..	C.. 0.33 B.. -0.42 S.. 1.14 N.. 227	C.. 0.00 B.. -0.22 S.. 1.23 N.. 373
PAZAN SHIPS)5/CELL	..	..	..	..	..	..	C.. 0.00 B.. -0.14 S.. 0.55 N.. 255
CLIMATOL	..	..	..	..	..	..	..

(k) March 1982, Global

Two Degree Average SST Anomaly Cross Correlations
Region: 56.0 deg N to 56.0 deg S, 0.0 deg E to 360.0 deg E

At least 1 observation(s) at common grid points
(C--Cross Correlation, B--Bias, S--Standard Deviation
about Bias, N--Number of common valid observations)
Bias is average over column temperatures minus row temperatures

	NOAA AVHRR DAY MAR	NOAA AVHRR NIGHT	NOAA AVHRR	SUSSKIND HIRS	NILMAN GMAR NIGHT CELL 234	NILMEIT/ HAN GMAR/SHIP COMPOSITE	BATES VAS	PAZAN SHIPS)5/CELL	PAZAN SHIPS)20/CELL	TRANSPAC XBT	CLIMATOL
NOAA	..	C.. 0.88	C.. 0.96	C.. 0.48	C.. 0.49	C.. 0.51	C.. 0.24	C.. 0.56	C.. 0.43	C.. 0.51	C.. 0.88
AVHRR	..	B. -0.37	B. -0.10	B. -0.43	B. -0.27	B. -0.11	B. 0.23	B. 0.09	B. 0.08	B. -0.07	B. -0.36
DAY	..	S.. 0.43	S.. 0.26	S.. 0.95	S.. 1.03	S.. 0.68	S.. 0.87	S.. 0.67	S.. 0.78	S.. 0.79	S.. 0.92
MAR	..	N.. 4294	N.. 4327	N.. 4327	N.. 3567	N.. 2295	N.. 435	N.. 691	N.. 215	N.. 364	N.. 4327
NOAA	..	..	C.. 0.96	C.. 0.35	C.. 0.54	C.. 0.61	C.. 0.24	C.. 0.69	C.. 0.67	C.. 0.58	C.. 0.88
AVHRR	..	..	B. 0.18	B. -0.62	B. 0.14	B. 0.29	B. 0.62	B. 0.49	B. 0.51	B. 0.27	B. 0.84
NIGHT	..	..	S.. 0.23	S.. 0.92	S.. 0.95	S.. 0.52	S.. 0.82	S.. 0.66	S.. 0.49	S.. 0.71	S.. 0.79
	..	..	N.. 4579	N.. 4579	N.. 3818	N.. 2474	N.. 439	N.. 795	N.. 265	N.. 443	N.. 4579
NOAA	..	..	..	C.. 0.35	C.. 0.54	C.. 0.58	C.. 0.20	C.. 0.67	C.. 0.64	C.. 0.59	C.. 0.88
AVHRR	..	..	..	B. -0.28	B. -0.06	B. 0.11	B. 0.48	B. 0.36	B. 0.39	B. 0.16	B. -0.14
	..	..	..	S.. 0.95	S.. 0.97	S.. 0.59	S.. 0.88	S.. 0.51	S.. 0.53	S.. 0.78	S.. 0.85
	..	..	..	N.. 4612	N.. 3848	N.. 2585	N.. 437	N.. 795	N.. 265	N.. 447	N.. 4612
SUSSKIND	..	..	..	..	C.. 0.13	C.. 0.13	C.. 0.31	C.. 0.18	C.. 0.13	C.. 0.11	C.. 0.88
HIRS	..	..	..	..	B. 0.10	B. 0.28	B. 0.37	B. -0.38	B. -0.27	B. -0.29	B. 0.86
	..	..	..	..	S.. 1.24	S.. 0.98	S.. 0.79	S.. 0.92	S.. 0.98	S.. 1.08	S.. 0.82
	..	..	..	..	N.. 3852	N.. 2517	N.. 439	N.. 795	N.. 265	N.. 450	N.. 4624
NILMAN	..	..	..	..	..	C.. 0.69	C..-0.04	C.. 0.24	C.. 0.07	C.. 0.26	C.. 0.88
GMAR NIGHT	..	..	..	..	..	B. 0.23	B. 0.86	B. 0.21	B. 0.15	B. -0.18	B. -0.14
CELL 234	..	..	..	..	..	S.. 0.62	S.. 1.29	S.. 1.11	S.. 1.15	S.. 1.10	S.. 1.12
	..	..	..	..	..	N.. 2261	N.. 425	N.. 670	N.. 240	N.. 410	N.. 3852
NILMEIT/	..	..	..	..	..	..	C..-0.10	C.. 0.58	C.. 0.62	C.. 0.47	C.. 0.88
HAN	..	..	..	..	..	..	B. 0.27	B. -0.04	B. -0.11	B. -0.23	B. -0.14
GMAR/SHIP	..	..	..	..	..	..	S.. 0.94	S.. 0.47	S.. 0.42	S.. 0.77	S.. 0.56
COMPOSITE	..	..	..	..	..	..	N.. 316	N.. 438	N.. 110	N.. 427	N.. 2517
BATES	..	..	..	..	..	..	..	C.. 0.48	C.. 0.42	C..-0.15	C.. 0.88
VAS	..	..	..	..	..	..	..	B. -0.90	B. -3.08	B. -0.07	B. -0.57
	..	..	..	..	..	..	..	S.. 0.56	S.. 0.57	S.. 0.95	S.. 0.88
	..	..	..	..	..	..	..	N.. 189	N.. 55	N.. 16	N.. 439
PAZAN	..	..	..	..	..	..	..	..	C.. 1.00	C.. 0.39	C.. 0.88
SHIPS	..	..	..	..	..	..	..	..	B. 0.00	B. -0.27	B. 0.09
)5/CELL	..	..	..	..	..	..	..	..	S.. 0.00	S.. 0.64	S.. 0.52
	..	..	..	..	..	..	..	..	N.. 265	N.. 242	N.. 795
PAZAN	..	..	..	..	..	..	..	..	..	C.. 0.33	C.. 0.88
SHIPS	..	..	..	..	..	..	..	..	..	B. -0.34	B. -0.02
)20/CELL	..	..	..	..	..	..	..	..	..	S.. 0.88	S.. 0.58
	..	..	..	..	..	..	..	..	..	N.. 76	N.. 265
TRANSPAC	..	..	..	..	..	..	..	..	..	..	C.. 0.88
XBT	..	..	..	..	..	..	..	..	..	..	B. 0.10
	..	..	..	..	..	..	..	..	..	..	S.. 0.85
	..	..	..	..	..	..	..	..	..	..	N.. 450
CLIMATOL	..	..	..	..	..	..	..	..	..	..	..
	..	..	..	..	..	..	..	..	..	..	..
	..	..	..	..	..	..	..	..	..	..	..

(1) March 1982, North Pacific

Two Degree Average SST Anomaly Cross Correlations
Region: 56.0 deg N to 20.0 deg N, 180.0 deg E to 298.0 deg E

At least 1 observation(s) at common grid points
(C--Cross Correlation, B--Bias, S--Standard Deviation about Bias, N--Number of common valid observations)
Bias is average over column temperatures minus row temperatures

	NOAA AVHRR DAY MAR	NOAA AVHRR NIGHT	NOAA AVHRR	SUSSKIND HIRS	MILMAN SMMR NIGHT CELL 234	WILHEIT/ HAN SMMR/SHIP COMPOSITE	PAZAN SHIPS >5/CELL	TRANSPAC XBT	CLIMATOL
NOAA AVHRR DAY MAR	..	C.. 0.78 B. -0.31 S.. 0.52 N.. 483	C.. 0.84 B. -0.28 S.. 0.48 N.. 483	C.. 0.11 B. 0.64 S.. 1.03 N.. 483	C.. 0.31 B. 0.11 S.. 1.12 N.. 429	C.. 0.45 B. 0.28 S.. 0.73 N.. 434	C.. 0.34 B. 0.22 S.. 0.66 N.. 344	C.. 0.44 B. 0.10 S.. 0.93 N.. 193	C.. 0.00 B. 0.38 S.. 0.73 N.. 483
NOAA AVHRR NIGHT	..	..	C.. 0.96 B. 0.09 S.. 0.17 N.. 595	C.. 0.18 B. 1.68 S.. 0.93 N.. 595	C.. 0.39 B. 0.49 S.. 1.01 N.. 534	C.. 0.62 B. 0.55 S.. 0.51 N.. 538	C.. 0.56 B. 0.59 S.. 0.46 N.. 434	C.. 0.51 B. 0.38 S.. 0.83 N.. 251	C.. 0.00 B. 0.74 S.. 0.57 N.. 595
NOAA AVHRR	..	..	..	C.. 0.19 B. 0.91 S.. 0.95 N.. 595	C.. 0.38 B. 0.48 S.. 1.03 N.. 534	C.. 0.60 B. 0.45 S.. 0.53 N.. 538	C.. 0.52 B. 0.58 S.. 0.49 N.. 434	C.. 0.52 B. 0.38 S.. 0.82 N.. 251	C.. 0.00 B. 0.64 S.. 0.59 N.. 595
SUSSKIND HIRS	..	..	..	..	C.. 0.09 B. -0.56 S.. 1.32 N.. 534	C.. 0.16 B. -0.58 S.. 0.97 N.. 539	C.. 0.13 B. -0.47 S.. 0.95 N.. 434	C.. 0.17 B. -0.62 S.. 1.24 N.. 251	C.. 0.00 B. -0.27 S.. 0.85 N.. 595
MILMAN SMMR NIGHT CELL 234	..	..	..	..	..	C.. 0.66 B. 0.05 S.. 0.83 N.. 538	C.. 0.37 B. -0.05 S.. 0.99 N.. 392	C.. 0.25 B. -0.38 S.. 1.26 N.. 226	C.. 0.00 B. 0.27 S.. 1.09 N.. 534
WILHEIT/ HAN SMMR/SHIP COMPOSITE	..	..	..	..	..	..	C.. 0.57 B. -0.03 S.. 0.46 N.. 394	C.. 0.36 B. -0.28 S.. 0.94 N.. 228	C.. 0.00 B. 0.22 S.. 0.68 N.. 538
PAZAN SHIPS >5/CELL	..	..	..	..	..	..	..	C.. 0.38 B. -0.29 S.. 0.91 N.. 227	C.. 0.00 B. 0.27 S.. 0.48 N.. 434
TRANSPAC XBT	..	..	..	..	..	..	..	..	C.. 0.00 B. 0.43 S.. 0.96 N.. 251
CLIMATOL	..	..	..	..	..	..	..	..	..

(m) March 1982, Mid Pacific

Two Degree Average SST Anomaly Cross Correlations
Region: 20.0 deg N to 20.0 deg S; 180.0 deg E to 290.0 deg E

At least 1 observation(s) at common grid points
(C--Cross Correlation, B--Bias, S--Standard Deviation
about bias, N--Number of common valid observations)
Bias is average over column temperatures minus row temperatures

	NOAA AVHRR DAY MAR	NOAA AVHRR NIGHT	NOAA AVHRR	SUSSKIND HIRS	MILHAM SMMR NIGHT CELL 234	WILHEIT/ HAN SMMR/SHIP COMPOSITE	BATES VAS	PAZAN SHIPS)5/CELL	TRANSPAC XBT	CLIMATOL
NOAA AVHRR DAY MAR	..	C.. 0.69 B.. -0.32 S.. 0.43 N.. 916	C.. 0.87 B.. -0.19 S.. 0.30 N.. 947	C.. 0.33 B.. -0.27 S.. 0.62 N.. 947	C.. 0.45 B.. -0.41 S.. 0.78 N.. 918	C.. 0.43 B.. -0.86 S.. 0.58 N.. 936	C.. 0.86 B.. -0.18 S.. 0.98 N.. 221	C.. 0.26 B.. 0.07 S.. 0.58 N.. 36	C.. 0.46 B.. -0.26 S.. 0.55 N.. 171	C.. 0.88 B.. -0.38 S.. 0.68 N.. 947
NOAA AVHRR NIGHT	..	..	C.. 0.92 B.. 0.11 S.. 0.18 N.. 1021	C.. 0.33 B.. 0.86 S.. 0.51 N.. 1021	C.. 0.57 B.. -0.86 S.. 0.61 N.. 993	C.. 0.61 B.. 0.38 S.. 0.39 N.. 1010	C.. 0.88 B.. 0.22 S.. 0.81 N.. 221	C.. 0.43 B.. 0.26 S.. 0.34 N.. 38	C.. 0.51 B.. 0.11 S.. 0.46 N.. 192	C.. 0.88 B.. 0.84 S.. 0.42 N.. 1021
NOAA AVHRR	..	..	..	C.. 0.34 B.. -0.88 S.. 0.55 N.. 1052	C.. 0.51 B.. -0.19 S.. 0.65 N.. 1023	C.. 0.51 B.. 0.16 S.. 0.48 N.. 1041	C.. 0.18 B.. 0.18 S.. 0.88 N.. 221	C.. 0.38 B.. 0.21 S.. 0.39 N.. 38	C.. 0.53 B.. -0.02 S.. 0.46 N.. 196	C.. 0.88 B.. -0.18 S.. 0.49 N.. 1052
SUSSKIND HIRS	..	..	..	..	C.. 0.21 B.. -0.12 S.. 0.79 N.. 1035	C.. 0.19 B.. 0.24 S.. 0.59 N.. 1053	C..-0.01 B.. 0.07 S.. 0.84 N.. 221	C.. 0.31 B.. -0.05 S.. 0.46 N.. 38	C.. 0.89 B.. 0.13 S.. 0.64 N.. 199	C.. 0.88 B.. -0.02 S.. 0.47 N.. 1064
MILHAM SMMR NIGHT CELL 234	..	..	..	..	..	C.. 0.78 B.. 0.37 S.. 0.48 N.. 1024	C.. 0.88 B.. 0.20 S.. 0.97 N.. 220	C.. 0.38 B.. 0.62 S.. 0.75 N.. 37	C.. 0.39 B.. 0.23 S.. 0.74 N.. 192	C.. 0.89 B.. 0.11 S.. 0.75 N.. 1035
WILHEIT/ HAN SMMR/SHIP COMPOSITE	..	..	..	..	..	..	C.. 0.81 B.. -0.87 S.. 0.83 N.. 220	C.. 0.43 B.. -0.14 S.. 0.49 N.. 35	C.. 0.49 B.. -0.16 S.. 0.58 N.. 199	C.. 0.89 B.. -0.26 S.. 0.46 N.. 1053
BATES VAS	..	..	..	..	..	..	..	C . 0.88 B.. 0.42 S.. 0.09 N.. 1	C..-0.15 B.. -0.07 S.. 0.95 N.. 16	C.. 0.88 B.. -0.16 S.. 0.74 N.. 221
PAZAN SHIPS)5/CELL	..	..	..	..	..	..	..	..	C.. 0.42 B.. -0.05 S.. 0.30 N.. 15	C.. 0.88 B.. -0.06 S.. 0.26 N.. 38
TRANSPAC XBT	..	..	..	..	..	..	..	..	..	C.. 0.98 B.. -0.14 S.. 0.52 N.. 199
CLIMATOL	..	..	..	..	..	..	..	..	..	..

(n) March 1982, South Pacific

Two Degree Average SST Anomaly Cross Correlations
Region: 28 0 deg S to 56 0 deg S, 180 0 deg E to 298 0 deg E

At least 1 observation(s) at common grid points
(C--Cross Correlation, B--Bias, S--Standard Deviation
about Bias, N--Number of common valid observations)
Bias is average over column temperatures minus row temperatures

	NOAA AVHRR DAY MAR	NOAA AVHRR NIGHT	NOAA AVHRR	SUSSKIND HIRS	WILMAN SAMR NIGHT CELL 234	WILHEIT/ HAN SAMR/SHIP COMPOSITE	BATES VAS	PAZAN SHIPS >5/CELL	CLIMATOL
NOAA AVHRR DAY MAR		C 0.98 B -0.43 S 0.36 N 1898	C 0.99 B -0.16 S 0.15 N 1898	C 0.59 B -0.82 S 0.77 N 1898	C 0.27 B -0.33 S 1.61 N 819	C 0.47 B -0.31 S 0.69 N 925	C 0.60 B 0.41 S 0.58 N 184	C -0.88 B -0.62 S 0.84 N 11	C 0.00 B -0.41 S 0.81 N 1898
NOAA AVHRR NIGHT			C 0.95 B 0.27 S 0.24 N 1899	C 0.57 B -0.39 S 0.75 N 1899	C 0.29 B 0.15 S 0.96 N 828	C 0.48 B 0.13 S 0.59 N 926	C 0.63 B 0.47 S 0.52 N 184	C 0.84 B -0.07 S 0.77 N 11	C 0.00 B 0.02 S 0.84 N 1899
NOAA AVHRR				C 0.59 B -0.64 S 0.75 N 1899	C 0.20 B -0.15 S 0.97 N 828	C 0.49 B -0.15 S 0.67 N 926	C 0.68 B 0.52 S 0.49 N 184	C 0.88 B -0.48 S 0.78 N 11	C 0.00 B -0.25 S 0.73 N 1899
SUSSKIND HIRS					C 0.16 B 0.44 S 1.15 N 828	C 0.28 B 0.55 S 0.91 N 926	C 0.42 B 0.68 S 0.64 N 184	C -0.41 B 0.85 S 1.40 N 11	C 0.00 B 0.41 S 0.98 N 1899
WILMAN SAMR NIGHT CELL 234						C 0.69 B 0.17 S 0.56 N 787	C 0.51 B 1.30 S 0.65 N 181	C 0.88 B -0.46 S 1.07 N 9	C 0.00 B -0.21 S 0.93 N 828
WILHEIT/ HAN SAMR/SHIP COMPOSITE							C 0.29 B 1.05 S 0.67 N 96	C 0.46 B -0.27 S 0.57 N 9	C 0.00 B -0.28 S 0.54 N 926
BATES VAS								C 0.97 B -2.43 S 0.17 N 2	C 0.00 B -0.97 S 0.67 N 184
PAZAN SHIPS >5/CELL									C 0.00 B -0.28 S 0.66 N 11
CLIMATOL									

(o) March 1982, North Atlantic

Two Degree Average SST Anomaly Cross Correlations
Region: 56.0 deg N to 0.0 deg S, 298.0 deg E to 360.0 deg E

At least 1 observation(s) at common grid points
(C--Cross Correlation, B--Bias, S--Standard Deviation about bias, N--Number of common valid observations)
Bias is average over column temperatures minus row temperatures

	NOAA AVHRR DAY MAR	NOAA AVHRR NIGHT	NOAA AVHRR	BUSSKIND HIRS	MILMAN SMMR NIGHT CELL 234	BATES VAS	FAZAN SHIPS)5/CELL	CLIMATOL
NOAA AVHRR DAY MAR	..	C.. 0.77 B.. -0.42 S.. 0.51 N.. 356	C.. 0.89 B.. -0.26 S.. 0.39 N.. 357	C.. 0.86 B.. 0.26 S.. 1.02 N.. 357	C..-0.15 B.. -1.02 S.. 1.34 N.. 277	C.. 0.46 B.. 0.08 S.. 0.63 N.. 118	C.. 0.57 B.. 0.04 S.. 0.60 N.. 255	C.. 0.88 B.. 0.02 S.. 0.81 N.. 357
NOAA AVHRR NIGHT	..	..	C.. 0.95 B.. 0.13 S.. 0.19 N.. 419	C.. 0.89 B.. 0.59 S.. 0.86 N.. 419	C..-0.06 B.. -0.62 S.. 1.15 N.. 335	C.. 0.59 B.. 1.35 S.. 0.48 N.. 114	C.. 0.66 B.. 0.44 S.. 0.41 N.. 267	C.. 0.38 B.. 0.42 S.. 0.57 N.. 419
NOAA AVHRR	..	..	..	C.. 0.86 B.. 0.47 S.. 0.86 N.. 428	C..-0.07 B.. -0.74 S.. 1.18 N.. 335	C.. 0.55 B.. 1.19 S.. 0.58 N.. 114	C.. 0.67 B.. 0.29 S.. 0.42 N.. 267	C.. 0.88 B.. 0.38 S.. 0.60 N.. 428
BUSSKIND HIRS	..	..	..	..	C.. 0.84 B.. -1.07 S.. 1.28 N.. 335	C.. 0.49 B.. 0.74 S.. 0.58 N.. 114	C..-0.01 B.. -0.16 S.. 0.84 N.. 267	C.. 0.88 B.. -0.18 S.. 0.69 N.. 428
MILMAN SMMR NIGHT CELL 234	..	..	..	..	..	C.. 0.18 B.. 1.85 S.. 1.18 N.. 184	C..-0.05 B.. 0.76 S.. 1.19 N.. 213	C.. 0.88 B.. 0.99 S.. 1.07 N.. 335
BATES VAS	..	..	..	..	..	..	C.. 0.50 B.. -0.69 S.. 0.52 N.. 184	C.. 0.88 B.. -1.02 S.. 0.58 N.. 114
FAZAN SHIPS)5/CELL	..	..	..	..	..	..	..	C.. 0.88 B.. -0.05 S.. 0.42 N.. 267
CLIMATOL	..	..	..	..	..	..	..	..

(p) July 1982, Global

Two Degree Average SST Anomaly Cross Correlations
Region: 56 0 deg N to 56 0 deg S, 0 0 deg E to 360 0 deg E

At least 1 observation(s) at common grid points
(C--Cross Correlation, B--Bias, S--Standard Deviation
about Bias, N--Number of common valid observations)
Bias is average over column temperatures minus row temperatures

	NOAA AVHRR DAY JUL	NOAA AVHRR NIGHT	NOAA AVHRR	BUSSEIKO MIES	BUSSEIKO MIES WEIGHTED	KILMAN SPMR NIGHT CELL 234	WILHEIT/ HAN SMMR/SMIP COMPOSITE	BATES VAS	PAZAN SHIPS >5/CELL	PAZAN SHIPS >20/CELL	TRANSPAC XBT
NOAA		C .. 0.65	C .. 0.85	C .. 0.45	C .. 0.47	C .. 0.32	C .. 0.51	C .. 0.47	C .. 0.52	C .. 0.63	C .. 0.28
AVHRR	..	B .. -0.24	B .. -0.13	B .. -0.28	B .. -0.43	B .. 0.06	B .. -0.01	B .. 0.36	B .. -0.43	B .. -0.61	B .. -0.27
DAY	..	S .. 0.65	S .. 0.42	S .. 0.72	S .. 0.73	S .. 1.05	S .. 0.68	S .. 0.63	S .. 1.05	S .. 1.15	S .. 1.20
JUL	..	N .. 2533	N .. 2558	N .. 2558	N .. 2558	N .. 2301	N .. 1369	N .. 481	N .. 375	N .. 113	N .. 147
NOAA	..	..	C .. 0.96	C .. 0.59	C .. 0.61	C .. 0.57	C .. 0.52	C .. 0.30	C .. 0.78	C .. 0.74	C .. 0.63
AVHRR	..	..	B .. 0.06	B .. 0.15	B .. -0.10	B .. 0.25	B .. 0.43	B .. 0.73	B .. 0.72	B .. 0.67	B .. 0.69
NIGHT	..	..	S .. 0.25	S .. 0.76	S .. 0.76	S .. 0.98	S .. 0.78	S .. 0.69	S .. 0.65	S .. 0.64	S .. 0.97
	..	..	N .. 4519	N .. 4513	N .. 4513	N .. 3752	N .. 2447	N .. 325	N .. 640	N .. 218	N .. 295
NOAA	..	..	..	C .. 0.59	C .. 0.61	C .. 0.54	C .. 0.50	C .. 0.42	C .. 0.62	C .. 0.71	C .. 0.57
AVHRR	..	..	..	B .. 0.06	B .. -0.17	B .. 0.20	B .. 0.25	B .. 0.68	B .. 0.68	B .. 0.64	B .. 0.69
	..	..	..	S .. 0.77	S .. 0.76	S .. 0.93	S .. 0.84	S .. 0.68	S .. 0.79	S .. 0.78	S .. 1.13
	..	..	..	N .. 4538	N .. 4538	N .. 3773	N .. 2468	N .. 336	N .. 644	N .. 218	N .. 280
BUSSEIKO	..	..	..	..	C .. 0.96	C .. 0.32	C .. 0.43	C .. 0.17	C .. 0.49	C .. 0.66	C .. 0.55
MIES	..	..	..	..	B .. -0.25	B .. 0.21	B .. 0.22	B .. 0.82	B .. 0.87	B .. -0.84	B .. 0.62
	..	..	..	..	S .. 0.21	S .. 1.01	S .. 0.69	S .. 0.73	S .. 0.69	S .. 0.73	S .. 0.90
	..	..	..	..	N .. 4623	N .. 3849	N .. 2516	N .. 339	N .. 662	N .. 220	N .. 277
BUSSEIKO	..	..	..	..	..	C .. 0.32	C .. 0.46	C .. 0.15	C .. 0.52	C .. 0.59	C .. 0.60
MIES	..	..	..	..	..	B .. 0.45	B .. 0.44	B .. 1.02	B .. 0.37	B .. 0.25	B .. 0.29
WEIGHTED	..	..	..	..	..	S .. 1.03	S .. 0.72	S .. 0.78	S .. 0.69	S .. 0.75	S .. 0.54
	..	..	..	..	..	N .. 3849	N .. 2516	N .. 339	N .. 662	N .. 220	N .. 277
KILMAN	..	..	..	..	..	..	C .. 0.75	C .. 0.44	C .. 0.46	C .. 0.58	C .. 0.52
SMMR NIGHT	..	..	..	..	..	..	B .. 0.16	B .. 0.48	B .. 0.43	B .. 0.36	B .. 0.14
CELL 234	..	..	..	..	..	..	S .. 0.57	S .. 0.73	S .. 0.77	S .. 0.76	S .. 1.06
	..	..	..	..	..	..	N .. 2253	N .. 362	N .. 522	N .. 155	N .. 259
WILHEIT/	..	..	..	..	..	..	..	C .. 0.58	C .. 0.76	C .. 0.86	C .. 0.68
HAN	..	..	..	..	..	..	..	B .. 0.36	B .. 0.04	B .. -0.03	B .. -0.05
SMMR/SMIP	..	..	..	..	..	..	..	S .. 0.54	S .. 0.53	S .. 0.45	S .. 0.88
COMPOSITE	..	..	..	..	..	..	..	N .. 491	N .. 316	N .. 70	N .. 269
BATES	..	..	..	..	..	..	..	..	C .. 0.49	C .. 0.45	C .. 0.26
VAS	..	..	..	..	..	..	..	..	B .. -0.48	B .. -0.84	B .. -0.28
	..	..	..	..	..	..	..	..	S .. 0.46	S .. 0.55	S .. 0.62
	..	..	..	..	..	..	..	..	N .. 92	N .. 33	N .. 16
PAZAN	..	..	..	..	..	..	..	.	..	C .. 1.09	C .. 0.50
SHIPS	..	..	..	..	..	..	..	..	..	S .. 0.88	S .. -0.22
>5/CELL	..	..	..	..	..	..	..	..	..	S .. 0.88	S .. 0.94
	..	..	..	..	..	..	..	..	..	N .. 220	N .. 154
PAZAN	..	..	..	..	..	..	..	..	.	..	C .. 0.56
SHIPS	..	..	..	..	..	..	..	..	.	..	S .. -0.17
>20/CELL	..	..	..	..	..	..	..	..	.	..	S .. 0.88
	..	..	..	..	..	..	..	..	.	..	N .. 55
TRANSPAC	..	..	..	..	..	..	..	..	..	..	..
XBT	..	..	..	..	..	..	..	..	..	..	.
	..	..	..	..	..	..	..	..	..	..	

(q) July 1982, North Pacific

Two Degree Average SST Anomaly Cross Correlations
Region: 56 0 deg N to 28 0 deg N, 180 0 deg E to 290 0 deg E

At least 1 observation(s) at common grid points
(C--Cross Correlation, B--Bias, S--Standard Deviation
about Bias, N--Number of common valid observations)
Bias is average over column temperatures minus row temperatures

		NOAA AVHRR DAY JUL	NOAA AVHRR NIGHT	NOAA AVHRR	BUSSEIND HIRS	BUSSEIND HIRS WEIGHTED	NILMAH SMMR NIGHT CELL 234	NILMEIT/ MAH SMMR/SHIP COMPOSITE	PAZAN SHIPS 1S/CELL	TRANSPAC XBT	CLIMATOL
NOAA	..	C .. 0.46	C .. 0.83	C .. 0.87	C .. 0.11	C .. 0.29	C .. 0.54	C .. 0.49	C .. 0.21	C .. 0.00
AVHRR	..	B .. -1.22	B .. -0.63	B .. -0.68	B .. -0.93	B .. -0.88	B .. -0.62	B .. -0.67	B .. -0.75	B .. -0.12
DAY	..	S .. 1.07	S .. 0.66	S .. 1.27	S .. 1.28	S .. 1.27	S .. 0.95	S .. 1.10	S .. 1.52	S .. 1.17
JUL	..	N .. 231	N .. 234	N .. 234	N .. 234	N .. 234	N .. 218	N .. 217	N .. 172	N .. 79	N .. 234
NOAA	..	..	..	C .. 0.86	C .. 0.87	C .. 0.58	C .. 0.39	C .. 0.48	C .. 0.64	C .. 0.66	C .. 0.00
AVHRR	..	..	..	B .. 0.23	B .. 0.73	B .. 0.42	B .. 0.68	B .. 0.83	B .. 0.73	B .. 0.63	B .. 1.20
NIGHT	..	..	..	S .. 0.51	S .. 0.77	S .. 0.76	S .. 0.97	S .. 0.79	S .. 0.73	S .. 1.16	S .. 0.00
	..	..	..	N .. 547	N .. 546	N .. 546	N .. 511	N .. 516	N .. 317	N .. 166	N .. 547
NOAA	..	..	..	..	C .. 0.39	C .. 0.39	C .. 0.32	C .. 0.41	C .. 0.59	C .. 0.62	C .. 0.00
AVHRR	..	..	..	..	B .. 0.49	B .. 0.18	B .. 0.39	B .. 0.61	B .. 0.37	B .. 0.33	B .. 1.05
	..	..	..	..	S .. 0.94	S .. 0.95	S .. 1.09	S .. 0.92	S .. 0.93	S .. 1.26	S .. 1.00
	..	..	..	..	N .. 569	N .. 569	N .. 513	N .. 518	N .. 323	N .. 169	N .. 570
BUSSEIND HIRS	..	..	..	..	..	C .. 0.92	C .. 0.22	C .. 0.27	C .. 0.43	C .. 0.32	C .. 0.00
	..	..	..	..	..	B .. -0.38	B .. -0.12	B .. 0.10	B .. -0.01	B .. -0.22	B .. 0.58
	..	..	..	..	..	S .. 0.25	S .. 1.08	S .. 0.09	S .. 0.72	S .. 1.11	S .. 0.41
	..	..	..	..	..	N .. 594	N .. 541	N .. 537	N .. 337	N .. 176	N .. 594
BUSSEIND HIRS WEIGHTED	..	..	..	..	..	..	C .. 0.23	C .. 0.28	C .. 0.45	C .. 0.37	C .. 0.00
	..	..	..	..	..	..	B .. 0.17	B .. 0.41	B .. 0.31	B .. 0.12	B .. 0.80
	..	..	..	..	..	..	S .. 1.01	S .. 0.82	S .. 0.74	S .. 1.08	S .. 0.65
	..	..	..	..	..	..	N .. 541	N .. 537	N .. 337	N .. 176	N .. 594
NILMAH SMMR NIGHT CELL 234	..	..	..	..	..	..	..	C .. 0.72	C .. 0.54	C .. 0.47	C .. 0.00
	..	..	..	..	..	..	..	B .. 0.21	B .. 0.22	B .. -0.13	B .. 0.68
	..	..	..	..	..	..	..	S .. 0.66	S .. 0.87	S .. 1.15	S .. 0.94
	..	..	..	..	..	..	..	N .. 520	N .. 278	N .. 145	N .. 532
NILMEIT/ MAH SMMR/SHIP COMPOSITE	..	..	..	..	..	..	..	..	C .. 0.74	C .. 0.59	C .. 0.00
	..	..	..	..	..	..	..	..	B .. 0.06	B .. -0.24	B .. 0.47
	..	..	..	..	..	..	..	..	S .. 0.54	S .. 0.97	S .. 0.71
	..	..	..	..	..	..	..	..	N .. 280	N .. 140	N .. 530
PAZAN SHIPS 1S/CELL	..	..	..	..	..	..	..	..	..	C .. 0.55	C .. 0.00
	..	..	..	..	..	..	..	..	..	B .. -0.23	B .. 0.67
	..	..	..	..	..	..	..	..	..	S .. 0.96	S .. 0.73
	..	..	..	..	..	..	..	..	..	N .. 146	N .. 330
TRANSPAC XBT	..	..	..	..	..	..	..	..	..	..	C .. 0.00
	..	..	..	..	..	..	..	..	..	..	B .. 0.92
	..	..	..	..	..	..	..	..	..	..	S .. 1.15
	..	..	..	..	..	..	..	..	..	..	N .. 177
CLIMATOL	..	..	..	..	..	..	..	..	..	..	..
	..	..	..	..	..	..	..	..	..	..	..
	..	..	..	..	..	..	..	..	..	..	..
	..	..	..	..	..	..	..	..	..	..	..

(r) July 1982, Mid Pacific

Two Degree Average SST Anomaly Cross Correlations
Region: 20.0 deg N to 20.0 deg S, 180.0 deg E to 279.0 deg E

At least 1 observation(s) at common grid points
(C--Cross Correlation, B--Bias, S--Standard Deviation
about bias, N--Number of common valid observations)
Bias is average over column temperatures minus row temperatures

	NOAA AVHRR DAY JUL	NOAA AVHRR NIGHT	NOAA AVHR2	SUSSKIND HIRS	SUSSKIND HIRS WEIGHTED	NILMAN SMMR NIGHT CELL 234	NILMEIT/ HAN SMMR/SHIP COMPOSITE	BATES VAS	PAZAN SHIPS)5/CELL	TRANSPAC XBT	CLIMATOL
NOAA AVHRR DAY JUL	C.. 0.56 B.. -0.10 S.. 0.44 N.. 551	C.. 0.89 B.. -0.06 S.. 0.25 N.. 573	C.. 0.31 B.. 0.12 S.. 0.68 N.. 576	C.. 0.33 B.. -0.12 S.. 0.64 N.. 570	C.. 0.24 B.. 0.03 S.. 0.77 N.. 548	C.. 0.48 B.. 0.08 S.. 0.52 N.. 542	C.. 0.67 B.. 1.69 S.. 0.42 N.. 161	C.. 0.61 B.. 0.58 S.. 0.37 N.. 7	C.. 0.57 B.. 0.38 S.. 0.54 N.. 68	C.. 0.88 B.. -0.19 S.. 0.55 N.. 570
NOAA AVHRR NIGHT		C.. 0.96 B.. 0.02 S.. 0.20 N.. 1016	C.. 0.68 B.. 0.24 S.. 0.54 N.. 1016	C.. 0.64 B.. 0.18 S.. 0.58 N.. 1016	C.. 0.49 B.. 0.43 S.. 0.73 N.. 979	C.. 0.45 B.. 0.61 S.. 0.67 N.. 1005	C.. 0.55 B.. 0.76 S.. 0.49 N.. 175	C.. 0.46 B.. 1.00 S.. 0.48 N.. 26	C.. 0.61 B.. 0.28 S.. 0.65 N.. 119	C.. 0.88 B.. 0.36 S.. 0.73 N.. 1016
NOAA AVHRR			C.. 0.67 B.. 0.38 S.. 0.58 N.. 1035	C.. 0.65 B.. 0.14 S.. 0.60 N.. 1035	C.. 0.48 B.. 0.43 S.. 0.76 N.. 995	C.. 0.46 B.. 0.58 S.. 0.70 N.. 1024	C.. 0.66 B.. 0.78 S.. 0.44 N.. 190	C.. 0.53 B.. 1.03 S.. 0.49 N.. 27	C.. 0.61 B.. 0.73 S.. 0.67 N.. 119	C.. 0.88 B.. 0.32 S.. 0.77 N.. 1035
SUSSKIND HIRS				C.. 0.97 B.. -0.16 S.. 0.18 N.. 1044	C.. 0.19 B.. 0.10 S.. 0.82 N.. 1022	C.. 0.31 B.. 0.27 S.. 0.82 N.. 1053	C.. 0.14 B.. 1.03 S.. 0.48 N.. 190	C.. 0.22 B.. 0.69 S.. 0.40 N.. 27	C.. 0.60 B.. 0.37 S.. 0.60 N.. 121	C.. 0.88 B.. 0.03 S.. 0.56 N.. 1044
SUSSKIND HIRS WEIGHTED					C.. 0.16 B.. 0.24 S.. 0.69 N.. 1022	C.. 0.30 B.. 0.43 S.. 0.68 N.. 1053	C.. 0.14 B.. 1.27 S.. 0.73 N.. 190	C.. 0.16 B.. 0.86 S.. 0.58 N.. 27	C.. 0.64 B.. 0.53 S.. 0.68 N.. 121	C.. 0.88 B.. 0.19 S.. 0.65 N.. 1044
NILMAN SMMR NIGHT CELL 234						C.. 0.72 B.. 0.19 S.. 0.58 N.. 1014	C.. 0.53 B.. 0.18 S.. 0.68 N.. 196	C.. 0.83 B.. 0.26 S.. 0.61 N.. 22	C.. 0.29 B.. 0.49 S.. 0.80 N.. 114	C.. 0.88 B.. -0.06 S.. 0.72 N.. 1023
NILMEIT/ HAN SMMR/SHIP COMPOSITE							C.. 0.66 B.. 0.35 S.. 0.46 N.. 197	C.. 0.81 B.. -0.01 S.. 0.27 N.. 25	C.. 0.33 B.. 0.16 S.. 0.67 N.. 121	C.. 0.88 B.. -0.25 S.. 0.48 N.. 1053
BATES VAS								C.. 0.95 B.. -0.04 S.. 0.43 N.. 4	C.. 0.26 B.. -0.28 S.. 0.62 N.. 16	C.. 0.88 B.. -0.05 S.. 0.59 N.. 190
PAZAN SHIPS)5/CELL									C.. 0.11 B.. -0.03 S.. 0.34 N.. 8	C.. 0.88 B.. -0.16 S.. 0.39 N.. 27
TRANSPAC XBT										C.. 0.88 B.. -0.39 S.. 0.70 N.. 121
CLIMATOL										

(8) July 1982, South Pacific

Two Degree Average SST Anomaly Cross Correlations
Region: 20.0 deg S to 56.0 deg S; 180.0 deg E to 290.0 deg E

At least 1 observation(s) at common grid points
(C--Cross Correlation, B--Bias, S--Standard Deviation about bias, N--Number of common valid observations)
Bias is average over column temperatures minus row temperatures

	NOAA AVHRR DAY JUL	NOAA AVHRR NIGHT	NOAA AVHRR	SUSSKIND HIRS	SUSSKIND HIRS WEIGHTED	MILMAN SMMR NIGHT CELL 234	MILMEIT/ MAN SMMR/SHIP COMPOSITE	BATES VAS	PATAN SHIPS >5/CELL	CLIMATOL
NOAA AVHRR DAY JUL	..	C.. 0.95 B.. -0.11 S.. 0.22 N.. 656	C.. 0.99 B.. -0.12 S.. 0.12 N.. 656	C.. 0.69 B.. -0.17 S.. 0.51 N.. 656	C.. 0.73 B.. -0.41 S.. 0.48 N.. 656	C.. 0.69 B.. 0.15 S.. 0.85 N.. 638	C.. 0.61 B.. 0.11 S.. 0.59 N.. 593	C.. 0.64 B.. -0.03 S.. 0.68 N.. 100	C.. 0.85 B.. 0.10 S.. 0.28 N.. 11	C.. 0.00 B.. -0.01 S.. 0.70 N.. 656
NOAA AVHRR NIGHT	..	..	C.. 0.99 B.. 0.05 S.. 0.12 N.. 1899	C.. 0.61 B.. -0.19 S.. 0.69 N.. 1899	C.. 0.64 B.. -0.44 S.. 0.65 N.. 1899	C.. 0.66 B.. 0.16 S.. 0.86 N.. 826	C.. 0.56 B.. 0.01 S.. 0.69 N.. 926	C.. 0.59 B.. 0.06 S.. 0.64 N.. 100	C.. 0.86 B.. 0.17 S.. 0.19 N.. 11	C.. 0.00 B.. 0.15 S.. 0.87 N.. 1899
NOAA AVHRR	..	..	..	C.. 0.64 B.. -0.24 S.. 0.66 N.. 1899	C.. 0.69 B.. -0.49 S.. 0.63 N.. 1899	C.. 0.66 B.. 0.10 S.. 0.85 N.. 826	C.. 0.58 B.. -0.05 S.. 0.67 N.. 926	C.. 0.64 B.. -0.01 S.. 0.61 N.. 100	C.. 0.86 B.. 0.11 S.. 0.19 N.. 11	C.. 0.00 B.. 0.10 S.. 0.86 N.. 1899
SUSSKIND HIRS	..	..	..	..	C.. 0.96 B.. -0.25 S.. 0.17 N.. 1899	C.. 0.27 B.. 0.34 S.. 0.93 N.. 826	C.. 0.44 B.. 0.24 S.. 0.78 N.. 926	C.. 0.85 B.. 0.47 S.. 0.85 N.. 100	C..-0.23 B.. -0.11 S.. 0.49 N.. 11	C.. 0.00 B.. 0.34 S.. 0.58 N.. 1899
SUSSKIND HIRS WEIGHTED	..	..	..	..	..	C.. 0.28 B.. 0.58 S.. 0.94 N.. 826	C.. 0.48 B.. 0.40 S.. 0.78 N.. 926	C..-0.01 B.. 0.61 S.. 0.89 N.. 100	C..-0.28 B.. 0.21 S.. 0.52 N.. 11	C.. 0.00 B.. 0.59 S.. 0.63 N.. 1899
MILMAN SMMR NIGHT CELL 234	..	..	..	..	..	..	C.. 0.68 B.. 0.07 S.. 0.60 N.. 711	C.. 0.58 B.. 0.17 S.. 0.88 N.. 99	C.. 0.74 B.. -0.48 S.. 0.91 N.. 7	C.. 0.00 B.. -0.12 S.. 0.92 N.. 826
MILMEIT/ MAN SMMR/SHIP COMPOSITE	..	..	..	..	..	..	..	C.. 0.46 B.. 0.38 S.. 0.67 N.. 94	C.. 0.44 B.. -0.38 S.. 0.44 N.. 9	C.. 0.00 B.. 0.06 S.. 0.74 N.. 926
BATES VAS	..	..	..	..	..	..	..	..	..	C.. 0.00 B.. -0.07 S.. 0.76 N.. 100
PATAN SHIPS >5/CELL	..	..	..	..	..	..	..	..	..	C.. 0.00 B.. 0.21 S.. 0.38 N.. 11
CLIMATOL	..	..	..	..	..	..	..	..	..	..

(t) July 1982, North Atlantic

Two Degree Average SST Anomaly Cross Correlations
Region: 56.0 deg N to 8.0 deg S; 298.0 deg E to 348.0 deg E

At least 1 observation(s) at common grid points
(C--Cross Correlation, B--Bias, S--Standard Deviation about bias, N--Number of common valid observations)
Bias is average over column temperatures minus row temperatures

	NOAA AVHRR DAY JUL	NOAA AVHRR NIGHT	NOAA AVHRR	SUSSKIND HIRS	SUSSKIND HIRS WEIGHTED	MILMAN SMMR NIGHT CELL 234	BATES VAS	PAZAN SHIPS >5/CELL	CLIMATOL
NOAA AVHRR DAY JUL	..	C.. 0.67 B. -0.98 S.. 0.88 N.. 181	C.. 0.81 B. -0.67 S.. 0.64 N.. 181	C.. 0.52 B. -0.32 S.. 0.92 N.. 181	C.. 0.59 B. -0.63 S.. 0.87 N.. 181	C.. 0.24 B. -1.25 S.. 1.23 N.. 138	C.. 0.58 B. -0.83 S.. 0.60 N.. 48	C.. 0.63 B. -0.35 S.. 0.85 N.. 144	C.. 0.88 B. 0.88 S.. 1.88 N.. 181
NOAA AVHRR NIGHT	..	..	C.. 0.95 B. 0.11 S.. 0.22 N.. 398	C.. 0.48 B. 0.67 S.. 0.61 N.. 398	C.. 0.53 B. 0.38 S.. 0.61 N.. 398	C.. 0.28 B. -0.13 S.. 0.85 N.. 308	C.. 0.58 B. 1.38 S.. 0.49 N.. 98	C.. 0.73 B. 0.73 S.. 0.52 N.. 258	C.. 0.88 B. 1.84 S.. 0.67 N.. 398
NOAA AVHRR	..	..	..	C.. 0.46 B. 0.56 S.. 0.66 N.. 398	C.. 0.51 B. 0.27 S.. 0.65 N.. 398	C.. 0.26 B. -0.23 S.. 0.89 N.. 339	C.. 0.53 B. 1.21 S.. 0.54 N.. 98	C.. 0.66 B. 0.57 S.. 0.68 N.. 258	C.. 0.88 B. 0.94 S.. 0.72 N.. 398
SUSSKIND HIRS	..	..	..	..	C.. 0.93 B. -0.38 S.. 0.21 N.. 428	C.. 0.16 B. -0.81 S.. 0.83 N.. 338	C.. 0.49 B. 0.76 S.. 0.47 N.. 92	C.. 0.51 B. 0.88 S.. 0.62 N.. 259	C.. 0.88 B. 0.39 S.. 0.58 N.. 428
SUSSKIND HIRS WEIGHTED	..	..	..	..	..	C.. 0.28 B. -0.52 S.. 0.85 N.. 338	C.. 0.52 B. 0.92 S.. 0.48 N.. 92	C.. 0.56 B. 0.37 S.. 0.61 N.. 259	C.. 0.88 B. 0.69 S.. 0.57 N.. 428
MILMAN SMMR NIGHT CELL 234	..	..	..	..	..	..	C.. 0.23 B. 1.48 S.. 0.86 N.. 87	C.. 0.32 B. 0.88 S.. 0.93 N.. 193	C.. 0.88 B. 1.17 S.. 0.76 N.. 338
BATES VAS	..	..	..	..	..	..	..	C.. 0.46 B. -0.50 S.. 0.45 N.. 88	C.. 0.88 B. -0.68 S.. 0.52 N.. 92
PAZAN SHIPS >5/CELL	..	..	..	..	..	..	..	..	C.. 0.88 B. 0.26 S.. 0.69 N.. 259
CLIMATOL	..	..	..	..	..	..	..	..	..

Table A-2. Statistical Comparisons Between 2° Latitude-Longitude Binned SST Anomaly Fields with 3 x 3 Cell Spatial Smoothing. All Data Masked up to 600 km from Land: (a) November 1979, Global.

Two Degree Average SST Anomaly Cross Correlations
Region: 56.0 deg N to 56.0 deg S; 0.0 deg E to 360.0 deg E

At least 1 observation(s) at common grid points
(C--Cross Correlation, B--Bias, S--Standard Deviation about bias, N--Number of common valid observations)
Bias is average over column temperatures minus row temperatures

	NOAA AVHRR NOV	SUSSKIND HIRS	WILHEIT/ MILMAN SMMR NIGHT CELL 234	PAZAN SHIPS >5/CELL	PAZAN SHIPS >20/CELL	FGGE BUOYS	TRANSPAC XBT	CLIMATOL
NOAA AVHRR NOV	..	C.. 0.34	C.. 0.46	C.. 0.78	C.. 0.87	C.. 0.00	C.. 0.78	C.. 0.00
	..	B. -0.53	B. -0.01	B. -0.24	B. -0.32	B. -0.16	B. -0.20	B. -0.65
	..	S.. 0.78	S.. 0.67	S.. 0.35	S.. 0.12	S.. 0.00	S.. 0.32	S.. 0.74
	..	N.. 3089	N.. 1502	N.. 324	N.. 6	N.. 1	N.. 30	N.. 3106
SUSSKIND HIRS	..	..	C.. 0.31	C.. 0.41	C.. 0.36	C.. 0.00	C..-0.03	C.. 0.00
	..	..	B. -0.34	B. 0.20	B. 0.45	B. 0.26	B. 0.26	B. -0.05
	..	..	S.. 0.89	S.. 0.62	S.. 0.56	S.. 0.00	S.. 0.68	S.. 0.64
	..	..	N.. 1846	N.. 324	N.. 6	N.. 1	N.. 30	N.. 3897
WILHEIT/ MILMAN SMMR NIGHT CELL 234	..	..	..	C.. 0.54	C.. 0.96	..	C.. 0.32	C.. 0.00
	..	..	..	B. -0.72	B. -2.11	..	B. -0.26	B. 0.14
	..	..	..	S.. 0.81	S.. 0.42	..	S.. 0.64	S.. 0.89
	..	..	..	N.. 152	N.. 6	..	N.. 27	N.. 1055
PAZAN SHIPS >5/CELL	..	..	..	..	C.. 1.00	..	C.. 0.68	C.. 0.00
	..	..	..	..	B. 0.00	..	B. 0.15	B. 0.00
	..	..	..	..	S.. 0.00	..	S.. 0.34	S.. 0.54
	..	..	..	..	N.. 6	..	N.. 29	N.. 324
PAZAN SHIPS >20/CELL	..	..	..	..	..	..	..	C.. 0.00
	..	..	..	..	..	..	..	B. -0.24
	..	..	..	..	..	..	..	S.. 0.13
	..	..	..	..	..	.	.	N.. 6
FGGE BUOYS	..	..	..	..	..	..	..	C.. 0.00
	..	..	..	..	..	..	..	B. -0.77
	..	..	..	..	..	..	..	S.. 0.00
	..	..	..	..	..	.	..	N.. 1
TRANSPAC XBT	..	..	..	..	..	..	..	C.. 0.00
	..	..	..	..	..	..	..	B. 0.33
	..	..	..	..	..	..	..	S.. 0.44
	..	..	..	..	..	..	..	N.. 30
CLIMATOL	..	..	..	..	..	..	..	..
	..	..	..	..	..	..	..	..
	..	..	..	..	..	..	..	..
	..	..	..	..	..	..	..	..

(b) November 1979, North Pacific

Two Degree Average SST Anomaly Cross Correlations
Region: 56.0 deg N to 20.0 deg N, 100.0 deg E to 298.0 deg E

At least 1 observation(s) at common grid points
(C--Cross Correlation, B--Bias, S--Standard Deviation
about bias, N--Number of common valid observations)
Bias is average over column temperatures minus row temperatures

	NOAA AVHRR NOV	SUSSKIND HIRS	WILHEIT/ MILMAN SMMR NIGHT CELL 234	PAZAN SHIPS >5/CELL	TRANSPAC XBT	CLIMATOL
NOAA AVHRR NOV	..	C.. 0.45	C.. 0.60	C.. 0.85	C.. 0.76	C.. 0.80
	..	B. -0.03	B. 0.16	B. -0.27	B. -0.21	B. 0.04
	..	S.. 0.61	S.. 0.75	S.. 0.33	S.. 0.32	S.. 0.63
	..	N.. 587	N.. 400	N.. 176	N.. 29	N.. 587
SUSSKIND HIRS	..	..	C.. 0.23	C.. 0.40	C..-0.28	C.. 0.80
	..	..	B. 0.28	B. 0.06	B. 0.26	B. 0.07
	..	..	S.. 0.97	S.. 0.65	S.. 0.69	S.. 0.52
	..	..	N.. 400	N.. 176	N.. 29	N.. 587
WILHEIT/ MILMAN SMMR NIGHT CELL 234	..	..	..	C.. 0.58	C.. 0.54	C.. 0.88
	..	..	..	B. -0.76	B. -0.34	B. -0.24
	..	..	..	S.. 0.78	S.. 0.53	S.. 0.94
	..	..	..	N.. 148	N.. 26	N.. 400
PAZAN SHIPS >5/CELL	..	..	..	..	C.. 0.68	C.. 0.88
	..	..	..	..	B. 0.15	B. 0.19
	..	..	..	..	S.. 0.34	S.. 0.61
	..	..	..	..	N.. 29	N.. 176
TRANSPAC XBT	..	..	..	..	..	C.. 0.80
	..	..	..	..	..	B. 0.37
	..	..	..	..	..	S.. 0.40
	..	..	..	..	..	N.. 29
CLIMATOL	..	..	..	..	..	..
	..	..	..	..	..	..
	..	..	..	..	..	..
	..	..	..	..	..	..

(c) November 1979, Mid Pacific

Two Degree Average SST Anomaly Cross Correlations
Region: 20.0 deg N to 20.0 deg S, 100.0 deg E to 290.0 deg E

At least 1 observation(s) at common grid points
(C--Cross Correlation, B--Bias, S--Standard Deviation
about bias, N--Number of common valid observations)
Bias is average over column temperatures minus row temperatures

	NOAA AVHRR NOV	SUSSKIND HIRS	WILHEIT/ MILMAN SMMR NIGHT CELL 234	PAZAN SHIPS >5/CELL	FGGE BUOYS	TRANSPAC XBT	CLIMATOL
NOAA AVHRR NOV	..	C.. 0.77	C.. 0.34	C.. 0.99	..	C.. 0.00	C.. 0.00
	..	B. -0.42	B. -1.08	B. -0.65	..	B. 0.06	B. -0.92
	..	S.. 0.38	S.. 0.67	S.. 0.04	..	S.. 0.00	S.. 0.61
	..	N.. 618	N.. 585	N.. 4	..	N.. 1	N.. 614
SUSSKIND HIRS	..	..	C.. 0.11	C.. 0.76	..	C.. 0.00	C.. 0.00
	..	..	B. -0.38	B. 0.65	..	B. 0.27	B. -0.43
	..	..	S.. 0.77	S.. 0.00	..	S.. 0.00	S.. 0.47
	..	..	N.. 928	N.. 4	..	N.. 1	N.. 963
WILHEIT/ MILMAN SMMR NIGHT CELL 234	..	..	..	C..-0.14	..	C.. 0.00	C.. 0.00
	..	..	..	B. 0.79	..	B. 1.66	B. -0.86
	..	..	..	S.. 0.21	..	S.. 0.00	S.. 0.66
	..	..	..	N.. 4	..	N.. 1	N.. 934
PAZAN SHIPS >5/CELL	..	..	..	..	..	..	C.. 0.00
	..	..	..	..	..	..	B. -0.21
	..	..	..	..	..	..	S.. 0.12
	..	..	..	..	..	..	N.. 4
FGGE BUOYS	..	..	..	..	..	..	..
	..	..	..	..	..	..	..
	..	..	..	..	..	..	..
	..	..	..	..	..	..	..
TRANSPAC XBT	..	..	..	..	..	..	C.. 0.00
	..	..	..	..	..	..	B. -0.63
	..	..	..	..	..	..	S.. 0.00
	..	..	..	..	..	..	N.. 1
CLIMATOL	..	..	..	..	..	..	..
	..	..	..	..	..	..	..
	..	..	..	..	..	..	..
	..	..	..	..	..	..	..

(d) November 1979, South Pacific

Two Degree Average SST Anomaly Cross Correlations
Region: 20.0 deg S to 56.0 deg S; 100.0 deg E to 290.0 deg E

At least 1 observation(s) at common grid points
(C--Cross Correlation, B--Bias, S--Standard Deviation
about bias, N--Number of common valid observations)
Bias is average over column temperatures minus row temperatures

	NOAA AVHRR NOV	SUSSKIND HIRS	WILHEIT/ MILMAN SMMR NIGHT CELL 234	PAZAN SHIPS >5/CELL	FGGE BUOYS	CLIMATOL
NOAA AVHRR NOV	..	C.. 0.23	C.. 0.79	..	..	C.. 0.80
	..	B. -0.82	B. -1.25	..	..	B. -0.65
	..	S.. 0.96	S.. 0.59	..	..	S.. 0.90
	..	N.. 831	N. 517	..	..	N.. 842
SUSSKIND HIRS	..	..	C.. 0.47	..	..	C.. 0.00
	..	..	B. -0.73	..	..	B. 0.23
	..	..	S.. 0.78	..	..	S.. 0.59
	..	..	N.. 518	..	..	N.. 994
WILHEIT/ MILMAN SMMR NIGHT CELL 234	..	..	..	..	..	C.. 0.00
	..	..	..	..	..	B. 0.79
	..	..	..	..	..	S.. 0.66
	..	..	..	..	..	N.. 521
PAZAN SHIPS >5/CELL	..	..	..	..	..	..
	..	..	..	..	..	..
	..	..	..	..	..	..
	..	..	..	..	..	..
FGGE BUOYS	..	..	..	..	..	..
	..	..	..	..	..	..
	..	..	..	..	..	..
	..	..	..	..	..	..
CLIMATOL	..	..	..	..	..	..
	..	..	..	..	..	..
	..	..	..	..	..	..
	..	..	..	..	..	..

(e) November 1979, North Pacific

Two Degree Average SST Anomaly Cross Correlations
Region: 56.0 deg N to 0.0 deg S; 290.0 deg E to 360.0 deg E

At least 1 observation(s) at common grid points
(C--Cross Correlation, B--Bias, S--Standard Deviation about bias, N--Number of common valid observations)
Bias is average over column temperatures minus row temperatures

	NOAA AVHRR NOV	SUSSKIND HIRS	PAZAN SHIPS >5/CELL	CLIMATOL
NOAA AVHRR NOV	..	C.. 0.15	C.. 0.41	C.. 0.00
	..	B. -0.30	B. -0.20	B. -0.36
	..	S.. 0.62	S.. 0.38	S.. 0.36
	..	N.. 296	N.. 144	N.. 296
SUSSKIND HIRS	..	..	C.. 0.49	C.. 0.00
	..	..	B. 0.35	B. -0.03
	..	..	S.. 0.52	S.. 0.56
	..	..	N.. 144	N.. 311
PAZAN SHIPS >5/CELL	..	..	..	C.. 0.00
	..	..	..	B. -0.23
	..	..	..	S.. 0.33
	..	..	..	N.. 144
CLIMATOL	..	..	..	..
	..	..	..	..
	..	..	..	..
	..	..	..	..

(f) December 1981, Global

Two Degree Average SST Anomaly Cross Correlations
Region: 56.0 deg N to 56.0 deg S, 0.0 deg E to 360.0 deg E

At least 1 observation(s) at common grid points
(C--Cross Correlation, B--Bias, S--Standard Deviation
about Bias, N--Number of common valid observations)
Bias is average over column temperatures minus row temperatures

	NOAA AVHRR DAY DEC	NOAA AVHRR NIGHT	NOAA AVHRR	SUSSKIND HIRS	WILHEIT/ NILMAN SMMR NIGHT CELL 234	PAZAN SHIPS)5/CELL	PAZAN SHIPS)20/CELL	TRANSPAC XBT	CLIMATOL
NOAA AVHRR DAY DEC	..	C.. 0.42 B. -0.45 S.. 0.84 N.. 3124	C.. 0.93 B. -0.17 S.. 0.29 N.. 3377	C.. 0.36 B. -0.36 S.. 0.88 N.. 3373	C.. 0.28 B. -0.10 S.. 1.01 N.. 2575	C.. 0.89 B. 0.36 S.. 0.29 N.. 232	C.. 1.00 B. 0.39 S.. 0.09 N.. 2	C.. 0.66 B. 0.67 S.. 0.37 N.. 13	C.. 0.00 B. -0.09 S.. 0.76 N.. 3377
NOAA AVHRR NIGHT	..	..	C.. 0.32 B. 0.27 S.. 0.87 N.. 3662	C..-0.02 B. 0.02 S.. 1.07 N.. 3685	C..-0.12 B. 0.33 S.. 1.20 N.. 2591	C..-0.11 B. 0.03 S.. 0.73 N.. 213	C..-1.00 B. 1.65 S.. 0.25 N.. 2	C.. 0.26 B. 1.27 S.. 0.53 N.. 11	C.. 0.00 B. 0.36 S.. 0.83 N.. 3689
NOAA AVHRR	..	..	..	C.. 0.47 B. -0.23 S.. 0.67 N.. 3970	C.. 0.23 B. 0.06 S.. 0.91 N.. 2831	C.. 0.91 B. 0.33 S.. 0.28 N.. 235	C.. 1.00 B. 0.38 S.. 0.07 N.. 2	C.. 0.73 B. 0.63 S.. 0.33 N.. 13	C.. 0.00 B. 0.09 S.. 0.64 N.. 3974
SUSSKIND HIRS	..	..	..	..	C.. 0.24 B. 0.14 S.. 0.87 N.. 2863	C.. 0.45 B. -0.21 S.. 0.42 N.. 235	C.. 1.00 B. -1.04 S.. 0.05 N.. 2	C.. 0.78 B. -0.38 S.. 0.37 N.. 13	C.. 0.00 B. 0.31 S.. 0.65 N.. 4017
WILHEIT/ NILMAN SMMR NIGHT CELL 234	..	..	..	..	..	C.. 0.48 B. -0.71 S.. 0.79 N.. 226	C.. 0.95 B. -0.81 S.. 0.17 N.. 2	C.. 0.38 B. -1.30 S.. 0.78 N.. 13	C.. 0.00 B. -0.05 S.. 0.83 N.. 2867
PAZAN SHIPS)5/CELL	..	..	..	..	..	..	C.. 1.00 B. 0.00 S.. 0.00 N.. 2	C.. 0.50 B. 0.24 S.. 0.27 N.. 8	C.. 0.00 B. 0.08 S.. 0.38 N.. 235
PAZAN SHIPS)20/CELL	..	..	..	..	..	..	..	C.. 0.00 B. -0.12 S.. 0.00 N.. 1	C.. 0.00 B. 0.30 S.. 0.18 N.. 2
TRANSPAC XBT	..	..	..	..	..	..	..	..	C.. 0.00 B. 0.24 S.. 0.48 N.. 13
CLIMATOL	..	..	..	..	..	..	..	..	..

(g) December 1981, North Pacific

Two Degree Average SST Anomaly Cross Correlations
Region: 56.0 deg N to 20.0 deg N; 100.0 deg E to 290.0 deg E

At least 1 observation(s) at common grid points
(C--Cross Correlation, B--Bias, S--Standard Deviation
about bias, N--Number of common valid observations)
Bias is average over column temperatures minus row temperatures

	NOAA AVHRR DAY DEC	NOAA AVHRR NIGHT	NOAA AVHRR	SUSSKIND HIRS	WILHEIT/ HILMAN SMMR NIGHT CELL 234	PAZAN SHIPS)5/CELL	TRANSPAC XBT	CLIMATOL
NOAA AVHRR DAY DEC	..	C.. 0.27 B. -0.69 S.. 0.81 N.. 414	C.. 1.00 B. 0.03 S.. 0.86 N.. 494	C.. 0.73 B. 0.71 S.. 0.53 N.. 494	C.. 0.06 B. 1.16 S.. 1.05 N.. 479	C.. 0.91 B. 0.45 S.. 0.33 N.. 127	C.. 0.66 B. 0.67 S.. 0.37 N.. 13	C.. 0.00 B. 0.55 S.. 0.75 N.. 494
NOAA AVHRR NIGHT	..	..	C.. 0.25 B. 0.73 S.. 0.81 N.. 421	C.. 0.04 B. 1.39 S.. 0.73 N.. 421	C.. 0.14 B. 1.71 S.. 0.85 N.. 402	C.. 0.46 B. 0.87 S.. 0.51 N.. 108	C.. 0.26 B. 1.27 S.. 0.53 N.. 11	C.. 0.00 B. 1.20 S.. 0.52 N.. 421
NOAA AVHRR	..	..	..	C.. 0.71 B. 0.68 S.. 0.51 N.. 507	C.. 0.06 B. 1.15 S.. 1.06 N.. 481	C.. 0.92 B. 0.43 S.. 0.29 N.. 127	C.. 0.73 B. 0.63 S.. 0.33 N.. 13	C.. 0.00 B. 0.51 S.. 0.73 N.. 507
SUSSKIND HIRS	..	..	..	..	C.. 0.09 B. 0.47 S.. 0.90 N.. 481	C.. 0.56 B. -0.21 S.. 0.45 N.. 127	C.. 0.78 B. -0.30 S.. 0.37 N.. 13	C.. 0.00 B. -0.17 S.. 0.50 N.. 507
WILHEIT/ HILMAN SMMR NIGHT CELL 234	..	..	..	..	..	C.. 0.34 B. -0.95 S.. 0.72 N.. 126	C.. 0.30 B. -1.30 S.. 0.78 N.. 13	C.. 0.00 B. -0.63 S.. 0.79 N.. 481
PAZAN SHIPS)5/CELL	..	..	..	..	..	..	C.. 0.50 B. 0.24 S.. 0.27 N.. 8	C.. 0.00 B. 0.12 S.. 0.41 N.. 127
TRANSPAC XBT	..	..	..	..	..	..	..	C.. 0.00 B. 0.24 S.. 0.48 N.. 13
CLIMATOL	..	..	..	..	..	..	..	..

(h) December 1981, Mid Pacific

Two Degree Average SST Anomaly Cross Correlations
Region: 20 0 deg N to 20 3 deg S; 180 0 deg E to 298 0 deg E

At least 1 observation(s) at common grid points
(C--Cross Correlation, B--Bias, S--Standard Deviation
about bias, N--Number of common valid observations)
Bias is average over column temperatures minus row temperatures

	NOAA AVHRR DAY DEC	NOAA AVHRR NIGHT	NOAA AVHRR	SUSSKIND HIRS	WILHEIT/ MILMAN SMMR NIGHT CELL 234	PAZAN SHIPS)S/CELL	TRANSPAC XBT	CLIMATOL
NOAA AVHRR DAY DEC	..	C.. 0.31 B -0 31 S.. 0.78 N.. 689	C.. 0.95 B -0 81 S 0 28 N. 794	C. 0 15 B -0 23 S . 0 63 N . 794	C 0 46 B -0 25 S 0 66 N . 714	C . 0 67 B 0 58 S . 0 25 N . 6	..	C . 0 89 B. 0 83 S. 0 56 N . . 794
NOAA AVHRR NIGHT	..	..	C . 0 26 B. 0 38 S . 0 68 N . . 887	C . -0 33 B. 0 02 S . . 0 97 N . . 825	C . . 0 14 B 0 85 S 0 91 N . 711	C . . 0 79 B 1 12 S 0 18 N 3	..	C . . 0 88 B 0 31 S . 0 66 N . 825
NOAA AVHRR	..	..	..	C . . 0 29 B -0 26 S . . 0 49 N . . 934	C . 0 48 B. -0 27 S . 0 63 N . 887	C . 0 71 B. 0 41 S . 0 21 N . . 6	..	C . . 0 88 B 0 81 S . . 0 44 N . . 934
SUSSKIND HIRS	..	..	..	..	C . -0 33 B -0 82 S . . 0 83 N . . 836	C . 0 79 B. 0 16 S . 0 12 N . . 6	..	C . . 0 88 B. 0 27 S . 0 39 N . . 969
WILHEIT/ MILMAN SMMR NIGHT CELL 234	..	..	..	..	..	C . -0 31 B 0 71 S . 0 16 N . . 4	..	C . . 0 88 B. 0 32 S . 0 72 N . 836
PAZAN SHIPS)S/CELL	..	..	..	..	..	..	..	C . 0 88 B 0 17 S 0 16 N. 6
TRANSPAC XBT	..	..	..	..	..	..	..	..
CLIMATOL	..	..	..	..	..	..	..	..

(i) December 1981, South Pacific

Two Degree Average SST Anomaly Cross Correlations
Region 20 0 deg S to 56 0 deg S, 100 0 deg E to 290 0 deg E

At least 1 observation(s) at common grid points
(C--Cross Correlation, B--Bias, S--Standard Deviation
about bias, N--Number of common valid observations)
Bias is average over column temperatures minus row temperatures

	NOAA AVHRR DAY DEC	NOAA AVHRR NIGHT	NOAA AVHRR	SUSSKIND HIRS	WILHEIT/ MILMAN SMMR NIGHT CELL 234	PAZAN SHIPS >5/CELL	TRANSPAC XBT	CLIMATOL
NOAA AVHRR DAY DEC		C 0 12 B -0 33 S 0 89 N 832	C 0 93 B -0 37 S 0 24 N 832	C 0 66 B -0 84 S 0 54 N 828	C 0 36 B -0 82 S 0 62 N 446			C 0 88 B -0 28 S 0 61 N 832
NOAA AVHRR NIGHT			C 0 37 B -0 09 S 0 81 N 968	C 0 84 B -0 54 S 1 05 N 964	C -0 27 B -0 28 S 1 04 N 402			C 0 89 B 0 17 S 0 81 N 968
NOAA AVHRR				C 0 64 B -0 46 S 0 56 N 964	C 0 24 B -0 31 S 0 65 N 402			C 0 86 N 0 25 S 0 58 N 968
SUSSKIND HIRS					C 0 32 B -0 85 S 3 67 N 478			C 0 88 B 0 71 S 0 78 N 964
WILHEIT/ MILMAN SMMR NIGHT CELL 234								C 0 88 B 0 34 S 0 68 N 482
PAZAN SHIPS >5/CELL								
TRANSPAC XBT								
CLIMATOL								

(j) December 1981, North Atlantic

Two Degree Average SST Anomaly Cross Correlations
Region: 56.0 deg N to 0.0 deg S; 298.0 deg E to 360.0 deg E

At least 1 observation(s) at common grid points
(C--Cross Correlation, B--Bias, S--Standard Deviation
about bias, N--Number of common valid observations)
Bias is average over column temperatures minus row temperatures

	NOAA AVHRR DAY DEC	NOAA AVHRR NIGHT	NOAA AVHRR	SUSSKIND HIRS	WILHEIT/ MILMAN SMMR NIGHT CELL 234	PAZAN SHIPS >5/CELL	CLIMATOL
NOAA AVHRR DAY DEC	..	C..-0.64 B. -0.94 S.. 0.93 N.. 198	C.. 0.97 B. 0.82 S.. 0.11 N.. 241	C.. 0.22 B. 0.19 S.. 0.50 N.. 241	C.. 0.98 B. 0.13 S.. 0.98 N.. 231	C.. 0.98 B. 0.22 S.. 0.17 N.. 99	C.. 0.80 B. -0.87 S.. 0.47 N.. 241
NOAA AVHRR NIGHT	..	..	C..-0.66 B. 1.88 S.. 0.95 N.. 236	C.. 0.11 B. 1.23 S.. 0.62 N.. 236	C..-0.55 B. 1.41 S.. 1.29 N.. 195	C..-0.88 B. 0.79 S.. 0.92 N.. 102	C.. 0.80 B. 1.81 S.. 0.57 N.. 236
NOAA AVHRR	..	..	..	C.. 0.17 B. 0.13 S.. 0.49 N.. 311	C.. 0.18 B. -0.82 S.. 0.95 N.. 267	C.. 0.93 B. 0.19 S.. 0.18 N.. 102	C.. 0.88 B. -0.14 S.. 0.44 N.. 311
SUSSKIND HIRS	..	..	..	..	C..-0.28 B. -0.15 S.. 1.04 N.. 267	C.. 0.84 B. -0.24 S.. 0.39 N.. 102	C.. 0.88 B. -0.27 S.. 0.38 N.. 311
WILHEIT/ MILMAN SMMR NIGHT CELL 234	..	..	..	..	..	C.. 0.59 B. -0.47 S.. 0.76 N.. 96	C.. 0.88 B. -0.18 S.. 0.93 N.. 267
PAZAN SHIPS >5/CELL	..	..	..	..	..	..	C.. 0.88 B. 0.01 S.. 0.35 N.. 102
CLIMATOL	..	..	..	..	..	..	..

(k) March 1982, Global

Two Degree Average SST Anomaly Cross Correlations
Region: 56 0 deg N to 56 0 deg S, 0 0 deg E to 360 0 deg E

At least 1 observation(s) at common grid points
(C--Cross Correlation, B--Bias, S--Standard Deviation about Bias, N--Number of common valid observations)
Bias is average over column temperatures minus row temperatures

	NOAA AVHRR DAY AND	NOAA AVHRR NIGHT	NOAA AVHRR	SUSSKIND HIRS	SUSSKIND HIRS VERSION 2	MILMAN SMMR NIGHT CELL 234	MILMIT/ MAN SMMR/SHIP COMPOSITE	BATES VAS	PA/AM SHIPS 35/CELL	PA/AM SHIPS 320/CELL	TRANSPAC XBT	CLIMATOL
NOAA	..	C .. 0.93	C 0.98	C 0.98	C 0.98	C 0.98	C 0.98	C 0.97	C 0.98	C 0.98	C 0.91	C 0.00
AVHRR	..	B -0.37	B -0.18	B -0.53	B -0.52	B -0.37	B -0.21	B 0.24	B 0.18	B 0.13	B 0.00	B -0.48
DAY	..	S 0.31	S 0.17	S 0.71	S 0.66	S 0.77	S 0.54	S 0.65	S 0.33	S 0.21	S 0.27	S 0.84
AND	..	N 3353	N 3486	N 3486	N 3486	N 2311	N 1606	N 291	N 229	N 9	N 9	N 3486
NOAA			C 0.98	C 0.95	C 0.99	C 0.95	C 0.71	C 0.29	C 0.82	C 0.99	C 0.00	C 0.00
AVHRR			B 0.17	B -0.86	B -0.86	B 0.87	B 0.47	B 0.69	B 0.57	B 0.07	B 0.00	B 0.00
NIGHT			S 0.10	S 0.72	S 0.66	S 0.72	S 0.48	S 0.57	S 0.23	S 0.21	S 0.00	S 0.72
			N 3921	N 3921	N 3921	N 2067	N 2103	N 301	N 348	N 23	N 10	N 3921
NOAA	..	..	..	C 0.95	C 0.98	C 0.95	C 0.66	C 0.21	C 0.77	C 0.92	C 0.78	C 0.00
AVHRR	..	..	..	B -0.24	B -0.24	B -0.12	B 0.08	B 0.51	B 0.48	B 0.00	B 0.00	B -0.05
	..	..	..	S 0.76	S 0.69	S 0.73	S 0.48	S 0.57	S 0.29	S 0.00	S 0.00	S 0.77
	..	..	..	N 3989	N 3989	N 2041	N 2150	N 301	N 348	N 23	N 10	N 3989
SUSSKIND HIRS	..	..	..	..	C 0.93	C 0.17	C 0.15	C 0.00	C 0.00	C 0.11	C 0.00	C 0.00
	..	..	..	..	B 0.15	B 0.02	B 0.12	B 0.00	B -0.00	B 0.00	B 0.00	B 0.15
	..	..	..	..	S 0.35	S 1.00	S 0.98	S 0.00	S 0.00	S 0.00	S 0.00	S 0.54
	..	..	..	..	N 4021	N 2067	N 2199	N 301	N 348	N 23	N 10	N 4021
SUSSKIND HIRS VERSION 2	..	..	..	..	..	C 0.17	C 0.14	C 0.00	C 0.00	C 0.00	C 0.00	C 0.00
	..	..	..	..	..	B 0.15	B 0.20	B 0.00	B -0.00	B 0.00	B 0.00	B 0.15
	..	..	..	..	..	S 0.97	S 0.81	S 0.00	S 0.00	S 0.00	S 0.00	S 0.54
	..	..	..	..	..	N 2067	N 2199	N 301	N 348	N 23	N 10	N 4021
MILMAN SMMR NIGHT CELL 234	..	..	..	..	..	..	C 0.82	C 0.00	C 0.15	C 0.00	C 0.00	C 0.00
	..	..	..	..	..	..	B 0.29	B 0.00	B 0.17	B 0.00	B 0.00	B 0.00
	..	..	..	..	..	..	S 0.57	S 0.00	S 0.79	S 0.00	S 0.00	S 0.54
	..	..	..	..	..	..	N 1618	N 258	N 308	N 21	N 10	N 2067
MILMIT/ MAN SMMR/SHIP COMPOSITE	..	..	..	..	..	..	..	C 0.00	C 0.00	C 0.00	C 0.00	C 0.00
	..	..	..	..	..	..	..	B 0.00	B 0.00	B 0.00	B 0.00	B 0.00
	..	..	..	..	..	..	..	S 0.00	S 0.00	S 0.00	S 0.00	S 0.00
	..	..	..	..	..	..	..	N 258	N 308	N 21	N 10	N 2199
BATES VAS	..	..	..	..	..	..	..	..	C 0.00	..	..	C 0.00
	..	..	..	..	..	..	..	..	B 0.00	..	..	B 0.00
	..	..	..	..	..	..	..	..	S 0.00	..	..	S 0.00
	..	..	..	..	..	..	..	..	N 301	..	..	N 301
PA/AM SHIPS 35/CELL	..	..	..	..	..	..	..	..	..	C 0.00	C 0.00	C 0.00
	..	..	..	..	..	..	..	..	..	B 0.00	B 0.00	B 0.00
	..	..	..	..	..	..	..	..	..	S 0.00	S 0.00	S 0.00
	..	..	..	..	..	..	..	..	..	N 348	N 23	N 348
PA/AM SHIPS 320/CELL	..	..	..	..	..	..	..	..	..	..	C 0.00	C 0.00
	..	..	..	..	..	..	..	..	..	..	B 0.00	B 0.00
	..	..	..	..	..	..	..	..	..	..	S 0.00	S 0.00
	..	..	..	..	..	..	..	..	..	..	N 23	N 23
TRANSPAC XBT	..	..	..	..	..	..	..	..	..	..	..	C 0.00
	..	..	..	..	..	..	..	..	..	..	..	B 0.00
	..	..	..	..	..	..	..	..	..	..	..	S 0.00
	..	..	..	..	..	..	..	..	..	..	..	N 10
CLIMATOL	..	..	..	..	..	..	..	..	..	..	..	..

(1) March 1982, North Pacific

Two Degree Average SST Anomaly Cross Correlations
Region 56.0 deg N to 28.0 deg N, 188.0 deg E to 298.0 deg E

At least 1 observation(s) at common grid points
(C--Cross Correlation, B--Bias, S--Standard Deviation about Bias, N--Number of common valid observations)
Bias is average over column temperatures minus row temperatures

	NOAA AVHRR DAY MAR	NOAA AVHRR NIGHT	NOAA AVHRR	SUSSKIND HIRS	SUSSKIND HIRS VERSION 2	MILHAM SMMR NIGHT CELL 234	WILMHIT/ HAN SAWN/SHIP COMPOSITE	PAZAN SHIPS)5/CELL	TRANSPAC XBT	CLIMATOL
NOAA	C .. 0.88	C .. 0.94	C .. 0.24	C .. 0.43	C .. 0.45	C .. 0.62	C .. 0.62	C .. 0.91	C .. 0.88
AVHRR	B .. -0.31	B .. -0.16	B .. 0.59	B .. 0.52	B .. -0.10	B .. 0.13	B .. 0.21	B .. -0.29	B .. 0.38
DAY	S .. 0.24	S .. 0.17	S .. 0.56	S .. 0.46	S .. 0.88	S .. 0.47	S .. 0.29	S .. 0.27	S .. 0.51
MAR	N .. 287	N .. 287	N .. 287	N .. 287	N .. 238	N .. 258	N .. 95	N .. 9	N .. 287
NOAA	..	..	C .. 0.98	C .. 0.33	C .. 0.43	C .. 0.45	C .. 0.72	C .. 0.69	C .. 0.75	C .. 0.88
AVHRR	..	..	B .. 0.16	B .. 0.99	B .. 0.89	B .. 0.36	B .. 0.52	B .. 0.65	B .. 0.25	B .. 0.76
NIGHT	..	..	S .. 0.10	S .. 0.49	S .. 0.41	S .. 0.76	S .. 0.36	S .. 0.24	S .. 0.32	S .. 0.44
	..	..	N .. 587	N .. 587	N .. 587	N .. 439	N .. 462	N .. 210	N .. 18	N .. 587
NOAA	..	..	..	C .. 0.31	C .. 0.48	C .. 0.43	C .. 0.70	C .. 0.58	C .. 0.78	C .. 0.88
AVHRR	..	..	..	B .. 0.89	B .. 0.79	B .. 0.26	B .. 0.42	B .. 0.54	B .. 0.14	B .. 0.44
	..	..	..	S .. 0.51	S .. 0.43	S .. 0.77	S .. 0.36	S .. 0.29	S .. 0.35	S .. 0.46
	..	..	..	N .. 587	N .. 587	N .. 439	N .. 462	N .. 210	N .. 18	N .. 587
SUSSKIND HIRS	..	..	..	..	C .. 0.67	C .. 0.11	C .. 0.27	C .. 0.39	C .. 0.48	C .. 0.88
	..	..	..	..	B .. -0.18	B .. -0.65	B .. -0.51	B .. -0.42	B .. -0.76	B .. -0.23
	..	..	..	..	S .. 0.38	S .. 0.98	S .. 0.54	S .. 0.41	S .. 0.52	S .. 0.48
	..	..	..	..	N .. 587	N .. 439	N .. 462	N .. 210	N .. 18	N .. 587
SUSSKIND HIRS VERSION 2	..	..	..	..	..	C .. 0.84	C .. 0.28	C .. 0.38	C .. 0.81	C .. 0.88
	..	..	..	..	..	B .. -0.55	B .. -0.48	B .. -0.44	B .. -0.62	B .. -0.13
	..	..	..	..	..	S .. 0.86	S .. 0.47	S .. 0.34	S .. 0.51	S .. 0.25
	..	..	..	..	..	N .. 439	N .. 462	N .. 210	N .. 18	N .. 587
MILHAM SMMR NIGHT CELL 234	..	..	..	..	..	..	C .. 0.83	C .. 0.56	C .. 0.59	C .. 0.88
	..	..	..	..	..	..	B .. 0.15	B .. -0.13	B .. -0.54	B .. 0.41
	..	..	..	..	..	..	S .. 0.52	S .. 0.67	S .. 0.54	S .. 0.84
	..	..	..	..	..	..	N .. 437	N .. 208	N .. 18	N .. 439
WILHELIT/ HAN SAWN/SHIP COMPOSITE	..	..	..	..	..	..	..	C .. 0.55	C .. 0.78	C .. 0.88
	..	..	..	..	..	..	..	B .. -0.07	B .. -0.44	B .. 0.27
	..	..	..	..	..	..	..	S .. 0.66	S .. 0.31	S .. 0.47
	..	..	..	..	..	..	..	N .. 283	N .. 18	N .. 462
PAZAN SHIPS)5/CELL	..	..	..	..	..	..	..	..	C .. 0.78	C .. 0.88
	..	..	..	..	..	..	..	..	B .. -0.47	B .. 0.29
	..	..	..	..	..	..	..	..	S .. 0.35	S .. 0.42
	..	..	..	..	..	..	..	..	N .. 18	N .. 210
TRANSPAC XBT	..	..	..	..	..	..	..	..	..	C .. 0.88
	..	..	..	..	..	..	..	..	..	B .. 0.77
	..	..	..	..	..	..	..	..	..	S .. 0.48
	..	..	..	..	..	..	..	..	..	N .. 18
CLIMATOL	..	..	..	..	..	..	..	..	..	..
	..	..	..	..	..	..	..	..	..	..
	..	..	..	..	..	..	..	..	..	..

(m) March 1982, Mid Pacific

Two Degree Average SST Anomaly Cross Correlations
Region: 28.0 deg N to 28.0 deg S, 180.0 deg E to 298.0 deg E

At least 1 observation(s) at common grid points
(C--Cross Correlation, B--Bias, S--Standard Deviation
about Bias, N--Number of common valid observations)
Bias is average over column temperatures minus row temperatures

	NOAA AVHRR DAY MAR	NOAA AVHRR NIGHT	NOAA AVHRR	SUSSKIND HIRS	SUSSKIND HIRS VERSION 2	MILMAN SMMR NIGHT CELL 234	MILWEIT/ HAN SMMR/SHIP COMPOSITE	BATES VAS	PATAN SHIPS)5/CELL	TRANSPAC XBT	CLIMATOL
NOAA AVHRR DAY MAR	C.. 0.75 B. -0.34 S.. 0.31 N.. 648	C.. 0.91 B. -0.21 S.. 0.21 N.. 686	C.. 0.49 B. -0.29 S.. 0.43 N.. 686	C.. 0.47 B. -0.39 S.. 0.44 N.. 686	C.. 0.63 B. -0.44 S.. 0.45 N.. 577	C.. 0.49 B. -0.12 S.. 0.44 N.. 683	C.. 0.84 B. -0.04 S.. 0.63 N.. 165	C.. 0.43 B. 0.10 S.. 0.21 N.. 5	..	C.. 0.88 B. -0.38 S.. 0.49 N.. 686
NOAA AVHRR NIGHT	..	..	C.. 0.95 B. 0.10 S.. 0.12 N.. 882	C.. 0.48 B. 0.06 S.. 0.36 N.. 882	C.. 0.42 B. -0.04 S.. 0.35 N.. 882	C.. 0.77 B. -0.06 S.. 0.44 N.. 785	C.. 0.76 B. 0.38 S.. 0.26 N.. 879	C.. 0.12 B. 0.36 S.. 0.50 N.. 165	C.. 0.72 B. 0.47 S.. 0.14 N.. 5	..	C.. 0.88 B. 0.06 S.. 0.34 N.. 882
NOAA AVHRR	..	..	..	C.. 0.42 B. -0.07 S.. 0.48 N.. 937	C.. 0.46 B. -0.16 S.. 0.39 N.. 937	C.. 0.72 B. -0.16 S.. 0.45 N.. 819	C.. 0.61 B. 0.17 S.. 0.35 N.. 934	C.. 0.11 B. 0.23 S.. 0.50 N.. 165	C.. 0.84 B. 0.43 S.. 0.10 N.. 5	..	C.. 0.83 B. -0.07 S.. 0.41 N.. 937
SUSSKIND HIRS	..	..	..	..	C.. 0.83 B. -0.06 S.. 0.19 N.. 969	C.. 0.26 B. -0.11 S.. 0.63 N.. 845	C.. 0.26 B. 0.23 S.. 0.43 N.. 966	C..-0.10 B. 0.26 S.. 0.53 N.. 165	C.. 0.77 B. 0.03 S.. 0.07 N.. 5	..	C.. 0.88 B. 0.08 S.. 0.31 N.. 969
SUSSKIND HIRS VERSION 2	..	..	..	..	..	C.. 0.19 B. -0.03 S.. 0.64 N.. 845	C.. 0.21 B. 0.31 S.. 0.44 N.. 966	C..-0.17 B. 0.36 S.. 0.54 N.. 165	C.. 0.96 B. 0.07 S.. 0.03 N.. 5	..	C.. 0.88 B. 0.07 S.. 0.38 N.. 969
MILMAN SMMR NIGHT CELL 234	..	..	..	..	..	..	C.. 0.89 B. 0.38 S.. 0.33 N.. 842	C.. 0.14 B. 0.48 S.. 0.68 N.. 163	C.. 0.83 B. 0.06 S.. 0.10 N.. 5	..	C.. 0.88 B. 0.13 S.. 0.63 N.. 845
MILWEIT/ HAN SMMR/SHIP COMPOSITE	..	..	..	..	..	..	..	C.. 0.86 B. 0.15 S.. 0.49 N.. 165	C.. 0.93 B. -0.01 S.. 0.08 N.. 4	..	C.. 0.88 B. -0.24 S.. 0.39 N.. 966
BATES VAS	..	..	..	..	..	..	..	..	..	..	C.. 0.89 B. -0.31 S.. 0.44 N.. 165
PATAN SHIPS)5/CELL	..	..	..	..	..	..	..	..	..	..	C.. 0.88 B. 0.10 S.. 0.11 N.. 5
TRANSPAC XBT	..	..	..	..	..	..	..	..	..	..	..
CLIMATOL	..	..	..	..	..	..	..	..	..	..	..

(n) March 1982, South Pacific

Two Degree Average SST Anomaly Cross Correlations
Region: 20.0 deg S to 56.0 deg S, 180.0 deg E to 298.0 deg E

At least 1 observation(s) at common grid points
(C--Cross Correlation, B--Bias, S--Standard Deviation about bias, N--Number of common valid observations)
Bias is average over column temperatures minus row temperatures

	NOAA AVHRR DAY M&B	NOAA AVHRR NIGHT	NOAA AVHRR	SUSSKIND HIRS	SUSSKIND HIRS VERSION 2	NILMAN SMMR NIGHT CELL 234	WILHEIT/ HAN SMMR/SSMI COMPOSITE	BATES VAS	PAZAN SHIPS JS/CELL	CLIMATOL
NOAA AVHRR DAY M&B	..	C.. 0.94 B.. -0.44 S.. 0.28 N.. 959	C.. 0.99 B.. -0.16 S.. 0.12 N.. 959	C.. 0.75 B.. -0.86 S.. 0.53 N.. 959	C.. 0.86 B.. -0.79 S.. 0.43 N.. 959	C.. 0.39 B.. -0.46 S.. 0.75 N.. 598	C.. 0.57 B.. -0.49 S.. 0.56 N.. 753	C.. 0.64 B.. 0.48 S.. 0.41 N.. 74	..	C.. 0.69 B.. -0.49 S.. 0.75 N.. 959
NOAA AVHRR NIGHT	..	..	C.. 0.97 B.. 0.28 S.. 0.18 N.. 968	C.. 0.73 B.. -0.43 S.. 0.52 N.. 968	C.. 0.79 B.. -0.35 S.. 0.48 N.. 968	C.. 0.36 B.. 0.02 S.. 0.78 N.. 599	C.. 0.55 B.. 0.08 S.. 0.45 N.. 762	C.. 0.64 B.. 0.62 S.. 0.41 N.. 74	..	C.. 0.88 B.. 0.64 S.. 0.58 N.. 968
NOAA AVHRR	..	..	..	C.. 0.74 B.. -0.78 S.. 0.52 N.. 968	C.. 0.81 B.. -0.63 S.. 0.41 N.. 968	C.. 0.38 B.. -0.28 S.. 0.72 N.. 599	C.. 0.58 B.. -0.22 S.. 0.58 N.. 762	C.. 0.64 B.. 0.58 S.. 0.48 N.. 74	..	C.. 0.88 B.. -0.23 S.. 0.67 N.. 968
SUSSKIND HIRS	..	..	..	..	C.. 0.95 B.. 0.08 S.. 0.24 N.. 968	C.. 0.19 B.. 0.32 S.. 0.86 N.. 599	C.. 0.35 B.. 0.50 S.. 0.72 N.. 762	C.. 0.65 B.. 0.51 S.. 0.48 N.. 74	..	C.. 0.88 B.. 0.47 S.. 0.75 N.. 968
SUSSKIND HIRS VERSION 2	..	..	..	..	..	C.. 0.19 B.. 0.27 S.. 0.88 N.. 599	C.. 0.34 B.. 0.42 S.. 0.63 N.. 762	C.. 0.64 B.. 0.62 S.. 0.48 N.. 74	..	C.. 0.88 B.. 0.39 S.. 0.64 N.. 968
NILMAN SMMR NIGHT CELL 234	..	..	..	..	..	..	C.. 0.88 B.. 0.23 S.. 0.32 N.. 539	C.. 0.73 B.. 1.24 S.. 0.38 N.. 42	..	C.. 0.88 B.. -0.84 S.. 0.69 N.. 599
WILHEIT/ HAN SMMR/SSMI COMPOSITE	..	..	..	..	..	..	..	C.. 0.45 B.. 0.95 S.. 0.48 N.. 69	..	C.. 0.88 B.. -0.14 S.. 0.41 N.. 762
BATES VAS	..	..	..	..	..	..	..	..	..	C.. 0.88 B.. -0.61 S.. 0.53 N.. 74
PAZAN SHIPS JS/CELL	..	..	..	..	..	..	..	..	..	..
CLIMATOL	..	..	..	..	..	..	..	..	..	..

(o) March 1982, North Atlantic

Two Degree Average SST Anomaly Cross Correlations
Region: 56.0 deg N to 0.0 deg S; 290.0 deg E to 360.0 deg E

At least 1 observation(s) at common grid points
(C--Cross Correlation, B--Bias, S--Standard Deviation
about bias, N--Number of common valid observations)
Bias is average over column temperatures minus row temperatures

	NOAA AVHRR DAY MAR	NOAA AVHRR NIGHT	NOAA AVHRR	SUSSKIND HIRS	SUSSKIND HIRS VERSION 2	MILMAN SMMR NIGHT CELL 234	BATES VAS	PAZAN SHIPS >5/CELL	CLIMATOL
NOAA AVHRR DAY MAR	..	C.. 0.82 B. -0.45 S.. 0.30 N.. 226	C.. 0.93 B. -0.27 S.. 0.21 N.. 227	C.. 0.38 B. 0.13 S.. 0.48 N.. 227	C.. 0.39 B. 0.20 S.. 0.47 N.. 227	C..-0.31 B. -1.23 S.. 0.95 N.. 148	C.. 0.46 B. 0.98 S.. 0.41 N.. 52	C.. 0.64 B. 0.03 S.. 0.35 N.. 139	C.. 0.88 B. -0.08 S.. 0.58 N.. 227
NOAA AVHRR NIGHT	..	..	C.. 0.96 B. 0.13 S.. 0.12 N.. 318	C.. 0.37 B. 0.55 S.. 0.42 N.. 318	C.. 0.37 B. 0.62 S.. 0.38 N.. 318	C..-0.14 B. -0.79 S.. 0.79 N.. 205	C.. 0.83 B. 1.40 S.. 0.22 N.. 62	C.. 0.83 B. 0.46 S.. 0.17 N.. 153	C.. 0.88 B. 0.40 S.. 0.36 N.. 318
NOAA AVHRR	..	..	..	C.. 0.39 B. 0.42 S.. 0.47 N.. 311	C.. 0.38 B. 0.49 S.. 0.48 N.. 311	C..-0.08 B. -0.93 S.. 0.79 N.. 205	C.. 0.68 B. 1.26 S.. 0.27 N.. 62	C.. 0.80 B. 0.30 S.. 0.21 N.. 153	C.. 0.83 B. 0.27 S.. 0.48 N.. 311
SUSSKIND HIRS	..	..	..	..	C.. 0.74 B. 0.67 S.. 0.27 N.. 311	C..-0.02 B. -1.22 S.. 0.83 N.. 205	C.. 0.76 B. 0.74 S.. 0.24 N.. 62	C.. 0.43 B. -0.12 S.. 0.35 N.. 153	C.. 0.88 B. -0.15 S.. 0.48 N.. 311
SUSSKIND HIRS VERSION 2	..	..	..	..	..	C.. 0.29 B. -1.29 S.. 0.75 N.. 205	C.. 0.78 B. 0.80 S.. 0.24 N.. 62	C.. 0.66 B. -0.21 S.. 0.22 N.. 153	C.. 0.69 B. -0.22 S.. 0.32 N.. 311
MILMAN SMMR NIGHT CELL 234	..	..	..	..	..	..	C.. 0.39 B. 2.22 S.. 0.78 N.. 33	C..-0.89 B. 0.77 S.. 0.67 N.. 95	C.. 0.89 B. 1.86 S.. 0.73 N.. 205
BATES VAS	..	..	..	..	..	..	..	C.. 0.79 B. -0.91 S.. 0.26 N.. 51	C.. 0.88 B. -1.13 S.. 0.37 N.. 62
PAZAN SHIPS >5/CELL	..	..	..	..	..	..	..	..	C.. 0.88 B. -0.10 S.. 0.27 N.. 153
CLIMATOL	..	..	..	..	..	..	..	..	..

(p) July 1982, Global

Two Degree Average SST Anomaly Cross Correlations
Region: 56 0 deg N to 56 0 deg S, 0 0 deg L to 360 0 deg E

At least 1 observation(s) at common grid points
(C--Cross Correlation, B--Bias, S--standard deviation about bias, N--Number of common valid observations)
Bias is average over column temperatures minus row temperatures

	NOAA AVHRR DAY JUL	NOAA AVHRR NIGHT	NOAA AVHRR	SUSSKIND HIRS	SUSSKIND HIRS WEIGHTED	MILMAN SMMR NIGHT CELL 234	WILHELIT/ HAN SMMR/SHIP COMPOSITE	BATES VAS	PAZAN SHIPS)5/CELL	PAZAN SHIPS)20/CELL	TRANSPAC XBT	CLIMATOL
NOAA AVHRR DAY JUL	..	C.. 0.82 B.. -0.12 S.. 0.36 N.. 1652	C.. 0.95 B.. -0.06 S.. 0.19 N.. 1640	C.. 0.60 B.. -0.10 S.. 0.47 N.. 1640	C.. 0.59 B.. -0.33 S.. 0.58 N.. 1640	C 0.39 B 0.08 S 0.77 N 1422	C 0.55 B 0.04 S 0.51 N 946	C. 0.55 B 0.05 S 0.48 N.. 183	C .0.83 B -0.79 S 0.52 N 74	C .1.08 B -0.48 S 0.58 N 2	..	C.. 0.00 B.. -0.11 S.. 0.59 N.. 1680
NOAA AVHRR NIGHT	..	..	C.. 0.98 B 0.05 S.. 0.17 N.. 3649	C 0.68 B 0.12 S 0.61 N 3683	C 0.69 B -0.14 S 0.60 N 3683	C 0.69 B 0.27 S 0.64 N 2641	C 0.59 B 0.41 S 0.61 N 1906	C. 0.48 B 0.67 S 0.54 N 247	C 0.83 B 0.67 S 0.35 N 269	C.. 0.89 B 0.54 S 0.48 N 7	C .-0.81 B 0.69 S 0.47 N 3	C .0.00 B 0.36 S 0.83 N.. 3689
NOAA AVHRR	..	..	..	C 0.66 B 0.06 S 0.60 N 3721	C 0.69 B -0.19 S 0.59 N 3721	C 0.65 B 0.21 S 0.67 N 2644	C 3.55 B 0.24 S 0.63 N 2015	C. 0.45 B 0.67 S 0.53 N 249	C 0.78 B 0.35 S 0.52 N 274	C. 0.98 B 0.45 S 0.43 N 7	C .-0.90 B 0.18 S 0.77 N 3	C .0.00 B 0.38 S 0.82 N.. 3727
SUSSKIND HIRS	..	..	..	..	C 0.98 B -0.26 S 0.14 N.. 4889	C 0.45 B 0.15 S 0.77 N.. 2883	C.. 0.53 B 0.21 S 0.52 N.. 2181	C. 0.24 B 0.65 S 0.53 N.. 254	C.. 0.78 B.. -0.07 S 0.38 N.. 327	C.. 0.82 B -0.15 S 0.26 N 7	C .-0.98 B 0.09 S 0.61 N 3	C .0.00 B 0.26 S 0.52 N.. 4889
SUSSKIND HIRS WEIGHTED	..	..	..	..	..	C 0.44 B 0.39 S 0.79 N 2883	C 0.54 B 0.43 S 0.55 N 2181	C.. 0.17 B 1.06 S 0.68 N.. 254	C.. 0.79 B 0.25 S 0.38 N.. 327	C.. 0.25 B 0.23 S 0.23 N.. 7	C .-0.95 B 1.42 S 0.61 N 3	C .0.00 B 0.52 S 0.65 N.. 4889
MILMAN SMMR NIGHT CELL 234	..	..	..	..	..	..	C 0.87 B 0.20 S 0.35 N 1783	C 0.58 B 0.55 S 0.60 N 241	C 0.55 B 0.69 S 0.60 N 230	C .-1.00 B 1.01 S 0.09 N 2	C .0.00 B 0.61 S 0.00 N 1	C .0.00 B 0.03 S 0.84 N.. 2891
WILHELIT/ HAN SMMR/SHIP COMPOSITE	..	..	..	..	..	..	..	C 0.73 B 0.42 S 0.34 N 211	C 0.86 B 0.10 S 0.27 N 137	..	C .0.00 B 0.04 S 0.00 N 1	C .0.00 B -0.01 S 0.57 N 2190
BATES VAS	..	..	..	..	..	..	..	..	C 0.42 B -0.55 S 0.22 N 34	..	..	C .0.00 B -0.05 S 0.67 N.. 254
PAZAN SHIPS)5/CELL	..	..	..	..	..	..	..	..	..	C 1.00 B 0.00 S 0.00 N.. 7	C .-0.77 B 0.06 S 0.29 N 2	C .0.00 B 0.78 S 0.63 N.. 336
PAZAN SHIPS)20/CELL	..	..	..	..	..	..	..	..	..	..	..	C .0.00 B 0.72 S 0.21 N 7
TRANSPAC XBT	..	..	..	..	..	..	..	..	..	..	..	C .0.00 B 0.65 S 0.23 N 3
CLIMATOL	..	..	..	..	..	..	..	..	..	..	..	..

(q) July 1982, North Pacific

Two Degree Average SST Anomaly Cross Correlations
Region: 56.0 deg N to 28.0 deg N, 188.0 deg E to 298.0 deg E

At least 1 observation(s) at common grid points
(C--Cross Correlation, B--Bias, S--Standard Deviation
about bias, N--Number of common valid observations)
Bias is average over column temperatures minus row temperatures

	NOAA AVHRR DAY JUL	NOAA AVHRR NIGHT	NOAA AVHRR	SUSSKIND HIRS	SUSSKIND HIRS WEIGHTED	MILMAN SMMR NIGHT CELL 234	MILMEIT/ HAN SMMR/SHIP COMPOSITE	PAZAN SHIPS >5/CELL	TRANSPAC XBT	CLIMATOL
NOAA AVHRR DAY JUL	..	C.. 0.43 B. -1.27 S.. 0.67 N.. 56	C.. 0.95 B. -0.52 S.. 0.23 N.. 58	C -0.13 B. -0.67 S.. 0.84 N.. 58	C. -0.82 B. -1.08 S.. 0.86 N.. 58	C.. 0.45 B. -1.37 S.. 0.75 N.. 52	C.. 0.66 B. -0.97 S.. 0.54 N.. 58	C.. 0.68 B. -1.07 S.. 0.59 N.. 27	..	C.. 0.88 B. -0.26 S.. 0.72 N.. 58
NOAA AVHRR NIGHT	..	..	C.. 0.83 B. 0.22 S.. 0.36 N.. 421	C.. 0.72 B. 0.78 S.. 0.36 N.. 418	C.. 0.72 B. 0.38 S.. 0.36 N.. 418	C.. 0.58 B. 0.44 S.. 0.58 N.. 367	C.. 0.52 B. 0.77 S.. 0.52 N.. 401	C.. 0.67 B. 0.68 S.. 0.41 N.. 112	C..-0.81 B. 0.69 S.. 0.47 N.. 3	C.. 0.86 B. 1.28 S.. 0.52 N.. 421
NOAA AVHRR	..	..	..	C.. 0.47 B. 0.47 S.. 0.56 N.. 423	C.. 0.42 B. 0.15 S.. 0.59 N.. 423	C.. 0.39 B. 0.24 S.. 0.73 N.. 371	C.. 0.33 B. 0.55 S.. 0.68 N.. 405	C.. 0.63 B. 0.17 S.. 0.62 N.. 117	C..-0.98 B. 0.18 S.. 0.77 N.. 3	C.. 0.88 B. 0.97 S.. 0.64 N.. 426
SUSSKIND HIRS	..	..	..	..	C.. 0.95 B. -0.32 S.. 0.13 N.. 498	C.. 0.35 B. -0.21 S.. 0.78 N.. 415	C. 0.41 B. 0.88 S.. 0.57 N.. 453	C.. 0.52 B. -0.14 S.. 0.39 N.. 178	C..-0.98 B. 0.69 S.. 0.61 N.. 3	C.. 0.88 B. 0.56 S.. 0.48 N.. 498
SUSSKIND HIRS WEIGHTED	..	..	..	..	..	C.. 0.37 B. 0.10 S.. 0.78 N.. 415	C.. 0.38 B. 0.39 S.. 0.60 N.. 453	C.. 0.45 B. 0.23 S.. 0.43 N.. 178	C..-0.95 B. 0.42 S.. 0.61 N.. 3	C.. 0.88 B. 0.87 S.. 0.44 N.. 498
MILMAN SMMR NIGHT CELL 234	..	..	..	..	..	..	C.. 0.85 B. 0.28 S.. 0.48 N.. 422	C.. 0.62 B. 0.39 S.. 0.48 N.. 127	C.. 0.88 B. 0.61 S.. 0.89 N.. 1	C.. 0.88 B. 0.77 S.. 0.74 N.. 423
MILMEIT/ HAN SMMR/SHIP COMPOSITE	..	..	..	..	..	..	..	C.. 0.86 B. 0.10 S.. 0.27 N.. 147	C.. 0.88 B. 0.54 S.. 0.88 N.. 1	C.. 0.88 B. 0.48 S.. 0.62 N.. 462
PAZAN SHIPS >5/CELL	..	..	..	..	..	..	..	..	C -0.99 B. 0.86 S.. 0.28 N.. 2	C.. 0.88 B. 0.76 S.. 0.58 N.. 179
TRANSPAC XBT	..	..	..	..	..	..	..	..	..	C.. 0.88 B. 0.65 S.. 0.23 N.. 3
CLIMATOL	..	..	..	..	..	..	..	..	..	..

(r) July 1982, Mid Pacific

Two Degree Average SST Anomaly Cross Correlations
Region: 20.0 deg N to 20.0 deg S, 180.0 deg E to 290.0 deg E

At least 1 observation(s) at common grid points
(C--Cross Correlation, B--Bias, S--Standard Deviation
about bias, N--Number of common valid observations)
Bias is average over column temperatures minus row temperatures

	NOAA AVHRR DAY JUL	NOAA AVHRR NIGHT	NOAA AVHRR	SUSSKIND HIRS	SUSSKIND HIRS WEIGHTED	MILMAN SMMR NIGHT CELL 234	WILHEIT/ HAN SMMR/SHIP COMPOSITE	BATES VAS	PAZAN SHIPS >5/CELL	TRANSPAC XBT	CLIMATOL
NOAA AVHRR DAY JUL	..	C.. 0.83 B.. 0.03 S.. 0.22 N.. 396	C.. 0.98 B.. -0.01 S.. 0.08 N.. 414	C.. 0.35 B.. 0.10 S.. 0.45 N.. 414	C.. 0.35 B.. 0.03 S.. 0.50 N.. 414	C.. 0.42 B.. 0.09 S.. 0.47 N.. 313	C.. 0.68 B.. 0.12 S.. 0.34 N.. 412	C.. 0.74 B.. 0.68 S.. 0.32 N.. 113	..	..	C.. 0.88 B.. -0.05 S.. 0.41 N.. 414
NOAA AVHRR NIGHT	..	..	C.. 0.98 B.. 0.01 S.. 0.13 N.. 825	C.. 0.77 B.. 0.35 S.. 0.42 N.. 825	C.. 0.74 B.. 0.28 S.. 0.45 N.. 825	C.. 0.64 B.. 0.37 S.. 0.54 N.. 785	C.. 0.58 B.. 0.55 S.. 0.50 N.. 823	C.. 0.68 B.. 0.71 S.. 0.36 N.. 141	..	..	C.. 0.88 B.. 0.31 S.. 0.44 N.. 825
NOAA AVHRR	..	..	..	C.. 0.77 B.. 0.33 S.. 0.45 N.. 848	C.. 0.75 B.. 0.18 S.. 0.46 N.. 848	C.. 0.63 B.. 0.37 S.. 0.57 N.. 715	C.. 0.53 B.. 0.52 S.. 0.59 N.. 846	C.. 0.76 B.. 0.76 S.. 0.33 N.. 143	..	..	C.. 0.88 B.. 0.28 S.. 0.78 N.. 848
SUSSKIND HIRS	..	..	..	..	C.. 0.99 B.. -0.15 S.. 0.12 N.. 969	C.. 0.36 B.. 0.06 S.. 0.68 N.. 817	C.. 0.42 B.. 0.22 S.. 0.49 N.. 966	C.. 0.29 B.. 1.08 S.. 0.51 N.. 140	..	..	C.. 0.88 B.. 0.08 S.. 0.49 N.. 969
SUSSKIND HIRS WEIGHTED	..	..	..	..	..	C.. 0.32 B.. 0.22 S.. 0.67 N.. 817	C.. 0.48 B.. 0.38 S.. 0.55 N.. 966	C.. 0.23 B.. 1.24 S.. 0.56 N.. 140	..	..	C.. 0.88 B.. 0.15 S.. 0.57 N.. 969
MILMAN SMMR NIGHT CELL 234	..	..	..	..	..	..	C.. 0.83 B.. 0.21 S.. 0.32 N.. 814	C.. 0.71 B.. 0.28 S.. 0.37 N.. 146	..	..	C.. 0.88 B.. -0.03 S.. 0.57 N.. 817
WILHEIT/ HAN SMMR/SHIP COMPOSITE	..	..	..	..	..	..	..	C.. 0.88 B.. 0.48 S.. 0.29 N.. 140	..	..	C.. 0.88 B.. -0.23 S.. 0.41 N.. 966
BATES VAS	..	..	..	..	..	..	..	..	..	..	C.. 0.88 B.. -0.82 S.. 0.48 N.. 140
PAZAN SHIPS >5/CELL	..	..	..	..	..	..	..	..	..	..	..
TRANSPAC XBT	..	..	..	..	..	..	..	..	..	..	..

(s) July 1982, South Pacific

Two Degree Average SST Anomaly Cross Correlations
Region: 28.0 deg S to 56.0 deg S, 188.0 deg E to 298.0 deg E

At least 1 observation(s) at common grid points
(C--Cross Correlation, B--Bias, S--Standard Deviation
about bias, N--Number of common valid observations)
Bias is average over column temperatures minus row temperatures

	NOAA AVHRR DAY JUL	NOAA AVHRR NIGHT	NOAA AVHRR	SUSSKIND HIRS	SUSSKIND HIRS WEIGHTED	MILMAN SMMR NIGHT CELL 234	MILMAN/ HAN SMMR/SHIP COMPOSITE	BATES VAS	PAZAN SHIPS >5/CELL	CLIMATOL
NOAA AVHRR DAY JUL	..	C.. 0.98 B. -0.12 S.. 0.12 N.. 586	C.. 1.00 B. -0.03 S.. 0.84 N.. 586	C.. 0.84 B. -0.11 S.. 0.38 N.. 586	C.. 0.87 B. -0.35 S.. 0.33 N.. 586	C.. 0.64 B. 0.04 S.. 0.59 N.. 445	C.. 0.69 B. 0.10 S.. 0.50 N.. 476	C.. 0.60 B. 0.10 S.. 0.44 N.. 66	..	C.. 0.80 B. -0.04 S.. 0.68 N.. 586
NOAA AVHRR NIGHT	..	..	C.. 0.99 B. 0.05 S.. 0.08 N.. 968	C.. 0.72 B. -0.17 S.. 0.57 N.. 968	C.. 0.77 B. -0.42 S.. 0.52 N.. 968	C.. 0.59 B. 0.11 S.. 0.60 N.. 611	C.. 0.59 B. 0.08 S.. 0.53 N.. 762	C.. 0.52 B. 0.15 S.. 0.47 N.. 66	..	C.. 0.89 B. 0.17 S.. 0.81 N.. 968
NOAA AVHRR	..	..	..	C.. 0.75 B. -0.22 S.. 0.54 N.. 968	C.. 0.88 B. -0.47 S.. 0.49 N.. 968	C.. 0.59 B. 0.04 S.. 0.59 N.. 611	C.. 0.61 B. 0.02 S.. 0.58 N.. 762	C.. 0.59 B. 0.11 S.. 0.44 N.. 66	..	C.. 0.89 B. 0.12 S.. 0.81 N.. 968
SUSSKIND HIRS	..	..	..	..	C.. 0.99 B. -0.25 S.. 0.11 N.. 960	C.. 0.45 B. 0.26 S.. 0.62 N.. 611	C.. 0.48 B. 0.28 S.. 0.51 N.. 762	C..-0.07 B. 0.60 S.. 0.62 N.. 66	..	C.. 0.88 B. 0.34 S.. 0.51 N.. 968
SUSSKIND HIRS WEIGHTED	..	..	..	..	..	C.. 0.45 B. 0.58 S.. 0.64 N.. 611	C.. 0.52 B. 0.51 S.. 0.51 N.. 762	C..-0.24 B. 0.75 S.. 0.68 N.. 66	..	C.. 0.88 B. 0.59 S.. 0.57 N.. 968
MILMAN SMMR NIGHT CELL 234	..	..	..	..	..	..	C.. 0.84 B. 0.13 S.. 0.33 N.. 547	C.. 0.63 B. 0.35 S.. 0.48 N.. 59	..	C.. 0.88 B. -0.06 S.. 0.67 N.. 611
WILMEIT/ HAN SMMR/SHIP COMPOSITE	..	..	..	..	..	..	..	C.. 0.61 B. 0.47 S.. 0.43 N.. 63	..	C.. 0.88 B. -0.03 S.. 0.53 N.. 762
BATES VAS	..	..	..	..	..	..	..	..	..	C.. 0.88 B. -0.95 S.. 0.53 N.. 66
PAZAN SHIPS >5/CELL	..	..	..	..	..	..	..	..	..	..

(t) July 1982, North Atlantic

Two Degree Average SST Anomaly Cross Correlations
Region: 56.0 deg N to 8.0 deg S, 290.0 deg E to 360.0 deg E

At least 1 observation(s) at common grid points
(C--Cross Correlation, B--Bias, S--Standard Deviation
about bias, N--Number of common valid observations)
Bias is average over column temperatures minus row temperatures

	NOAA AVHRR DAY JUL	NOAA AVHRR NIGHT	NOAA AVHRR	SUSSKIND HIRS	SUSSKIND HIRS WEIGHTED	MILMAN SMMR NIGHT CELL 234	BATES VAS	PAZAN SHIPS >5/CELL	CLIMATOL
NOAA AVHRR DAY JUL	..	C.. 0.91 B.. -1.83 S.. 0.41 N.. 58	C.. 0.94 B.. -0.71 S.. 0.34 N.. 58	C.. 0.84 B.. -0.43 S.. 0.62 N.. 58	C.. 0.87 B.. -0.75 S.. 0.53 N.. 58	C.. 0.79 B.. -1.55 S.. 0.67 N.. 51	C.. 0.94 B.. -0.36 S.. 0.88 N.. 4	C.. 0.94 B.. -0.62 S.. 0.39 N.. 47	C.. 0.89 B.. -0.13 S.. 0.93 N.. 58
NOAA AVHRR NIGHT	..	..	C.. 0.97 B.. 0.14 S.. 0.15 N.. 236	C.. 0.81 B.. 0.65 S.. 0.34 N.. 236	C.. 0.83 B.. 0.34 S.. 0.31 N.. 236	C.. 0.68 B.. -0.42 S.. 0.45 N.. 158	C.. 0.84 B.. 1.38 S.. 0.19 N.. 48	C.. 0.89 B.. 0.65 S.. 0.31 N.. 157	C.. 0.88 B.. 1.01 S.. 0.57 N.. 236
NOAA AVHRR	..	..	..	C.. 0.79 B.. 0.51 S.. 0.39 N.. 236	C.. 0.88 B.. 0.28 S.. 0.37 N.. 236	C.. 0.57 B.. -0.58 S.. 0.49 N.. 158	C.. 0.88 B.. 1.29 S.. 0.28 N.. 48	C.. 0.84 B.. 0.48 S.. 0.37 N.. 157	C.. 0.88 B.. 0.87 S.. 0.61 N.. 236
SUSSKIND HIRS	..	..	..	..	C.. 0.97 B.. -0.32 S.. 0.14 N.. 311	C.. 0.44 B.. -0.97 S.. 0.42 N.. 231	C.. 0.78 B.. 0.74 S.. 0.15 N.. 48	C.. 0.85 B.. -0.84 S.. 0.36 N.. 157	C.. 0.88 B.. 0.48 S.. 0.37 N.. 311
SUSSKIND HIRS WEIGHTED	..	..	..	..	..	C.. 0.49 B.. -0.67 S.. 0.44 N.. 231	C.. 0.87 B.. 0.89 S.. 0.12 N.. 48	C.. 0.88 B.. 0.27 S.. 0.38 N.. 157	C.. 0.88 B.. 0.72 S.. 0.47 N.. 311
MILMAN SMMR NIGHT CELL 234	..	..	..	..	..	..	C.. 0.61 B.. 1.71 S.. 0.35 N.. 38	C.. 0.66 B.. 1.67 S.. 0.51 N.. 193	C.. 0.88 B.. 1.38 S.. 0.42 N.. 231
BATES VAS	..	..	..	..	..	..	..	C.. 0.42 B.. -0.55 S.. 0.22 N.. 38	C.. 0.88 B.. -0.79 S.. 0.24 N.. 48
PAZAN SHIPS >5/CELL	..	..	..	..	..	..	..	..	C.. 0.88 B.. 0.48 S.. 0.64 N.. 157
CLIMATOL	..	..	..	..	..	..	..	..	..

Table A-3. Same as Table A-2 Except HIRS and HIRS Version 2 Replaced by HIRS Version 2 Weighted and HIRS Version 2 Weighted Smoothed. (All Other Data Sets Smoothed.) (a) March 1982, Global.

Two Degree Average SST Anomaly Cross Correlations
Region: 56.0 deg N to 56.0 deg S, 0.0 deg E to 360.0 deg E

At least 1 observation(s) at common grid points
(C--Cross Correlation, B--Bias, S--Standard Deviation about bias, N--Number of common valid observations)
Bias is average over column temperatures minus row temperatures

	NOAA AVHRR DAY MAR	NOAA AVHRR NIGHT	NOAA AVHRR	SUSSKIND HIRS	SUSSKIND HIRS VERSION 2	MILMAN SMMR NIGHT CELL 234	WILHEIT/ HAN SMMR/SHIP COMPOSITE	BATES VAS	PAZAN SHIPS >5/CELL	PAZAN SHIPS >20/CELL	TRANSPAC XBT	CLIMATOL
NOAA AVHRR DAY MAR	..	C.. 0.93 B.. -0.37 S.. 0.31 N.. 3353	C.. 0.98 B.. -0.18 S.. 0.17 N.. 3404	C.. 0.58 B.. -0.53 S.. 0.71 N.. 3404	C.. 0.62 B.. -0.52 S.. 0.66 N.. 3404	C.. 0.62 B.. -0.37 S.. 0.77 N.. 2311	C.. 0.60 B.. -0.21 S.. 0.54 N.. 1686	C.. 0.17 B.. 0.24 S.. 0.65 N.. 291	C.. 0.74 B.. 0.18 S.. 0.33 N.. 239	C.. 0.21 B.. 0.13 S.. 0.21 N.. 9	C.. 0.91 B.. -0.29 S.. 0.27 N.. 9	C.. 0.00 B.. -0.48 S.. 0.84 N.. 3404
NOAA AVHRR NIGHT	..	..	C.. 0.98 B.. 0.17 S.. 0.18 N.. 3921	C.. 0.45 B.. -0.06 S.. 0.72 N.. 3921	C.. 0.49 B.. -0.06 S.. 0.66 N.. 3921	C.. 0.65 B.. 0.07 S.. 0.72 N.. 2807	C.. 0.71 B.. 0.27 S.. 0.40 N.. 2163	C.. 0.20 B.. 0.64 S.. 0.59 N.. 381	C.. 0.82 B.. 0.57 S.. 0.23 N.. 368	C.. 0.94 B.. 0.67 S.. 0.23 N.. 23	C.. 0.75 B.. 0.25 S.. 0.32 N.. 18	C.. 0.00 B.. 0.84 S.. 0.72 N.. 3921
NOAA AVHRR	..	..	..	C.. 0.45 B.. -0.24 S.. 0.76 N.. 3989	C.. 0.58 B.. -0.24 S.. 0.69 N.. 3989	C.. 0.65 B.. -0.12 S.. 0.73 N.. 2841	C.. 0.66 B.. 0.08 S.. 0.48 N.. 2158	C.. 0.21 B.. 0.51 S.. 0.59 N.. 381	C.. 0.77 B.. 0.44 S.. 0.29 N.. 368	C.. 0.92 B.. 0.60 S.. 0.28 N.. 23	C.. 0.78 B.. 0.14 S.. 0.35 N.. 18	C.. 0.00 B.. -0.14 S.. 0.79 N.. 3989
SUSSKIND HIRS	..	..	..	..	C.. 0.93 B.. 0.00 S.. 0.25 N.. 4021	C.. 0.17 B.. 0.02 S.. 1.00 N.. 2867	C.. 0.15 B.. 0.17 S.. 0.68 N.. 2198	C.. 0.48 B.. 0.41 S.. 0.58 N.. 381	C.. 0.48 B.. -0.29 S.. 0.41 N.. 368	C.. 0.11 B.. -0.18 S.. 0.47 N.. 23	C.. 0.48 B.. -0.76 S.. 0.52 N.. 18	C.. 0.00 B.. 0.18 S.. 0.64 N.. 4021
SUSSKIND HIRS VERSION 2	..	..	..	..	..	C.. 0.17 B.. 0.05 S.. 0.97 N.. 2867	C.. 0.14 B.. 0.20 S.. 0.61 N.. 2198	C.. 0.49 B.. 0.52 S.. 0.49 N.. 381	C.. 0.55 B.. -0.29 S.. 0.31 N.. 368	C.. 0.38 B.. -0.27 S.. 0.32 N.. 23	C.. 0.81 B.. -0.82 S.. 0.51 N.. 18	C.. 0.00 B.. 0.18 S.. 0.54 N.. 4021
MILMAN SMMR NIGHT CELL 234	..	..	..	..	..	..	C.. 0.02 B.. 0.28 S.. 0.39 N.. 1818	C.. -0.84 B.. 0.89 S.. 0.83 N.. 258	C.. 0.15 B.. 0.17 S.. 0.79 N.. 368	C.. -0.16 B.. -0.18 S.. 0.42 N.. 23	C.. 0.59 B.. -0.54 S.. 0.54 N.. 18	C.. 0.00 B.. -0.84 S.. 0.94 N.. 2867
WILHEIT/ HAN SMMR/SHIP COMPOSITE	..	..	..	..	..	..	..	C.. -0.88 B.. 0.39 S.. 0.61 N.. 234	C.. 0.75 B.. -0.87 S.. 0.25 N.. 207	C.. 0.51 B.. -0.85 S.. 0.15 N.. 14	C.. 0.78 B.. -0.46 S.. 0.31 N.. 18	C.. 0.00 B.. -0.18 S.. 0.46 N.. 2198
BATES VAS	..	..	..	..	..	..	..	..	C.. 2.79 B.. -0.91 S.. 0.26 N.. 51	..	..	0.00 -0.68 0.56 301
PAZAN SHIPS >5/CELL	..	..	..	..	..	..	..	..	..	C.. 1.00 B.. 0.00 S.. 0.00 N.. 23	C.. 0.78 B.. -0.47 S.. 0.35 N.. 18	0.00 13
PAZAN SHIPS >20/CELL	..	..	..	..	..	..	..	..	..	..	C.. 0.98 B.. -0.49 S.. 0.15 N.. 4	C.. 0.00 B.. 0.01 S.. 0.23 N.. 23
TRANSPAC XBT	..	..	..	..	..	..	..	..	..	..	..	C.. 0.00 B.. 0.77 S.. 0.48 N.. 18
CLIMATOL												

APPENDIX B

ERROR-PARTITIONING TABLES

Table B-1. Partitioned rms Error Between Triplet Combinations of the 2° - Binned SST Anomaly Data Sets: AVHRR, SMMR, HIRS, and Climatology: (a) November 1979, AVHRR.

RMS ERROR TABLE FOR DATA SET 1

FILE NAME: SSTSHOP:[SST]AAE60004.BLY
DESCRIPTION: NOAA AVHRR
LATITUDE BOUNDS= -55 TO 55 LONGITUDE BOUNDS= 0 TO 360

OVERALL AVERAGE RMS ERROR= 0.53

	1	2	3	4
1	-----	-----	-----	-----
2	-----	-----	0.34	0.59
3	-----	3772	-----	0.67
4	-----	3773	4538	-----

UPPER RIGHT TRIANGLE OF TABLE CONTAINS RMS ERROR IN TRIAD

LOWER LEFT TRIANGLE OF TABLE CONTAINS NUMBER COMMON GRID POINTS IN TRIAD

ROW AND COLUMN NUMBER OF TABLE DEFINE THE 2ND AND 3RD DATA SETS IN TRIAD

ROW/COLUMN	FILE NAME	DESCRIPTION
1	SSTSHOP:[SST]AAE60004.BLY	NOAA AVHRR
2	SSTSHOP.[SST]SDC60004.BLY	SMMR CELLS 234
3	SSTSHOP:[SST]hcg60004.BLY	HIRS/MSU2
4	SSTSHOP:[SST]tgz600.bin	CLIMATOLOGY

(b) November 1979, SMMR

RMS ERROR TABLE FOR DATA SET 2

FILE NAME: SSTSHOP:[SST]SDC80004.BLY
DESCRIPTION: SMMR CELLS 234
LATITUDE BOUNDS= -55 TO 55 LONGITUDE BOUNDS= 0 TO 360

OVERALL AVERAGE RMS ERROR= 0.87

	1	2	3	4
1	-----	-----	0.91	0.77
2	-----	-----	-----	-----
3	3772	-----	-----	0.94
4	3773	-----	3849	-----

UPPER RIGHT TRIANGLE OF TABLE CONTAINS RMS ERROR IN TRIAD

LOWER LEFT TRIANGLE OF TABLE CONTAINS NUMBER COMMON GRID POINTS IN TRIAD

ROW AND COLUMN NUMBER OF TABLE DEFINE THE 2ND AND 3RD DATA SETS IN TRIAD

ROW/COLUMN	FILE NAME	DESCRIPTION
1	SSTSHOP:[SST]AAE80004.BLY	NOAA AVHRR
2	SSTSHOP:[SST]SDC80004.BLY	SMMR CELLS 234
3	SSTSHOP:[SST]hcg80004.BLY	HIRS/MSU2
4	SSTSHOP:[SST]tgz600.bin	CLIMATOLOGY

(c) November 1979, HIRS

RMS ERROR TABLE FOR DATA SET 3

FILE NAME: SSTSHOP:[SST]hcg60804.BLY
DESCRIPTION: HIRS/MSU2
LATITUDE BOUNDS= -55 TO 55 LONGITUDE BOUNDS= 0 TO 360

OVERALL AVERAGE RMS ERROR= 0.56

	1	2	3	4
1	-----	0.66	-----	0.40
2	3772	-----	-----	0.62
3	-----	-----	-----	-----
4	4538	3849	-----	-----

UPPER RIGHT TRIANGLE OF TABLE CONTAINS RMS ERROR IN TRIAD

LOWER LEFT TRIANGLE OF TABLE CONTAINS NUMBER COMMON GRID POINTS IN TRIAD

ROW AND COLUMN NUMBER OF TABLE DEFINE THE 2ND AND 3RD DATA SETS IN TRIAD

ROW/COLUMN	FILE NAME	DESCRIPTION
1	SSTSHOP:[SST]RAE60804.BLY	NOAA AVHRR
2	SSTSHOP:[SST]SOC60804.BLY	SMMR CELLS 234
3	SSTSHOP:[SST]hcg60804.BLY	HIRS/MSU2
4	SSTSHOP:[SST]tgz680.bin	CLIMATOLOGY

(d) November 1979, Climatology

RMS ERROR TABLE FOR DATA SET 4

FILE NAME: SSTSHOP:[SST]tgz600.bin
DESCRIPTION: CLIMATOLOGY
LATITUDE BOUNDS= -55 TO 55 LONGITUDE BOUNDS= 0 TO 360

OVERALL AVERAGE RMS ERROR= 0.63

	1	2	3	4
1	-----	0.70	0.76	-----
2	3773	-----	0.45	-----
3	4538	3849	-----	-----
4	-----	-----	-----	-----

UPPER RIGHT TRIANGLE OF TABLE CONTAINS RMS ERROR IN TRIAD

LOWER LEFT TRIANGLE OF TABLE CONTAINS NUMBER COMMON GRID POINTS IN TRIAD

ROW AND COLUMN NUMBER OF TABLE DEFINE THE 2ND AND 3RD DATA SETS IN TRIAD

ROW/COLUMN	FILE NAME	DESCRIPTION
1	SSTSHOP:[SST]AAE60004.BLY	NOAA AVHRR
2	SSTSHOP:[SST]SDC60004.BLY	SMMR CELLS 234
3	SSTSHOP:[SST]hcg60004.BLY	HIRS/MSU2
4	SSTSHOP:[SST]tgz600.bin	CLIMATOLOGY

(e) December 1981, AVHRR

RMS ERROR TABLE FOR DATA SET 1

FILE NAME: SSTSHOP:[SST]AAE60003.BLY
DESCRIPTION: NOAA AVHRR
LATITUDE BOUNDS= -55 TO 55 LONGITUDE BOUNDS= 0 TO 360

OVERALL AVERAGE RMS ERROR= 0.49

	1	2	3	4
1	-----	-----	-----	-----
2	-----	-----	0.38	0.45
3	-----	3840	-----	0.72
4	-----	3840	4612	-----

UPPER RIGHT TRIANGLE OF TABLE CONTAINS RMS ERROR IN TRIAD

LOWER LEFT TRIANGLE OF TABLE CONTAINS NUMBER COMMON GRID POINTS IN TRIAD

ROW AND COLUMN NUMBER OF TABLE DEFINE THE 2ND AND 3RD DATA SETS IN TRIAD

ROW/COLUMN	FILE NAME	DESCRIPTION
1	SSTSHOP:[SST]AAE60003.BLY	NOAA AVHRR
2	SSTSHOP:[SST]SDC60003.BLY	SMMR CELLS 234
3	SSTSHOP:[SST]hcg60003.BLY	HIRS/MSU2
4	SSTSHOP:[SST]tgz600.bin	CLIMATOLOGY

(f) December 1981, SMMR

RMS ERROR TABLE FOR DATA SET 2

FILE NAME: SSTSHOP:[SST]SDC60003.BLY
DESCRIPTION: SMMR CELLS 234
LATITUDE BOUNDS= -55 TO 55 LONGITUDE BOUNDS= 0 TO 360

OVERALL AVERAGE RMS ERROR= 0.95

	1	2	3	4
1	-----	-----	0.92	0.86
2	-----	-----	-----	-----
3	3840	-----	-----	1.08
4	3840	-----	3352	-----

UPPER RIGHT TRIANGLE OF TABLE CONTAINS RMS ERROR IN TRIAD

LOWER LEFT TRIANGLE OF TABLE CONTAINS NUMBER COMMON GRID POINTS IN TRIAD

ROW AND COLUMN NUMBER OF TABLE DEFINE THE 2ND AND 3RD DATA SETS IN TRIAD

ROW/COLUMN	FILE NAME	DESCRIPTION
1	SSTSHOP:[SST]AAE60003.BLY	NOAA AVHRR
2	SSTSHOP:[SST]SDC60003.BLY	SMMR CELLS 234
3	SSTSHOP:[SST]hcg60003.BLY	HIRS/MSU2
4	SSTSHOP:[SST]tgz600.bin	CLIMATOLOGY

(g) December 1981, HIRS

RMS ERROR TABLE FOR DATA SET 3

FILE NAME: SSTSHOP:[SST]hcg60003.BLY
DESCRIPTION: HIRS/MSU2
LATITUDE BOUNDS= -55 TO 55 LONGITUDE BOUNDS= 0 TO 360

OVERALL AVERAGE RMS ERROR= 0.53

	1	2	3	4
1	-----	0.74	-----	0.40
2	3840	-----	-----	0.46
3	-----	-----	-----	-----
4	4612	3852	-----	-----

UPPER RIGHT TRIANGLE OF TABLE CONTAINS RMS ERROR IN TRIAD

LOWER LEFT TRIANGLE OF TABLE CONTAINS NUMBER COMMON GRID POINTS IN TRIAD

ROW AND COLUMN NUMBER OF TABLE DEFINE THE 2ND AND 3RD DATA SETS IN TRIAD

ROW/COLUMN	FILE NAME	DESCRIPTION
1	SSTSHOP:[SST]AAE60003.BLY	NOAA AVHRR
2	SSTSHOP:[SST]SDC60003.BLY	SMMR CELLS 234
3	SSTSHOP:[SST]hcg60003.BLY	HIRS/MSU2
4	SSTSHOP:[SST]tgz000.bin	CLIMATOLOGY

(h) December 1981, Climatology

RMS ERROR TABLE FOR DATA SET 4

FILE NAME: SSTSHOP:[SST]tgz600.bin
DESCRIPTION: CLIMATOLOGY
LATITUDE BOUNDS= -55 TO 55 LONGITUDE BOUNDS= 0 TO 360

OVERALL AVERAGE RMS ERROR= 0.50

	1	2	3	4
1	-----	0.73	0.48	-----
2	3340	-----	0.30	-----
3	4612	3852	-----	-----
4	-----	-----	-----	-----

UPPER RIGHT TRIANGLE OF TABLE CONTAINS RMS ERROR IN TRIAD

LOWER LEFT TRIANGLE OF TABLE CONTAINS NUMBER COMMON GRID POINTS IN TRIAD

ROW AND COLUMN NUMBER OF TABLE DEFINE THE 2ND AND 3RD DATA SETS IN TRIAD

ROW/COLUMN	FILE NAME	DESCRIPTION
1	SSTSHOP:[SST]AAE60003.BLY	NOAA AVHRR
2	SSTSHOP:[SST]SDC60003.BLY	SMMR CELLS 234
3	SSTSHOP:[SST]hcg60003.BLY	HIRS/MSU2
4	SSTSHOP:[SST]tgz600.bin	CLIMATOLOGY

(i) March 1982, AVHRR

RMS ERROR TABLE FOR DATA SET 1

FILE NAME: SSTSHOP:[SST]AAE60002.BLY
DESCRIPTION: NOAA AVHRR
LATITUDE BOUNDS= -55 TO 55 LONGITUDE BOUNDS= 0 TO 360

OVERALL AVERAGE RMS ERROR= 0.60

	1	2	3	4
1	-----	-----	-----	-----
2	-----	-----	0.60	0.62
3	-----	3780	-----	0.59
4	-----	3781	4612	-----

UPPER RIGHT TRIANGLE OF TABLE CONTAINS RMS ERROR IN TRIAD

LOWER LEFT TRIANGLE OF TABLE CONTAINS NUMBER COMMON GRID POINTS IN TRIAD

ROW AND COLUMN NUMBER OF TABLE DEFINE THE 2ND AND 3RD DATA SETS IN TRIAD

ROW/COLUMN	FILE NAME	DESCRIPTION
1	SSTSHOP:[SST]AAE60002.BLY	NOAA AVHRR
2	SSTSHOP:[SST]SDC60002.BLY	SMMR CELLS 234
3	SSTSHOP:[SST]hag60002.BLY	HIRS/MSU2
4	SSTSHOP:[SST]tgz600.bin	CLIMATOLOGY

(j) March 1982, SMMR

RMS ERROR TABLE FOR DATA SET 2

FILE NAME: SSTSHOP:[SST]SDC60002.BLY
DESCRIPTION: SMMR CELLS 234
LATITUDE BOUNDS= -55 TO 55 LONGITUDE BOUNDS= 0 TO 360

OVERALL AVERAGE RMS ERROR= 0.98

	1	2	3	4
1	-----	-----	0.98	0.97
2	-----	-----	-----	-----
3	3780	-----	-----	0.98
4	3781	-----	3790	-----

UPPER RIGHT TRIANGLE OF TABLE CONTAINS RMS ERROR IN TRIAD

LOWER LEFT TRIANGLE OF TABLE CONTAINS NUMBER COMMON GRID POINTS IN TRIAD

ROW AND COLUMN NUMBER OF TABLE DEFINE THE 2ND AND 3RD DATA SETS IN TRIAD

ROW/COLUMN	FILE NAME	DESCRIPTION
1	SSTSHOP:[SST]AAE60002.BLY	NOAA AVHRR
2	SSTSHOP:[SST]SDC60002.BLY	SMMR CELLS 234
3	SSTSHOP:[SST]hag60002.BLY	HIRS/MSU2
4	SSTSHOP:[SST]tgz600.bin	CLIMATOLOGY

(k) March 1982, HIRS

RMS ERROR TABLE FOR DATA SET 3

FILE NAME: SSTSHOP:[SST]hag60002.BLY
DESCRIPTION: HIRS/MSU2
LATITUDE BOUNDS= -55 TO 55 LONGITUDE BOUNDS= 0 TO 360

OVERALL AVERAGE RMS ERROR= 0.68

	1	2	3	4
1	-----	0.65	-----	0.72
2	3780	-----	-----	0.66
3	-----	-----	-----	-----
4	4612	3790	-----	-----

UPPER RIGHT TRIANGLE OF TABLE CONTAINS RMS ERROR IN TRIAD

LOWER LEFT TRIANGLE OF TABLE CONTAINS NUMBER COMMON GRID POINTS IN TRIAD

ROW AND COLUMN NUMBER OF TABLE DEFINE THE 2ND AND 3RD DATA SETS IN TRIAD

ROW/COLUMN	FILE NAME	DESCRIPTION
1	SSTSHOP:[SST]AAE60002.BLY	NOAA AVHRR
2	SSTSHOP:[SST]SDC60002.BLY	SMMR CELLS 234
3	SSTSHOP:[SST]hag60002.BLY	HIRS/MSU2
4	SSTSHOP:[SST]tgz600.bin	CLIMATOLOGY

(1) March 1982, Climatology

RMS ERROR TABLE FOR DATA SET 4

FILE NAME: SSTSHOP:[SST]tgz600.bin
DESCRIPTION: CLIMATOLOGY
LATITUDE BOUNDS= -55 TO 55 LONGITUDE BOUNDS= 0 TO 360

OVERALL AVERAGE RMS ERROR= 0.43

	1	2	3	4
1	-----	0.40	0.50	-----
2	3781	-----	0.38	-----
3	4612	3790	-----	-----
4	-----	-----	-----	-----

UPPER RIGHT TRIANGLE OF TABLE CONTAINS RMS ERROR IN TRIAD

LOWER LEFT TRIANGLE OF TABLE CONTAINS NUMBER COMMON GRID POINTS IN TRIAD

ROW AND COLUMN NUMBER OF TABLE DEFINE THE 2ND AND 3RD DATA SETS IN TRIAD

ROW/COLUMN	FILE NAME	DESCRIPTION
1	SSTSHOP:[SST]AAE60002.BLY	NOAA AVHRR
2	SSTSHOP:[SST]SDC60002.BLY	SMMR CELLS 234
3	SSTSHOP:[SST]hag60002.BLY	HIRS/MSU2
4	SSTSHOP:[SST]tgz600.bin	CLIMATOLOGY

(m) July 1982, AVHRR

RMS ERROR TABLE FOR DATA SET 1

FILE NAME: SSTSHOP:[SST]AAE60001.BLY
DESCRIPTION: NOAA AVHRR
LATITUDE BOUNDS= -55 TO 55 LONGITUDE BOUNDS= 0 TO 360

OVERALL AVERAGE RMS ERROR= 0.87

	1	2	3	4
1	-----	-----	-----	-----
2	-----	-----	0.76	0.88
3	-----	2138	-----	0.98
4	-----	2139	4094	-----

UPPER RIGHT TRIANGLE OF TABLE CONTAINS RMS ERROR IN TRIAD

LOWER LEFT TRIANGLE OF TABLE CONTAINS NUMBER COMMON GRID POINTS IN TRIAD

ROW AND COLUMN NUMBER OF TABLE DEFINE THE 2ND AND 3RD DATA SETS IN TRIAD

ROW/COLUMN	FILE NAME	DESCRIPTION
1	SSTSHOP:[SST]AAE60001.BLY	NOAA AVHRR
2	SSTSHOP:[SST]SDC60001.BLY	SMMR CELLS 234
3	SSTSHOP:[SST]hag60001.BLY	HIRS/MSU2
4	SSTSHOP:[SST]tgz600.bin	CLIMATOLOGY

(n) July 1982, SMMR

RMS ERROR TABLE FOR DATA SET 2

FILE NAME: SSTSHOP:[SST]SDC60001.BLY
DESCRIPTION: SMMR CELLS 234
LATITUDE BOUNDS= -55 TO 55 LONGITUDE BOUNDS= 0 TO 360

OVERALL AVERAGE RMS ERROR= 1.01

	1	2	3	4
1	-----	-----	1.05	0.95
2	-----	-----	-----	-----
3	2138	-----	-----	1.03
4	2139	-----	2305	-----

UPPER RIGHT TRIANGLE OF TABLE CONTAINS RMS ERROR IN TRIAD

LOWER LEFT TRIANGLE OF TABLE CONTAINS NUMBER COMMON GRID POINTS IN TRIAD

ROW AND COLUMN NUMBER OF TABLE DEFINE THE 2ND AND 3RD DATA SETS IN TRIAD

ROW/COLUMN	FILE NAME	DESCRIPTION
1	SSTSHOP:[SST]ARE60001.BLY	NOAA AVHRR
2	SSTSHOP:[SST]SDC60001.BLY	SMMR CELLS 234
3	SSTSHOP:[SST]hag60001.BLY	HIRS/MSU2
4	SSTSHOP:[SST]tgz000.bin	CLIMATOLOGY

(o) July 1982, HIRS

RMS ERROR TABLE FOR DATA SET 3

FILE NAME: SSTSHOP:[SST]hag60001.BLY
DESCRIPTION: HIRS/MSU2
LATITUDE BOUNDS= -55 TO 55 LONGITUDE BOUNDS= 0 TO 360

OVERALL AVERAGE RMS ERROR= 0.75

	1	2	3	4
1	-----	0.74	-----	0.76
2	2138	-----	-----	0.75
3	-----	-----	-----	-----
4	4094	2385	-----	-----

UPPER RIGHT TRIANGLE OF TABLE CONTAINS RMS ERROR IN TRIAD

LOWER LEFT TRIANGLE OF TABLE CONTAINS NUMBER COMMON GRID POINTS IN TRIAD

ROW AND COLUMN NUMBER OF TABLE DEFINE THE 2ND AND 3RD DATA SETS IN TRIAD

ROW/COLUMN	FILE NAME	DESCRIPTION
1	SSTSHOP:[SST]RAE60001.BLY	NOAA AVHRR
2	SSTSHOP:[SST]SDC60001.BLY	SMMR CELLS 234
3	SSTSHOP:[SST]hag60001.BLY	HIRS/MSU2
4	SSTSHOP:[SST]tgz600.bin	CLIMATOLOGY

(p) July 1982, Climatology

RMS ERROR TABLE FOR DATA SET 4

FILE NAME: SSTSHOP:[SST]tgz600.bin
DESCRIPTION: CLIMATOLOGY
LATITUDE BOUNDS= -55 TO 55 LONGITUDE BOUNDS= 0 TO 360

OVERALL AVERAGE RMS ERROR= 0.47

	1	2	3	4
1	-----	0.58	0.45	-----
2	2139	-----	0.39	-----
3	4094	2305	-----	-----
4	-----	-----	-----	-----

UPPER RIGHT TRIANGLE OF TABLE CONTAINS RMS ERROR IN TRIAD

LOWER LEFT TRIANGLE OF TABLE CONTAINS NUMBER COMMON GRID POINTS IN TRIAD

ROW AND COLUMN NUMBER OF TABLE DEFINE THE 2ND AND 3RD DATA SETS IN TRIAD

ROW/COLUMN	FILE NAME	DESCRIPTION
1	SSTSHOP:[SST]RAE60001.BLY	NOAA AVHRR
2	SSTSHOP:[SST]SDC60001.BLY	SMMR CELLS 234
3	SSTSHOP:[SST]hag60001.BLY	HIRS/MSU2
4	SSTSHOP:[SST]tgz600.bin	CLIMATOLOGY

Table B-2. Partitioned rms Error Between Triplet Combinations of the 2° - Binned SST Anomaly Data Sets With 3 x 3 Cell Spatial Filter Applied: AVHRR, SMMR, HIRS, and Climatology. (a) November 1979, AVHRR.

RMS ERROR TABLE FOR DATA SET 1

FILE NAME: SSTSHOP:[SST]AREs60001.BLY
DESCRIPTION: NOAA AVHRR
LATITUDE BOUNDS= -55 TO 55 LONGITUDE BOUNDS= 0 TO 360

OVERALL AVERAGE RMS ERROR= 0.82

	1	2	3	4
1	-----	-----	-----	-----
2	-----	-----	0.70	0.88
3	-----	1496	-----	0.86
4	-----	1502	3889	-----

UPPER RIGHT TRIANGLE OF TABLE CONTAINS RMS ERROR IN TRIAD

LOWER LEFT TRIANGLE OF TABLE CONTAINS NUMBER COMMON GRID POINTS IN TRIAD

ROW AND COLUMN NUMBER OF TABLE DEFINE THE 2ND AND 3RD DATA SETS IN TRIAD

ROW/COLUMN	FILE NAME	DESCRIPTION
1	SSTSHOP:[SST]AREs60001.BLY	NOAA AVHRR
2	SSTSHOP:[SST]SDCs60001.BLY	SMMR CELLS 234
3	SSTSHOP:[SST]hgs60001.BLY	HIRS/MSU2
4	SSTSHOP:[SST]tgzs600.bin	CLIMATOLOGY

(b) November 1979, SMMR

RMS ERROR TABLE FOR DATA SET 2

FILE NAME: SSTSHOP:[SST]SDCs60001.BLY
DESCRIPTION: SMMR CELLS 234
LATITUDE BOUNDS= -55 TO 55 LONGITUDE BOUNDS= 0 TO 360

OVERALL AVERAGE RMS ERROR= 0.87

	1	2	3	4
1	-----	-----	0.98	0.82
2	-----	-----	-----	-----
3	1496	-----	-----	0.82
4	1502	-----	1846	-----

UPPER RIGHT TRIANGLE OF TABLE CONTAINS RMS ERROR IN TRIAD

LOWER LEFT TRIANGLE OF TABLE CONTAINS NUMBER COMMON GRID POINTS IN TRIAD

ROW AND COLUMN NUMBER OF TABLE DEFINE THE 2ND AND 3RD DATA SETS IN TRIAD

ROW/COLUMN	FILE NAME	DESCRIPTION
1	SSTSHOP:[SST]AAEs60001.BLY	NOAA AVHRR
2	SSTSHOP:[SST]SDCs60001.BLY	SMMR CELLS 234
3	SSTSHOP:[SST]hags60001.BLY	HIRS/MSU2
4	SSTSHOP:[SST]tgzs600.bin	CLIMATOLOGY

(c) November 1979, HIRS

RMS ERROR TABLE FOR DATA SET 3

FILE NAME: SSTSHOP:[SST]hags60001.BLY
DESCRIPTION: HIRS/MSU2
LATITUDE BOUNDS= -55 TO 55 LONGITUDE BOUNDS= 0 TO 360

OVERALL AVERAGE RMS ERROR= 0.37

	1	2	3	4
1	-----	0.26	-----	0.37
2	1496	-----	-----	0.48
3	-----	-----	-----	-----
4	3089	1845	-----	-----

UPPER RIGHT TRIANGLE OF TABLE CONTAINS RMS ERROR IN TRIAD

LOWER LEFT TRIANGLE OF TABLE CONTAINS NUMBER COMMON GRID POINTS IN TRIAD

ROW AND COLUMN NUMBER OF TABLE DEFINE THE 2ND AND 3RD DATA SETS IN TRIAD

ROW/COLUMN	FILE NAME	DESCRIPTION
1	SSTSHOP:[SST]AREs60001.BLY	NOAA AVHRR
2	SSTSHOP:[SST]SDCs60001.BLY	SMMR CELLS 234
3	SSTSHOP:[SST]hags60001.BLY	HIRS/MSU2
4	SSTSHOP:[SST]tgzs600.bin	CLIMATOLOGY

(d) November 1979, Climatology

RMS ERROR TABLE FOR DATA SET 4

FILE NAME: SSTSHOP:[SST]tgzs600.bin
DESCRIPTION: CLIMATOLOGY
LATITUDE BOUNDS= -55 TO 55 LONGITUDE BOUNDS= 0 TO 360

OVERALL AVERAGE RMS ERROR= 0.42

	1	2	3	4
1	-----	0.44	0.47	-----
2	1502	-----	0.36	-----
3	3089	1846	-----	-----
4	-----	-----	-----	-----

UPPER RIGHT TRIANGLE OF TABLE CONTAINS RMS ERROR IN TRIAD

LOWER LEFT TRIANGLE OF TABLE CONTAINS NUMBER COMMON GRID POINTS IN TRIAD

ROW AND COLUMN NUMBER OF TABLE DEFINE THE 2ND AND 3RD DATA SETS IN TRIAD

ROW/COLUMN	FILE NAME	DESCRIPTION
1	SSTSHOP:[SST]AAEs60001.BLY	NOAA AVHRR
2	SSTSHOP:[SST]SDCs60001.BLY	SMMR CELLS 234
3	SSTSHOP:[SST]hags60001.BLY	HIRS/MSU2
4	SSTSHOP:[SST]tgzs600.bin	CLIMATOLOGY

(e) December 1981, AVHRR

RMS ERROR TABLE FOR DATA SET 1

FILE NAME: SSTSHOP:[SST]AAEs60002.BLY
DESCRIPTION: NOAA AVHRR
LATITUDE BOUNDS= -55 TO 55 LONGITUDE BOUNDS= 0 TO 360

OVERALL AVERAGE RMS ERROR= 0.47

	1	2	3	4
1	-----	-----	-----	-----
2	-----	-----	0.48	0.50
3	-----	2827	-----	0.44
4	-----	2831	3970	-----

UPPER RIGHT TRIANGLE OF TABLE CONTAINS RMS ERROR IN TRIAD

LOWER LEFT TRIANGLE OF TABLE CONTAINS NUMBER COMMON GRID POINTS IN TRIAD

ROW AND COLUMN NUMBER OF TABLE DEFINE THE 2ND AND 3RD DATA SETS IN TRIAD

ROW/COLUMN	FILE NAME	DESCRIPTION
1	SSTSHOP:[SST]AAEs60002.BLY	NOAA AVHRR
2	SSTSHOP:[SST]SDCs60002.BLY	SMMR CELLS 234
3	SSTSHOP:[SST]hagsC0002.BLY	HIRS/MSU2
4	SSTSHOP:[SST]tgzs600.bin	CLIMATOLOGY

(f) December 1981, SMMR

RMS ERROR TABLE FOR DATA SET 2

FILE NAME: SSTSHOP:[SST]SDCs60002.BLY

DESCRIPTION: SMMR CELLS 234

LATITUDE BOUNDS= -55 TO 55 LONGITUDE BOUNDS= 0 TO 360

OVERALL AVERAGE RMS ERROR= 0.77

	1	2	3	4
1	-----	-----	0.78	0.76
2	-----	-----	-----	-----
3	2827	-----	-----	0.77
4	2831	-----	2863	-----

UPPER RIGHT TRIANGLE OF TABLE CONTAINS RMS ERROR IN TRIAD

LOWER LEFT TRIANGLE OF TABLE CONTAINS NUMBER COMMON GRID POINTS IN TRIAD

ROW AND COLUMN NUMBER OF TABLE DEFINE THE 2ND AND 3RD DATA SETS IN TRIAD

ROW/COLUMN	FILE NAME	DESCRIPTION
1	SSTSHOP:[SST]AAEs60002.BLY	NOAA AVHRR
2	SSTSHOP:[SST]SDCs60002.BLY	SMMR CELLS 234
3	SSTSHOP:[SST]hags60002.BLY	HIRS/MSU2
4	SSTSHOP.[SST]tgzs600.bin	CLIMATOLOGY

(g) December 1981, HIRS

RMS ERROR TABLE FOR DATA SET 3

FILE NAME: SSTSHOP:[SST]hags60002.BLY
DESCRIPTION: HIRS/MSU2
LATITUDE BOUNDS= -55 TO 55 LONGITUDE BOUNDS= 0 TO 360

OVERALL AVERAGE RMS ERROR= 0.47

	1	2	3	4
1	-----	0.42	-----	0.55
2	2827	-----	-----	0.44
3	-----	-----	-----	-----
4	3970	2863	-----	-----

UPPER RIGHT TRIANGLE OF TABLE CONTAINS RMS ERROR IN TRIAD

LOWER LEFT TRIANGLE OF TABLE CONTAINS NUMBER COMMON GRID POINTS IN TRIAD

ROW AND COLUMN NUMBER OF TABLE DEFINE THE 2ND AND 3RD DATA SETS IN TRIAD

ROW/COLUMN	FILE NAME	DESCRIPTION
1	SSTSHOP:[SST]AAEs60002.BLY	NOAA AVHRR
2	SSTSHOP:[SST]SDCs60002.BLY	SMMR CELLS 234
3	SSTSHOP:[SST]hagsf0002.BLY	HIRS/MSU2
4	SSTSHOP:[SST]tgzs600.bin	CLIMATOLOGY

(h) December 1981, Climatology

RMS ERROR TABLE FOR DATA SET 4

FILE NAME: SSTSHOP:[SST]tgzs600.bin
DESCRIPTION: CLIMATOLOGY
LATITUDE BOUNDS= -55 TO 55 LONGITUDE BOUNDS= 0 TO 360

OVERALL AVERAGE RMS ERROR= 0.38

	1	2	3	4
1	-----	0.34	0.48	-----
2	2831	-----	0.32	-----
3	3970	2863	-----	-----
4	-----	-----	-----	-----

UPPER RIGHT TRIANGLE OF TABLE CONTAINS RMS ERROR IN TRIAD

LOWER LEFT TRIANGLE OF TABLE CONTAINS NUMBER COMMON GRID POINTS IN TRIAD

ROW AND COLUMN NUMBER OF TABLE DEFINE THE 2ND AND 3RD DATA SETS IN TRIAD

ROW/COLUMN	FILE NAME	DESCRIPTION
1	SSTSHOP:[SST]RAEs60002.BLY	NOAA AVHRR
2	SSTSHOP:[SST]SDCs60002.BLY	SMMR CELLS 234
3	SSTSHOP:[SST]hags60002.BLY	HIRS/MSU2
4	SSTSHOP:[SST]tgzs600.bin	CLIMATOLOGY

(i) March 1982, AVHRR

RMS ERROR TABLE FOR DATA SET 1

FILE NAME: SSTSHOP:[SST]AAEs60003.BLY
DESCRIPTION: NOAA AVHRR
LATITUDE BOUNDS= -55 TO 55 LONGITUDE BOUNDS= 0 TO 360

OVERALL AVERAGE RMS ERROR= 0.42

	1	2	3	4
1	-----	-----	-----	-----
2	-----	-----	0.23	0.38
3	-----	2841	-----	0.66
4	-----	2841	3989	-----

UPPER RIGHT TRIANGLE OF TABLE CONTAINS RMS ERROR IN TRIAD

LOWER LEFT TRIANGLE OF TABLE CONTAINS NUMBER COMMON GRID POINTS IN TRIAD

ROW AND COLUMN NUMBER OF TABLE DEFINE THE 2ND AND 3RD DATA SETS IN TRIAD

ROW/COLUMN	FILE NAME	DESCRIPTION
1	SSTSHOP:[SST]AAEs60003.BLY	NOAA AVHRR
2	SSTSHOP:[SST]SDCs60003.BLY	SMMR CELLS 234
3	SSTSHOP:[SST]hcgs60003.BLY	HIRS/MSU2
4	SSTSHOP:[SST]tgzs600.bin	CLIMATOLOGY

(j) March 1982, SMMR

RMS ERROR TABLE FOR DATA SET 2

FILE NAME: SSTSHOP:[SST]SDCs60003.BLY
DESCRIPTION: SMMR CELLS 234
LATITUDE BOUNDS= -55 TO 55 LONGITUDE BOUNDS= 0 TO 360

OVERALL AVERAGE RMS ERROR= 0.75

	1	2	3	4
1	-----	-----	0.71	0.64
2	-----	-----	-----	-----
3	2841	-----	-----	0.91
4	2841	-----	2867	-----

UPPER RIGHT TRIANGLE OF TABLE CONTAINS RMS ERROR IN TRIAD

LOWER LEFT TRIANGLE OF TABLE CONTAINS NUMBER COMMON GRID POINTS IN TRIAD

ROW AND COLUMN NUMBER OF TABLE DEFINE THE 2ND AND 3RD DATA SETS IN TRIAD

ROW/COLUMN	FILE NAME	DESCRIPTION
1	SSTSHOP:[SST]AREs60003.BLY	NOAA AVHRR
2	SSTSHOP:[SST]SDCs60003.BLY	SMMR CELLS 234
3	SSTSHOP:[SST]hcgs60003.BLY	HIRS/MSU2
4	SSTSHOP:[SST]tgzs600.bin	CLIMATOLOGY

(k) March 1982, HIRS

RMS ERROR TABLE FOR DATA SET 3

FILE NAME: SSTSHOP:[SST]hcgs60003.BLY
DESCRIPTION: HIRC/MSU2
LATITUDE BOUNDS= -55 TO 55 LONGITUDE BOUNDS= 0 TO 360

OVERALL AVERAGE RMS ERROR= 0.45

	1	2	3	4
1	-----	0.67	-----	0.32
2	2841	-----	-----	0.36
3	-----	-----	-----	-----
4	3989	2867	-----	-----

UPPER RIGHT TRIANGLE OF TABLE CONTAINS RMS ERROR IN TRIAD

LOWER LEFT TRIANGLE OF TABLE CONTAINS NUMBER COMMON GRID POINTS IN TRIAD

ROW AND COLUMN NUMBER OF TABLE DEFINE THE 2ND AND 3RD DATA SETS IN TRIAD

ROW/COLUMN	FILE NAME	DESCRIPTION
1	SSTSHOP:[SST]AAEs60003.BLY	NOAA AVHRR
2	SSTSHOP:[SST]SDCs60003.BLY	SMMR CELLS 234
3	SSTSHOP:[SST]hcgs60003.BLY	HIRS/MSU2
4	SSTSHOP:[SST]tgzs600.bin	CLIMATOLOGY

(1) March 1982, Climatology

RMS ERROR TABLE FOR DATA SET 4

FILE NAME: SSTSHOP:[SST]tgzs600.bin
DESCRIPTION. CLIMATOLOGY
LATITUDE BOUNDS= -55 TO 55 LONGITUDE BOUNDS= 0 TO 360

OVERALL AVERAGE RMS ERROR= 0.47

	1	2	3	4
1	-----	0.69	0.45	-----
2	2841	-----	0.26	-----
3	3989	2867	-----	-----
4	-----	-----	-----	-----

UPPER RIGHT TRIANGLE OF TABLE CONTAINS RMS ERROR IN TRIAD

LOWER LEFT TRIANGLE OF TABLE CONTAINS NUMBER COMMON GRID POINTS IN TRIAD

ROW AND COLUMN NUMBER OF TABLE DEFINE THE 2ND AND 3RD DATA SETS IN TRIAD

ROW/COLUMN	FILE NAME	DESCRIPTION
1	SSTSHOP:[SST]AVHRRs60003.BLY	NOAA AVHRR
2	SSTSHOP:[SST]SMMRs60003.BLY	SMMR CELLS 234
3	SSTSHOP:[SST]hcgs60003.BLY	HIRS/MSU2
4	SSTSHOP:[SST]tgzs600.bin	CLIMATOLOGY

(m) July 1982, AVHRR

RMS ERROR TABLE FOR DATA SET 1

FILE NAME: SSTSHOP:[SST]AREs60004.BLV
DESCRIPTION: NOAA AVHRR
LATITUDE BOUNDS= -55 TO 55 LONGITUDE BOUNDS= 0 TO 360

OVERALL AVERAGE RMS ERROR= 0.39

	1	2	3	4
1	-----	-----	-----	-----
2	-----	-----	0.20	0.44
3	-----	2661	-----	0.53
4	-----	2664	3721	-----

UPPER RIGHT TRIANGLE OF TABLE CONTAINS RMS ERROR IN TRIAD

LOWER LEFT TRIANGLE OF TABLE CONTAINS NUMBER COMMON GRID POINTS IN TRIAD

ROW AND COLUMN NUMBER OF TABLE DEFINE THE 2ND AND 3RD DATA SETS IN TRIAD

ROW/COLUMN	FILE NAME	DESCRIPTION
1	SSTSHOP:[SST]AREs60004.BLV	NOAA AVHRR
2	SSTSHOP:[SST]SDCs60004.BLV	SMMR CELLS 234
3	SSTSHOP:[SST]hcgs60004.BLV	HIRS/MSU2
4	SSTSHOP:[SST]tgzs600.bin	CLIMATOLOGY

(n) July 1982, SMMR

RMS ERROR TABLE FOR DATA SET 2

FILE NAME: SSTSHOP:[SST]SDCs60004.BLY
DESCRIPTION: SMMR CELLS 234
LATITUDE BOUNDS= -55 TO 55 LONGITUDE BOUNDS= 0 TO 360

OVERALL AVERAGE RMS ERROR= 0.65

	1	2	3	4
1	-----	-----	0.67	0.55
2	-----	-----	-----	-----
3	2661	-----	-----	0.72
4	2664	-----	2893	-----

UPPER RIGHT TRIANGLE OF TABLE CONTAINS RMS ERROR IN TRIAD

LOWER LEFT TRIANGLE OF TABLE CONTAINS NUMBER COMMON GRID POINTS IN TRIAD

ROW AND COLUMN NUMBER OF TABLE DEFINE THE 2ND AND 3RD DATA SETS IN TRIAD

ROW/COLUMN	FILE NAME	DESCRIPTION
1	SSTSHOP.[SST]AAEs60004.BLY	NOAA AVHRR
2	SSTSHOP:[SST]SDCs60004.BLY	SMMR CELLS 234
3	SSTSHOP:[SST]hcgs60004.BLY	HIRS/MSU2
4	SSTSHOP:[SST]tgzs600.bin	CLIMATOLOGY

(o) July 1982, HIRS

RMS ERROR TABLE FOR DATA SET 3

FILE NAME: SSTSHOP:[SST]hcgs60004.BLY
DESCRIPTION: HIRS/MSU2
LATITUDE BOUNDS= -55 TO 55 LONGITUDE BOUNDS= 0 TO 360

OVERALL AVERAGE RMS ERROR= 0.46

	1	2	3	4
1	-----	0.57	-----	0.33
2	2661	-----	-----	0.50
3	-----	-----	-----	-----
4	3721	2883	-----	-----

UPPER RIGHT TRIANGLE OF TABLE CONTAINS RMS ERROR IN TRIAD

LOWER LEFT TRIANGLE OF TABLE CONTAINS NUMBER COMMON GRID POINTS IN TRIAD

ROW AND COLUMN NUMBER OF TABLE DEFINE THE 2ND AND 3RD DATA SETS IN TRIAD

ROW/COLUMN	FILE NAME	DESCRIPTION
1	SSTSHOP:[SST]AREs60004.BLY	NOAA AVHRR
2	SSTSHOP:[SST]SDCs60004.BLY	SMMR CELLS 234
3	SSTSHOP:[SST]hcgs60004.BLY	HIRS/MSU2
4	SSTSHOP:[SST]tgzs000.bin	CLIMATOLOGY

(p) July 1982, Climatology

RMS ERROR TABLE FOR DATA SET 4

FILE NAME: SSTSHOP:[SST]tgzs600.bin
Description: Climatology
Latitude Bounds = -55 to 55
Longitude Bounds = 0 to 360
Overall Average rms Error = 0.59

1	-----	0.64	0.69	-----
2	2664	-----	0.46	-----
3	3721	2883	-----	-----
4	-----	-----	-----	-----

UPPER RIGHT TRIANGLE OF TABLE CONTAINS RMS ERROR IN TRIAD

LOWER LEFT TRIANGLE OF TABLE CONTAINS NUMBER COMMON GRID POINTS IN TRIAD

ROW AND COLUMN NUMBER OF TABLE DEFINE THE 2ND AND 3RD DATA SETS IN TRIAD

ROW/COLUMN	FILE NAME	DESCRIPTION
1	SSTSHOP:[SST]AAEs60004.BLY	NOAA AVHRR
2	SSTSHOP:[SST]SDCs60004.BLY	SMMR CELLS 234
3	SSTSHOP:[SST]hcgs60004.BLY	HIRS/MSU2
4	SSTSHOP:[SST]tgzs600.bin	CLIMATOLOGY

Table B-3. Average Partitioned rms Error for Each Sensor: (a) No Smoothing; (b) 3 x 3 Spatial Filter Applied to all 2° - Binned Data.

		November 1979	December 1981	March 1982	July 1982
(a)	AVHRR	0.53	0.49	0.60	0.87
	SMMR	0.87	0.95	0.98	1.01
	HIRS	0.56	0.53	0.68	0.75
	Climatology	0.63	0.50	0.43	0.47
(b)	AVHRR	0.82	0.47	0.42	0.39
	SMMR	0.87	0.77	0.75	0.65
	HIRS	0.37	0.47	0.45	0.46
	Climatology	0.42	0.38	0.47	0.59

APPENDIX C

COLOR IMAGES

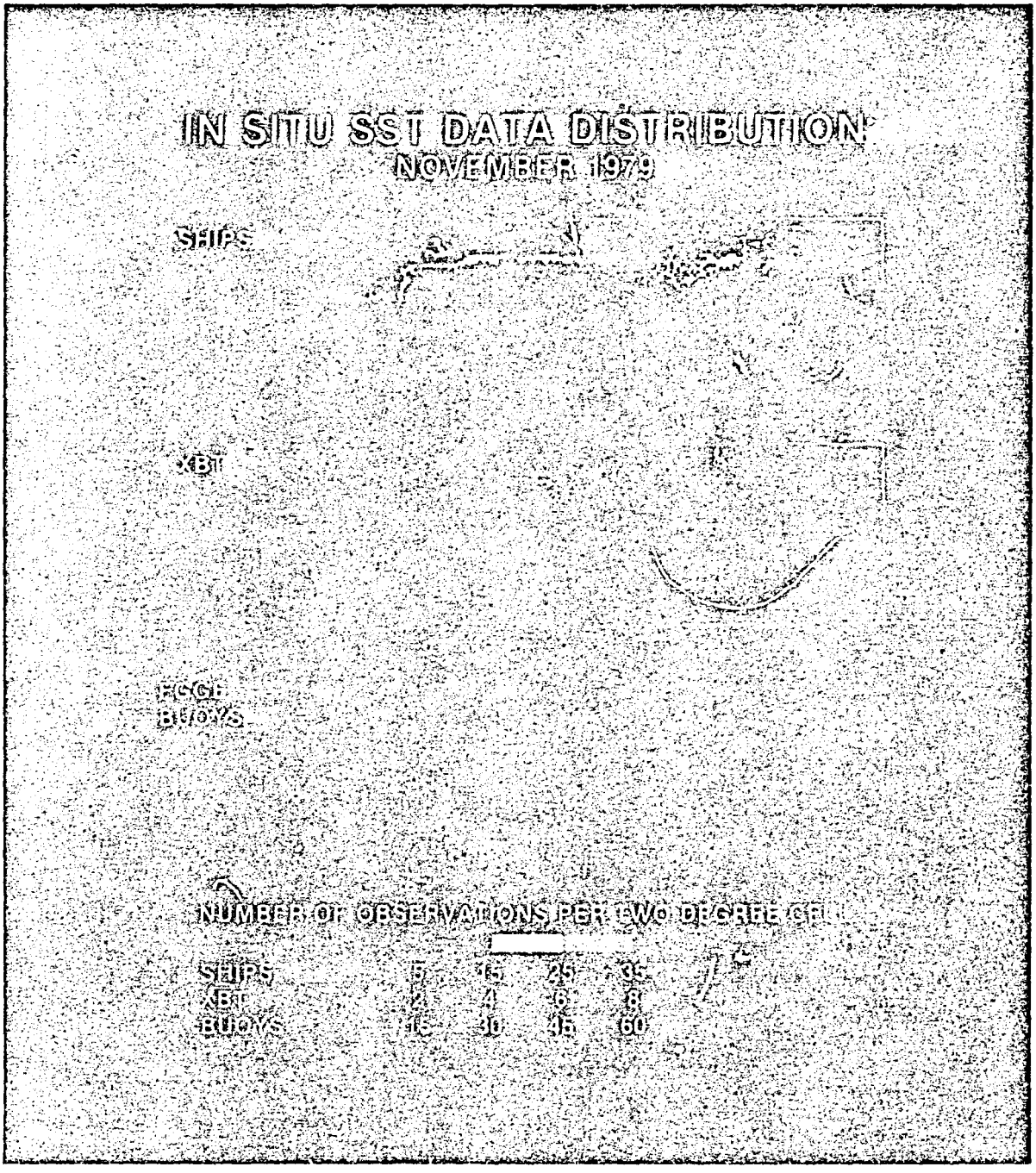

Figure C-1. In situ data distribution for November 1979 showing the number of SST measurements per month per 2° latitude-longitude bin for (a) ships, (b) XBT's, (c) FGGE buoys.

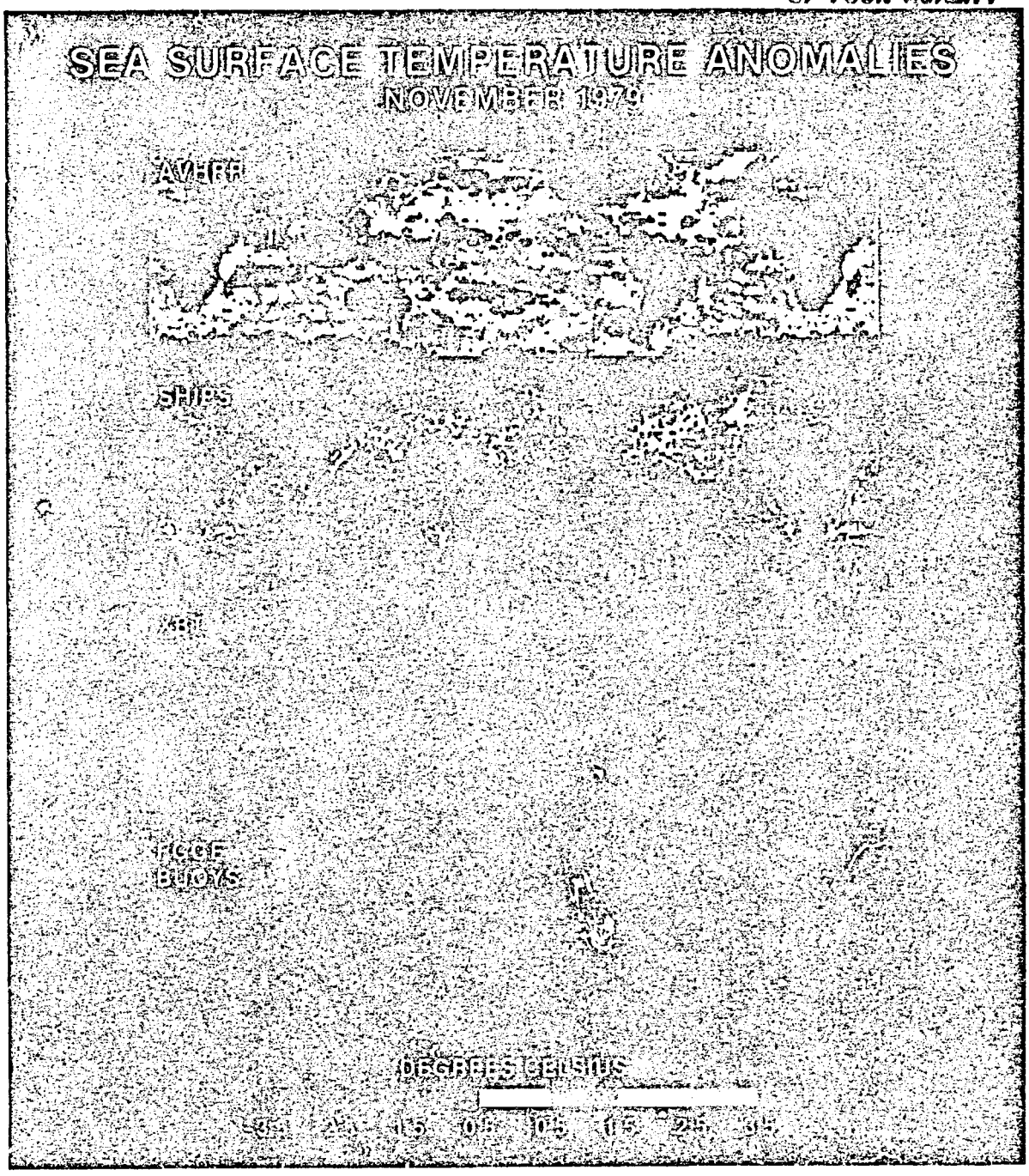

Figure C-2. SST anomalies for November 1979: (a) AVHRR, (b) ships, (c) XBT's, (d) FGGE buoys.

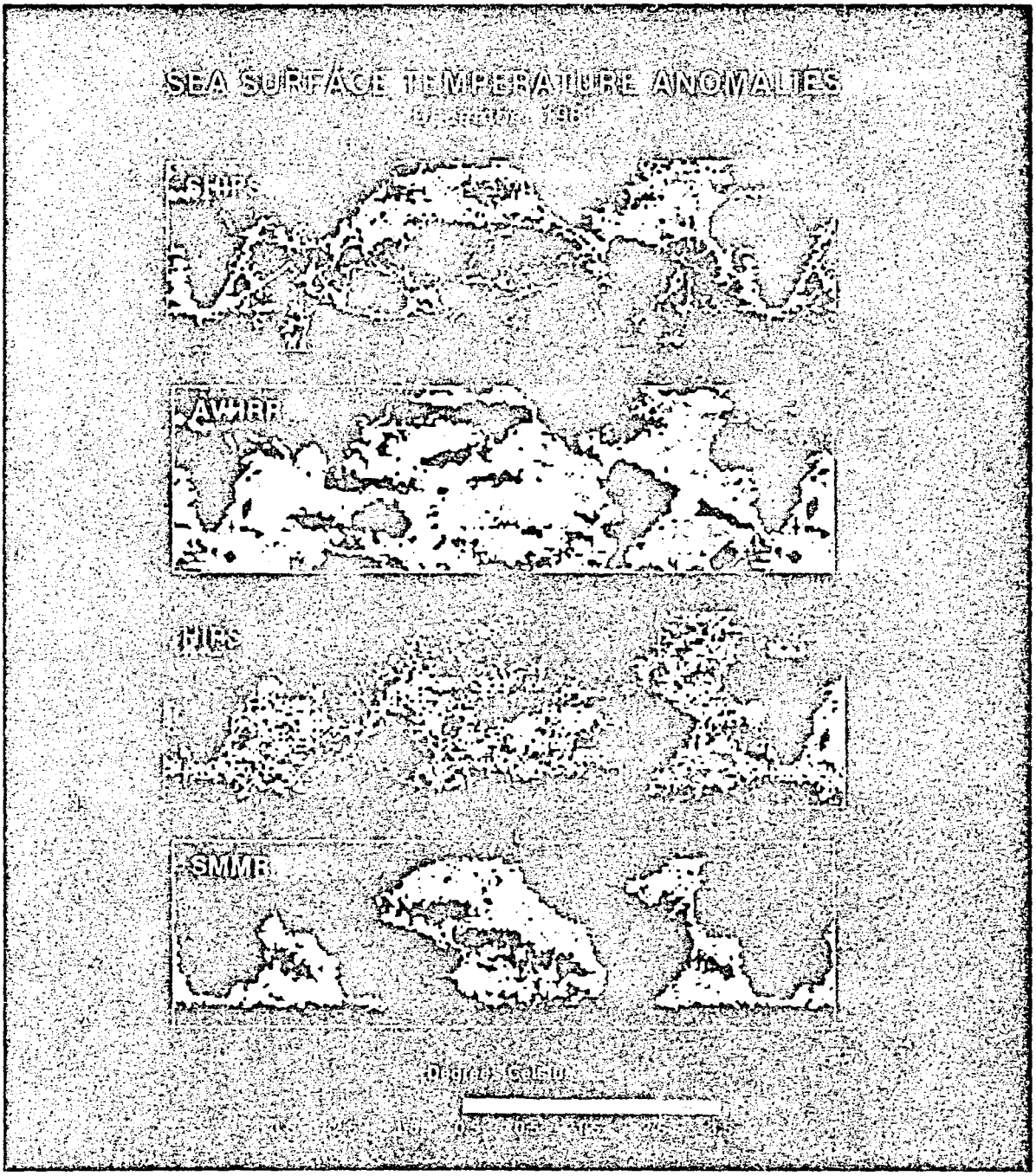

Figure C-3. SST anomalies for December 1981: (a) ships, (b) AVHRR, (c) HIRS, (d) SMMR.

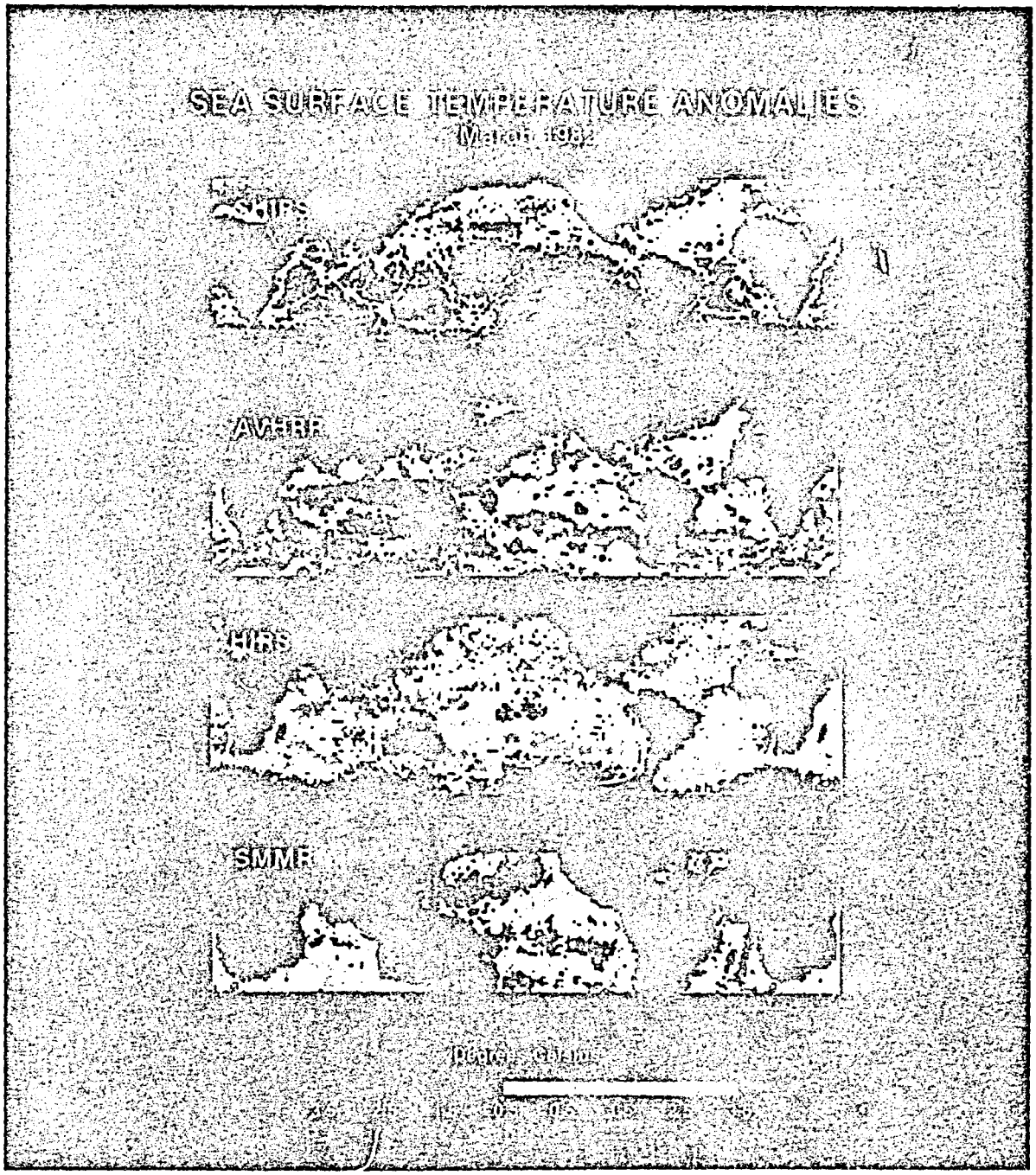

Figure C-4. SST anomalies for March 1982: (a) ships, (b) AVHRR, (c) HIRS, (d) SMMR.

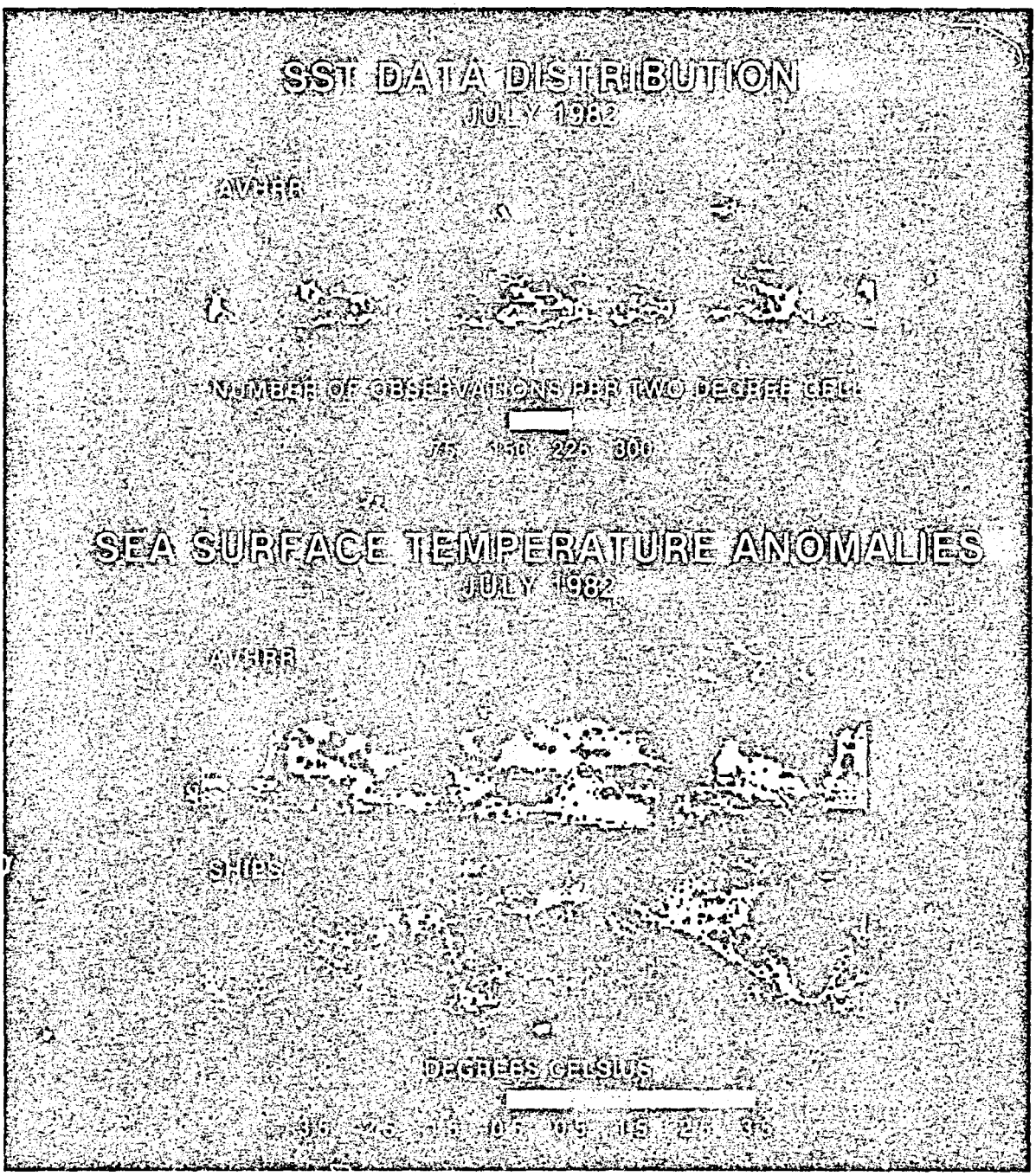

Figure C-5. For July, 1982: (a) AVHRR SST data distribution, (b) AVHRR SST anomalies, (c) ship SST anomalies.

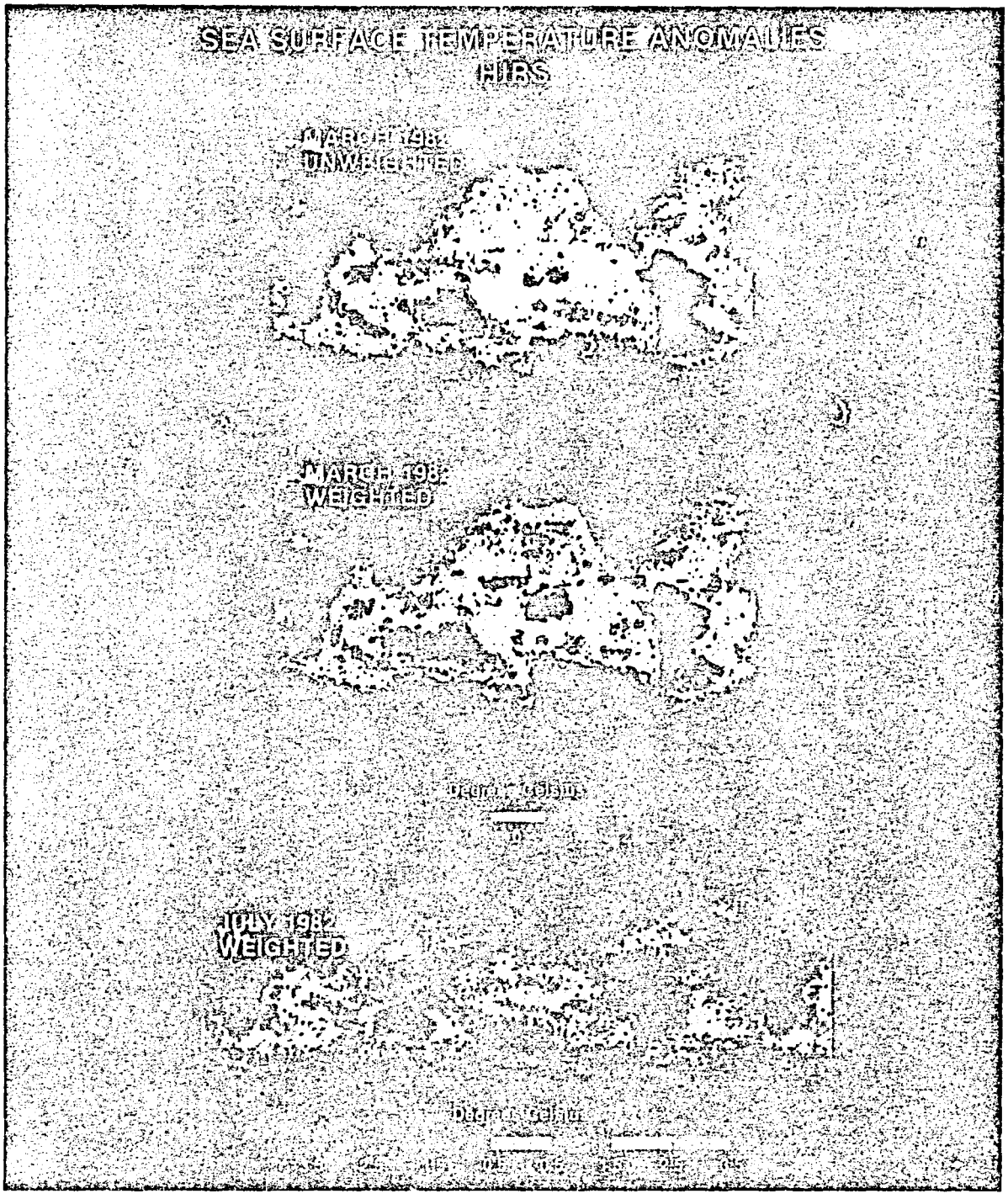

Figure C-6. HIRS SST anomalies for: (a) March 1982 unweighted (supplied by J. Susskind), (b) March 1982 weighted (supplied by J. Susskind), (c) July 1982 weighted.

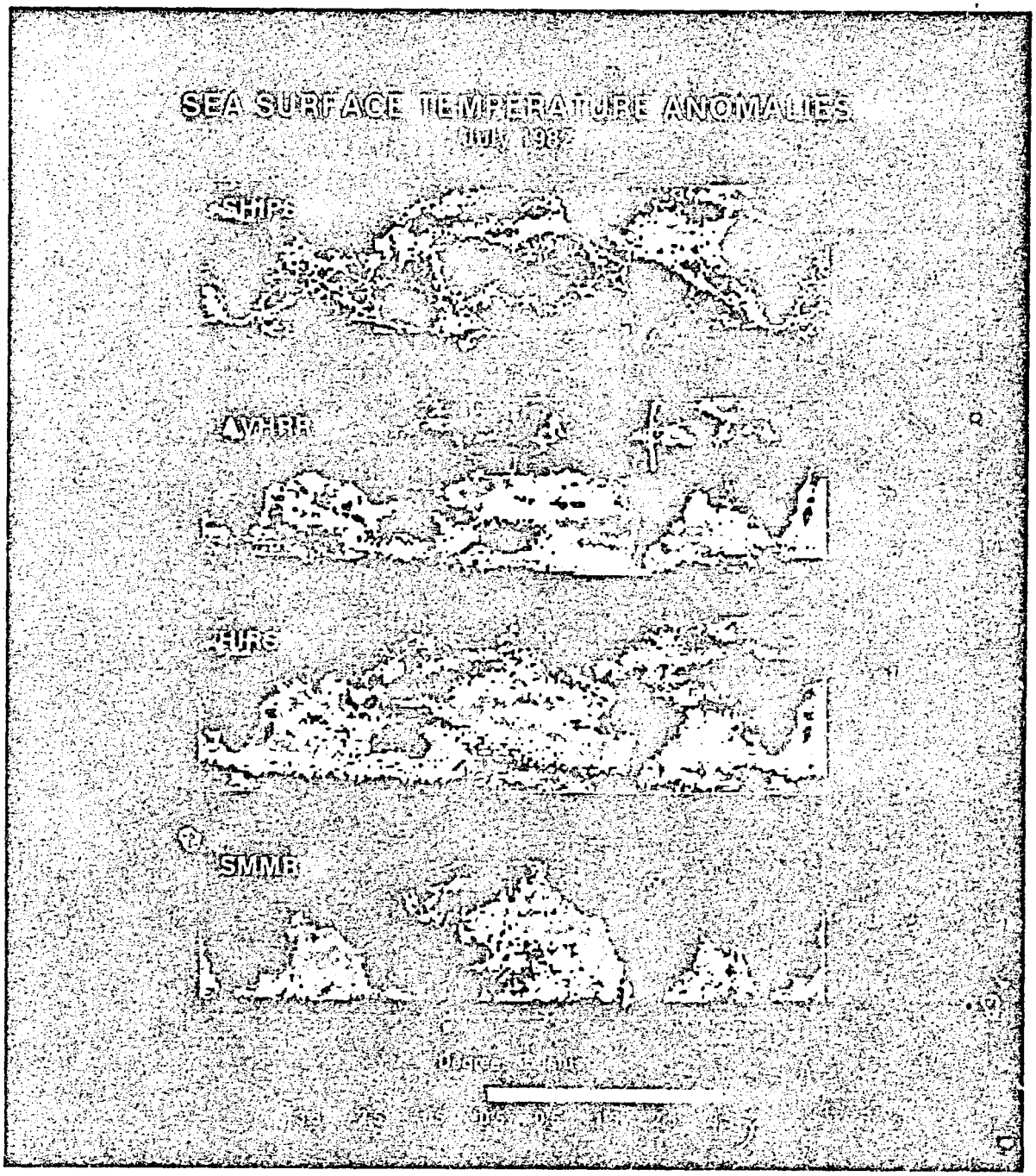

Figure C-7. SST anomalies for July 1982: (a) ships, (b) AVHRR, (c) HIRS, (d) SMMR.

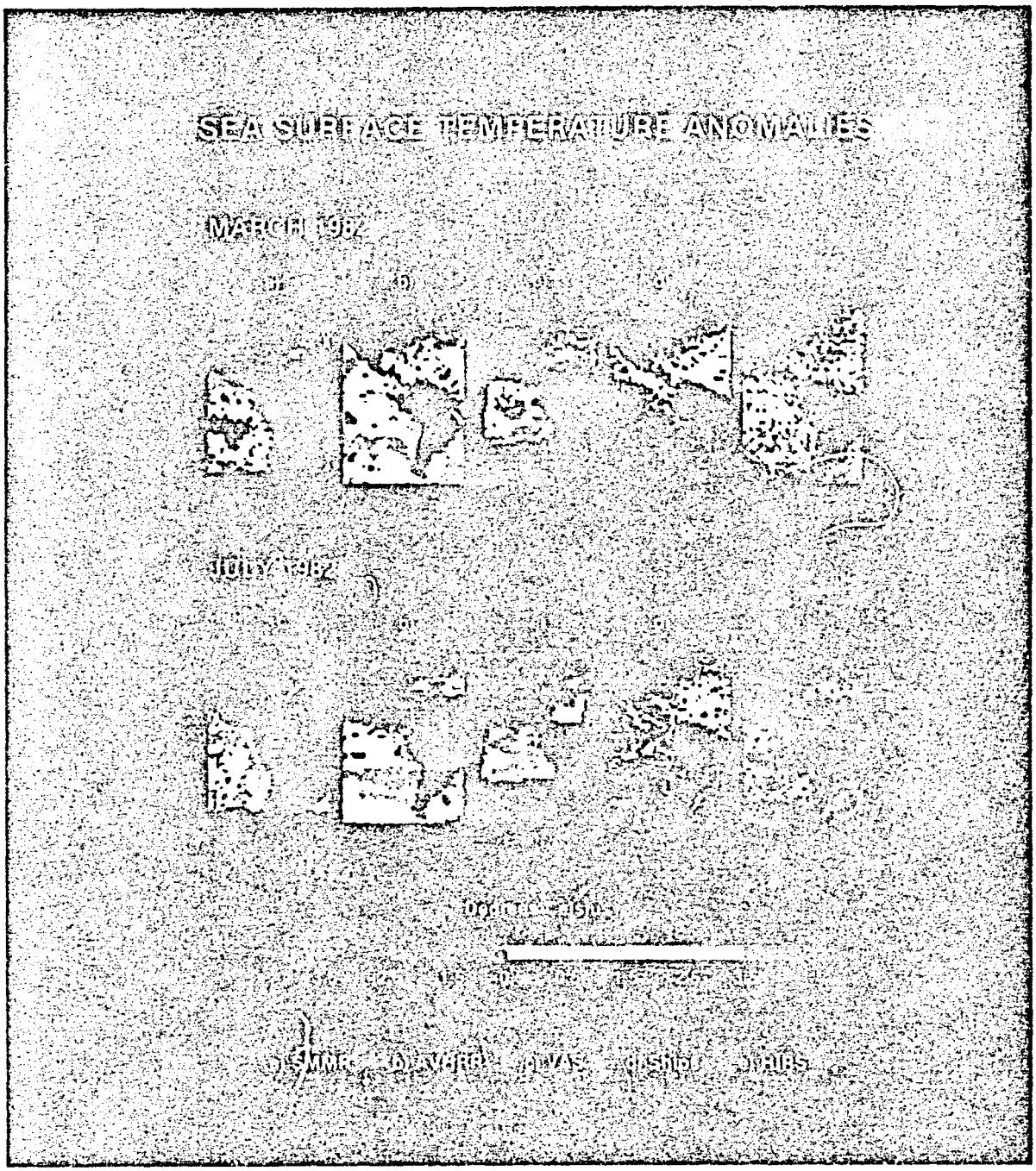

Figure C-8. SST anomalies for March and July 1982 in the VAS observation region.

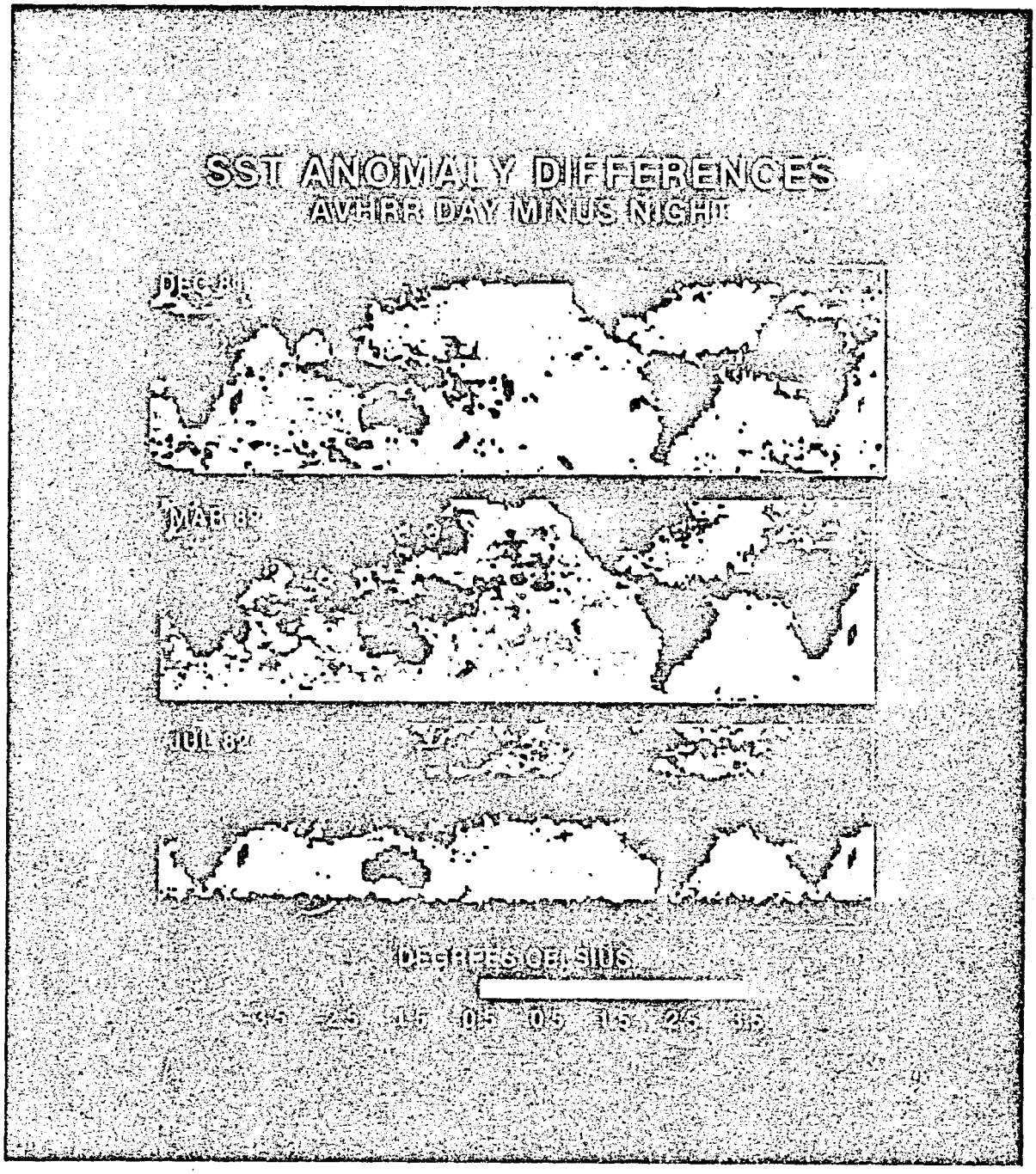

Figure C-9. AVHRR SST anomaly differences, day minus night: (a) December 1981, (b) March 1982, (c) July 1982.

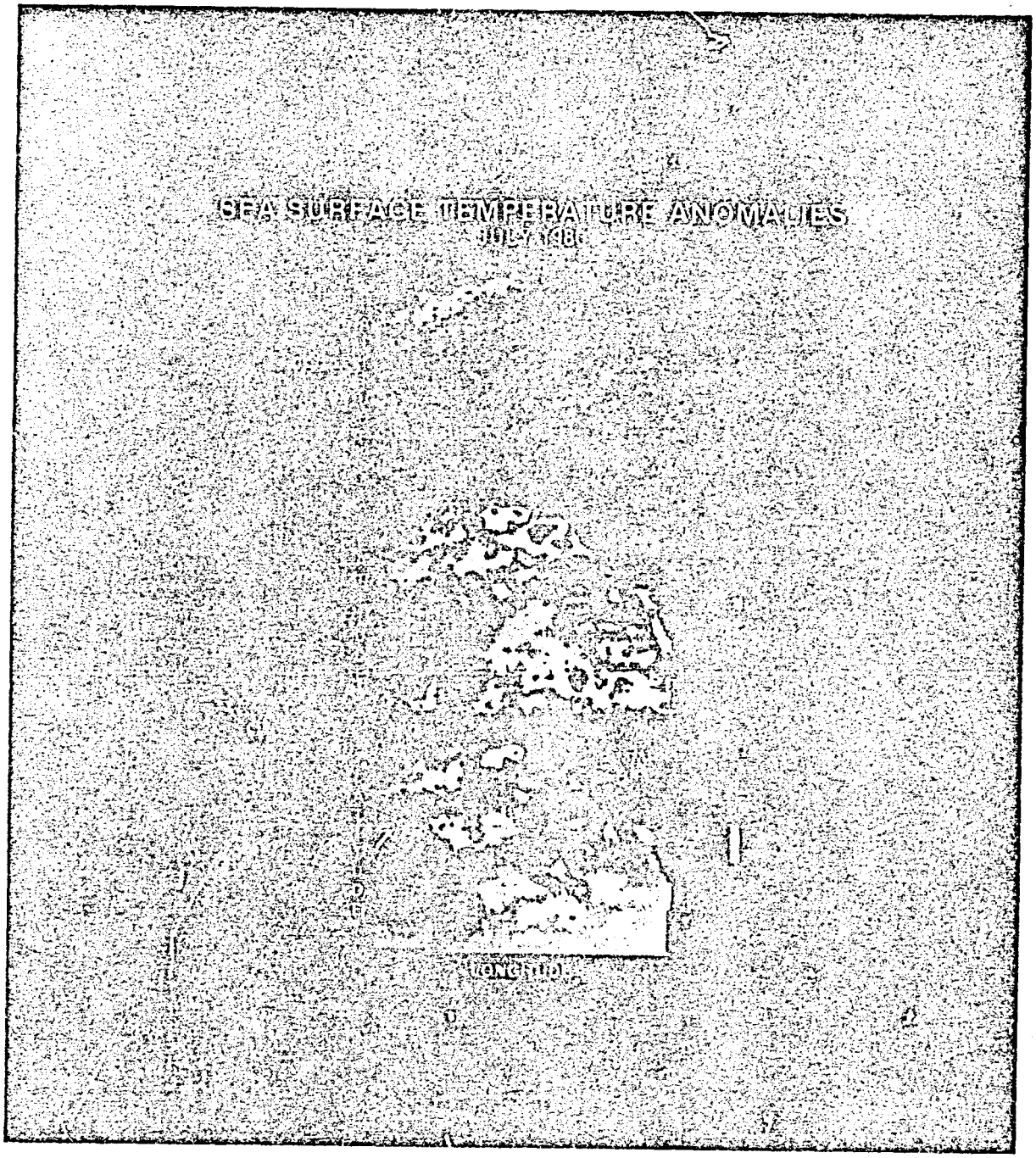

Figure C-10. SST anomalies for July 1980: (a) ship, (b) SMMR, (c) blended SMMR/ship (supplied by T. Wilheit).

APPENDIX D

LIST OF PARTICIPANTS

(Workshop III)

Mark R. Abbott
Jet Propulsion Laboratory, 169-236
4800 Oak Grove Drive
Pasadena, CA 91109

Larry Armi
A-030
Scripps Institute of Oceanography
La Jolla, CA 92093

John J. Bates
Space Science & Engineering Center
University of Wisconsin
Madison, WI 53706

Robert L. Bernstein
SeaSpace
5360 Bothe Avenue
San Diego, CA 92122

Moustafa T. Chahine
Jet Propulsion Laboratory, 180-904
4800 Oak Grove Drive
Pasadena, CA 91109

Dudley B. Chelton
College of Oceanography
Oregon State University
Corvallis, OR 97331

Donald Collins
Jet Propulsion Laboratory, 169-236
4800 Oak Grove Drive
Pasadena, CA 91109

Wayne E. Esaias
Code EE
NASA/Headquarters
Washington, D.C. 20546

Daesoo Han
Systems & Applied Sciences Corporation
5809 Annapolis Road
Hyattsville, MD 20784

Jeffrey E. Hilland
Jet Propulsion Laboratory, 138-308
4800 Oak Grove Drive
Pasadena, CA 91109

Paul H. Hwang
Code 910.2
NASA/Goddard Space Flight Center
Greenbelt, MD 20771

W. Timothy Liu
Jet Propulsion Laboratory, 169-236
4800 Oak Grove Drive
Pasadena, CA 91109

E. Paul McClain
NOAA/National Environmental Satellite,
Data, and Information Service
Washington, D.C. 20233

Andrew S. Milman
Hughes Aircraft/Space & Comm. Div.
P.O. Box 92919
Los Angeles, CA 90009

Eni G. Njoku
Jet Propulsion Laboratory, 168-314
4800 Oak Grove Drive
Pasadena, CA 91109

Stephen E. Pazan
A-030
Scripps Institution of Oceanography
La Jolla, CA 92093

John Penrose
School of Physics and Geosciences
Western Australia Institute of Technology
Kent Street
Bentley 6102
Western Australia

Joel Susskind
Code 911
NASA/Goddard Space Flight Center
Greenbelt, MD 20771

Thomas T. Wilheit
Code 913
NASA/Goddard Space Flight Center
Greenbelt, MD 20771

Yoshizumi Yasuda
Chika University
1-33, Yayoi-cho
Chiba 260, JAPAN

APPENDIX E

GLOSSARY

AMTS	Advanced Moisture and Temperature Sounder
AVHRR	Advanced Very High Resolution Radiometer
FGGE	First GARP Global Experiment
FNOC	Fleet Numerical Oceanography Center
GARP	Global Atmospheric Research Project
GLA	Goddard Laboratory for Atmospheres
GMT	Greenwich Mean Time
GOES	Geostationary Operational Environmental Satellite
GOSSTCOMP	Global Operational SST Computation
GSFC	Goddard Space Flight Center
HIRS	High-Resolution Infrared Sounder
JPL	Jet Propulsion Laboratory
LST	Local Standard Time
McIDAS	Man-Computer Interactive Data Access System
MCSST	Multi-Channel SST
MSI	Multi-Spectral Imaging
MSU	Microwave Sounding Unit
NASA	National Aeronautics and Space Administration
NCAR	National Center for Atmospheric Research
NDBO	National Data Buoy Office
NESDIS	National Environmental Satellite, Data, and Information Service
NOAA	National Oceanic and Atmospheric Administration
PODS	Pilot Ocean Data System
SIO	Scripps Institution of Oceanography
SMMR	Scanning Multichannel Microwave Radiometer
SR	Scanning Radiometer
SST	Sea Surface Temperature
SSU	Stratospheric Sounding Unit
STD	Salinity, Temperature, Density Probe
TIROS	Television-Infrared Observational Satellite
TOVS	TIROS Operational Vertical Sounder
VAS	VISSR Atmospheric Sounder

VISSR	Visible-Infrared Spin-Scan Radiometer
VTPR	Vertical Temperature Profiling Radiometer
XBT	Expendable Bathythermograph

NASA—JPL—Conf., L.A., Calif.

TECHNICAL REPORT STANDARD TITLE PAGE

1. Report No.	2. Government Accession No.	3. Recipient's Catalog No.
4. Title and Subtitle Satellite-Derived Sea Surface Temperature Workshop III		5. Report Date October 15, 1985 6. Performing Organization Code
7. Author(s)		8. Performing Organization Report No. JPL Publication 85-63
9. Performing Organization Name and Address JET PROPULSION LABORATORY California Institute of Technology 4800 Oak Grove Drive Pasadena, California 91109		10. Work Unit No. 11. Contract or Grant No. NAS7-918 13. Type of Report and Period Covered JPL Publication
12. Sponsoring Agency Name and Address NATIONAL AERONAUTICS AND SPACE ADMINISTRATION Washington, D.C. 20546		14. Sponsoring Agency Code

15. Supplementary Notes

16. Abstract

This is the third report in a series of three workshops, sponsored by the National Aeronautics and Space Administration, to investigate the state of the art in global sea surface temperature measurements from space. Three workshops were necessary to process and analyze sufficient data from which to draw conclusions on the accuracy and reliability of the satellite measurements. In this workshop (Workshop III), the final two (out of a total of four) months of satellite and in situ data chosen for study were processed and evaluated. Results from the AVHRR, HIRS, SMMR, and VAS sensors, in comparison with in situ data from ships, XBTs, and buoys, confirmed satellite rms accuracies in the 0.5 to 1.0°C range, but with variable biases. These accuracies may degrade under adverse conditions for specific sensors. A variety of color maps, plots, and statistical tables are provided for detailed study of the individual sensor SST measurements.

17. Key Words (Selected by Author(s))	18. Distribution Statement
Geosciences and Oceanography (General) Meteorology and Climatology Physical Oceanography	Unclassified/Unlimited

19. Security Classif. (of this report)	20. Security Classif. (of this page)	21. No. of Pages	22. Price
Unclassified	Unclassified		

JPL 0184 R 9/83

END

DATE

FILMED

MAR 14 1986

End of Document